ENVIRONMENTAL PROGRESS

Vol. 12, No. 3 • August 1993

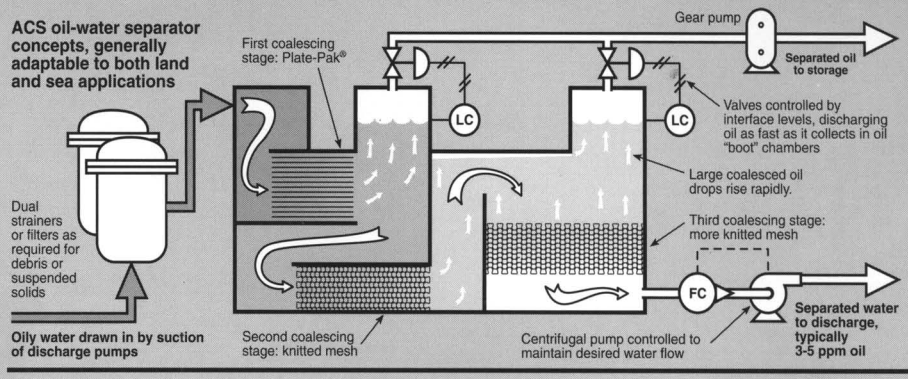

The optimum configuration of Plate-Pak and mesh

ACS INDUSTRIES, INC. Land and Sea Oil-water separators

for environmental treatment of industrial wastewater and marine skimmer discharge

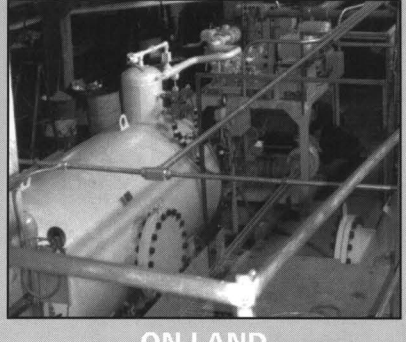

ON LAND

Documented case histories available for ACS separators now working at electric generating plants, refineries and chemical plants.

AT SEA

Because of their proven high speed and high efficiency, ACS oil-water separators were chosen for use aboard all 16 MSRC vessels recently built to respond to spills in U.S. coast waters.

ACS Industries., Separations Technology Group
14208 Industry Road • Houston, Texas 77053
Telephone (713) 434-0934 or (800) 231-0077
Telefax (713) 433-6201

Established in 1939
ACS INDUSTRIES, INC.

ENVIRONMENTAL PROGRESS

Environmental Progress is a publication of the American Institute of Chemical Engineers. It will deal with multifaceted aspects of the pollution problem. It will provide through coverage of abatement, control, and containment of effluents and emissions within compliance standards. Papers will cover all aspects including water, air, liquid and solid wastes. Progress and technological advances vital to the environmental engineer will be reported.

Published four times a year (February, May, August, and November) by the American Institute of Chemical Engineers, 345 E 47th St., New York, N.Y. 10017 [ISSN 0278-4491]. Manuscripts should be submitted to the Manuscript Center, AIChE 345 E 47th St., New York, N.Y. 10017. Statements and opinions in *Environmental Progress* are those of the contributors,and the American Institute of Chemical Engineers, assumes no responsibility for them. Subscription price per year $125. AIChE Environmental Division Members $29 included in dues. Outside the U.S. please add $12 per subscription for postage and handling. Single copies $37. Outside the U.S. please add $3 for postage and handling. Payment must be made in U.S. dollars. Second-class postage paid at New York, N.Y. and additional mailing offices.

Contents

Cover: Modular solvent concentrator currently treating 400,000 SCFM from a printing operation in Michigan. Photo courtesy of Dürr Industries, Plymouth, MI. (See article on page 226).

Departments

Superfund:
focusing on the real problems

Joel S. Hirschhorn

Once again reports, articles, and conferences on fixing Superfund are appearing everywhere, as Congress is soon to consider the reauthorization of the program. Sadly, most of the talk centers around non-technical issues, such as, liability and who pays. At the core of the problem, however, are a host of technology-related issues. Among the issues being debated are the use of innovative remediation technologies which have the potential to lower costs, and produce speedy and more effective cleanups which are acceptable to the public.

Superfund and other cleanups which are both financed and managed by the government are often considerably more costly than private sector cleanups of similar sites. Several structural reasons exist for this unacceptable situation which have nothing to do with liability and need much more attention.

A key problem is that the government views site remediation as construction, which must be preceded by a design phase. This effectively blocks the use of rapid and cost-effective turnkey approaches to remediation. The two-phase design-construction system is based on several, faulty assumptions.

First, consulting firms that are used for design work often have no significant experience in actual site remediation technologies and field work. More importantly, they are unlikely to have in-depth experience with the most innovative, cost-effective remediation technologies. The concept of standard designs for remediation is largely inappropriate, even if generic technologies are appropriate as standard or presumptive remedies for classes of sites.

Second, design is often based on incomplete and inaccurate information about what needs to be remediated, because Remedial Investigation and Feasibility Study data are incomplete and unreliable. The most meaningful data are only likely to become available through actual site remediation work itself. Given the uncertainties about site data, many design projects result in over-design to provide for contingency conditions (the expensive gold plated design) or under-designs which lead to repeated fixes, incredible delays and also excessive costs.

Third, the construction concept applied to remediation ignores the fact that usually 70 to 80% of site cleanup costs are for technical services, rather than standard construction actions, materials and equipment. Companies that often get construction work, however, do not have the special technical expertise required for first class work. Sometimes they are using patented technology without licensing it; this is the case, for example, for many firms using vacuum extraction or soil vapor extraction technology which is, in fact, patented and available through license.

One of the key solutions for fixing using Superfund and other governmenta cleanup programs is to procure remediation services from a single vendor that can provide interactive design/construction/operation capabilities, particularly for innovative treatment technologies. For example, this approach was used by TerraVac at the Verona Superfund site in Michigan.

Technology oriented firms have unique expertise in innovative remediation technology which they have developed and, in some cases, patented. Procurement should be oriented to technical services rather than construction, and procuring turnkey remediation according to the Brooks Act should be used so that quality, experience and previous performance are the basis for selection, rather than low price. Only in this way will all the talk about using more innovative and cost-effective remediation technology be turned into a reality.

Fixing Superfund, restoring public confidence in it, and reducing the multi-billion dollar cost of cleanup in the United States requires a focus on technology and on using administrative and procurement systems which maximize the use of companies with truly unique technological capabilities and also giving less attention to liability and legal issues.

Joel S. Hirschhorn, Ph.D. is President of Hirschhorn & Associates, Inc., an environmental consulting firm in Lanham, Maryland. He was formerly with the Congressional Office of Technology Assessment, where he directed several key studies of the Superfund program which has influenced many actions by Congress and the EPA.

Workshop on the prevention of waste and emissions in the fine chemicals/ pharmaceutical industries

This International Workshop is to be held in Cork, Ireland, October 4th and 5th, 1993. The workshop is organized by The Clean Technology Centre (Ireland), Storsøms Amt. (Denmark), and The PREPARE Secretariat (The Netherlands). (PREPARE is the waste prevention working group operating under EUREKA). The workshop brings together industrialists and experts from the European Community and the USA with the objective of improving competitiveness by optimizing operations and minimizing wastes. For further information please contact: The Clean Technology Centre, Cork RTC, Bishopstown, Cork, Ireland. Telephone: 011 353 21 344864 • FAX: 011 353 21 344865.

Course offered on preparing for EPA/OSHA inspections

EPA and OSHA have signed a memorandum of understanding to coordinate their compliance and enforcement activities, referring possible violations, exchanging information and cross-training agency personal. To help companies understand how to handle inspections, before, during and after the inspector arrives, Government Institutes Inc., is offering a one-day intensive course on October 26, 1993 at the Stouffer Concourse Hotel in Arlington, VA.

Course attendees will learn how to protect their company from needless penalties and violations, what the role of audits are in ensuring a company's compliance preparation for an inspection, legal obligations during an inspection and more.

For more information contact Coleen Sullivan at Government Institutes Inc., Suite 200, Rockville, MD 20850; (301) 921-2345 • FAX: (301) 921-0373.

Economic Growth Spurs the Hazardous Waste Management Market

The increase in industrial production following the recession of the early 1990s will increase the generation of hazardous waste in the U.S. by 3% annually to over 400 million tons in 1997. As a result, commercial hazardous waste management services are expected to expand 12.4 % per year (in dollar terms) through 1997 according to a new study from The Freedonia Group Inc., of Cleveland, Ohio. In addition to economic factors, legislative, regulatory, social and technological trends also influence hazardous waste management activities which range from pretreatment and land disposal, to incineration, remediation and resource recovery. Industry analyst Eric Mundy forecasts that most of these management services will experience double-digit growth, except collection/transportation and asbestos abatement services. Freedonia's new study #480 entitled *Hazardous Waste Materials, Management and Services* offers a detailed look into this industry.

Service revenues generated in the hazardous waste remediation segment will expand over 13% per annum to nearly $17 billion in 1997. Mr. Mundy cites increased clean-up activity of Superfund sites and contaminated federal weapons facilities as the main reasons for this growth. In addition, greater activity related to private-party voluntary compliance and corrective action will also contribute to gains, as will greater remediation activity of obsolete underground storage tanks. Land disposal and incineration revenues will see good growth due to higher operating and liability costs. Consulting, engineering and analytical testing services will also see favorable gains.

Wastewaters and other liquids will continue to account for over 80% of the U.S. hazardous stream. The treatment and release of these solutions will remain the most widely implemented hazardous waste management method, and Mr. Mundy attributes gains in this management technique to more stringent regulations and enforcement measures.

Although land disposal facilities (landfills, injection wells, etc.) are the final resting place of many hazardous materials, particularly solid wastes, land ban restrictions recently implemented by the EPA will limit activity in this sector. Both incineration and resource recovery and recycling will consequently see excellent gains of nearly 12% and 10% respectively over the forecast period. The volume of illegally or improperly disposed hazardous waste will continue to decline as enforcement activity becomes more stringent.

Although over 90% of hazardous waste materials is handled captively, the quantity of commercially managed wastes (i.e., managed by waste management specialists) will continue to increase. Mr. Mundy believes that as regulations become more complex and liabilities mount, waste generators will turn to professional hazardous waste management firms. The quantity of commercially managed hazardous wastes is forecast to increase over twice as fast as overall waste generation, reaching 24.5 million tons in 1997.

The complete 153-page #480, *Hazardous Waste Materials, Management and Services* is available for $2700.00 from the Freedonia Group Inc., 3570 Warrensville Center Road, Ste. 201, Cleveland, OH 44122-5226. For more information please call (216) 921-6800 or FAX (216) 921-5459.

Hazardous Waste Management by Method
(million tons)

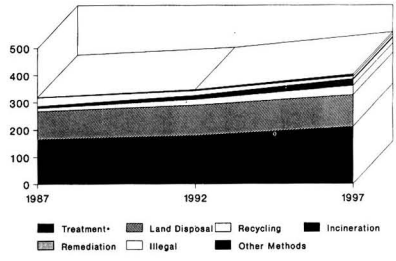

*Excludes waste exempt from RCRA permits

Washington Environmental Newsletter

The Environmental Agenda - 1993/1994

The 103rd Congress has set an ambitious environmental agenda even though almost all Members are carryovers from the last Congress. What happens to the key environmental issues is usually measured in two-year cycles, such as, the length of the term of a Congress. What transpires is influenced by those involved in the discussions and their particular aspirations or agenda. Even though there are many new faces in the 103rd Congress the people who influence the pace and outcome of these environmental debates, namely, the committee and subcommittee chairs, are basically the same as they were in the 102nd Congress. This cannot be said of the new administration where everyone in a policy-making role is new and they are beginning to get involved in these issues. It is important, therefore, to examine this group as they will be the ones who will set the administration's environmental agenda.

A New Administration - The People

The major goal of the Clinton administration, in the environmental area, is to strike a balance between economic growth and environmental compliance. This will present a significant challenge to the new people who have already been named or are soon to be named to key environmental positions. This challenge will extend beyond the EPA to other agencies and departments as well as the Office of Management and Budget (OMB) and the President's immediate White House staff.

The success of the new administration in achieving their environmental goals will be dependent on the people involved and the process they establish for dealing with the issues. The process, that is, how issues are to be moved through the administration in order to develop administration positions and by whom, is still not well defined.

As for the people, Vice President Al Gore appears to be key as to what will transpire in the environmental area. The Vice President has been successful in placing many of his key aides and friends from his Senate and House days into important environmental positions. For example, EPA Administrator Carol Browner worked for then Senator Gore as his legislative director. Kathleen McGinty, who is Assistant to the President and Director of the new Office of Environmental Policy was his legislative assistant for environmental matters. Roy Neel, now Deputy Chief of Staff to the President, was the Vice President's Administrative Assistant when Al Gore was in the Senate. He was also the Vice President's Chief of Staff prior to moving to the Presidents office. When the Vice President was in the House of Representatives, he worked closely with former Office of Technology Assessment Director and now the new Assistant to the President for Science and Technology, Dr. John Gibbons. There are others in key positions, in areas such as the Department of Energy and the Department of Commerce, who will assist the Vice President extend his influence in the environmental area.

On the economic side some of these same people who are aligned with the Vice President participated in the administration's deliberations on the President's budget and econimic stimulus packages before they were sent to the Congress. They were particularly active during deliberations on the BTU tax.

The Environmental Issues

The 103rd Congress is expected to consider amendments to the following statutes: the Clean Water Act; the Comprehensive Environmental Response, Compensation and Liability Act (CERCLA) or as it is commonly referred to, Superfund; the Resource Conservation and Recovery Act (RCRA), as it pertains to the interstate transportation and the recycling of waste materials; the Endangered Species Act and elevating the EPA to Cabinet status.

The administration has formed task forces to develop policy positions and legislation on superfund and the wetlands provisions of the Clean Water Act. The influence of the administration will become more significant in dealing with the environmental issues before Congress when the people named to the remaining senior environmental policy positions are confirmed by the Senate and they more clearly define the respective roles each entity will play in the development of policy.

This newsletter was prepared by AIChE's Washington representative, Dale Brooks, 1300 I Street, N.W., Suite 1090, East Tower, Washington, D.C. 20005. Telephone (202) 962-8690 • FAX: (202) 962-8699

Occupation and Environmental Safety: Engineering and Management by Hamid R. Kavianian and Charles A. Wentz, Jr.,Van Nostrand Reinhold Company, New York, NY,(1990). [ISBN No.: 0-442-23822-3],U.S. List Price: $ 55.95

Having reviewed Wentz's first excellent text, *Hazardous Waste Management*, I turned to this book eagerly. I was not disappointed. As chemical engineers, Kavianian and Wentz have written especially for our profession. They have done a good job, covering almost all the essential elements of safety management for the process industries.

Clearly, safety is an important topic to the Chemical Engineer who may be in danger to his/her subordinate, for whom he/she as a professional is responsible. The community may also be in danger as tragically evidenced by the spill of methyl isocyanate at Bhopal, India where more than 2,000 people died and more than 200,000 were injured. In the United States, numerous chemical plant workers have been killed or injured recently in spills, fires, and explosions. Lawsuits and fines levied by the EPA and OSHA make these accidents terribly painful (and expensive) for the corporate coffers. Hence, prevention of accidents is the key goal in the chemical and allied industries.

ABET, the engineer's accrediting body, has encouraged (to us academics, ABET's encouragement is a mandate) the inclusion of safety examples and problems in appropriate courses. That is a good first step, but I feel a separate course of safety is needed (along with another course on environmental engineering, although my academic colleagues are not sure where "we'll find room for it in the curriculum".

If we do add a safety course, Kavianian and Wentz have the text to use. It is logically designed and well written. It is comprehensive and full of good examples. Perhaps best of all, from an academic perspective, it has suggested student exercises at the end of each chapter.

After an introductory chapter in which the authors express concern (which I share) about the need for inclusion of safety in the curriculum, they dive into the law and create what I term a "need to know". Clearly, safety is driven by rules and regulations established by OSHA; for environmental safety (hazardous wastes and chemical spills), it is driven by the U.S. EPA. The discussion is quite up-to-date. I looked for and found a discussion of OSHA 1910:120 standard HAZWOPER (Hazardous Waste Operation and Emergency Response Standard) which governs actions at hazardous waste sites and hazardous chemical spill cleanups.

The law is not easy to read, but it is necessary. Appropriately, the authors devoted almost 80 pages to it. Included in this chapter is an interesting (and well done) discussion of hazard labelling including DOT placards and NFPA diamonds. Material Safety Data Sheets (MSDSs) are also discussed.

Chapter 3 is devoted to Industrial Toxicology which the authors define as: "...a science that deals with the potential harmful effects of materials, products, and wastes on health, and the environment. Bringing together knowledge from many scientific fields, including chemistry, biology, pharmacology, physiology, and pathology, it has been given a name meaning 'the science of poisons' ". Clearly this is an important topic, especially so for chemical engineers who are not usually privy to toxicology courses or even discussions of toxicology during their undergraduate course of study. Covered are the basics of exposure (under the title of "Transport of Toxic Substances in the Body"), Carcinogens, Relationship between Dose and Response, Lethal Dose, Threshold Limit Values, Acute and Chronic Toxicity, Effect of Toxicity and,finally,the Toxicity of Dioxins, Dibenzofurans, and PCBs (an appropriate ending to the chapter as these three groups of chemicals are much discussed in the scientific and popular literature. My only criticism of the chapter is that it is too short (only 14 pages). More space, I feel, could have been devoted to these three topics.

The next four chapters (4 through 7) have the following headings:

- The management of Personal Protective Equipment
- Managing Fire Hazards
- Industrial Noise Control
- Electrical Safety

Chapters 8 and 9 return to the central theme of the book (the central theme for chemical engineers). Their titles are:

- Determining the Cause of Accidents and Conducting Effective Safety Audits
- System Safety Analysis in Program Design

Chapter 10 was of personal interest to me; Containment and Spill Management. Although it was short, the authors have a good discussion of the legal and practical aspects of handling hazardous wastes. However, they stopped far too short of the problem. Not covered was the potential for spills of raw materials and finished products - tanks, drums, and transport pose more serious problems when they contain virgin chemicals than when they carry hazardous waste. I would have significantly extended the chapter to products of the chemical industry.

Chapters 11 and 12 discuss radiation hazards and first aid. The book ends with a seemingly "tacked on" chapter entitled Computer Systems and Statistical Methods for Occupational Safety and Health Management. There are four lengthy appendices:

- Extremely hazardous substances and t hreshold planning qualities
- Known carcinogens
- Suspected carcinogens
- OSHA permissible exposure limits.

As a safety course text, I highly recommend the book. Each section has suggested student assignments that will markedly assist an instructor. However, using the book and text will require supplementation and a courageous (and forward-looking) Chemical Engineering faculty to put such a course into the curriculum.

Gary F. Bennett
Prof., Emeritus of Biochemical Engineering
Department of Chemical Engineering
University of Toledo
Toledo, OH 43606

Risk Management of Chemicals in the Environment by Hans M. Seip and Anders B. Heiberg, Plenum Press, New York, NY, (1989). [ISBN No.: 0-306-43081-9], U.S. List Price: $65.00

Risk assessment and management is a critical element of implementing programs for occupational safety and environmental protection. Risk assessment is also the underlying foundation for the development of occupational safety and environmental legislation, regulation, and standards.

This book which is organized into twelve chapters presents the results of an international pilot study on environmental protection risk assessment and risk management. Chapter 1 begins with a good introduction to the pilot study of risk management of chemicals in the environment. Chapter 2 presents an excellent description of methods for quantification of health risks due to exposure to chemicals, while Chapter 3 discusses the methods for assessing the risk of environmental contamina-

tion. The fourth chapter presents an excellent summary of the methods used in the United States for assessment and management of health risks due to chemicals. The next chapter discusses methods used in the U. S . for assessment of ecological risks related to chemical exposure

Chapter 6 discusses attitude toward risk-benefit analysis for managing effects of chemical exposures. The seventh chapter presents a discussion of modelling behavior of pollutant in soil for risk assessment purposes. The environmental and health impact assessment of soil pollutants are addressed in Chapter 8. The next chapter presents a good discussion of mathematical and biological uncertainties in the assessment of permissible blood lead concentration. Chapter 10 presents a case study dealing with the use of formal methods in evaluating countermeasures to coastal water pollution. Methods used to control air pollution in Oslo, Norway are presented. The last chapter presents a good summary of individual chapters in the report along with the editors' conclusions and recommendations.

This book, although not recommended as a textbook for risk assessment and management, should prove to be an extremely useful tool as a reference guide for these individuals involved with risk assessment and management of chemicals in the environment.

Hamid R. Kavianian, Ph.D.
Professor
Department of Chemical Engineering
California State University at Long Beach
Long Beach, CA 90840

Occupational Hygiene Management Guide by Stanley E. Jones, H. Roland Hosein, Glenn R. Swalm and Jack F. Yablonsky, Lewis Publishers Inc., Chelsea, MI (1990) [ISBN No. : 0-87371-255-2],U.S. List Price: $45.00

This book provides guidelines and procedures for upper and middle management to develop and implement effective programs to minimize occupational exposure to acute and chronic harmful substances in the workplace. In recent years, the public pressure on industry for creating an occupationally and environmentally safe workplace has resulted in promulgation of strict, legislation, regulations, and standards. It is the management's responsibility to ensure compliance with occupational and environmental management to understand the hazards of harmful substances in the workplace and to develop and implement programs to manage worker exposure to these hazards.

This book is divided into four sections. The first section presents an overview of the management role in occupational safety and provides guidelines for allocation of occupational hygiene responsibilities within the organization.

The second section provides guidelines for hazard recognition, evaluation and control. Section 3 discusses procedures for monitoring and measuring the effectiveness of the overall program.

Section 4 is a set of six appendices. Appendix A is a summary of a typical management program elements. Appendix B is a summary of typical chemical and physical harmful agents which can be found in the

workplace along with their potential adverse effects. Appendix C is a summary of the principles of industrial toxicology. Appendix D contains the 1989-1990 Threshold Limit Values and Biological Exposure Indices published by the American Conference of Governmental Industrial Hygienists. Appendix E is a list of suggested references and Appendix F is a glossary of terms used by health professionals.

This book should prove to be useful as a general guidelines for managing occupational exposure to harmful physical and chemical agents.

Hamid R. Kavianian, Ph.D
Professor
Department of Chemical Engineering
California State University at Long Beach
Long Beach, CA 90840

Retrofitting Publicly-Owned Treatment Works for Compliance, Pollution Technology Review No. 190 by Bob A. Hegg, Larry DeMers and John Barber, Noyes Data Corp., Park Ridge, N.J. (1990), 271 pages, [ISBN No.: 0-8155-1251-1], U.S. List Price: $45.00

Members of Process Applications Inc., of Ft. Collins, Colorado, Hegg, DeMers and Barber authored this manual for the U.S. EPA to describe methods for retrofitting publicly-owned treatment works (POTWs) for compliance with federal regulations. They were assisted by almost a dozen contributing authors from the U.S. EPA, other consulting firms and academia. This book was thoroughly peer reviewed owing to the fact that it is a U.S. EPA report.

The goal of the manual was to assist non-complying (i.e., non-complying with effluent limitations) POTWs to achieve compliance or more reliable performance from their existing facilities. The manual provides procedures for:

(1) Conducting performance evaluations,
(2) Implementing performance improvement activities, and
(3) Selecting facility modifications for secondary treatment plants that have identified design limitations.

The manual focuses on conventional secondary (biological) treatment systems. Innovative/alternative technologies are presented as potentials for modifying (and improving) existing conventional facilities.

Chapter 2 discusses an evaluation approach to identifying reasons for noncompliance and to assess the suitability of existing facilities for improved performance. Chapter 3 discusses the composite corrective approach which details methods of optimizing existing facilities without major capital expenditures. Procedures to address design, operation, maintenance, and administration factors limiting performance are outlined. Implementation of a composite correction program ensures optimization of existing facilities, and if compliance is not achieved, the design factors limiting performance are identified.

Chapter 4 provides the reader with a detailed description of facility modifications that can result with improved performance. This portion of the manual can be used with procedures outlined in the two previous chapters, or it can be used alone if the reader had already determined the facility modifications necessary to achieve compliance. Chapter 4 utilizes a tabular format to list design factors that can potentially limit compliance of major unit processes, describes briefly the manner in which compliance is affected, and directs the reader to this section of the chapter where specific information regarding suggestion facility modifications are discussed.

Approximately one-half of the book (and probably the most useful part) is appendices which are check-lists with work sheets for:

Appendix A: CPE Classification Ssytem, Factors Checklist, and Definitions for Assessing Performance-Limiting Factors.

Appendix B: CPE Summary Sheet for Ranking Performance-Limiting Factors.

Appendix C: Examination of CPE Report.

Appendix D: Data Collection Form Used in Conducting CPEs.

Appendix E: Procedure for Converting Oxygen Rates and Flows

Appendix F: Guidelines for Field Estimating Equipment Power Usage.

Appendix G: Example Form for Evaluating Maintenance Program for Small POTWs.

Appendix H: Example Wastewater Treatment Plant Administrative and Management Audit

Appendix I: Example Process Monitoring Summary for an RBC POTW.

Appendix J: Example Process Monitoring Summary for an Activated Sludge POTW.

Appendix K: Parameters Used to Monitor the ABF Treatment Process.

Appendix L: Suspended Growth Major Unit Process Evaluation Worksheet..

Appendix M: Trickling Filter Major Unit Process Evaluation Worksheet.

Appendix N: RBC Major Unit Process Evaluation Worksheet.

Appendix O: ABF Major Unit Process Evaluation Worksheet.

Appendix P: Stabilization Plant Major Unit Process Evaluation Worksheet.

Gary F. Bennett
Prof., Emeritus
of Biochemical Engineering
Department of Chemical Engineering
University of Toledo
Toledo, OH 43606

Environmental Software From Flyers

A. Kumar, S. Sahore and N.K. Bellam
Department of Civil Engineering, The University of Toledo, Toledo, OH 43606

Introduction

As compliance with environmental regulations increasingly becomes part of routine business operations, more environmental managers are turning to computers for help in performing their jobs. The proliferation of environmental regulations during the 1980s has been accompanied by rapid growth in the volume and variety of commercial software available to aid compliance. From relatively simple programs that run on personal computers, and generate Material Safety Data Sheets (MSDS) and shipping labels to complex relational databases that can be used for multiple compliance tasks, computer software has become an indispensable tool for many environmental managers. Therefore, entry level environmental jobs generally require a good working knowledge of environmental software.

With this perspective, environmental software deserves some close attention in this decade - as we experience a transformation at the local, regional, national and global level. The number of users of environmental software is constantly increasing and the prices for software are plummeting.

With an environmentally-concerned, conscious people at the helm, new rules and regulations can be expected which will cause organizations to restructure and reshape themselves in order to meet the growing environmental needs of the day. Also top executives are and will use lower-cost, high performance information technology to build leaner, more adaptive, and competitive companies.

So environmental managers, too, must build and maintain lean, adaptive, and competitive compliance programs keeping in mind that a restructured, overhauled environmental program should not be managed as an entity apart from the core business enterprise [*1*].

In the coming years, the single most important role for environmental software and Management Information Systems is to link environmental management judiciously and comprehensively into the core information flows of the business.

This paper in a simplified way attempts to bridge the gap between available software and the end-user, in order to make a leviathan and often fruitless task of searching for relevant software a successful one. In the past reviews published in this column mainly concentrated on software taken from directories, reports and scientific papers [*2, 3, 4*]. The material presented in the following pages is from flyers, which are an invaluable source of knowledge and may be overlooked or ignored by many environmental managers. The software discussed in this paper have been divided into the five main areas of environmental engineering: (i)Air Pollution Modeling, (ii) Waste Management (iii) Environmental Geotechnology, (iv) Regulatory Compliance, and (v) Information Technology.

Air Pollution Modeling Software

Computerized modeling of air pollution has come as a welcome and more economic replacement for the age-old method of ambient air monitoring. The technological breakthrough in this field has been so intense and rapid that the variety of commercial software available is literally mind boggling [*5*]. The software under this category (see Table 1) cover a broad range of issues from estimating the impact of source emissions on air quality, analyzing the effect of stack height on pollutant dispersion, establishing ambient air monitoring stations in order to assess compliance under the Air Toxics Program of Clean Air Act Amendments of 1990, to providing a crucial component of an environmental impact assessment.

Waste Management Software

Software under this category (see Table 2) cover the numerous processes viz., filtration, clarification, sedimentation, flocculation, coagulation, ion exchange, reverse osmosis, activated sludge system and many more employed at a water/wastewater treatment plant. They incorporate features such as maintaining control of the processes related to a wastewater treatment facility, performing design calculations for an activated sludge system, evaluating the hardness of water and quantifying the tendency of water to scale or corrode by calculating the Langelier and Ryznar indexes, and managing the humongous amount of records needed by an industrial plant to ensure compliance under the NPDES by setting a discharge limitation.

Environmental Geotechnology Software

The specialization in this field include multiphase, multicomponent flow, techniques of characterization and remediation, determining hydraulic properties of aquifers from pumping and slug tests, performing simple flood routing and more detailed surface water/groundwater interaction. A number of software programs (see Table 3) have been used successfully for the investigation and remediation of Superfund sites. Being a handy and easy referring tool, they are immensely useful and have gained huge popularity among the environmental managers today.

Regulatory Compliance Software

Because the regulatory climate is dynamic and increasingly complex, regulatory compliance software has a combination of scientific, engineering, and management expertise. No manual system can ever handle the sheer volume and complexity of information generated when dealing with legalities. Thus automating environmental information is indispensable for the professionals in the field to efficaciously manage the regulatory workload. A list of software is given in Table 4.

In addition to tracking the dynamics of law, they help in maintaining records and generating reports like TierI, Tier II, Tier III, Title 313 Form R, MSDS records, environmental audits and groundwater monitoring reports.

Information Technology

Of late there has been an increasing tendency to store a broad spectrum of factual information and data electronically. On-site and off-site experts, researchers, and other professionals as well as novices can tap resources worldwide through such bulletin boards. They provide information that is comprehensive and all encompassing. This helps in tackling real world problems innovatively and with a very high degree of precision. The popularity of the system is increasing. Generally all information can be found on these systems which are available from either commercial or public vendors. Extensive air pollution-related data bases are also available from bulletin boards and publishers (see Table 5).

Concluding Remarks

A number of different software were found from flyers during this review. Contact information is given for each organization. It is hoped that you will find information useful for environmental activities at your plant.

Literature Cited

1. Ferguson, R. A., "Information Management", AT, pp. O & P 16, February 1993.
2. Kumar, A. and S. Sahore, "A Review of Four Software Directories", *Environmental Progress*, **12** (2), pp. M9-M14 (1993).
3. Kumar, A. and S. Kode, "Sources of Environmental Software" *Environmental Progress*, **11** (3), pp. A10-A14 (1992).
4. Kumar, A. and J. B. Lee, "Software to Study Environmental Effects of Hazardous Waste Sites", *Environmental Progress*, **10** (2), pp. M7-M10 (1991).
5. Sadar, A. J., "Dispersion Modeling", *Environmental Protection*, pp. 15 - 20, March 1993.
6. Rich, G., "Picking Environmental Software", *Pollution Engineering*, pp. 45- 66, January 1992.

Table 1. Software for Air Pollution

NAME	*VENDOR*	*DESCRIPTION*
ADEPT 2	Alberta Environment	Estimates seasonal and annual average concentrations and deposition of sulfur compounds.
BEE-line SLAB	Bowman Environmental Engineering (214) BEE-LINE	Tool containing dense gas algorithms, allowing heavier-than-air gas releases to be accurately modeled.
BREEZE AIR ISCST model	Trinity Consultants, Inc. (214) 661-8100	Model used to predict short-term pollutant concentration produced by continuous emissions from point, area and volume sources.
BREEZE AIR ISCLT model	Trinity Consultants, Inc. (214) 661-8100	Model used to predict annual or seasonal pollutant concentrations produced by continuous emissions from point, area, and volume sources.
BREEZE AIR SCREEN	Trinity Consultants, inc. (214) 661-810	Model used to analyze single point, area or flare sources in simple or complex terrain.
BREEZE WAKE	Trinity Consultants, inc. (214) 661-8100	Tool designed to produce the direction-specific, building heights and widths necessary for downwash analysis in the latest versions of ISCST and ISCLT.
CHEMMIX	Environmental Systems, Inc., (419) 353-8540	Design program to determine potential chemical reactivity as a result of unplanned chemical mixing.
CHEMS-PLUS VERSION 2.0	Arthur D. Little, Inc. (617) 864-5770	Detailed package of simplified hazard assessment models for emergency planning
DANA	Ingenieurburo Kunzler, Switzerland	Software package of emission monitoring and sampling of stack gases and other industrial processes.
ENVICOM/PLUS REVISION 5.02	Odessa Engineering, Inc. (512) 834-4141	Tool used to acquire, store and analyze air quality data.
ENVAID REVISION 5.01	Odessa Engineering, Inc.	Tool used to acquire, store and analyze air quality data
EPI CODE VERSION 4.1	Homann Associates, Inc. (415) 490-6370	Software tool to evaluate the atmospheric release of toxic substances.
HAZOP-PC	Prima Tech (614) 841-9800	Tool used for hazard and operational studies at facilities handling hazardous materials.
OILMAP	Applied Science Associates, Inc., (401) 789-6224	Tool used for rapid oil spill response, full fates modeling, contingency planning and risk assessment.
PHA-PC	Prima Tech	Tool used for preliminary hazard analysis at facilities handling hazardous materials.
PRISE	Computational Mechanics Publications (508) 667-5841	Calculates airborne effluent dispersion using plume rise model and a Gaussian model.
SUPERCHEMS	Arthur D. Little, Inc. (617) 864-5770	Detailed hazard modeling package containing models for release rate, pool behavior, vapor dispersion, different types of fires and explosions.
TOXIC 3.1	HMCRI (800) 397-7161	Calculates risk of processing hazardous waste.
WHAT-IF	Prima Tech (614) 841-9800	Tool used for formal "what-if" studies at facilities handling hazardous materials.
WHAZAN-II	DNV Technical software products division	Calculates indoor concentrations as cloud passes a building, pool spread and evaporation.

Table 2. Software for Waste Management

NAME	VENDOR	DESCRIPTION
ACT	TECHDATA (713) 498-0798	A LOTUS 1-2-3 template which performs design calculations for activated sludge system design. It considers four common process modifications including extended aeration.
Audit Master	UtiliCom Pittsford, NY	A program capable of tracking the mass of records necessary to insure a chemical plant is safe and in compliance with government regulations.
The Collection System Manager	J & H Software Inc., (419) 473-9611	Contains detailed information on manholes, sewers, catchbasins/inlets, taps, laterals, and regulators.
The Distribution System Manager	J & H Software Inc., (419) 473-9611	Maintains detailed information on meters, valves, hydrants, pipes, service connections, backflow prevention devices, and more.
The Industrial Pretreatment Program Manager	J & H Software Inc., (419) 473-9611	A menu-driven program to assist the pretreatment program coordinator / manager in administering the local pretreatment program.
The Maintenance Manager/Equipment	J & H Software Inc., (419) 473-9611	A database that maintains detailed information on all plant equipment including name plate data, catalog information, special operating requirements and more.
PC Environmental Fate database	Syracuse Research, Syracuse, NY	Contains physical/chemical properties, transport information, abiotic and biological degradation data, and ambient food, and occupational monitoring data. Has four files that contain actual experimental data or identify environmental fate and monitoring data.
Process Adviser / NPDES Reporter	J & H Software Inc., (419) 473-9611	Incorporates a pull-down menu system that allows the user to maintain control of the process related to a wastewater treatment facility.
SAMPLINK	ISCO Inc., (402) 474-2233	Allows data transfer between an enhanced ISCO 3700 Automatic Wastewater Sampler and an IBM-PC or compatible computer.
Sludge Manager	Softcare Computer Services Inc., (315) 597-2385	A software that is designed specifically for record keeping and database management in sludge and other byproduct use programs
WATER	TECHDATA (713) 498-0798	A template that calculates Langelier and Ryznar indexes, which indicate the water's tendency to scale or corrode.
WATERMAX	The Pitometer Associates (800) 347-5990	A powerful, user friendly, fast EPS water system analysis program that doesn't require other costly graphics or spreadsheet software.
The Well System Manager	J & H Software Inc., (419) 473-9611	Permits the user to monitor and determine the operating condition of water wells.

Table 3. Software for Geotechnology

NAME	VENDOR	DESCRIPTION
AQTESOLV	Geraghty and Miller, Inc. (703) 758-1200	Determines hydraulic properties of aquifers from pumping tests and slug tests.
MODCAD	Geraghty and Miller, Inc.	Tool used as a computer aided design for groundwater modeling.
MODFLOW	Geraghty and Miller, Inc.	Tool with applications in isothermal groundwater flow systems.
QUICKFLOW	Geraghty and Miller, Inc.	Simulat groundwater flow in a horizontal plane.
SUTRA	Geraghty and Miller, Inc.	Simula unsaturated flow and transport, variable viscosi thermal transport and variable density solute transpo

Table 4. Software for Regulatory Compliance

NAME	VENDOR	DESCRIPTION
BEE-Line Permitting Package	Bowman Environmental Engineering (214) BEE-LINE	Contains a complete set of models, data entry software, and support software to meet most air permitting modeling needs, including PSD and state and regional toxics modeling.
Compliance Manager	OSHA-SOFT Inc. (603) 672-7230	Tool designed to aid compliance with OSHA's hazard communication standard. Provides a computerized link between chemical inventory and MSDS information.
Earthlaw	ERM Computer Services, Inc., (800) 544-3118	A main-frame based product that integrates ENFLEX INFO, the most comprehensive resource for existing federal and state laws, with three well-known database services that track developing laws and regulations.
ENFLEX DATA	ERM Computer Services, Inc., (800) 544-3118	A comprehensive modular software system with a fully integrated database manager, is designed to ease the burden of environmental record-keeping and reporting.
ENFLEX INFO	ERM Computer Services (800) 544-3118	An environmental regulatory Information system that gives you access to the full text of current Federal and State laws and regulations.
Facility Tracking System	Quantum Compliance Systems, Inc. (313) 761-2175	Creates a comprehensive framework for storing, retrieving and tracking data required under today's most demanding environmental regulations viz., SARA Title III, RCRA, EPCRA etc.,
Fast-Regs	OSHA-SOFT Inc., (603) 672-7230	Tool designed to help companies keep abreast of federal regulations.
FORM-R	AV Systems Inc., (313) 662-0035	It covers the complicated rules of EPA SARA Title III Section 313 toxic release reporting
Hazardous Materials Manager	Jordan Systems Inc.,	Tool designed to help environmental coordinators generate Tier I and II and Form R reports for annual submission.
HITS version 2.3 (HazMat Inventory Tracking System)	BSI Systems, Inc. (619) 673-8420	Easy to use software for SARA Title III and OSHA hazard communication standard compliance. It includes a built in chemical data base created by SIGMA-ALDRICH Chemical Corp.

(Continued on following page)

Table 4. (Continued from previous page)

NAME	VENDOR	DESCRIPTION
MIRS	AV Systems Inc., (313) 662-0035	An integrated, comprehensive software compliance tool with many module options to simplify environmental compliance.
MSDS+	AV Systems Inc., (313) 662-0035	Is designed for OSHA HAZCOM compliance and material safety data sheet (MSDS) generation.
RI/FS	Environmental Software and Systems Inc., (419) 353-8540	A package that is concerned with the requirements for submitting a Remedial Investigation/Feasibility Study for RCRA sites.
SARA!	OSHA-SOFT Inc., (603) 672-7230	Simplifies compliance with Title III of the EPA's SARA regulations by producing required Tier reports for all chemicals, including those contained in mixtures.
VOC	AV Systems, Inc. (313) 662-0355	A versatile air permit and emissions data tracking module, with a range of reports to assist with permit requests and state and federal emissions reporting requirements.
WASTE	AV Systems, Inc. (313) 662-0355	Is a container and manifest module that handles cradle to grave waste tracking, incorporating the RCRA biennial report and a multitude of management reports.
WASTE db	Envirogenics Inc., (800) 527-7213	Tracks waste materials and keeps historical disposal records by TSDF or transporter, types of material disposed of, work area generating the waste and/or cost of disposal.
WITS (Waste Inventory Tracking System)	BSI Systems, Inc. (619) 673-8420	Makes compliance with EPA and DOT hazardous waste regulations easy by guiding applicable manifesting, labeling and record-keeping requirements for hazardous waste.

Table 5. Information Technology

SYSTEM	ACCESS INFORMATION	PURPOSE / COMMENTS
ATTIC	Computer: (301) 670-3808 Settings: 8-N-1-F	It provides the most up-to-date information available on alternative technologies for hazardous waste treatment. It also contains a listing of the experts in the field, publications etc.
AERB	Computer: (919) 541-1325 Settings: 8-N-1-1200/2400	It contains numerous air models used in the field for both regulatory compliance as well as for general purposes.
Air Docket	Helpline: (919) 541-0888	Contains information used in the rule making and decisions under the Clean Air Act.
Air RISC	Helpline: (919) 541-0850	This system offers information to state and local governmental agencies that are developing or have implemented programs to control toxic air pollutants.
CEAM	Computers: (706) 546-3402 Settings: 8-N-1-F-1200/2400/9600	Supports environmental risk-based decisions concerning protection of air, water, and soil
NATICH	Helpline: (919) 541-0850	It contains all the materials gathered by the clearinghouse. Material is indexed according to agency, pollutant, emission source and research information.
OAQPS TNN	Computer: (919) 541-5742 Helpline: (919) 541-5384 Settings: 8-N-1-F	A very comprehensive air pollution information bulletin board
PIES	Computer: (703) 506-1025 Settings: 8-N-1-F Helpline: (202) 260-7548	This system includes e-mail features, contacts directory, documentation, pollution prevention case-studies, legislation and other things.

NOXSO SO_2/NO_x Flue Gas Treatment Process Proof-of-Concept Test

W. T. Ma and J. L. Haslbeck

NOXSO Corporation, P.O. Box 469, Library, PA 15129

The NOXSO process uses a regenerable sorbent that removes SO_2 and NO_x simultaneously from flue gas. The sorbent is a γ alumina bead impregnated with sodium carbonate. The process was successfully tested at three different scales, equivalent to 0.017, 0.06 and 0.75 MW of flue gas generated from a coal-fired power plant. The Proof-of-Concept (POC) Test is the last test prior to a full-scale demonstration. A slip stream of flue gas equivalent to a 5 MW coal-fired power plant was used for the POC test. This paper summarizes the NOXSO POC process and its current test results.

INTRODUCTION

The NOXSO process is a dry, regenerable flue gas treatment system that simultaneously removes 90% of the SO_2 and 70–90% of the NO_x from flue gas generated from the combustion of coal. The process has been successfully tested at a small scale (0.017 MW) on high sulfur coal (2.5%) at the TVA Shawnee Steam Plant. The test results are contained in two U.S. Department of Energy reports [*1*, *2*].

Tests of a NOXSO Process Development Unit (PDU, 0.75 MW) were conducted at the Pittsburgh Energy Technology Center (PETC) under a cooperative research agreement between NOXSO and the Department of Energy (DOE). Testing in the adsorber was done by continuously feeding a batch of sorbent into a fluidized bed adsorber and collecting the spent sorbent from the adsorber overflow. Regeneration took place in a separate batch reactor. The test results were reported by Yeh *et al.* in 1987 [*3*], and by Haslbeck *et al.* in 1988 [*4*].

A Life-Cycle Test Unit (LCTU, 0.06 MW) was built at PETC in 1988 to test the NOXSO process in an integrated, continuous-operation mode. The LCTU test program was designed to determine long-term effects of the process on the sorbent reactivity and attrition properties. Three lock hoppers were used to transport sorbent from the regenerator, through the sorbent cooler, through the adsorber, then to the sorbent heater. In order to conserve the sorbent temperature, the hot sorbent (621°C) overflow to the moving bed regenerator from the sorbent heater was fed by gravity. Due to the direct sorbent flow between sorbent heater and regenerator, nitrogen was used to inert the sorbent heater at all times. The test results were published by Ma *et al.* in 1991 [*6*], and by Yeh *et al.* in 1992 [*7*].

The Proof-of-Concept (POC) Test is the last test prior to the full-scale demonstration. The test will collect all the design information for the full-scale NOXSO plant, especially in the area of process safety, process control, sorbent activity, sorbent attrition, heat recovery, and regeneration off-gas composition. The POC plant (5 MW) is located at Ohio Edison's Toronto Station in Toronto, Ohio. Flue gas was first introduced to the plant on November 23, 1991. The flue gas test will continue until September 1993. The current test results and process performance are presented in this report.

PROCESS DESCRIPTION

The NOXSO POC at Toronto, Ohio is shown schematically in Figure 1. A slip stream of flue gas (equivalent to 5 MW coal-fired power) is extracted from either Boiler #10 or #11 of Ohio Edison's Toronto Power Plant. The flue gas first flows through a 250 HP, I.D. fan, then is cooled to 160°C (320°F) by spraying water into the flue gas ducts. The cooled flue gas then enters a 3.2-m (126″) diameter single-stage fluid-bed adsorber. The NOXSO sorbent, which is 1.6 mm (1/16″) diameter γ alumina beads impregnated with 5.2 wt% Na, in the adsorber removes the SO_2 and NO_x simultaneously from the flue gas. The cleaned flue gas mixes with the hot off-gas from the sorbent heater, then passes through the baghouse to remove all the attrited sorbent before the gas vents to the atmosphere through the power plant's stack. A cyclone is installed after the adsorber to recycle fines to the bed (50% efficient on 50 micron diameter particles).

The spent sorbent in the adsorber overflows into the dense-phase conveying system where 128.9 kPa (40 psig) air lifts the sorbent 24.4-m (80 ft) high to the top of the sorbent heater, which is a 2.34-m (92″) diameter, 3-stage, fluid-bed vessel. A natural-gas-fired air heater supplies the hot air to heat the sorbent in the sorbent heater to 621°C. During the sorbent heating process, all the adsorbed NO_x and a small portion of adsorbed SO_2 desorbs from the sorbent. The hot sorbent heater off-gas can either be directly vented to the atmosphere through the power plant's stack or can be mixed with the cleaned flue gas to enter the baghouse. Mixing with the flue gas is needed to protect the baghouse from exceeding the high temperature limit of the bags. No cyclone is installed on the top of the sorbent heater.

The hot sorbent in the bottom-bed sorbent heater underflows into a J-valve (hereafter called top J-valve). Either nitrogen or steam can be used to carry the sorbent through the J-valve into the 1.22-m (48″) diameter moving-bed regenerator. Natural gas is the first regenerant to treat the hot sorbent in the regenerator; the sulfate on the sorbent is reduced to SO_2, H_2S, and sulfide. Steam is then used to drive all the sulfide out of the sorbent. The off-gas from the natural gas treater mixes with that from the steam treater before the combined stream

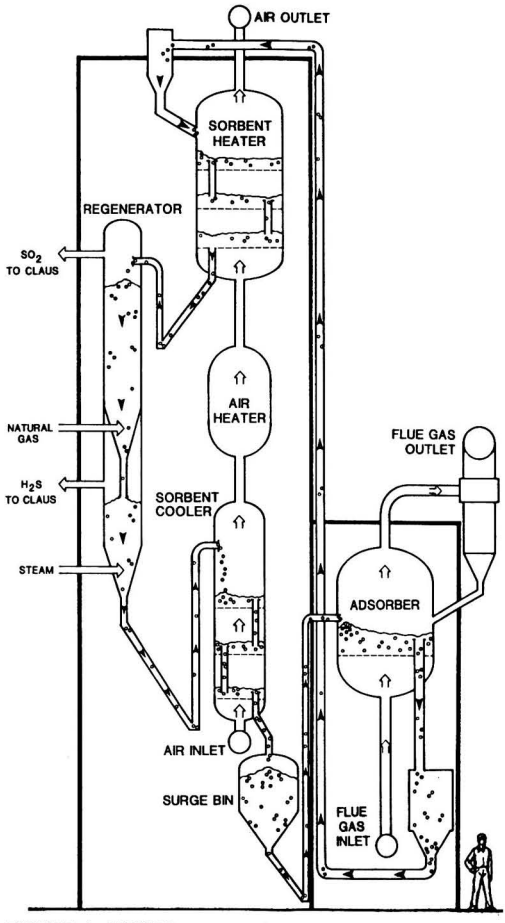

FIGURE 1. NOXSO process tower.

enters the incinerator, in which all the sulfur species are converted to SO_2.

The regenerated sorbent flows into a second J-valve (hereafter called middle J-valve because of its relative elevation to other J-valves) from which it enters the 1.73-m (68″) diameter, 3-stage fluid-bed cooler. A fan supplies ambient air to cool the sorbent. The heat of the regenerated sorbent is recovered by the cooling air which is then used as the combustion air in the air heater. The cool sorbent in the bottom bed of the cooler overflows into a 1.83-m (72″) diameter surge tank. A third J-valve (called bottom J-valve) is used to transport the sorbent from the surge tank to the adsorber.

The top and middle J-valves isolate the reducing section (regenerator) of the NOXSO plant from its oxidation section (heater and cooler train). The steam (for normal operation) or nitrogen (for start-up) enters the middle or top J-valve to carry the sorbent upward. Since the steam is introduced at the lowest point of the J-valve, which is also the highest pressure point between the two vessels, a steam barrier is therefore created to prevent the mixing of the reducing gas with the oxygen or vice versa. The bottom J-valve is operated with air to lift the sorbent from the surge tank to the adsorber.

Since the POC plant uses only a slip stream of flue gas from the power plant, the amount of NO_x evolved from the sorbent heater is too small to effect the NO_x thermal equilibrium inside the coal combustor. NO_x was not recycled to the coal combustor during the POC testing. However, the ability of a coal combustor to reduce excess NO_x introduced into the combustion chamber was proven in a series of simulated NO_x recycle tests. The simulated NO_x recycle tests were carried out in PETC's tunnel furnace and 227 kg/hr (500 lb/hr) pulverized coal combustor [*3*, *4*]. In order to obtain the NO_x recycle data to design the NOXSO full-scale demonstration plant in Niles, Ohio, a simulated NO_x recycle test program is being conducted in the Babcock and Wilcox (B&W) modular cyclone coal combustor in Alliance, Ohio, in parallel to the POC tests.

Table 1 Sorbent Properties

	Fresh	after 1500 flue gas hours
Sodium, wt%	5.2	5.2
Surface Area, m^2/g	250	175
Bulk Compact Density, g/cc	0.64	0.64
Crush Strength, kg	3.8	2.4–3.8
Porosity	0.65	0.65

PLANT PERFORMANCE AND SORBENT PROPERTIES

The POC plant began to treat flue gas on November 23, 1991, then was shut-down on December 21, 1991. A decision was made to replace all the 20-gauge fluid-bed distributor plates with 6.35 mm (1/4″) thick perforated plates. The plant was back on flue gas on March 23, 1992. Since then, only a few short shut-down periods were required to repair or install instruments. Generally speaking, the plant is trouble free and runs automatically with minimal operator intervention. The POC flue gas test is ongoing and will be completed in September 1993.

The sorbent has experienced more than 2400 hours on flue gas and 1200 hours of hot inert operation. The properties of fresh sorbent and the cycled sorbent are listed in Table 1. The major change in the properties of aged sorbent is surface area. The sorbent surface area drops from 250 m^2/g to 175 m^2/g after 1500 hours on flue gas. However, the trend plot of surface area (Figure 2) shows that the surface area is virtually stabilized at 175 m^2/g after 750 hours on flue gas.

The sorbent attrition rate was determined by plotting the cumulative makeup sorbent versus the cumulative operating hours, then applying the least-squares method to determine the best fit straight line through the experimental data. The slope of the line is equal to the attrition rate. Figure 3 shows the result which yields 1.59 kg/hr (3.5 lb/hr) attrition for the 3636.4 kg/hr (8000 lb/hr) sorbent circulation rate in the POC plant. The design attrition rate for the POC plant is 4 lb/hr, which is calculated according to 0.03%/hr attrition of the entire fluid-bed sorbent inventory.

TEST RESULTS AND DISCUSSION

The test program of the POC plant consists of parametric and duration tests. The parametric tests are statistically de-

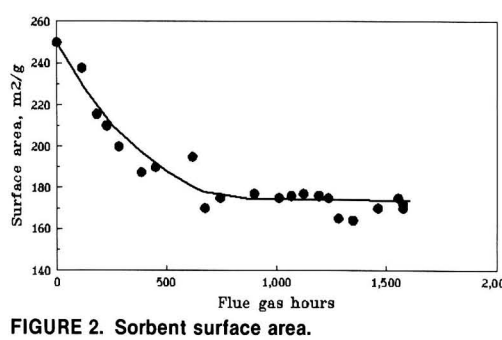

FIGURE 2. Sorbent surface area.

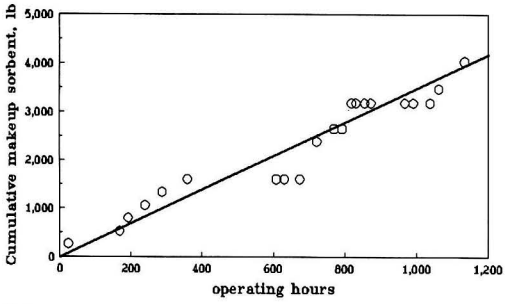

FIGURE 3. Sorbent attrition.

signed to obtain the optimal operating conditions for the subsequent duration test. Currently, parametric tests are being conducted.

NO_x and SO_2 Removal Fraction

The NO_x and SO_2 removal fraction is defined as follows:

$$\phi_i = 1 - \frac{y_{fi}}{y_{oi}} \tag{1}$$

where y_{oi} is the inlet concentration, y_{fi} is the outlet concentration, and subscript i stands for pollutants ($i=A$ for SO_2 and $i=B$ for NO_x). The amount of NO_x and SO_2 removed by the NOXSO sorbent is dependent on the temperature, sorbent properties, NO_x and SO_2 concentrations, flue gas flow rate, reaction time, etc. In an integrated NOXSO process, the sorbent is continuously circulating through adsorber and regenerator. Both NO_x and SO_2 removal fractions are further effected by the regeneration results. It is hard to isolate the effect of one variable on the removal fraction from others. To overcome this difficulty, an adsorption model is used in this report to analyze the data collected from the NOXSO POC plant. Based on the results of earlier small scale tests, an adsorption mechanism was proposed. A fluid-bed reactor model was then incorporated with the adsorption mechanism to develop the adsorber model. The POC test results were next used to determine the model parameters. A brief summary is given in the following to show the model and level of agreement between the predicted and actual results.

Several phenomena were observed during the earlier NOXSO adsorption tests:

1. The sorbent does not remove any NO_x unless there is SO_2 in the flue gas.
2. The sorbed NO_x will desorb from the sorbent if more SO_2 is fed into the reactor.
3. The spent sorbent, when heated to desorb all the NO_x but not treated with regenerants to remove sulfur, loses its NO_x removal ability.
4. The NO_x and SO_2 sorption reaction is NO_x sorption limited.

The following mechanism is proposed to explain these observations.

$$A + l_2 \underset{k1'}{\overset{k1}{\rightleftarrows}} Al_2 \tag{2}$$

$$Al_2 + 2B \underset{k2'}{\overset{k2}{\rightleftarrows}} B_2l_2 + A \tag{3}$$

$$Al_2 \xrightarrow{k3} Rl_2 \tag{4}$$

where A stands for SO_2, B for NO_x, l_2 for Na_2O, and Rl_2 for Na_2SO_4. Equation (2) shows that SO_2 first reacts with sorbent to form the NO_x sorption sites, Al_2. But the NO_x sorption sites have a limited life span, and will lose their NO_x activity to become Rl_2 as Eq. (4) shows. The Al_2 which reacts with NO_x forms B_2l_2 according to Eq. (3). The presence of excess SO_2 will reverse the reaction of Eq. (3) to desorb the NO_x from the sorbent. The reaction rate of Eq. (2) is the fastest according to the fourth observation.

Consider a chemisorption scheme with the following order of rate magnitude.

$$r_1 \gg r_2, r_3 \tag{5}$$

and

$$r_1 = k_1\left[Py_AC_{l_2} - \frac{1}{K_1}C_{Al_2}\right] \tag{6}$$

Since $k_1 \gg 1$ and r_1 is finite, then

$$Py_AC_{l_2} - \frac{1}{K_1}C_{Al_2} \approx 0 \tag{7}$$

$$C_{Al_2} = K_1Py_AC_{l_2} \tag{8}$$

where $K_1 = k_1/k_1'$, P is the gas pressure, y_A is the concentration fraction, and Cl_2 is the equivalent sorbent active sites in terms of Na_2O kmole/kg sorbent. Because the total number of Na_2O sites is constant, so

$$C_t = C_{l_2} + C_{Al_2} + C_{B_2l_2} + C_{Rl_2} + X_0C_t \tag{9}$$

where X_0 is the initial sorbent conversion factor, which is defined as

$$X_0 \equiv \frac{S_r}{3200 \cdot C_t} \tag{10}$$

where S_r is the sulfur content of the regenerated sorbent in wt%, C_t is the total number of Na_2O sites in kmole/kg sorbent, and 3200 is the sulfur molecular weight times 100. Define the sorbent conversion factor as follows:

$$X = X_0 + \frac{C_{Al_2} + C_{B_2l_2} + C_{Rl_2}}{C_t} \tag{11}$$

The rate of sorbent conversion factor will be

$$\frac{dX}{dt} = \frac{1}{C_t}\left\{\frac{dC_{Al_2}}{dt} + \frac{dC_{B_2l_2}}{dt} + \frac{dC_{Rl_2}}{dt}\right\} \tag{12}$$

In order to apply the adsorption mechanism to a fluid-bed adsorber model, a time averaged sorbent conversion factor is used in this report. To simplify the mathematics, mean gas concentrations were introduced into Eq. (12) and then integrated to obtain the time function for the sorbent conversion factor. A time average scheme was applied next to give the averaged sorbent conversion factor as follows:

$$\overline{X} = 1 - \frac{F}{E} - \frac{\frac{D}{E}\left(1 - X_0 - \frac{F}{E}\right)(1 - e^{-E/D\,t})}{t} \tag{13}$$

where

$$D = 1 + K_1 P\overline{y_A}$$

$$E = \left(k_2 P^2 \overline{y_B}^2 + k_3 + \frac{k_2}{K_1 K_2}\right) K_1 P \overline{y_A}$$

$$F = \frac{k_2}{K_2} P \overline{y_A}\left[1 - \frac{S_a}{3200 C_t}\right] \qquad (14)$$

S_a = sulfur content of spent sorbent, wt%
y_B = the mean gas fraction of NO_x
y_A = the mean gas fraction of SO_2
t = the sorbent residence time, sec.

Incorporating Eq. (13) with the fluid-bed model of gas phase plug-flow and solid phase mixed-flow assumptions results in the adsorber model equation, which is given by

$$\frac{F_g}{C_t F_s}\left[\phi_A y_{0_A} + \frac{\phi_B}{2} y_{0_B}\right] = \left(1 - X_0 - \frac{F}{E}\right)(1 - e^{-E/D\ W/F_s}) \qquad (15)$$

where F_g is the flue gas flow rate, kmole/sec
F_s is the sorbent flow rate, kg/sec
W is the adsorber sorbent inventory, kg.

Before applying Eq. (15) to correlate the POC data, the value of C_t and mean values of y_A and y_B across the fluid-bed must be defined. It can be proved that the mean concentrations for the first order and second order reaction in a plug-flow reactor can be expressed by their logarithmetic mean as follows:

$$\text{1st order } \overline{y_A} = \frac{y_{f_A} - y_{0_A}}{\ln\left[\frac{y_{f_A}}{y_{0_A}}\right]} = \frac{-y_{0_A}\phi_A}{\ln(1-\phi_A)}$$

$$\text{2nd order } \overline{y_B} = y_{0_B} y_{f_B} \cdot \frac{\ln\left(\frac{y_{f_B}}{y_{0_B}}\right)}{y_{f_B} - y_{0_B}} = \frac{-y_{0_B}(1-\phi_B)\ln(1-\phi_B)}{\phi_B} \qquad (16)$$

Since the alumina substrate alone also adsorbs NO_x and SO_2 from flue gas, the stoichiometric ratio of the reactant gas to the active sorbent material must include the contribution from both sodium and alumina. The active site which is expressed in terms of Na_2O concentration is determined in the NOXSO laboratory by testing the sorbent substrate with or without sodium at different temperatures. The result is expressed by

$$C_t = \frac{1}{2}\left[\frac{Na}{2300}\right] + \frac{0.6 - 0.0075 T_a}{1000} \qquad (17)$$

where Na is the sorbent sodium content, wt %
T_a is the adsorber temperature, °C
2300, is the sodium molecular weights times 100

The second term in the right hand side of Eq. (17) is the equivalent Na_2O site contributed by alumina substrate. The alumina contribution decreases when the temperature increases. With Eq. (17), the left hand side of Eq. (15) becomes a measurable quantity, which is called the measured sorbent conversion. The right hand side of Eq. (15) is called the estimated sorbent conversion, which can be calculated from the modal parameter and mean gas concentrations. To obtain the estimated sorbent conversion, the terms D, E, and F in Eq. (15) must be replaced with the mean gas concentrations expressed in Eq. (14) and (16). This results in an equation with four unknowns, i.e. K_1, K_2, k_2 and k_3. The POC data were then used to determine these unknowns.

The best values for K_1, K_2, k_2 and k_3 are determined as follows:

1). Assume K_1, K_2, k_2, k_3 values.
2). Calculate the estimated sorbent conversion for each POC data point.
3). Obtain the measured sorbent conversion for each POC data point.
4). Calculate the standard deviation between the estimated and measured sorbent conversion according to Eq. (18).

$$\sigma = \sqrt{\frac{1}{n}\sum_{i=1}^{n}(X_i - X_{m_i})^2} \qquad (18)$$

where σ is the standard deviation, n is the number of data point, X_i is the estimated value, and X_{mi} is the measured value.
5). Repeat steps 1) to 4) until a lowest σ is found.

The final values for K_1, K_2, k_2 and k_3 obtained from 71 data points are given below

$$K_1 = 2000 \quad K_2 = 1.2 \quad k_2 = 5.8 \quad k_3 = 0.0012 \qquad (19)$$

with the corresponding standard deviation = 0.087. The relative magnitude of K_1, K_2, k_2 and k_3 confirms the proposed chemsorption scheme, $r_1 \gg r_2$ and r_3. Figure 4 shows the comparison between the measured and calculated sorbent conversion for the POC tests at different temperatures (from 153 to 180°C with the averaged temperature equals to 167.3°C). The evenly distributed data points shown in Figure 4 indicates that the temperature dependence was accounted for by the adsorber model. Since the sorption sites contributed by alumina substrate is the only temperature dependent variable of the model, it is concluded that the temperature dependence of NO_x and SO_2 sorption on NOXSO sorbent is mainly due to the alumina substrate. The agreement between the measured and estimated sorbent conversion as shown in Figure 4 encourages the use of the model to design other NOXSO plants. The design equation is obtained by rewriting Eq. (15) into the following form:

$$W = -\frac{DF_s}{E}\ln\left[1 - \frac{\frac{F_g}{C_t F_s}\left(\phi_A y_{O_A} + \frac{\phi_B}{2} y_{O_B}\right)}{1 - X_0 - \frac{F}{E}}\right] \qquad (20)$$

Please note that Eq. (20) contains both NO_x and SO_2 removal fractions. Different combinations of NO_x and SO_2 removal fractions may end up yielding the same sorbent inventory. However, the application of Eq. (20) to design does not present any difficulties. The y_{OA}, y_{OB} and F_g are fixed by the flue gas of the power plant. With the required SO_2 removal fraction, F_s is determined by the gas-solid sulfur balance. A series of W are next calculated from variously assumed ϕ_B. The criteria of process economy is used to determine the best sorbent inventory and the corresponding NO_x removal fraction. The

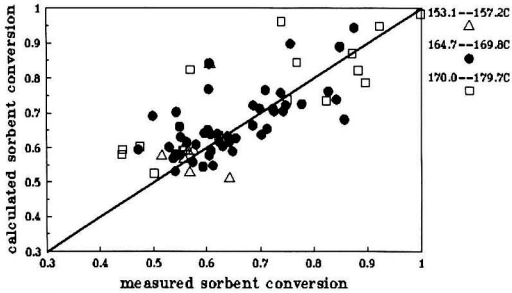

FIGURE 4. Spent-sorbent conversion of POC tests.

relationship between the process economy and sorbent inventory will be discussed at the end of this section.

Since the NOXSO process is limited by the NO_x removal fraction, it is important to understand various effects on the NO_x removal fraction. To assist the study, Eq. (15) is recast into NO_x removal fraction as shown in the following:

$$\phi_B = 2\left(\frac{y_{O_A}}{y_{O_B}}\right)\left[\chi\left(1-\frac{1-\frac{\phi_A}{\chi}}{\alpha}\right)(1-e^{-k_2\alpha/\beta\tau_s}) - \phi_A\right] \quad (21)$$

where χ is the ratio of sorbent active site to SO_2 feed rate, which is defined as

$$\chi = \frac{C_t(1-X_0)F_s}{y_{O_A}F_g} \quad (22)$$

$$\alpha = 1 + K_1K_2\frac{k_3}{k_2} + K_1K_2P^2\overline{y_B}^2$$

$$\beta = K_1K_2 - \frac{K_2\ln(1-\phi_A)}{Py_{O_A}\phi_A}$$

$$\tau_s = \frac{W}{F_s} \quad (23)$$

A flue gas of 2500 ppm SO_2 and 91% SO_2 removal requirement was used with Eq. (21) to calculate the NO_x removal fraction at different active-site to SO_2-feed ratio. The plots of ϕ_B versus χ were then prepared for different y_{OA}/y_{OB} at different sorbent residence times. The results are shown in Figure 5, which indicates that NO_x removal fraction can be improved by increasing the active-site/SO_2-feed ratio, the inlet SO_2/NO_x ratio, and the sorbent residence time in the adsorber. It should be pointed out that earlier NOXSO tests showed that using a lower adsorption temperature or a completely regenerated sorbent also improves the NO_x removal fraction. Both the temperature and regeneration effects are included by the use of χ, of which C_t is the function of adsorption temperature and X_0 is related to the sulfur content of regenerated sorbent. Lower adsorption temperature and completely regenerated sorbent provide more active sites, which gives a higher χ value. The increase of χ value yields a higher NO_x removal fraction.

The reason for improving the NO_x removal fraction by increasing SO_2/NO_x ratio as shown in Figure 5 is discussed next. Equation (1) describes that more SO_2 will provide more NO_x sorption sites. But Eq. (2) says higher SO_2 concentration will reverse the NO_x sorption. Since the SO_2 concentration of Figure 5 is fixed at 2500 ppm, the increase of SO_2/NO_x ratio decreases the NO_x concentration. Earlier NOXSO tests also showed that the NO_x removal fraction is decreased by increasing the NO_x concentration. The improvement of NO_x removal fraction by

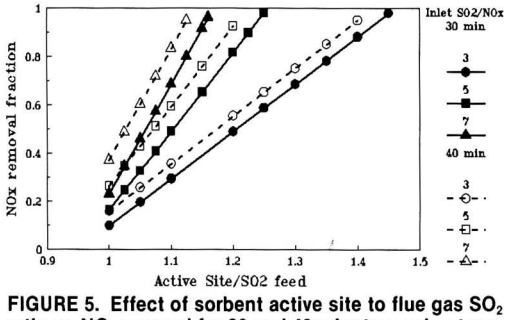

FIGURE 5. Effect of sorbent active site to flue gas SO_2 ratio on NO_x removal for 30 and 40 minutes sorbent residence time.

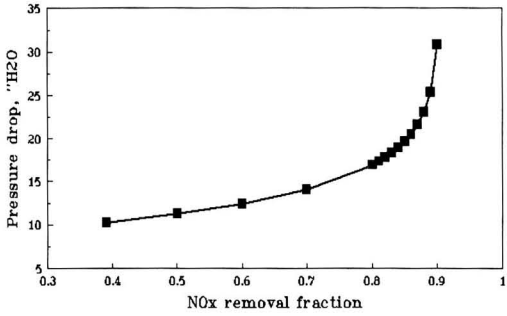

FIGURE 6. Adsorber grid plus bed pressure drop versus NO_x removal efficiency.

increasing SO_2/NO_x ratio is more likely caused by a lower NO_x concentration. It should be emphasized that the sorbent has to contain excess SO_2 sorption sites (i.e., $\chi > 1$) in order to improve the NO_x removal fraction.

The significance of individual effects on NO_x removal fraction can also be judged by comparing the NO_x removal fraction as shown in Figure 5. Take 30-minute sorbent residence time and inlet $SO_2/NO_x = 3$, for example. Increasing the active site/SO_2 feed ratio from 1 to 1.1 results in a 0.2 increase of NO_x removal fraction; while a 33% increase in sorbent residence time gives only a 0.05 improvement. Furthermore, the increase of sorbent residence time always gives a higher pressure drop in the fluid-bed adsorber. As a result, the flue gas fan has to consume more power to deliver the flue gas through the adsorber. The improvement of NO_x removal fraction is not a linear function of sorbent residence time. Figure 6 is the result of a case study to demonstrate the relationship between NO_x removal fraction and the adsorber pressure drop. The case study used $\chi = 1.39$, and inlet $SO_2/NO_x = 2.86$. The pressure drop shown in Figure 6 is the total pressure drop across the adsorber, of which 23% belongs to the gas distributor. Figure 6 shows that the pressure drop is linearly increased with the increasing of NO_x removal fraction until 0.7. Once the NO_x removal fraction exceeds 0.8, the pressure drop increases rapidly. The desired NO_x removal fraction for this case study is 0.8 and the corresponding sorbent residence time is 28.7 minutes.

NO_x and Sulfur Regeneration

The amount of NO_x removed in the adsorber was found to completely evolve from sorbent in the sorbent heater. The same NO_x balance result was also found during the LCTU test conducted at PETC. However, the LCTU test used an inert sorbent heater, the evolved NO_x remains intact, mainly in NO form. The POC sorbent heater contains about 17% oxygen, therefore, most evolved NO becomes NO_2 at the POC. The presence of NO_2 in the sorbent heater off-gas may effect the efficiency of NO_x destruction when recycling the NO_x back to the coal combustor. However, the simulated NO_x recycle tests conducted in B&W's modular cyclone coal-combustor shows the NO_x destruction is independent of the form of the recycled NO_x. Moreover, the B&W tests agree with the earlier PETC tunnel furnace test results.

The regeneration temperature was controlled by the bottom bed temperature of the 3-stage sorbent heater. Figure 7 shows that the sulfur content of the regenerated and spent sorbent at different bottom-bed temperatures of the sorbent heater. The sulfur content increases linearly with decreasing temperature. Also the sulfur difference between the spent and regenerated sorbent seems to be a constant. However, a lower regeneration temperature is preferred in terms of energy conservation and sorbent life. For the sake of process safety, the

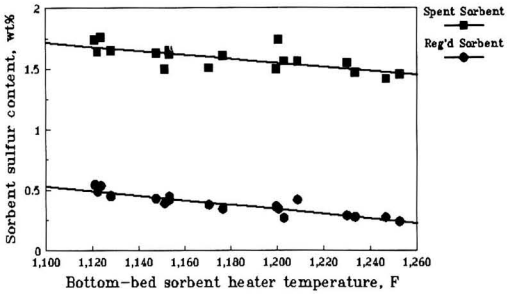

FIGURE 7. Sorbent sulfur content versus bottom-bed sorbent heater temperature.

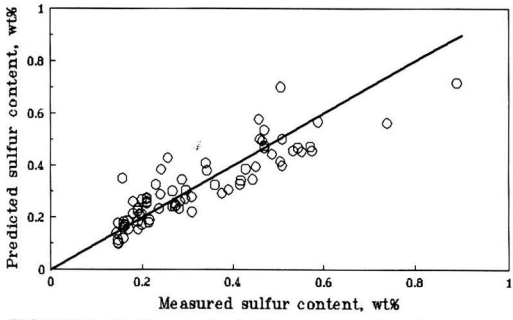

FIGURE 8. Sulfur content of regenerated sorbent.

bottom bed temperature of sorbent heater is controlled at 621°C (1150°F). Since the auto ignition temperature of natural gas is 602°C (1116°F), any natural gas which slips into the sorbent heater due to the process upset will burn out by itself.

To determine the rate of sulfur regeneration for spent sorbent, an *i*th order rate equation was used to fit the POC test data. The rate equation has the following form.

$$\frac{dS}{dt_r} = -KS^i \tag{24}$$

where S is the sorbent sulfur content, wt% and t_r is the regeneration time, min. Integrating Eq. (24) gives

$$\begin{aligned} S_r^{1-i} &= S_a^{1-i} + (i-1)Kt_r \quad \text{for } i \neq 1 \\ \ln \frac{S_a}{S_r} &= Kt_r \qquad\qquad\quad \text{for } i = 1 \end{aligned} \tag{25}$$

where S_a and S_r are the sulfur content of the spent and regenerated sorbent, respectively. The Arrhenius' law is inserted into Eq. (25) to assess the temperature effect on sulfur regeneration. The final equations are given by

$$\begin{aligned} S_r^{1-i} &= S_a^{1-i} + (i-1)K_0 e^{-E/RT} t_r \quad \text{for } i \neq 1 \\ \ln \frac{S_a}{S_r} &= K_0 e^{-E/RT} t_r \qquad\qquad\quad \text{for } i = 1 \end{aligned} \tag{26}$$

The measured S_a and S_r of POC test data were used to determine the K_0 and E/R for different i values of Eq. (26). The resulting K_0 and E/R were then used to calculate the standard deviation between the measured S_r and that estimated from Eq. (26) according to Eq. (18). The results obtained from 79 data points are listed in Table 2.

Table 2 The Standard Deviation of S_r for Rate of Regeneration, Equation (26)

i	0	0.2	0.4	0.5	0.6	0.8	1.0	1.5	2.0
σ	.159	.099	.073	.072	.076	.091	.107	.135	.148

Table 2 shows the best i value is equal to 0.5. Equation (26) is further reduced to

$$\sqrt{S_r} = \sqrt{S_a} - \frac{1}{2}[0.2971 e^{-2580/T}] t_r \tag{27}$$

where T is the bottom-bed absolute temperature of the sorbent heater, °K. Figure 8 shows the comparison between the predicted and measured sulfur content of the regenerated sorbent. The agreement between the predicted and measured results encourages the use of Eq. (27) to size the regenerator for future NOXSO plants.

CONCLUSION

The NOXSO POC plant has been operated for more than 2400 flue gas hours, and the operation will be continued until September 1993. The test results collected until now agree with the findings obtained in the earlier small scale PETC tests. The POC data was successfully correlated with adsorption and regeneration models. The resulting correlations can be used to size the adsorber and regenerator for other NOXSO processes. The adsorber model has further been used to study the individual effect on the NO_x removal fraction. It is concluded that the most effective way to improve the NO_x removal fraction is to increase the ratio of sorbent active sites to SO_2 feed rate.

LITERATURE CITED

1. Haslbeck, J. L., C. J. Wang, H. P. Tseng, and J. D. Tucker, "Evaluation of the NOXSO Combined NO_x/SO_2 Flue Gas Treatment Process," NOXSO Corporation Contract Report submitted to U.S. DOE, Report No. DOE/FE/60148-T5 (Nov. 1984).
2. Haslbeck, J. L., L. G. Neal, C. P. Perng, and C. J. Wang, "Evaluation of the NOXSO Combined NO_x/SO_2 Flue Gas Treatment Process," NOXSO Corporation Contract Report submitted to U.S. DOE, Report No. DOE/PC/73225-T2 (April, 1988).
3. Yeh, J. T., C. J. Drummond, J. L. Haslbeck, and L. G. Neal, "The NOXSO Process: Simultaneous Removal SO_2 and NO_x from Flue Gas," presented at the Houston, Texas Spring National Meeting of the AIChE (March 29-April 2, 1987).
4. Haslbeck, J. L., W. T. Ma, and L. G. Neal, "A Pilot-Scale Test of the NOXSO Flue Gas Treatment Process," NOXSO Corporation Cooperative Agreement submitted to U.S. DOE, Contract No. DE-FC22-85PC81503 (June, 1988).
5. Haslbeck, J. L. and L. G. Neal, "The NOXSO Process Development: An Update," The Ninth EPA-EPRI Symposium on Flue Gas Desulfurization, Cincinnati, Ohio (June 4-7, 1985).
6. Ma, W. T., J. L. Haslbeck, L. G. Neal, and J. T. Yeh, "Life Cycle Test of the NOXSO SO_2 and NO_x Flue Gas Treatment Process: Process Modeling," *Separations Technology*, **1**, pp. 195-204, 1991.
7. Yeh, J. T., W. T. Ma, H. W. Pennline, J. L. Haslbeck, J. I. Joubert, and F. N. Gromicko, "Integrated Testing of the NOXSO Process: Simultaneous Removal of SO_2 and NO_x from Flue Gas," *Chemical Engineering Communication*, **114**, pp. 65-88, 1992.

Implementing the New Water Quality Standards—Fitting the Puzzle Together

Edmund A. Kobylinski, Gary L. Hunter, and Elizabeth A. Quinlan
Black & Veatch, 8400 Ward Parkway, P.O. Box 8405, Kansas City, MO 64114

INTRODUCTION

The Clean Water Act gave EPA the authority to implement the National Pollutant Discharge Elimination System (NPDES). Under the NPDES program, industries and municipalities have to obtain a permit to discharge wastewaters into waters of the United States. This program initially targeted direct discharges of untreated wastes. Since its inception, the NPDES program has been evolving. As a result of this evolution, EPA has developed water quality standards designed to keep our lakes and rivers suitable for fishing and swimming.

The Water Quality Standards were published several years ago. EPA has been encouraging each State with primacy to incorporate water quality standards into their permitting process. Thirty-one states have some form of approved water quality standards. The remaining states were directed by EPA in December 1992 to implement their water quality standards program immediately, or to use EPA's national program. As NPDES permits are renewed, the new permits will include water quality standards.

The water quality standards consist of two separate criteria. The first of these criterion is aquatic toxicity testing. Basically, the aquatic testing program uses selected species of aquatic life to determine whether the wastewater exhibits toxicity. The second criterion is chemical-specific numerical limits or water quality standards. These numerical limits are based on toxicological research data using one chemical in solution. The aquatic toxicity tests are designed to determine whether chemical mixtures act to enhance the toxicity of substances present at concentrations below the limits set by water quality standards, or whether other chemicals in the water cause toxicity.

As far as the NPDES program is concerned, every permittee must comply with both criteria. Many industries have found that they can comply with one of the two standards, but fail the other. For example, the effluent can comply with the numerical standards, but may have a high salt content (composed of non-hazardous materials) and fail the aquatic toxicity test.

Industries that discharge through a publicly-owned treatment works (POTW) are not required to have an NPDES permit. The POTW is designed to remove suspended solids and biochemical oxygen demand. Therefore, to maintain compliance with its discharge permit, the POTW's pretreatment program requires industry to limit the discharge of metals and toxic organic compounds. By limiting the discharge of these materials, the POTW is protected from process upsets, pass-through, and sludge contamination.

Since the water quality standards affecting the POTW's NPDES permit limits, the POTW, in turn limits, the concentration or mass of specific pollutants discharged by industry. Therefore, even the industries discharging through a POTW can be faced with stringent discharge limits.

HOW PERMIT LIMITS ARE DERIVED

How are NPDES permit limits developed? Will all of the chemicals listed in the water quality standards appear in my permit? Why are my permit limits different from similar industries in other areas?

These and similar questions are often voiced as a permit is reviewed. Basically an NPDES permit is site-specific. Permit limits depend on the size and the water quality of the receiving stream use and on its use. In general, the smaller the receiving stream, the stricter the permit limits.

There has been a fundamental shift in how permit limits are being derived. Until recently, Best Available Technology (BAT) was used to determine allowable discharges of pollutants into receiving waters of the United States. Now however, water quality standards must be used to derive permit limits. In other words, permit limits must be such that water quality standards will not be violated.

Basic Concept

The basic concept of water quality-based permit limits is fairly simple. Knowing flow rates and concentrations of pollutants for both the receiving water and the effluent stream, the resultant concentration after mixing can be calculated from Eq. (1):

$$C = (QeCe + QsCs)/(Qe + Qs) \quad (1)$$

where Qe = volume discharge of effluent,
Qs = volume discharge of the receiving stream (or the amount available for mixing)
Ce = concentration of a constituent in the effluent
Cs = concentration of a constituent in the receiving stream
C = resultant concentration of a constituent in the receiving stream after mixing.

Remember, the water quality standards are in-stream concentration limits.

The maximum value of C should not exceed the limit established in the water quality standard. Therefore, the allowable value of Ce could be calculated by solving Equation 1 after setting C equal to the water quality standard. However, while the basic concept is simple, the actual calculations must take into account many other factors and the procedure can become quite complex. These other factors include different types of water quality criteria, e.g., chronic or acute, variations in effluent quality, appropriate dilution factors, and the influence of multiple discharges into the same receiving waters. The Technical Support Document (TSD) for Water Quality-based Toxics Control [*1*] provides permit writers with guidance on how permit limits should be derived. The discussion on permit limits in this paper follows the EPA guidance.

Steps in the Process

Several steps must be taken to develop permit limits, including the following:

- Characterize the effluent in terms of average and maximum concentrations and variability.
- Identify the pollutants of concern, those that have a reasonable potential to exceed the limits set by water quality standards.
- Determine the appropriate dilution factors.
- Calculate the wasteload allocation.
- Calculate permit limits.

Each of these steps is discussed in subsequent sections.

Pollutants of Concern

Information on the concentrations and variability of pollutants in industry's effluent is used to determine whether specific constituents have a reasonable potential to exceed the limits set by water quality standards. If a reasonable potential exists, a permit limit must be derived for that constituent. If sufficient effluent data is available, the potential to exceed these limits can be calculated. According to EPA guidelines,

> "... a permittee has a reasonable potential to exceed a water quality standard if it cannot be demonstrated with a high confidence level that the upper bound of the lognormal distribution of effluent concentrations is below the receiving water criteria at specified low-flow conditions."

The TSD describes the steps to be followed to determine if reasonable potential exists. The procedure is based on the assumption that the range of concentrations of a constituent in an effluent follows a lognormal distribution such as shown on Figure 1. Using this distribution and the average and maximum values measured in the effluent, a probable high value is calculated. This value is used with the appropriate dilution to project a maximum receiving water concentration. If the concentration in the receiving water is greater than the water quality standard, there is a reasonable potential to exceed water quality standards.

Mixing Zone Analysis

A mixing zone analysis is conducted to determine the appropriate dilution to use in calculating the projected concentration in receiving waters. The mixing zone analysis must consider the design periods for different types of receiving waters and also the method by which dilution and the size of the mixing zone is calculated. Dilutions are usually calculated for low flow or quiescent conditions.

For a river or stream, the 7Q10 flow is often used to calculate dilution. This is the low flow that would occur for a 7 day interval once every ten years. The 7Q10 flow is appropriate to use with chronic water quality standards. EPA suggests using

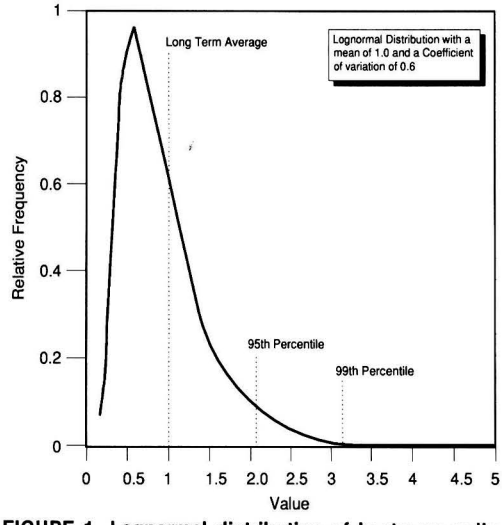

FIGURE 1. Lognormal distribution of in-stream pollutant concentrations.

the 1Q10 (lowest daily flow within a ten-year interval) when calculating dilutions for the acute water quality limits. For lakes and reservoirs, water levels and seasonal changes in wind-induced circulation should be considered. In estuaries, density stratification, river flow, and tidal currents all affect the dilution. The specific conditions to be used in the calculations are normally dictated by State policy and can vary greatly. However, conditions are usually selected to be conservative.

Dilutions can be determined through calculations, by modeling, or through field measurements. The size of the mixing zone will be specified in the NPDES permit. It is important to ensure that the size of the mixing zone is consistent with the method by which the dilution was determined. For river discharges it is common for a portion of the flow (at 7Q10) to be allocated for mixing. In estuaries, dilution is commonly calculated using a plume model.

Wasteload Allocation

After the appropriate dilution has been determined, the wasteload allocation can be established. The wasteload allocation is the amount of a constituent that can be discharged without violating water quality standards. The wasteload allocation is equivalent to Ce in the first equation and is determined from the Eq. (2):

$$WLA = [(WQC(Qe+Qs)) - QsCs]/Qe \qquad (2)$$

where WQC = water quality standard, either acute or chronic.

Wasteload allocations can be calculated for either steady state or dynamic conditions. Normally, steady state conditions are used. Under these conditions constant values are used for both the effluent concentration and the receiving water conditions. With a dynamic model the inputs would vary by using either a time series of data or probability distributions. A dynamic model requires more data, but reduces the duplication of conservative assumptions and, therefore, may result in higher WLA.

Wasteload allocations for a specific facility can differ from the example above when there are multiple dischargers into the receiving stream or when a total maximum daily load (TMDL) has been established for a receiving water. In this case the wasteload allocation for the receiving stream must be

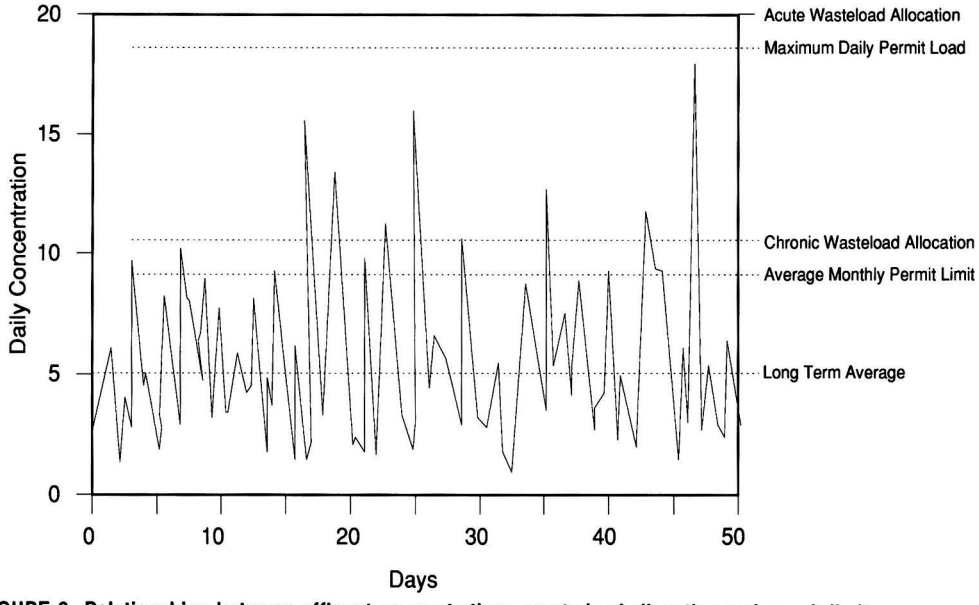

FIGURE 2. Relationships between effluent concentrations, waste load allocation and permit limits.

divided among all dischargers. Several approaches can be used to allocate the wasteload among dischargers, and several of these are discussed in the TSD.

Develop Permit Limits

The final step in the process of developing permit limits is to convert the wasteload allocations into actual numeric limits. This step again takes into account the variability of effluent quality expressed by the lognormal distribution discussed earlier. First, the long-term average effluent concentration (LTA) is calculated based on the wasteload allocation, the coefficient of variation determined for the effluent, and the probability basis of the calculation (usually either 99 or 95 percent). This calculation, in effect, defines the long-term average concentration needed in the effluent to ensure that the maximum concentration, or wasteload allocation, is not exceeded. The long-term average is calculated for both acute and chronic conditions and the lower of the two values is selected as the controlling number.

Next the long-term average is converted to a maximum daily limit (MDL) and an average monthly limit (AML). Again, this is based on a statistical relationship, or probability distribution, of effluent quality. The MDL and AML are then compared to BAT limits; the more stringent limits will apply. Finally, if the water quality-based limits are more stringent, the MDL and AML are converted to loads, such as pounds per day, and these become the permit limits.

The equations used to calculate the LTA, MDL and AML are given in Eqs. (3) and (4)

$$LTA_{a,c} = WLA_{a,c} \cdot e^{[0.5\sigma^2 - Z\sigma]}$$

$$LTA_c = WLA_c \cdot e^{[0.5\sigma_4^2 - Z\sigma_4]} \quad (3)$$

where $\sigma^2 = \ln(cv^2+1)$
$\sigma_4 = \ln(cv^2/4+1)$
$Z = 1.645$ for 95th Percentilé Probability Basis
$Z = 2.326$ for 99th Percentile Probability Basis

$$MDL = LTA \cdot e^{[Z\sigma - 0.5\sigma^2]}$$

$$AML = LTA \cdot e^{[Z\sigma_n - 0.5\sigma_n^2]} \quad (4)$$

where $\sigma^2 = \ln(cv^2+1)$
$\sigma_n^2 = \ln(cv^2/n+1)$
$Z = 1.645$ for 95th Percentile Probability Basis
$Z = 2.326$ for 99th Percentile Probability Basis

Figure 2 shows an example of a time series of daily effluent concentrations, along with the WLAs, permit limits, and long-term average. It is important to note that for a given WLA, the long-term average will increase as the coefficient of variation decreases. In effect, this means that, as the variability of effluent quality decreases (CV decreases), the long-term average can be closer to the WLA and still maintain a high probability of not exceeding water quality standards.

PERMITTEE RESPONSIBILITY

The permit holder is indirectly responsible for the development of permit limits. Even though the State or the EPA performs the statistical analysis to determine permit limits, the permittee supplies the water quality data. The preceding discussion has shown how the permit writers manipulate the data to determine numerical limits.

Implementation of water quality-based permit limits begins with data collection. At some point in time, your discharge permit will require monitoring for certain constituents. In the past, this data was not always used to develop permit limits; however, this has now changed. Under the current program that monitoring data "becomes the basis for numerical limits." Since the permittee collects that data, the permittee has indirect responsibility for the numerical limits.

Each permit holder should develop a formal quality assurance/quality control (QA/QC) plan. The QA/QC plan will define all sample collection procedures, proper sample preservation methods, chain of custody documentation, and analytical QC procedures. Why is the QA/QC plan so important? Since the in-stream water quality standards are in the μg/L range, and are at, or near, analytical detection limits, analytical error can have a large impact on the analytical results. It is therefore, critical for the permittee that the samples are not contaminated during collection, while being transported, or during analysis. Duplicate samples, trip blanks, and spiked samples should be submitted, in addition to standard QC sam-

ples used by the laboratory, to verify the reliability and accuracy of the analytical data. Probably the best approach for a permittee is to treat the monitoring requirements as if they were numerical limits. Improper sampling and analysis techniques will produce poor data. Poor data will usually result in more strict permit limits.

Another area to consider is process plant operations. Batch processing and process upsets invariably lead to slug discharges of materials. Batch discharges will, therefore, create scatter in the data, causing the coefficient of variation to increase and the permit limit to be reduced. It is to an industry's advantage to locate the slug discharges and install provisions for equalization. Equalization does not change the mass of material discharged, but it can significantly reduce variations in contaminant concentrations.

Spills and accidents will happen. A log should be kept to document such occurrences, particularly with respect to effluent quality. A single occurrence can significantly affect the outcome of the statistical analysis if the data set is small. For example, quarterly sampling results in only 20 data points over a 5-year period typical for NPDES permits. If a spill or other accident occurs which can be shown to have an impact on effluent quality, corrective action should be taken to prevent the recurrence of such accidents, and documented as justification for invalidating that data point.

As wastewater data is collected, an industry may discover a pollutant source that can be removed or at least reduced. An active, aggressive pollution prevention program can, in some cases, significantly reduce pollutant discharges without a large capital investment. It is necessary to understand why specific wastes are discharged, and to quantify these sources to effectively prevent pollution.

Industry should evaluate data as it is collected. Sampling frequency could be increased to dampen the effect of occasional anomalous data on statistical analysis, or in-plant projects may be initiated to reduce pollutant discharges. All in-plant modifications must be documented to explain why waste characteristics have changed. Without this documentation the permit writer may use data which no longer represent actual conditions. It is industry's responsibility to ensure that the data is representative and reliable. Under the water quality standards program consistency in effluent data will produce the least stringent discharge limits.

Why should an industry go to all this trouble to ensure the quality of its data and reduce data scatter? Even if equalization, QA/QC procedures, and source control measures are implemented, there is no guarantee that the industry will not be issued numerical water quality limits. However, the efforts will not be wasted, because they will help assure that the discharge limits are reasonable. This is particularly important in states that have strict anti-backsliding policies. Some state policies stipulate that once a numerical discharge limit has been set, it can never be relaxed. In this case, if poor or unreliable data is used to develop a permit, the numerical limit will be unreasonably low. Therefore, it is critical for industry to be aware of state policy regarding backsliding.

The NPDES permit program is changing. Industries need to understand the new policies and rules, or their NPDES discharge permits could include very strict numerical discharge limits. Compliance with these new numerical limits will be expensive and may involve implementation of advanced treatment technologies. Industry must realize that the water quality standards program begins with data collection and that this is the area where they must be proactive or suffer the consequences.

PRETREATMENT PROGRAM

The National Pretreatment Program was established to regulate the introduction of pollutants from nondomestic sources into POTWs. The goals of local pretreatment programs are to prevent interference with liquid wastewater or sludge treatment processes and to control pollutants that pass through the treatment processes. "Interference" is defined in 40 CFR 403 as a "discharge which, alone or in conjunction with a discharge or discharges from other sources, both:

(1) Inhibits or disrupts the POTW, its treatment processes or operations, or its sludge processes, use, or disposal.
(2) Therefore, is a cause of a violation of a requirement of the POTW's NPDES permit or other federal, state, or local regulations."

40 CFR 403.8 [2] defines who must develop industrial pretreatment programs. All treatment plants which receive flow from categorically regulated industries must develop a pretreatment program regardless of their size. POTWs which have a design flow greater than 18,930 m^3/day (5 mgd) and receive flow from industrial users must also develop a pretreatment program. The EPA regional administrator may require POTWs with design flows less than 18,930 m^3/day (5 mgd) to develop pretreatment programs if the industrial flow is causing treatment process upsets, violations of NPDES permits, or contamination of sludge.

NPDES permits contain specific information regarding the discharge of conventional and nonconventional pollutants. Nationwide, renewed permits are beginning to contain limits for the discharge of toxic pollutants regulated under state and federal water quality standards. NPDES permits may also contain regulations on pollutant removal efficiencies, as well as restrictions concerning sludge disposal. As limits for additional toxic pollutants are included in the NPDES permit and increasingly stricter regulations are imposed to govern sludge disposal, local industrial pretreatment limits may need to be modified.

Technically Based Local Limits

Local pretreatment limits regulate the discharge of specific substances to the POTW. The development of local limits requires a POTW to use site-specific data to identify pollutants of concern which might reasonably be expected to be discharged in quantities sufficient to interfere with operation of the POTW or to cause environmental problems. These site-specific data include treatment plant removal data, NPDES permit limits, sludge disposal permits and limits, POTW effluent toxicity data, and industrial discharge data. This site-specific data is used in a wastewater collection and treatment system mass balance, and the mass contribution from all domestic and industrial sources is used to develop allowable loadings on POTW headworks. Existing POTW performance data is used to work backwards from the NPDES permit limits to calculate a maximum allowable headworks loading. The maximum allowable headworks loading is then compared to the headworks loading from all domestic and industrial sources to ensure that the POTW can meet all permits and regulations.

EPA has developed a mass balance computer model called PRELIM [3] to assist regulatory authorities in developing allowable loadings on POTWs. Site-specific data can be entered into the model to develop either mass discharge limits for each individual user or uniform concentration limits. Mass proportion limits are developed to account for changing discharge flows from industries. Uniform concentration limits would require all industries to meet a specific concentration limit, regardless of the discharge volume.

If site-specific data is unavailable, the "literature" values in PRELIM can be used. However, the use of PRELIM literature values will diminish the validity of local limits developed from the computer program.

The inputs required to produce technically-based local limits using PRELIM are:

- POTW Flow and Process Information
- POTW Removal Efficiencies

Table 1 Domestic and Industrial Contributions

Parameter	Domestic	Battery Manufacturer	Aluminum Former
BOD, mg/L	78		
TSS, mg/L	100	1,166	63
NH_3-N, mg/L	25.0		
Cadmium, mg/L	0.01	0.004	0.002
Chromium, mg/L	0.01	0.004	0.004
Copper, mg/L	0.03	0.09	0.004
Cyanide, mg/L	0.01	0.003	0.003
Lead, mg/L	0.02	0.104	0.018
Mercury, mg/L	0.0001	0.004	
Nickel, mg/L	0.02	0.004	0.004
Silver, mg/L	0.005	0.004	0.002
Zinc, mg/L	0.10	0.12	0.032
Phenol, mg/L		0.160	0.004
Arsenic, mg/L	0.01	0.001	

- Sludge Flow, Disposal Method, and Permit Limits
- POTW NPDES Permit Limits
- State Water Quality Standards
- Individual Industry—Flow and Concentrations
- Domestic Flow and Concentrations
- Concentrations of Inhibitory Substances
- Desired Safety Factor

CASE HISTORY

A small community has an extended aeration activated sludge plant which received domestic and industrial flow (Table 1). A battery manufacturer and an aluminum fabricator are the major industries in the community. NPDES permit limits and water quality criteria are listed in Table 2. In this case, the water quality standards are applied directly to the POTW effluent because the plant effluent constitutes the stream in the summer.

NPDES Permit Criteria

Determine the headworks loading criterion for lead based on stream water quality. The first step is to calculate the mass of lead (Pb) allowed in the plant influent without violating the NPDES permit or the water quality standards. Development of headworks loading limits is the area in which the water quality standards have the greatest impact.

Table 2 Limits and Criteria

Parameter	NPDES Limits mg/L	Water Quality Criteria mg/L	Sludge Criteria mg/kg
BOD	30.0		
TSS	30.0		
NH_3-N			
Cadmium		0.020	8.933
Chromium		0.190	
Copper	0.02	0.043	223.31
Cyanide		0.005	
Lead		0.020	893.322
Mercury		0.001	
Nickel		0.006	89.332
Silver		0.0001	
Zinc		1.505	446.661
Phenol		0.100	
Arsenic		0.020	

Effluent Quality

Allowable headworks loading (kg/day) =

$$\frac{(0.001)[(C_{WQ}(Q_{STR}+Q_{POTW}))-((C_{STR})(Q_{STR}))]}{(1-R_{POTW})}$$

C_{WQ} = limiting effluent quality criteria, mg/L (for Pb = 0.02 mg/L)
C_{STR} = background concentration in receiving stream (mg/L) (assume 0.003 mg/L Pb)
Q_{POTW} = influent flow to treatment facility, m^3/d (3407 m^3/day)
Q_{STR} = 7Q10 receiving stream flow m^3/day (assume 1:1 dilution, so 7Q10 = 3407 m^3/day)
R_{POTW} = overall removal efficiency of treatment facility (calculated from actual plant data) (i.e., 13% removal, $R_{POTW} = 0.13$)

Allowable headworks loading (kg/Day)

$$= \frac{(0.001)[(0.02(3407+3407))-((3407)(.003))]}{(1.0-0.13)}$$

$$= \underline{0.1446 \text{ kg/day}}$$

Sludge Quality

The second criterion for comparison is sludge quality. The limit for a given constituent in wastewater sludge differs depending on the disposal method used. The sludge regulations should be consulted to determine the limiting concentration of each constituent in the sludge based on the method of disposal. A sample calculation for the mass of lead removed from the liquid and wasted in the sludge, based on disposal by land application, is as follows:

$$L_{SLUDGE\text{-}DISP} = \frac{(0.001)(C_{SLCRIT})(PS/100)(Q_{SLDG})}{R_{POTW}}$$

where,

$L_{SLUDGE\text{-}DISP}$ = Maximum allowable headworks loading (kg/day) based on sludge disposal options
PS = Sludge percent solids to disposal (%) assume (0.5)
Q_{SLDG} = Sludge flow to disposal (m^3/d) assume 13.6 m^3/day
R_{POTW} = POTW removal efficiency (as a decimal) assume (0.87)
C_{SLCRIT} = Minimum of $C_{LIM(DISP)}$, $C_{LIM(A)}$, and $C_{LIM(C)}$ sludge criterion greater than zero

where,

$C_{LIM(DISP)}$ = Sludge disposal criteria or standard (mg/kg)

$$C_{LIM(A)} = \frac{(AAR)(SA)}{(Q_{SLDG})(PS/100)(3046)}$$

$$C_{LIM(c)} = \frac{(CAR)(SA)}{(SL)(Q_{SLDG})(PS/100)(3046)}$$

where,

$C_{LIM(A)}$ = Sludge disposal limit based on annual application (mg/kg)
$C_{LIM(C)}$ = Sludge disposal limit based on cumulative application (mg/kg)
AAR = Annual application rate limit (kg/hectare/year)
CAR = Cumulative application rate limit (lbs/hectare/life)
SA = Site area (hectares) (assume 740 hectares)
SL = Site use duration (years) (25 years)

Table 3 Summary of Headworks Loading Criteria

Criteria	Allowable Loading
Effluent Quality	0.1446 kg/day (Limiting Criterion)
Sludge Quality	0.467 kg/day
Process Inhibition—Activated Sludge	0.392 kg/day

Allowable headworks loading (kg/day)

$$= \frac{(0.001)(893.3 \text{ mg/kg})(0.5/100)(13.6)}{(0.13)}$$

$$= \underline{0.467 \text{ kg/day}}$$

Process Inhibition

The final criterion for comparison is process inhibition. Any biological process can undergo inhibition, and it is important to make sure that the concentrations of individual constituents do not exceed these inhibitory concentrations. Example calculations are shown to determine the concentration of lead at the headworks to prevent inhibition in activated sludge.

Allowable headworks loading (kg/day)

$$= \frac{(0.001)(K5, \text{ mg/L})(Q1, \text{ m}^3/\text{d})}{1-(R2)}$$

where, 0.001 = metric conversion factor
K5 = limiting process inhibiting criterion, mg/L (based on field or PRELIM data)
Q1 = influent flow to treatment facility, m^3/day (3407 m^3/day)
R2 = removal efficiency of treatment process (i.e., 13% removal, R2 = 0.13)

For activated sludge, Pb inhibition = 0.1 mg/L (from PRELIM data base)

Allowable headworks loading (kg/day)

$$= \frac{(0.001)(0.1 \text{ mg/L})(3407)}{(1.00-0.13)}$$

$$= \underline{0.392 \text{ kg/day}}$$

The next step is to compare the calculated headworks loadings to determine the loading criterion that results in the lowest daily mass loading. Based on the preceding calculations, the most stringent loading criterion is effluent quality, resulting in a lead loading of 0.1446 kg/day at the headworks. The calculation results are summarized in Table 3.

Determine Loadings From Uncontrollable Sources

Evaluate the lead loading attributable to uncontrollable (domestic/commercial) sources. Lead loadings from domestic sources must be determined from sampling. A good source of data for domestic/commercial sources is the local water treatment facility. As an example of this calculation, sampling data on the domestic part of a wastewater collection system indicated a lead concentration of 0.02 mg/L.

kg/day of Pb from domestic sources
= (0.001)(0.02 mg/L)(3210 m^3/day domestic flow)
= $\underline{0.0642 \text{ kg/day}}$

Available Industrial Loading

The allowable lead loading from industrial sources can then be determined by subtracting the loading from domestic/commercial sources from the allowable headworks loading and applying a factor of safety as shown in Table 4.

Table 4

Loading Condition	10% Safety Factor	25% Safety Factor
Allowable Headworks	0.1446 kg/day	0.1446 kg/day
Safety Factor	0.0145 kg/day	0.0362 kg/day
Domestic/Commercial	0.0642 kg/day	0.0642 kg/day
Available To Industry	0.0658 kg/day	0.0443 kg/day

Calculation of Pretreatment Limit

The available industrial loading calculated previously is converted to a concentration. This concentration would be the uniform local pretreatment limit which each industry would need to meet. Conversion of the allowable loading to an allowable concentration is as follows:

Lead loading available to industry = 0.0658 kg/day
Daily industry flow, mgd (from historical data) = 197 m^3/day
kg/day = Flow (m^3/day) concentration (mg/L) 0.001
0.0658 kg/day = (0.001)(mg/L)(197 m^3/day)
Lead concentration = $\underline{0.334}$ mg/L

SUMMARY

The Water Quality Standards will have a profound effect on many industries. Numerical limits on specific chemicals will continue to become more strict. Aquatic toxicity standards will also be imposed. Even industries that discharge through POTWs will feel the impact of water quality standards.

Some key items to remember are:

- Permits will include only those chemicals in the effluent that have a reasonable potential of violating water quality standards.
- Pretreatment permit limits will be changed to reflect the impact of water quality standards.
- The actual numerical limit in NPDES permits will be a function of discharge concentration, size of receiving stream, and receiving stream water quality.

Are the Water Quality Standards the final stage in EPAs management of stream water quality? The answer is NO! The State of Washington has adopted sediment criteria and EPA is working to develop national sediment standards. It is expected that these standards will be applied nationwide in a few years. EPA is also considering biomonitoring (which is not to be confused with aquatic toxicity monitoring) as part of the NPDES program. Biomonitoring involves stream sampling to assess the health of the food chain organisms. Does the stream support only pollution hardy-biota? If the answer is yes, more stringent discharge limits will probably be imposed.

To keep pace with the changing regulations, talk to your state NPDES permit writers regularly to determine how your state is implementing these programs. Watch the Federal Register for advanced warning of changes to the Federal Programs. The key is communication.

LITERATURE CITED

1. U.S. EPA, *Technical Support Document for Water Quality-based Toxics Control*, EPA 505/2-90-001, March 1991.
2. 40 CFR part 403.
3. EPA, PRELIM Version 4.0 User's Guide, Documentation for the EPA Computer Program for Development of Local Discharge Limitations Under the Pretreatment Program, May 1990.

Chemical Barriers for Controlling Groundwater Contamination

S. J. Morrison and R. R. Spangler

Environmental Sciences Laboratory, Grand Junction Projects Office*,
P.O. Box 14000, Grand Junction, CO 81502

Chemical barriers are being explored as a low-cost means of controlling groundwater contamination. The barrier can intercept a contaminant plume and prevent migration by transferring contaminants from the groundwater to immobile solids. A chemical barrier can be emplaced in a landfill liner or in an aquifer cutoff wall or can be injected into a contaminant plume. Chemical barriers can be classified as either precipitation barriers or sorption barriers depending upon the dominant mode of contaminant extraction. In a precipitation barrier, contaminants are bound in the structures of newly formed phases; whereas, in a sorption barrier, contaminants attach to the surfaces of preexisting solids by adsorption or some other surface mechanism. Sorption of contaminants is pH dependent. A precipitation barrier can control the pH of the system, but alkaline groundwater may dominate the pH in a sorption barrier. A comparison is made of the characteristics of precipitation and sorption barriers. Experimental data on the extraction of uranium and molybdenum from simulated groundwater are used to demonstrate these concepts.

INTRODUCTION

Much of the research on groundwater† remediation has focused on the removal of contaminated water from the subsurface and treating it at the surface. While removal of the contaminants is desirable, the costs often are prohibitive and rarely are contaminant concentrations lowered to the required levels. Chemical barriers are being considered as a low-cost alternative to protect groundwater. To construct a barrier, chemicals are emplaced into the subsurface. As groundwater passes through the barrier, reactions occur that cause dissolved contaminants to become part of the immobile solids in the aquifer. The barrier could be emplaced by lining a disposal site, by trench and fill, or by injection into the subsurface (Figure 1). A chemical barrier is essentially a passive *in situ* water-treatment system. A discussion is presented of some early results of a project to design and implement a chemical barrier for a uranium mill tailings disposal site at Monticello, Utah. A pilot-scale field demonstration is planned for the summer of 1992.

*Operated by RUST Geotech, Inc., for the U.S. Department of Energy under DOE Contract No. DE-AC04-86ID12584.

†The term "groundwater" as used in this paper refers to any subsurface water and includes the water contained in partially saturated pores of mill tailings repositories.

Several factors are important to the successful implementation of chemical barriers, which we classify as precipitation barriers and sorption barriers. Dissolved contaminants are extracted by precipitation of newly formed minerals in precipitation barriers or by attachment to surfaces of preexisting minerals by adsorption, absorption, or chelation in sorption barriers. Some characteristics of precipitation barriers contrast with those of sorption barriers. These distinctions (for example, the tendency for the barrier to become clogged) can be used to help select an appropriate barrier design for site remediation. The discussion examples focus on uranium and molybdenum extraction by hydrated lime [$Ca(OH)_2$], ferrous sulfate ($FeSO_4$), and ferric oxyhydroxide ($Fe_2O_3 \cdot nH_2O$).

Previous published research on chemical barrier technology is limited. Several industrial materials such as iron oxides, titanium oxides, lime, peat, and phosphate have been used effectively in laboratory experiments to reduce dissolved concentrations of contaminants characteristic to uranium millsites [*1*, *2*]. Laboratory research by Burruss and Antworth [*3*] reports that organic surfactants can increase sorption of organic contaminants; they concluded that these surfactants may be used as a sorption barrier for organics.

Waste sites typically contain more than one contaminant and each contaminant possesses unique chemical properties. Designing a chemical barrier that will lower concentration of

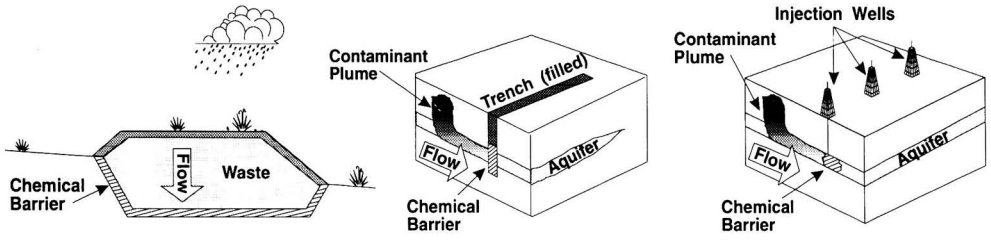

FIGURE 1. Potential methods of emplacement for chemical barriers

all contaminants to their regulated limits is a significant challenge. At millsites, the contaminants are the waste products of ore processing. Because the contaminants were extracted from groundwater during ore genesis, these contaminants should be reprecipitated if the ore-forming processes are duplicated in a chemical barrier. For example, ferrous hydroxide [$Fe(OH)_2$] can produce redox conditions similar to those that occurred during roll-front-type uranium ore deposition [*4*].

METHODS AND MATERIALS

The columns used in the experiments were constructed from 10-cm-diameter cylindrical acrylic pipe. Except where indicated, the columns were filled with about 1,250 mL of sand mixed with the test material. Test solutions (Table 1) were simulations of the pore fluids expected in uranium mill tailings. The test solution was pumped from the bottom to the top through the column at a constant flow rate. Measurements of pH, Eh, and conductivity were made immediately after sample collection. Uranium and molybdenum concentrations were measured within 3 days; however, most measurements were made within 2 hours of sample collection. Uranium concentrations were measured by laser-induced fluorometry (Scintrex UA-3) and molybdenum concentrations were determined by the ternary complex or the mercaptoacetic acid photometric method.

Ferric oxyhydroxide was prepared by dissolving $FeCl_3 \cdot 6H_2O$ in deionized water and then adding 10 normal NaOH until the pH reached about 10. The flocculent was then washed twice in 4 liters of deionized water and centrifuged to about 100 mL. Concentrated nitric acid was used to adjust pH to the desired value. Because the hydration state of ferric oxyhydroxide is uncertain, the weights of ferric oxyhydroxide given in the text are actually the weights of $FeCl_3 \cdot 6H_2O$ used in its preparation.

DEPENDENCY OF CHEMICAL BARRIERS ON pH, Eh, AND SOLUTION COMPOSITION

Both precipitation and sorption reactions in a chemical barrier depend on the chemistry of the groundwater that contacts it. In a precipitation barrier, the groundwater chemistry is modified by the barrier materials to exceed the solubility limits of a desired mineral phase. This can be accomplished by the addition of another solid; for example, hydrated lime [$Ca(OH)_2$] can be placed in a barrier to promote precipitation of uranium as calcium uranate:

$$3Ca(OH)_2 + (UO_2)_3(OH)_5^+ + (OH)^- = 3CaUO_4 + 6H_2O. \quad (1)$$

The hydrated lime yields calcium ions for the precipitation reaction and maintains solution pH above about 12. Many heavy metals (e.g., Pb, Cd, and Cu) precipitate as hydroxides at this pH. However, some contaminants such as molybdenum become more mobile at elevated pH.

Precipitation also may be induced by lowering the oxidation/reduction state. Many contaminant-bearing minerals have extremely low solubilities at low Eh. For example, dissolved uranium is limited to about 2.4 ppb over the pH range 4 to 14 if the solution is sufficiently reducing to form amorphous $UO_2 \cdot xH_2O$ [*5*]. If dissolved sulfur is present, as is the case with most mine and mill wastes, contaminant-bearing sulfides are likely to form at low Eh but may require microbial mediation to enhance the relatively slow conversion of sulfate to sulfide.

Precipitation barriers are less dependent than sorption barriers on groundwater composition. For example, the increase in pH associated with hydrated lime is the dominant factor determining the fate of the contaminants. The extent of contaminant extraction by a precipitation barrier will be nearly the same regardless of the incoming groundwater composition. Adsorption processes that would occur in a sorption barrier also are pH dependent, but the sorbents are less capable of controlling the solution parameters. The range of pH for optimal adsorption of a contaminant will be different for each solution composition. Also, each contaminant has a different optimal adsorption pH range. Thus, accurate groundwater characterization is probably more critical to predicting the performance of sorption barriers than to predicting the performance of precipitation barriers.

Sorption is strongly pH dependent (Figure 2) and the optimal

Table 1 Compositions of Test Solutions

Solution Number	Concentration[a]													
	Na	K	Ca	Mg	SO_4	Cl	Alk	As	U	V	Mo	Pb	^{226}Ra	pH
F1	3680	23	304	65	6178	1000	1902	1.0	30.0	1.60	8.9	2.0	20	7.0
F2	3680	0	304	0	5894	1000	1902	1.0	30.0	0.00	8.9	0.0	0	7.0
F3	2468	16	455	81	5204	40	330	0.0	10.0	0.34	33.0	2.0	100	7.0
F4	296	32	540	140	1975	7	268	1.0	23.3	0.04	5.0	2.0	100	7.4
F5	137	67	538	106	2025	18	10	0.0	7.0	0.07	1.2	0.0	69	7.5
F6	0	0	0	0	0	0	0	0.0	20.0	0.00	10.0	0.0	0	7.0

[a]Concentrations in mg/L; ^{226}Ra in pCi/L; Alk (alkalinity) in mg/L as $CaCO_3$.

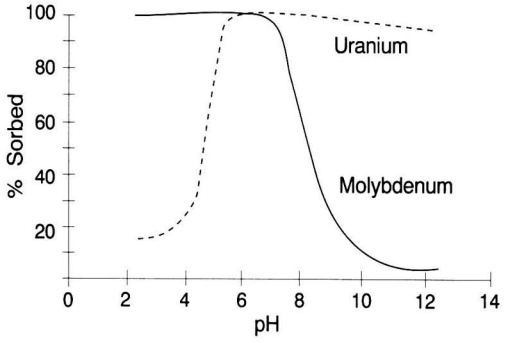

FIGURE 1. Potential methods of emplacement for chemical barriers

range varies with the solution composition and the contaminant. We reasoned that a sorption barrier may be most effective if it causes the groundwater to pass through a wide range of pH values as it flows through the barrier. To test this concept, the pH of ferric oxyhydroxide was adjusted by equilibrating it with water at several pH values.

Three column experiments were run using ferric oxyhydroxide adjusted to pH values of 5, 6, and 7; all other conditions were held constant. Deionized water containing 20 mg/L of uranium and 10 mg/L of molybdenum at pH 7 was passed through the column. Figure 3 shows the results of these experiments. The column with ferric oxyhydroxide conditioned at pH 7 was most effective in removing uranium and molybdenum concentrations in contrast to our expectation that pH 5 would be most effective. Ferric oxyhydroxide conditioned at pH 7 also was more effective than other pH values when a more complex solution (test solution F1, Table 1) was used (Figure 4). Batch tests indicated that the optimal pH for U and Mo adsorption for test solution F1 was about 6.0 to 6.5 (Figure 2). Ferric oxyhydroxide was able to buffer the pH by releasing hydrogen ions in the deionized water experiments (Figure 3c) but not in the experiments using the complex solution (Figure 4c). The high alkalinity of the complex solution apparently was able to take up any excess hydronium released from the ferric oxyhydroxide surfaces.

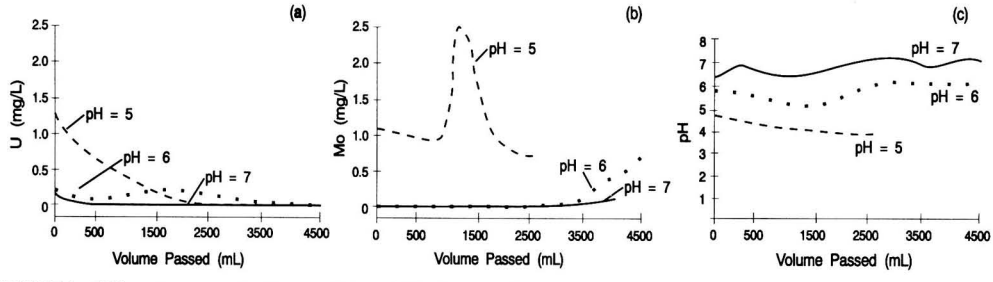

FIGURE 3. Effluent concentrations of U and Mo from column experiments. Ferric oxyhydroxide was conditioned at pH values of 5, 6, and 7. These column experiments contained 26 g of ferric oxyhydroxide and the test solution contained 20 mg/L of U and 10 mg/L of Mo in deionized water at pH 7. (a) U, (b) Mo, (c) pH.

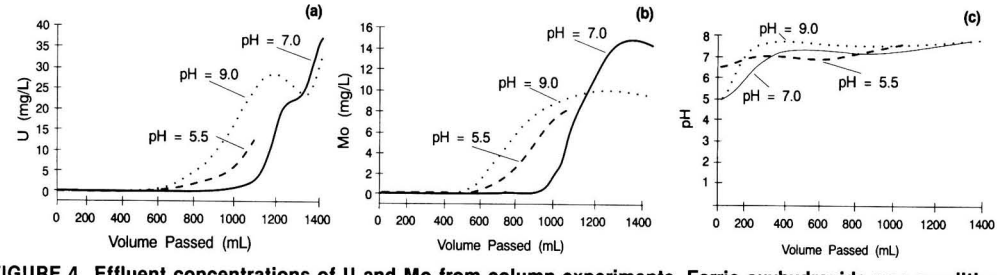

FIGURE 4. Effluent concentrations of U and Mo from column experiments. Ferric oxyhydroxide was conditioned at pH values of 5.5, 7.0, and 9.0. These column experiments contained 6.5 g of ferric oxyhydroxide and the test solution was F1 (Table 1). (a) U, (b) Mo, (c) pH.

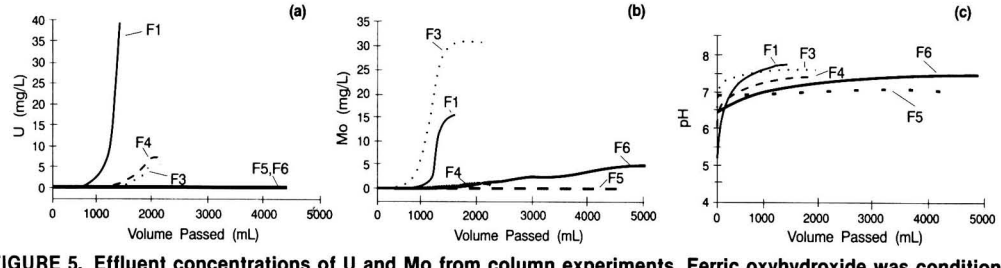

FIGURE 5. Effluent concentrations of U and Mo from column experiments. Ferric oxyhydroxide was conditioned at pH value of 7.0. These experiments contained 6.5 g of ferric oxyhydroxide; compositions of test solutions, F1, F3, F4, F5, and F6 are given in Table 1. (a) U, (b) Mo, (c) pH.

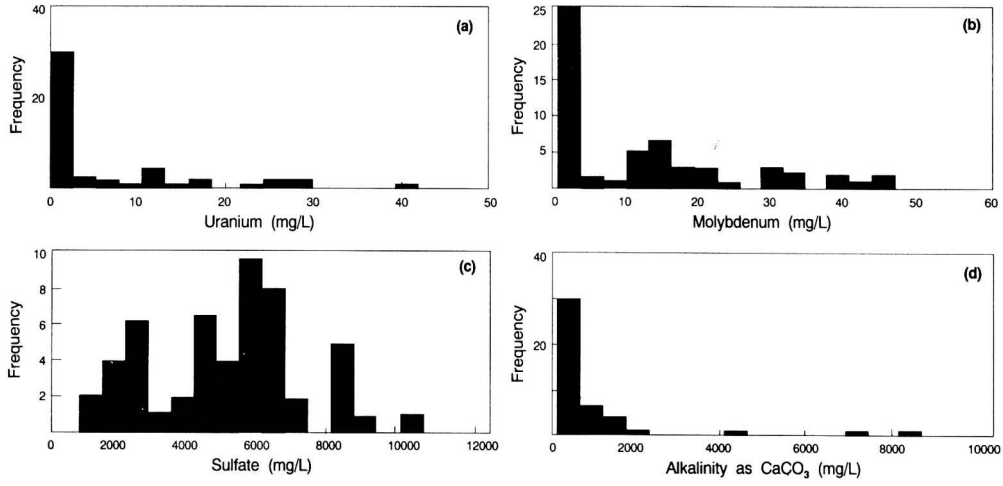

FIGURE 6. Histograms showing distribution of U, Mo, SO_4, and alkalinity in uranium mill tailings pore fluids

Additional column experiments were run to examine the extraction of uranium and molybdenum by ferric oxyhydroxide (conditioned at pH 7) for a range of complex solution compositions. The results indicate that the extraction efficiency is very dependent on solution composition (Figure 5). For solutions with high salt content, ferric oxyhydroxide is less effective in extracting U and Mo. Aqueous complexing of uranium by carbonate is well known. Uranium extraction was greatest from those solutions having the least amount of carbonate (as indicated by the alkalinities), which suggests uranyl carbonate complexing as a possible explanation of the uranium trends. The solutions differ in so many other ways, however, that more controlled experiments will be required to determine if carbonate complexing is the dominant control on uranium.

GROUNDWATER CHARACTERIZATION

The characterization of site-specific groundwater composition is critical in evaluating the performance of a chemical barrier, particularly a sorption barrier. Groundwater at a uranium mill tailings repository will include pore fluids present in the tailings, a large volume of water introduced during site construction to control dust, and infiltration water. Groundwater characterization in our study consists of 50 samples of pore waters from 11 lysimeters during a period of about 8 years and five solutions formed by interacting water with tailings to simulate the construction water. Histograms showing distributions of U, Mo, SO_4, and alkalinity in tailings pore fluids (Figure 6) and in water interacted with tailings (Figure 7) demonstrate the diversity of chemical compositions. Using these characterization data, it is possible to estimate the water compositions most likely to pass through the chemical barrier. Modeling of water-tailings interactions and of mixing of these waters is needed to predict the fluid compositions more accurately. Because the composition of the test fluids is critical to evaluating the potential effectiveness of sorption barriers, site-specific groundwater characterization is needed.

RELATIONSHIP OF GROUNDWATER FLUX TO BARRIER PERFORMANCE

Chemicals used in the barrier must be positioned so that more chemical material is placed in areas that will receive higher flux of contaminated groundwater. One of the most likely failure scenarios for a chemical barrier is miscalculation of groundwater fluxes. An accurate flow model of the site is necessary for proper placement of chemical barrier material.

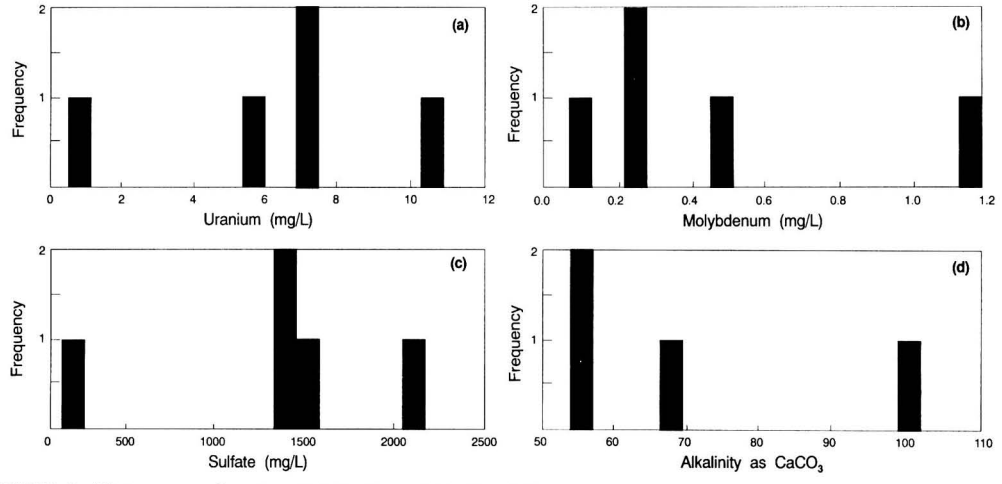

FIGURE 7. Histograms showing distribution of U, Mo, SO_4, and alkalinity in water reacted with uranium mill tailings

It may be possible, in some cases, to engineer a repository with an underground drain that will localize the flow. In this case, barrier materials can be placed in the drain to reduce the risk associated with the possibility of flow missing the barrier.

Chemical reactions in the barrier may precipitate minerals in the pores and cause reduction of hydraulic conductivity so that flow is diverted away from the barrier. This effect is likely to be more dominant in precipitation barriers than in sorption barriers. Theoretical considerations of precipitation chemistry can help to determine the likelihood of porosity plugging; however, properly instrumented laboratory columns and field-scale pilot studies are needed to evaluate this aspect more completely.

BARRIER AGING

A barrier can fail (in the sense that it can no longer immobilize contaminants) if the chemicals become modified by aging. If enough groundwater passes through, all barriers eventually will become loaded and no longer will be effective for immobilizing contaminants. Ferric oxyhydroxide is known to convert to goethite (FeOOH) over time periods of weeks to years, but it is not known what *in situ* conditions control the rate of conversion. Goethite adsorbs many of the same contaminants as ferric oxyhydroxide; thus, experiments using goethite are needed to quantify its adsorption capacity. Recrystallization of ferric oxyhydroxide (either to goethite or to a more crystalline ferric oxyhydroxide) can cause a decrease in sorption capacity and rates because of decreasing surface area.

Lime can react with silicate minerals in the chemical barrier to produce calc silicates and limit the amount of free lime available for the desired precipitation reactions. The chemical conditions required for these reactions and their rates in geologic media are not well known. If these reactions are not considered, the barrier could be depleted of hydrated lime sooner than predicted.

UNDESIRABLE MODIFICATIONS TO AQUIFERS FROM CHEMICAL BARRIERS

Potential risks of using a chemical barrier must be evaluated as well as the potential benefits. The technology for chemical barriers is not well developed. Field experiments and actual usage will be needed before it can be reasonably certain that laboratory data and model concepts will predict accurately the performance desired at a site. However, field usage will only be permitted if minimal risks are associated with the barrier.

Precipitation barriers are more likely than sorption barriers to degrade the groundwater composition. Hydrated lime will add a significant amount of calcium and will increase the pH, but ferric oxyhydroxide (a sorbent) is not likely to contribute any significant amounts of chemicals to the groundwater. Ferric oxyhydroxide (the naturally occurring form often is referred to as ferrihydrite) is present in most soils and aquifers and probably accounts for much of the retardation of contaminants that occurs as contaminated fluids flow through the subsurface. By concentrating ferric oxyhydroxide in a barrier, contaminants are simply extracted in a more limited area than would occur by natural processes alone.

CHEMICAL KINETICS

The reaction rates for the examples in these experiments appear to be sufficiently fast with respect to groundwater flow; they can be considered to go to equilibrium instantaneously. Chemical water-treatment plants must use processes that react quickly because of the large flow rates that are required. Groundwater flow through a chemical barrier, however, typically is slow (1 to 100 meters per year) and reactions are more likely to go to completion. Rates for many reactions of interest to chemical barriers are not well known. No generalizations can be made comparing reaction rates in precipitation versus sorption barriers.

Failure to recognize slow reaction rates in laboratory simulations may cause useful barrier materials to be overlooked. As an example, consider the reaction of hydrated lime on the precipitation of uranium minerals. An experiment was set up with 3 g of hydrated lime placed in a sand column. The flow rate was set to take about 20 minutes for the fluid to pass through the hydrated lime layer. On the basis of the results of long-term (3-day equilibrations) batch experiments, 3 g of $Ca(OH)_2$ should have been able to maintain uranium concentrations below 0.500 mg/L for about 4 L of solution. The results of uranium concentrations in the column effluent are shown in Figure 8a. The uranium concentration was never lower than 0.944 mg/L and concentrations increased dramatically after only 400 mL of solution. This result can be explained by considering the rate of the reaction as determined from a timed batch test. An excess amount of hydrated lime was added quickly to test solution F1 (Table 1) that contained 30 mg/L of uranium. Samples were taken at timed intervals, quenched with water, and immediately measured for uranium concentration. The results are compared with a first-order rate curve in Figure 8b. More than 1 hour was required for the uranium concentration to fall below 0.500 mg/L (representing approximately complete reaction). This length of time is more than the contact time (about 20 minutes) with hydrated lime

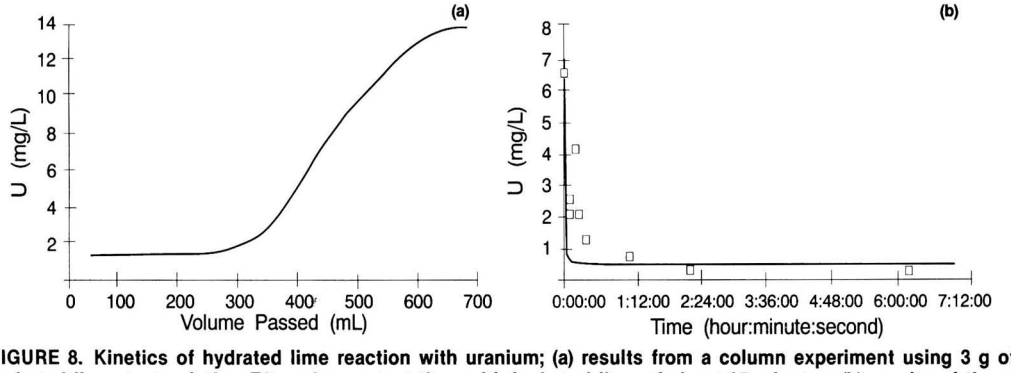

FIGURE 8. Kinetics of hydrated lime reaction with uranium; (a) results from a column experiment using 3 g of hydrated lime, test solution F2, and a contact time with hydrated lime of about 25 minutes; (b) results of timed batch experiments in which excess hydrated lime was reacted with test solution F1.

in the column experiment. Therefore, slower flow rates likely will improve the performance of the hydrated lime.

PERFORMANCE MODELING OF CHEMICAL BARRIERS

The ability to predict long-term performance accurately is as important to the success of chemical barrier remediation as with any other groundwater remediation technology. Because chemical barriers rely on chemical reactions, it is particularly important to use accurate chemical models. Traditional contaminant transport models that invoke a single bulk distribution coefficient to simulate all the chemical processes are not desirable for predicting interactions in chemical barriers.

Ideally, models can be constructed that use fundamental thermodynamic and kinetic principles to predict the contaminant interactions with a chemical barrier. The most widely accepted models used to describe chemical processes such as those that would occur in chemical barriers invoke mass-action principles to describe aqueous complexation, mineral precipitation and dissolution, and surface-site binding. These models accurately predict the distribution of contaminants between solid and aqueous phases in static, closed, and relatively simple chemical systems. However, few studies are available that validate their application to the more complex, dynamic, open systems that will occur in chemical barriers.

Successful models will need to simulate two- and three-dimensional dynamic flow-through systems. They will have to account for flow patterns in both saturated and unsaturated media and have the capability to predict the chemical interactions. Much progress has been made in recent years to develop coupled modeling codes capable of performing these tasks. Probably the most advanced of these codes is HYDROGEOCHEM [*6*], which is able to partially couple equilibrium aqueous-solid chemical reactions with two-dimensional variably saturated flow. Chemical reactions included in the model are aqueous complexation and precipitation/dissolution based on mass-action principles; adsorption, using site complexation constants adjusted for surface charge in the electrical double layer, and ion exchange. Currently lacking in HYDROGEOCHEM is the ability to calculate kinetics; however, the code was written in a way that readily will allow the implementation of a kinetic algorithm [7]. Permeability modifications that are due to mineral precipitation in the chemical barrier may be important in chemical barriers but cannot be modeled using HYDROGEOCHEM. Small field-scale simulations using HYDROGEOCHEM have been run efficiently on a DEC5000 desk-top computer workstation in our laboratory.

We are using HYDROGEOCHEM to simulate the effects of chemical barriers on contaminant plumes. Partial results of a "model validation" study are shown in Figure 9. The method of goethite (FEOOH) synthesis, goethite surface properties, and thermodynamic constants are those of Tripathi [*8*]. Simple site complexation without correction for electrical double-layer charge distribution was used to model adsorption of uranium on goethite. Deionized water with 0.1 molar $NaNO_3$, 1.0 mg/L uranium, and pH 4 was passed through the column at a flow rate of about 2.8 liters per day in a carbon dioxide-free environment. Figure 9 shows the predicted and observed concentrations of uranium for the fourth day. The model did not quantitatively predict the observed uranium distributions but did predict the uranium concentration to rise above the incoming value, which is consistent with the results of the column experiment. Prediction of a concentration above the incoming value is mathematically impossible using traditional distribution-coefficient approaches. Refinements are needed, probably, in both the HYDROGEOCHEM model parameters and the experimental design.

Successful models will have to, at a minimum, be able to predict accurately contaminant distributions of complex aqueous solutions with barrier materials such as those presented in Figure 5. Fortunately, one of the favored chemical barrier materials, ferric oxyhydroxide, has been studied in great detail [*9*, *10*] so there is reasonable hope that accurate models can be generated with only a limited amount of additional laboratory work. The effect of ferric oxyhydroxide on hydraulic conductivity probably is minimal, which also is fortunate because no models exist that can predict reliably that aspect of coupling.

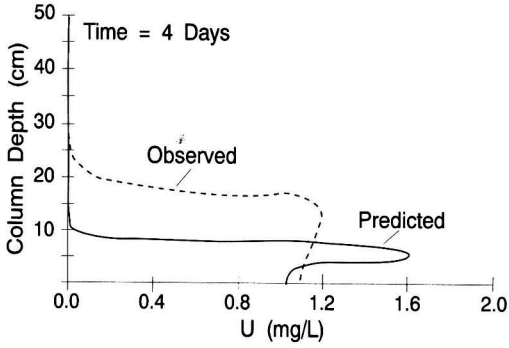

FIGURE 9. Dissolved uranium for day 4 of a model validation column experiment

CONCLUSIONS

Chemical barriers can offer a low-cost alternative to pump-and-treat groundwater remediation. Characteristics of chemical barriers can be evaluated more meaningfully by considering them as two general types: precipitation and sorption barriers. Some industrial materials have been shown to be effective in extracting some types of contaminants from solution and may be cost effective for some chemical barriers. Most of the chemical barrier research performed to date has focused on evaluating the extraction potential of select industrial materials using laboratory testing on a variety of groundwater compositions, contaminant types, and pH ranges. More efforts are required to develop accurate predictive chemical models, evaluate flow patterns at specific sites, and integrate chemical barriers into large-scale remediation designs. It is unlikely that a "standardized" chemical barrier can be developed for routine use at waste sites. Rather, the characteristics of each site will need to be evaluated before determining the appropriateness and type of chemical barrier for a specific site.

ACKNOWLEDGMENTS

We gratefully acknowledge Dave Emilia, Brian Wilson, and Hal Langner for their support throughout the project and to Vijay Tripathi for many discussions of the chemical systems. We thank Sarah Morris for providing technical assistance. The work was funded by the U.S. Department of Energy Office of Environmental Restoration and Waste Management (DOE Contract No. DE-AC04-86ID12584), Monticello Remedial Action Project, and Grand Junction Projects Office's Laboratory-Directed Research and Development program.

LITERATURE CITED

1. Longmire, P. A., D. G. Brookins, B. M. Thompson, and P. G. Eller, "Application of Sphagnum Peat, Calcium

Carbonate, and Hydrated Lime for Immobilizing Uranium Tailing Leachate," pp. 623-631 in *Scientific Basis for Nuclear Waste Management XIV*, T. A. Abrajano, Jr., and L. H. Johnson, eds., Material Research Society, Pittsburgh, PA (1991).
2. Morrison, S. J., and R. R. Spangler, "Chemical Barriers for Uranium Mill Tailings Remediation: Extraction of Uranium and Molybdenum from Aqueous Solutions Using Industrial Materials," *Environmental Science & Technology*, 26, pp. 1922-1931 (1992).
3. Burruss, D. R., and C. P. Antworth, "*In Situ* Modification of an Aquifer Material by a Cationic Surfactant to Enhance Retardation of Organic Contaminants," *Jour. Contaminant Hydrology*, **11** (1992).
4. Spangler, R. R., and S. J. Morrison, "Laboratory-Scale Tests of a Chemical Barrier for Use at Uranium Mill Tailings Disposal Sites," in *ER '91 Conference Proceedings*, Pasco, WA (1991).
5. Rai, Dhanpat, A. R. Felmy, and J. L. Ryan, "Uranium(IV) Hydrolysis Constants and Solubility Product of $UO_2 \cdot xH_2O$(am)," *Inorg. Chem.*, **29**, pp. 260-264 (1990).
6. Yeh, G. T., and V. S. Tripathi, *HYDROGEOCHEM: A Coupled Model of HYDROlogic Transport and GEOCHEMical Equilibria in Reactive Multicomponent Systems*, ORNL-6371, Oak Ridge National Laboratory, Oak Ridge, TN (1990).
7. Yeh, G. T., and V. S. Tripathi, "A Critical Evaluation of Recent Developments in Hydrogeochemical Transport Models of Reactive Multichemical Components," *Water Resources Research*, **29**, pp. 93-108 (1989).
8. Tripathi, V. S., *Uranium(IV) Transport Modeling: Geochemical Data and Submodels*, Ph.D. dissertation, Stanford University (1984).
9. Hsi, C. D., and D. Langmuir, "Adsorption of Uranyl Onto Ferric Oxyhydroxides: Application of the Surfaced Complexation Site-Binding Model," *Geochimica et Cosmochimica Acta*, **49**, pp. 1931-1941 (1985).
10. Dzombak, D. A., and F. M. M. Morel, *Surface Complexation Modeling—Hydrous Ferric Oxide*, John Wiley & Sons, New York (1990).

Economic Effects of Catalyst Deactivation During VOC Oxidation

Sanjay K. Agarwal and James J. Spivey

Research Triangle Institute, Center for Process Research, P.O. Box 12194, Research Triangle Park, NC 27709-2194

Catalytic oxidation of volatile organic compounds (VOCs) is widely used for air pollution control. While catalytic oxidation offers several advantages over alternative processes, the catalyst can deactivate over time, resulting in changes in activity and selectivity with time-on-stream. To maintain constant catalyst activity, required for environmental regulations, the temperature is generally increased gradually to compensate for catalyst deactivation. This results in an increase in fuel consumption with time. Since the fuel costs can account for 50 to 70 percent of the total operating costs, the effect of catalyst deactivation on fuel costs and hence total operating costs should be considered. This paper shows how the catalyst deactivation affects the total operating costs using an example of the oxidation of a VOC-containing gas stream over a commercial hopcalite catalyst.

INTRODUCTION

Control of volatile organic compounds (VOCs) in gas streams is an important environmental concern. The wide variety of sources has suggested the development of techniques that can be applied to gases with a correspondingly wide variety of chemically different VOCs. One such source is air strippers, which are used to remove VOCs from contaminated groundwater. A recent survey identified 177 air strippers in the United States, of which only 17 had controls on the air emissions from the stripper [*1*]. Typically, emissions from air strippers contain a wide range of compound types and concentrations. Of particular concern in many air strippers are chlorinated organics (which pose problems of byproduct formation in thermal oxidation systems that operate at high temperature), humidity (which can decrease the capacity of adsorption beds), and the need to control sources with inlet concentrations as low as 10 to 100 ppm (which may require unacceptably large and costly systems).

Catalytic oxidation systems address some of these concerns by operating at low temperatures, being relatively humidity-insensitive, and being applicable to gases with low inlet concentrations. However, as in any catalytic process, the catalyst used for VOC oxidation can deactivate. Catalyst deactivation can result in the emission of unreacted and/or partially oxidized compounds, i.e., both the activity and selectivity can change with time-on-stream. Whereas HCl and H_2SO_4 may be the initial acidic products of complete oxidation of chlorine, and sulfur containing compounds, different and perhaps more toxic products such as Cl_2 or SO_2 could be formed as the catalyst deactivates [*2, 3*]. For example, Cl_2 selectivities in the 3 to 7 percent range have been observed in the catalytic oxidation of CH_3Cl over 19 percent Cr_2O_3 on alumina at temperatures from 613 to 745 K and space velocities from 2.6×10^4 to 3.6×10^4 h^{-1} [*2*]. Laidig et al. observed Cl_2 selectivities as high as 19 to 42 percent using copper-based catalysts [*4*]. The production of Cl_2 is not environmentally desirable. In contrast, HCl can be scrubbed with a mild caustic solution or water.

Correspondence concerning this paper should be addressed to S. K. Agarwal.

If the catalyst continues to deactivate and no measures are taken to offset it, the catalyst activity will drop to an unacceptable level. The reduced activity may not be desirable for environmental applications where a constant activity is required to meet the government regulations. The catalyst activity can be maintained at a constant level by increasing the temperature gradually to compensate for catalyst deactivation. Provided the conversion is measured periodically, it is less expensive to operate at the lowest reaction temperature needed to maintain a target conversion. Ideally, this reaction temperature is gradually raised in small increments as the catalyst deactivates. This minimizes the cost of preheating the inlet gas to the reaction temperature. In practice, it is difficult to measure the outlet composition and adjustments to the reaction temperature are frequently either not made at all or made only when the conversion has fallen well below the target level. Since the cost of the fuel needed to raise the inlet gas is generally 50 to 70 percent of the operating cost [*5*], the catalyst deactivation can considerably change the operating costs.

The purpose of this paper is to couple an experimental model of the deactivation of catalysts used for VOC oxidation in environmental control applications with the fuel cost. This is done by examining the results of deactivation tests carried out on a ceria-promoted hopcalite (copper-manganese oxide) catalyst. These experimental results are then used to show the economic consequences of catalyst deactivation.

DEACTIVATION DURING VOC OXIDATION

Because all catalysts deactivate over time, it is important to have the best possible understanding of catalyst deactivation so that the economics of catalyst replacement or regeneration are taken into account.

The VOC-containing gas stream is burned in a catalytic chamber as shown in Figure 1. Because the temperature of the inlet gas stream, T_{wi}, is generally much lower than that required for combustion, T_{ri}, energy is required to raise the gas temperature to the reaction temperature. The concentration of organics is usually low enough that the energy released by their combustion is not sufficient to sustain an adequate tempera-

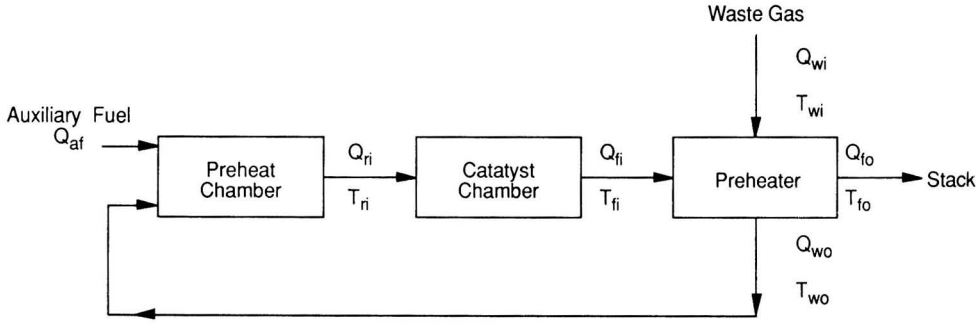

FIGURE 1. Schematic of catalytic incinerator.

ture, and thus auxiliary fuel is required. Generally, the auxiliary fuel cost is the largest single operating cost for the entire system, accounting for as much as 50 to 70 percent of the total operating costs [5]. Deactivation of the catalyst causes more fuel to be used to maintain constant conversion with time. As a result, fuel usage and thus the total operating costs increase as the catalyst deactivates.

Most economic studies consider a constant feed temperature during the entire catalyst lifetime. Since this is not true for a deactivating catalyst, a temperature-time relationship is required to predict the true process economics. It is impossible to predict a priori the temperature required to maintain a given level of conversion with time-on-stream. The required temperature-time relationship can be obtained in a laboratory-scale microreactor. Once such a relationship is available, the fuel usage can be determined as a function of time-on-stream. Agarwal et al. conducted such a study to predict the operating cost of a commercial hopcalite catalyst for the oxidation of a VOC stream with composition typical of that expected from air strippers used for groundwater cleanup [6].

Deactivation of the hopcalite catalyst for the oxidation of a humidified air stream containing 500 ppm of a mixture of C_5 to C_9 hydrocarbons was studied in a fixed-bed reactor. The reaction was conducted continuously (24 h/day, 7 days/week) over an extended period of time (297 days). The composition of the feed stream is shown in Table 1. The gas stream was humidified to a dew point of 288 K. This water vapor concentration is typical of streams from air strippers. The reaction was conducted at constant total carbon conversion of 99 percent. The temperature was increased, when needed, to compensate for the catalyst deactivation and maintain a constant conversion. Agarwal et al. give experimental details [6].

The hopcalite catalyst deactivated during 297 days of operation, as shown in Figure 2, which summarizes the temperature required to maintain a constant conversion of greater than 99 percent. The initial temperature over the hopcalite catalyst was 588 K and the total conversion was close to 99.9 percent at the start of the run. As the catalyst started deactivating, the conversion dropped below 99.9 percent. The temperature was increased when the total conversion dropped below 99 percent. The total conversion was maintained above 99 percent by periodically increasing the temperature to compensate for the loss of intrinsic catalytic activity. The temperature had to be increased to 673 K over 297 days to maintain the conversion above 99 percent. A sharp loss in catalyst activity was observed after 225 days on stream, as expected given the exponential nature of the deactivation rate for constant conversion operation [7].

There were also differences in the conversion of different compounds with time. The conversion of all compounds, except pentane and benzene, was above 99 percent. The conversion of pentane was about 98 percent and was constant with time-on-stream. However, the conversion of benzene decreased steadily from >99 percent conversion at the start of the run to 88 percent after 297 days on stream.

A simple mathematical model was developed for the temperature versus time-on-stream data over the hopcalite catalyst. The model is given by Agarwal et al. [6].

$$t = D\left[1 - \exp B\left(\frac{1}{T_{ri}} - \frac{1}{T_o}\right)\right] + C \tag{1}$$

where

$$D = \frac{E_a}{E_d A_d} \exp\left[\frac{E_d}{RT_o}\right] \tag{2}$$

$$B = \frac{-E_d}{R}. \tag{3}$$

The experimental data fitted to equation (1) by a least-square method gave the following: B = 4,770 K, C = 106 days, and D = 299.3 days. The model can be used to predict the catalyst lifetime using a maximum recommended temperature of 773 K for this catalyst. Equation (1) gives a catalyst lifetime of 362 days for T_{ri} = 773 K. The time-temperature relationship predicted by equation (1) is compared with the experimental

Table 1 Feed Stream Composition

Compound	Concentration (ppm)
Pentane	132.5
2,3-Dimethylbutane	5.0
Methylcyclopentane	24.0
Cyclohexane	206.5
Benzene	29.0
Ethylbenzene	26.0
m,p-xylene	66.5
Cumene	10.5
Water vapor	1.6×10^4
Total (moisture free)	500

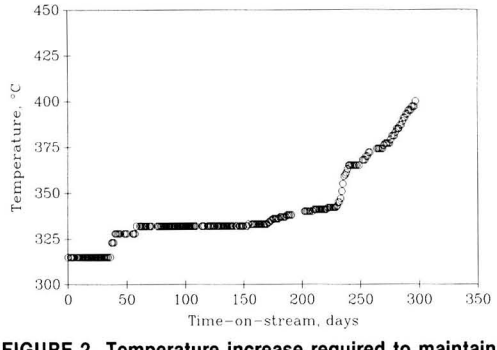

FIGURE 2. Temperature increase required to maintain a constant conversion (>99%) of VOCs over the hopcalite catalyst.

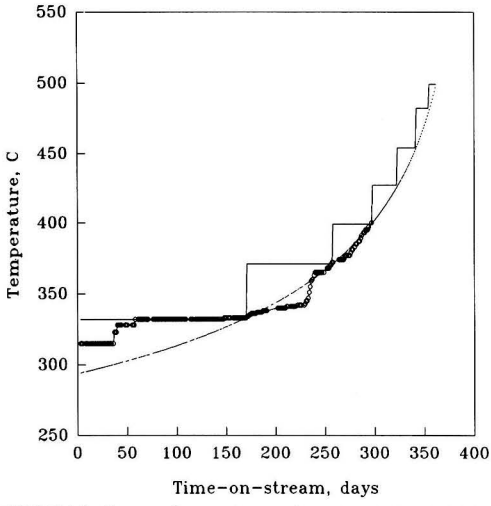

FIGURE 3. Comparison of experimental data with that predicted by the model. Symbols represent experimental values. Dashed line represents predicted value. Solid line represents a practical case where the temperature is arbitrarily increased, in steps, well above the minimum required temperatures.

data in Figure 3. The parameter C has the units of time and is believed to be related to the breakthrough of the deactivation wave, after which the decrease in conversion with time-on-stream becomes observable at bed exit. Figure 3 shows this time to be about 160 days. This is comparable with the value of C (106 days).

The predicted temperature compares very well with the experimental results after 160 days on stream. Before 160 days on stream, the actual temperature is higher than that predicted by the model. This is because recommended startup temperature is higher than the minimum required for greater than 99 percent conversion. The intrinsic activity of the catalyst gradually decreases and the required temperature to maintain constant conversion increases after 160 days on stream. After this period, the temperature is increased daily whenever the total carbon conversion falls below 99 percent. In practice, however, it may not be feasible to continuously increase the temperature to compensate for the loss of catalyst activity. Generally, the temperature is increased to a level much above the minimum required for a given conversion. This allows the combustion reaction to be conducted at this temperature for a longer time before another temperature increase is required. This type of temperature increase behavior, corresponding more closely to commercial practice, is also shown in Figure 3. In this case, the temperature is increased only six times over the entire catalyst lifetime.

ECONOMICS

Equation (1) relates the reaction temperature with time-on-stream. The auxiliary fuel usage rate is a function of the temperature T_{ri} given by an energy balance around the incinerator shown in Figure 1.

$$Q_{af}=\frac{\rho_{wo}Q_{wo}\left[C_{pm_{air}}\left\{1.1\left(T_{ri}-\frac{\Delta h_{cwo}}{C_{pm_{air}}}\right)-0.5\left(T_{ri}-\frac{\Delta h_{c_{wo}}}{C_{pm_{air}}}+T_{wi}\right)-0.1T_{ref}\right\}+\Delta h_{c_{wo}}\right]}{\rho_{af}\left[-\Delta h_{c_{af}}-1.1C_{pm_{air}}\left(T_{ri}-\frac{\Delta h_{c_{wo}}}{C_{pm_{air}}}-T_{ref}\right)\right]} \quad (4)$$

The derivation of this function and the assumptions leading to it are given by Agarwal and Spivey [8]. Equations (1) and (4) can be combined to express the auxiliary fuel usage rate as a function of time-on-stream. The result is an expression of the form:

$$Q_{af}=\left(\frac{aT_n(t)+b}{cT_n(t)+d}\right). \quad (5)$$

In equation (5) constants a, b, c, and d are defined only by the properties of the gases and the system size (i.e., total volumetric flow rate). They do not depend on the deactivation of the catalyst. Equation (4) becomes a time-dependent function, $Q_{af}(t)$, by substituting equation (1) into equation (4), yielding an expression of the form

$$Q_{af}(t)=\frac{[aET_o+bE]+bT_o\ln\left[1-\frac{t-F}{G}\right]}{[cET_o+dE]+dT_o\ln\left[1-\frac{t-F}{G}\right]} \quad (6)$$

where E, F, and G depend only on the experimental deactivation results and are defined by the deactivation model given in equation (3). For the hopcalite catalyst, tested in this study

$E=4770$ K
$F=1.526\times10^5$ min
$G=4.310\times10^5$ min.

For the hydrocarbon gas tested on the hopcalite catalyst and for a 283 m^3/min system the values of a, b, c, and d are given by:

$a=214.8$ kJ/min-K
$b=-26{,}375$ kJ/min
$c=0.7671$ kJ/m^3-K
$d=3.265\times10^4$ kJ/m^3

Figure 4 shows the fuel consumption as a function of time-on-stream for three different cases. In the first case, when the catalyst does not deactivate, the fuel consumption is constant with time-on-stream as shown by the flat line. In the second case, where the temperature is continuously increased to compensate the catalyst deactivation, the fuel consumption increases continuously following the same behavior as the temperature-time relationship. This curve has been generated by using the experimental time-temperature data until 297 days on stream followed by the data predicted by the model between 297 and 362 days-on-stream. Under practical conditions, it would not be feasible to continuously measure the effluent stream and increase the temperature when the catalyst loses some activity. It is more practical to keep the operating temperature considerably higher than the minimum required. The temperature is increased when the catalyst activity falls below the requirement. The third curve in Figure 4 shows the fuel consumption for this situation. As expected, the fuel consumption in this case is slightly higher than the case in which the temperature is continuously increased to compensate for the loss of catalyst intrinsic activity.

Figure 4 shows that catalyst deactivation significantly affects the fuel consumption and hence the operating cost. Table 2 summarizes the fuel consumption and the associated fuel cost

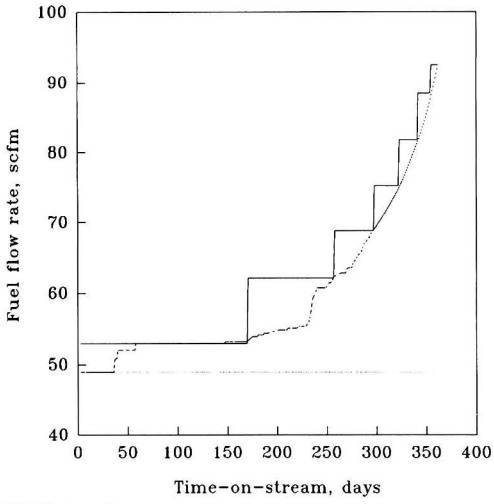

FIGURE 4. Comparison of fuel consumption for a nondeactivating catalyst with a deactivating catalyst. Dotted line represents a nondeactivating catalyst. Dashed line represents continuous temperature adjustment (from experimental data). Solid line represents step temperature change.

over the entire catalyst lifetime for the three cases. Since the cost difference between continuous temperature adjustment and step temperature adjustment is not much, the latter operation is justified in practice.

In conclusion, catalyst deactivation can have considerable effect on fuel consumption. Since the fuel cost accounts for as much as 50 to 70 percent of the total operating costs, catalyst deactivation increases the total operating costs and should be considered in economic analysis.

ACKNOWLEDGMENT

The financial support provided by the U.S. Air Force Engineering Services Center (Tyndall AFB, FL) under contract FO8635-89-C-0276 is greatly acknowledged. Trademarks and trade names of materials and equipment do not constitute endorsement or recommendation for use by the U.S. Air Force nor can this paper be used for advertising any product.

NOTATION

A_d = preexponential factor for deactivation reaction
E_a = activation energy for primary reaction
E_d = activation energy for deactivation reaction
R = gas constant
t = time-on-stream, day
T_{ri} = catalyst temperature, K
T_o = initial catalyst temperature, K

Table 2 Fuel Consumption and Cost for Catalytic Oxidation for 362 Days of Operation

Case	Fuel consumption (m^3)	Fuel cost[a] ($)
No deactivation	5.9×10^5	69,300
Continuous temperature adjustment	7.4×10^5	85,800
Step temperature adjustment	7.6×10^5	89,430

[a]Fuel cost is based on \$0.117/m^3 (\$3.30/1,000 ft^3).

Q_{af} = flow rate of natural gas auxiliary fuel to the unit preheater, scfm
ρ_{wo} = density of the inlet waste gas, 1.19 kg/m^3 at 298 K, 1 atm
Q_{wo} = flow rate of waste gas from the air stripper through the preheater, 283 m^3/min (10,000 scfm)
$C_{pm_{air}}$ = mean heat capacity of air over the range of operation of the incinerator, 1.065 kJ/kg-K
T_{ri} = inlet temperature to the catalyst combustion chamber, K
$\Delta h_{c_{wo}}$ = heat of combustion of waste gas, kJ/kg
T_{wi} = inlet temperature of the waste gas from the air stripper to the catalytic oxidation unit, chosen to be 298 K in this example
T_{ref} = reference temperature, 298 K
ρ_{af} = density of natural gas, calculated as methane, 0.657 kg/m^3 at 298 K
$\Delta h_{c_{af}}$ = heat of combustion of the natural gas auxiliary fuel, 49,900 kJ/kg

LITERATURE CITED

1. Vancil, M. A., R. H. Howle, D. J. Herndon, S. A. Shareef, "Air Strippers Air Emissions and Controls," Report DCN 87-231-020-32-16 for EPA (Research Triangle Park, NC), May 1987.
2. Weldon, J., and S. M. Senkan, "Catalytic Oxidation of CH_3Cl by Cr_2O_3," *Combustion Science and Technology*, **47**, pp. 229-237 (1986).
3. Agarwal, S. K., J. J. Spivey, and J. B. Butt, "Catalyst Deactivation During Deep Oxidation of Chlorohydrocarbons," Applied Catalysis A: General, **82**, p. 259 (1992).
4. Laidig, G., D. Hoenicke, and K. Griesbaum, Erdol. Kohle, Erdgas Petrochem., **34**, p. 329 (1981).
5. U.S. Environmental Protection Agency, "OAQPS Control Cost Manual," EPA-450/3-90-006, U.S. EPA, OAQPS (Research Triangle Park, NC), pp. 3-1 to 3-64 (1990).
6. Agarwal, S. K., J. J. Spivey, and J. B. Butt, "Deep Oxidation of Hydrocarbons," Applied Catalysis A: General, **81**, p. 239 (1992).
7. Butt, J. B., and E. E. Petersen, "Activation, Deactivation, and Poisoning of Catalysts," Academic Press, 1988.
8. Agarwal, S. K., and J. J. Spivey, "Deactivation of Oxidation Catalysts," Final Report prepared for the U.S. Air Force, Tyndall Air Force Base, FL. Research Triangle Institute, Research Triangle Park, NC, November 1991.

Carbon Decontamination of Activated Sludge From Plastics Processing

Y. El-Shoubary and D. E. Woodmansee

General Electric Research and Development Center, Schenectady, NY 12301

INTRODUCTION

This paper is concerned with the site treatment of wastes generated at a plastic manufacturing plant. Most of the waste produced in the plastic manufacture process is transferred to an onsite treatment facility. Figure 1 shows a flow diagram of the sludge process. The waste, containing approximately 400 ppm COD, is first mixed with powder-activated carbon to enhance bioreaction and then goes through a two-stage operation. The first stage, known as thickening, is physiochemical and involves the conversion of discrete, unflocculated particles of the suspension into a thickened underflow with a clear overflow, which is accomplished by the addition of a coagulant or a flocculent. This process is of vital importance in terms of establishing the conditions required for the biodegradation (biomass) which will start on the carbon substrates. The second stage is to reduce the remaining water content of the thickened underflow by a suitable solid liquid separation process, thereby transforming it into a compact rigid solid containing only smaller quantities of water (sludge).

The objective of this work is to try to break the biocell mass and separate the fine carbon from the sludge using hydroclones and/or flotation equipment. The carbon will be regenerated for reuse.

LITERATURE SURVEY

The art of separation using flotation techniques is well known. The flotation techniques are used to separate minerals from their raw materials, coal, from its gangue and contaminant from soils (1:4, 18:24). No attempts to separate the processed sludge carbon were found in the published literature. However, several books and publications were found on sludge process control, kinetics, microbial theory, factors affecting the process and sludge activation methods (5:17). This literature was studied to find a method to break the carbon biocell mass and liberate the carbon. Once the cell mass is broken, techniques to float the carbon away from the rest of the sludge components could be developed.

EQUIPMENT

The equipment used in this study is a hydroclone and a flotation cell. Figure 2 shows a schematic diagram of a hydroclone and a flotation cell. The hydroclone used in this study was supplied by Mozley Corporation located in the United Kingdom.

The flotation cell used in this study was a 4-cell flotation device model #5-DR float supplied by Denver Equipment Company, Colorado Springs, Colorado. Air is pumped through a vein-type rotor revolving within a fixed stator.

In addition, Perkin Elmer Thermogravimetric Analyzer 7, thermal analyzer controller (TAC/PC), IBM personal system 2 and Perkin Elmer graphics plotter 8 were used to estimate the carbon separation performance.

The materials used were Fine Activated Charcoal (400 mesh) and coconut activated charcoal (8–12 mesh). The two types of carbon were obtained from EM Science. The surface area of the two carbons are 750,000 and 1,200,000 sqm/kg respectively.

Finally, two different types of sludge were obtained. The first one will be referred to as agglomerated sludge. The second will be referred to as nonagglomerated sludge. The first was collected from the clarifier after the coagulant or flocculent

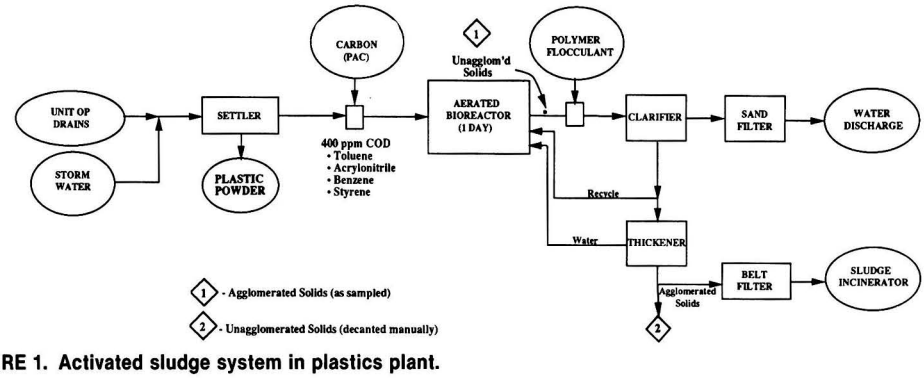

FIGURE 1. Activated sludge system in plastics plant.

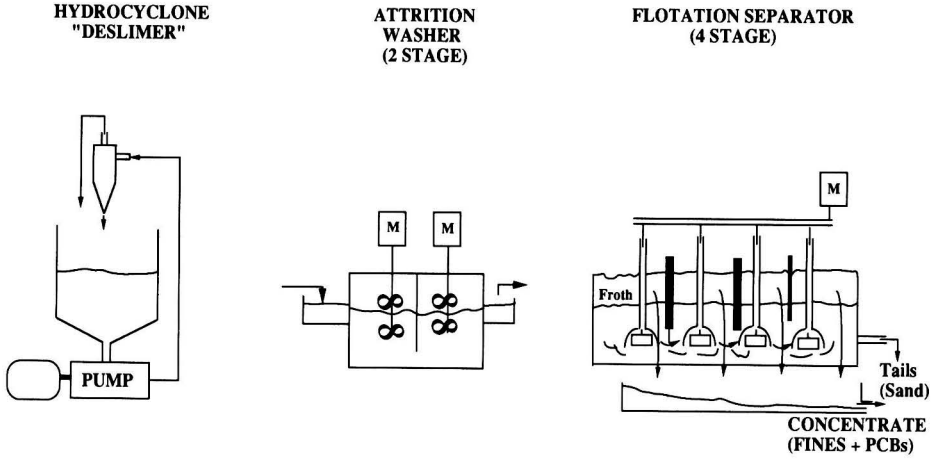

FIGURE 2. Schematic diagram of the flotation equipment used in this study.

was added. The second was obtained from the thickener prior to the addition of the coagulant or the flocculent (see Figure 1).

MEASUREMENT PERFORMED ON SLUDGE SAMPLES

Moisture Content

Several samples of each sludge were dried for 14 hours at 105°C. A Fisher Isotemp oven 200 Series, obtained from Fisher Scientific, Springfield, NJ was used for the drying. The difference between the dry weight and the wet weight was considered to be the weight of the sludge liquid. Accordingly, the percent solid in each sample was determined. The agglomerated sludge contained 18–20% solids, while the nonagglomerated sludge contained 2–4% solids.

Carbon Content

The carbon content of both types of sludge was difficult to determine. However, using thermogravimetric techniques the value of the carbon content could be accurately estimated. A clean virgin carbon sample was obtained and run in a nitrogen atmosphere. Table 1 gives the run conditions. A sample of the dried sludge was run under the same conditions and the difference in weight loss was assumed to be due to other materials that exist in the sludge, i.e., materials other than carbon. It should be mentioned here that the carbon content obtained using this technique was in total agreement with the values obtained from the plant manager. The carbon content for the agglomerated sludge was found to be 20% with respect to dry weight and 40 to 60% based on dry weight for the nonagglomerated sludge. The wide range was due to the sample date of collection. On any given day the waste produced at the facility may vary in concentration but not in content.

Table 1 Thermogravimetric Analyzer Run Conditions for the Sludge Work

1	Sample Weight	20–30 mg
2	Gas Used	Nitrogen
3	Heating Rate	10°C/min
4	Gas Flow Rate	40 cc/min
5	Start Temp	35°C
6	Pressure	1 atm
7	Final Temp	800°C

Two runs were performed by adding granular-activated carbon (GAC) to the sludge. The two runs were performed to clarify the possibility of depressing the fine carbon and other fine materials and floating the coarse contents of the sludge with the GAC. Also, the possibility of using GAC instead of PAC is attractive since screening separation is possible.

In several other runs, it was eminent to add powder-activated carbon to the sludge to prevent the generation of any faint odors and to magnify the visual observations of the carbon separation. The intent of this work was to study the separation of carbon from sludge and not to differentiate between both added carbon and biological cell-mass carbon.

Screen Analysis

Each type of sludge was screened using wet-sieving techniques. The screen analysis showed that both sludges contained more than 70% of their weight in particles finer than 200 mesh (0.074 mm diameter). These results show that the total separation of carbon may be difficult, if not impossible, because there is little difference in the size or density between the carbon particles and the other fine particles. Figure 3 shows the screen analysis results for both sludges.

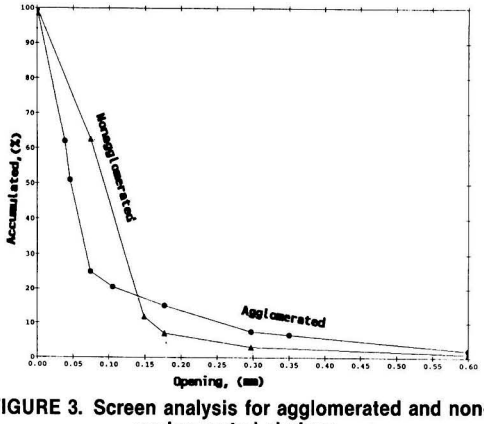

FIGURE 3. Screen analysis for agglomerated and nonagglomerated sludges.

Table 2 Sludge Runs Measurements

Run No.	Code No.	SLUDGE FEED	FEED Flot'n Feed (gms)	Flot'n Solids (FS/Tot)	Tot Carb. Solids (TC/FS)	Coll'r (gms)	Froth'r (gms)	PH	FROTH Tot. Mass [TM] (gms)	Tot Solids (TS/TM)	Tot Carbon (TC/TS)	Color	TAILS Tot. Mass [TM] (gms)	Tot Solids (TS/TM)	Tot Carbon (TC/TS)	Color
1	S1	Agglom.,	20257	0.069	0.493	None	3		10562	0.071	0.375	Tan	9695	0.067	0.625	Dk Brn
4	S4	Agglom.,	27779	0.102	0.631	398	3	7	9190	0.112	0.229	Tan	18589	0.097	0.721	Black
5	6	Agglom.,	23100	0.131	0.716	None	3	7	9800	0.1	0.68	Tan	13300	0.154	0.766	Gray
6	NS-1	Agglom.,	3975	0.208	0.204	None	15	7	1984	0.13	0.189	Dark Tan	2462	0.231	0.2	Gray
7	NS-4	Agglom.,	7141	0.17	0.369	60	3	10	1635	0.151	0.198	Dark Tan	5506	0.175	0.39	Dk Brn
8	S5	Unagglom.,	16630	0.029	0.742	None	3	7	13170	0.034	0.74	Dark Blk	3460	0.008	0.784	Lt Tan
9	S7	Unagglom.,	13931	0.028	0.490	None	3	7	5532	0.019	0.619	Dark Blk	8323	0.034	0.447	Gray
10	NS-3	Unagglom.,	80182	0.046	0.660	202	3	8	2179.2	0.045	0.3	Tan	5839	0.046	0.8	Black
12	NS-5	Unagglom.,	8213	0.036	0.600	604	1	7.5	1681	0.036	13.33	Tan	6532	0.036	0.72	Lt Brn
13	NS-6	Unagglom.,	8667	0.099	0.703	454	3	10	2655	0.082	0.44	Dark Tan	5549	0.12	0.3	Lt Black
14	NS-7	Unagglom.,	6712	0.093	0.660	250	3	<6	4293	0.1	0.14	Red	2419	0.089	0.93	Brick Red

Table 3 Summary of Separation Results

Run No.	Code No.	SLUDGE FEED	Composition As Recd Solids (SS/Tot)	Blol. Carbon (BC/SS)	CLASS'N Hydroclone Time (min)	Sorptive Carbon (SC/SS)	WASHING Attrition Time (min)	FLOTATION COLLECTOR (name)	FROTHER (name)	RESULTS CARBON ENRICHM'T [%C (talls)/ %C (feed)	CARBON YIELD [TC (talls)/ TC (feed)]
1	S1	Agglom.,	0.074	0.388	0	0.207	30	—	Pine Oil	1.268	0.589
4	S4	Agglom.,	0.175	0.420	0	0.57	20	Ca(OH)2	4M,2 Pentanone	1.143	0.847
5	6	Agglom.,	0.231	0.630	0	0.301	35		4M,2 Pentanone	1.070	0.702
6	NS-1	Agglom.,	0.208	0.204	0	0	25		Triton X100	0.980	0.702
7	NS-4	Agglom.,	0.197	0.270	0	0.157	30	H_2O_2 + Starch	Pine Oil	1.057	0.880
8	S5	Unagglom.,	0.015	0.500	0	0.935	15		Pine Oil	1.057	0.060
9	S7	Unagglom.,	0.028	0.490	0	0	12		Pine Oil	0.912	0.060
10	NS-3	Unagglom.,	0.047	0.660	0	0	10	Rubber cem.	Pine Oil	1.212	0.890
12	NS-5	Unagglom.,	0.042	0.600	0	0	15	Starch	Pine Oil	1.200	0.950
13	NS-6	Unagglom.,	0.049	0.703	0	0	12	Na silicate	Pine Oil	0.427	0.702
14	NS-7	Unagglom.,	0.036	0.600	0	0	15	Pot. perman.	Pine Oil	1.409	0.486

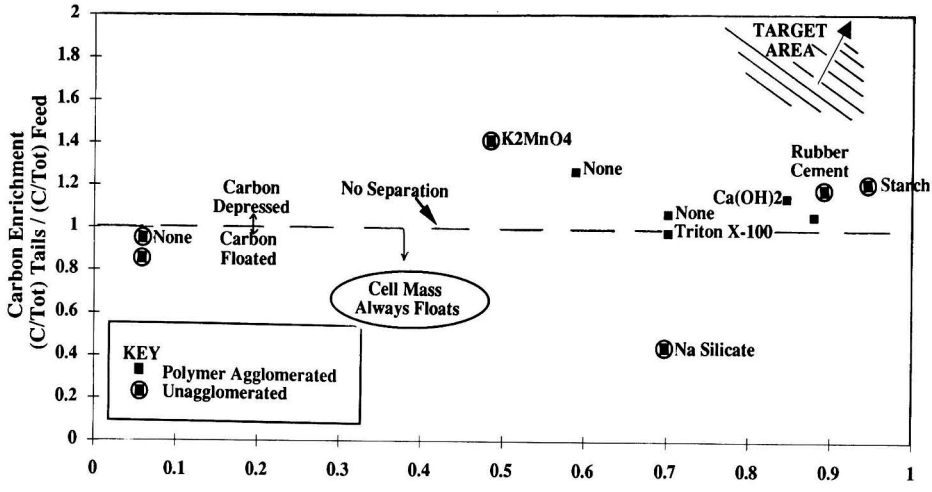

FIGURE 4. Yield of carbon to tails (C in tails/C in feed).

Soxhlet Extraction

The dried samples of each sludge were extracted using soxhlet equipment and methylene chloride. Although no numerical values were obtained from the analysis, it was virtually obvious from the extract, that the majority of the samples consisted of plastics.

EXPERIMENTAL RUNS

A total of 14 runs (12 flotation and 2 hydroclone) were performed in this study. Tables 2 and 3, attached, give the type of equipment and additive used in each run.

In each flotation run a sample was collected from the feed, froth and tails. In case of the hydroclone runs, a sample was collected from the overflow and underflow. Each sample was dried at 105°C and the percent solid in each sample was calculated. Each sample was run in the TGA equipment in the same manner described above, to determine the percent carbon in the matrix. When an additive was added to the sludge as a depressant, a pure sample of the additive was run in the TGA module in nitrogen atmosphere. Three temperatures were chosen to carry the following calculation.

Total weight loss = Carbon weight loss

+ Other material weight loss + Depressant weight loss

DISCUSSION

The separation results presented in Tables 2 and 3 are shown graphically in Figure 4 for those runs involving flotation. The carbon enrichment on the ordinate can be viewed as a separation factor, while the abscissa reflects how much of the feed carbon ends up in the tails. These results show that the permanganate provided the best separation, but at a low carbon yield of only 50%. The starch additive was good at depressing all the carbon to the tails, but too much of the plastic and cell mass came down with the carbon to make its use practical.

It is apparent that two major issues need to be addressed separately in order to recover more completely the biological and decontaminating carbon added to the wastewater. The first is to effect a separation of the other materials (probably plastic particles) from the rest of the sludge. These particles do not float with the cell mass, but instead appear to be depressed with the carbon. Either these particles should be filtered prior to processing the cell mass, or they should be separated from the flotation tails before the carbon is returned for reactivation. The large burden of nonactivated carbon combustibles in the tails would overload any carbon reactivation system.

From the results in Figure 4, one process option that might be followed is first to float the cell mass and carbon away from the plastic particles, and then to separate the carbon from the cell mass. The sodium silicate appears to be an excellent collector for the carbon and cell mass, floating it away from the plastic particles. Once this separation is accomplished, a second attrition washing would be performed using a potassium permanganate to break up the cell mass with a second flotation to follow using the starch as a carbon depressant.

To break the cell mass, hot water (80°C) was mixed with the agglomerated sludge in the attrition scrubber (Run 5). In Run 7, hydrogen peroxide was added to the agglomerated sludge in the attrition scrubber to achieve the same purpose. In both runs, the bacteria might have been destroyed, but the cell mass was only partially broken. This partial breakdown of the cell mass is reflected in the carbon percentage of yield of Runs 5 and 7 (see Table 3). The percentage of yield was 7.2% and 88% for Runs 5 and 7, respectively, compared to 58.9% for Run 1, in which no steps were taken to break the cell mass. It was felt that a longer mixing time of the sludge with both or any of the above additives with a reasonable residence attrition time will increase the cell mass breakdown and consequently the percentage of carbon yield.

Table 4 Comparison Between Agglomerated and Unagglomerated Sludges

	Unagglomerated	Agglomerated
Percentage Solid	1.5-5%	18-20%
Odor	Weak	Very Strong
Cell Mass	Did not exist	Exists and always floated
Carbon Separation	Moderately difficult	Extremely difficult
Color	Black	Gray
Sample Location	Thickener No coagulant or flocculant	Clarifier with coagulant or flocculant

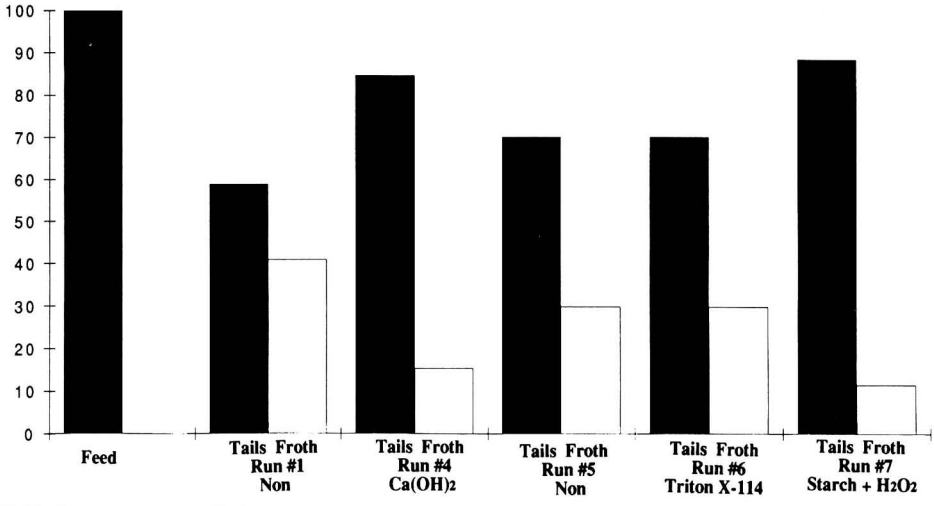

FIGURE 5. Carbon percent split for agglomerated sludge using flotation equipment.

AGGLOMERATED VS. NONAGGLOMERATED SLUDGE

A comparison between the two sludges is given in Table 4. The two sludges behaved differently in the flotation cell. The cell mass of the agglomerated sludge always floated even when depressant was used. Accordingly, it was easier to depress the carbon and contain it to the tails and let the cell mass float. This idea was successful in most runs.

MASS BALANCE AND PERCENTAGE OF CARBON

Table 2 summarizes the mass balance obtained for each run. Mass balance error never exceeded 7%. This is considered satisfactory, keeping in mind the large dilutions in the process and the scale of the experiments. The mass balance was forced to close through the increase or decrease on the added clean water in the flotation cell.

AGGLOMERATED SLUDGE RESULTS

The results of the agglomerated sludge are summarized as carbon percentage split in Figure 5, and as percentage of carbon in both the froth and the tail in Figure 6. The carbon split itself between the tails and the froth at the values are shown in Figure 5. The percentage of carbon showed in the tails ranged from 59% with no additive (Run 1) to 89% when calcium hydroxide was added (Run 4). Although these result appear to be satisfactory, it has no value without finding the actual carbon concentration in every produced flotation stream (see Figure 6). If successful separation is to be achieved, the percentage of carbon in the tails or even in the froth should be high enough to grant economical carbon regeneration. The existence of impurities with the carbon will translate into more energy input for the regeneration and consequently higher cost. On the other hand, the existence of the depressant with the regenerated carbon will allow saving the addition of the fresh depressant. This balance should be studied in each run. The

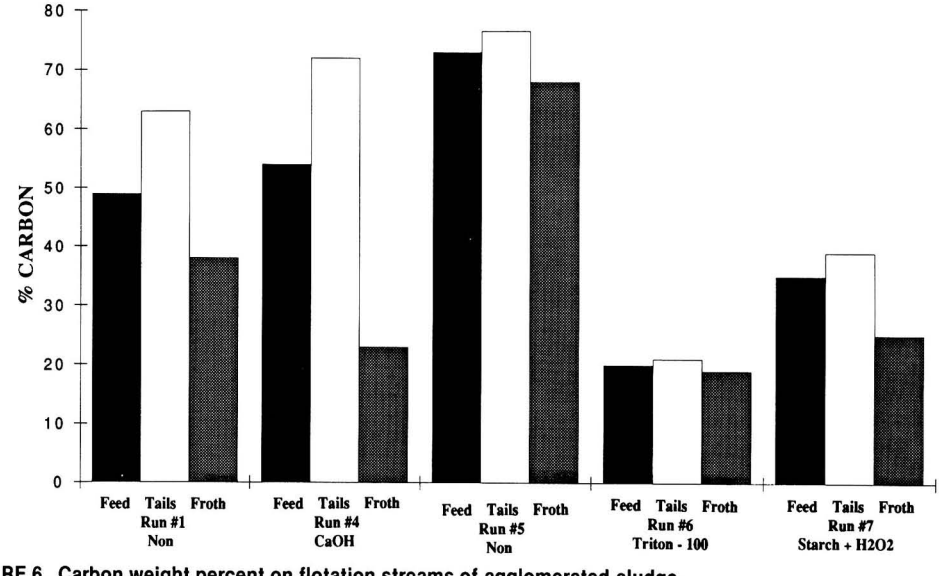

FIGURE 6. Carbon weight percent on flotation streams of agglomerated sludge.

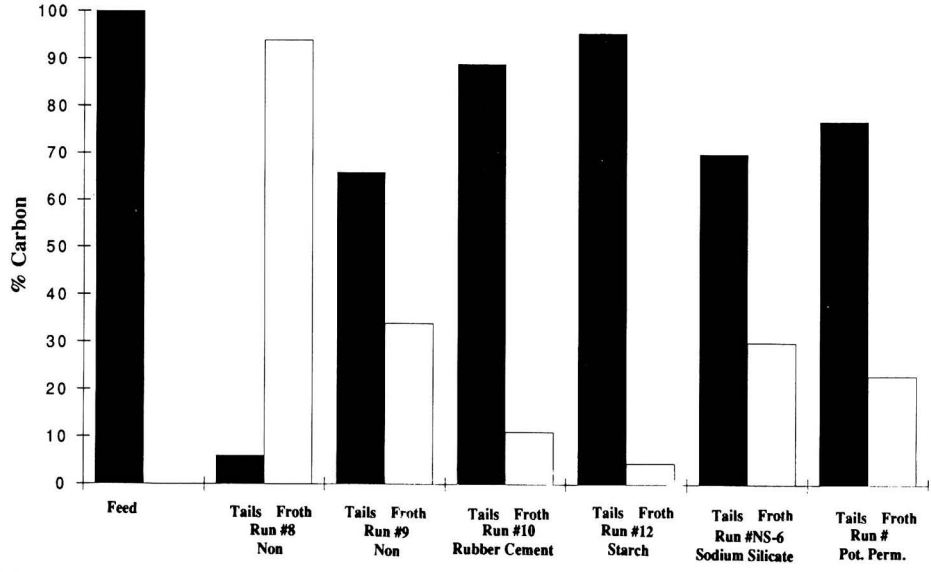

FIGURE 7. Carbon percent split for nonagglomerated sludge using flotation equipment.

calcium hydroxide (Run 4) had the highest success since the percentage of carbon in the tails was 72% and only 28% impurities, which were mostly starch.

NONAGGLOMERATED SLUDGE RESULTS

The same analysis was applied to the nonagglomerated sludge. Figure 7 shows the carbon percentage split in the tails and the froth and Figure 8 shows the percentage of carbon in each flotation stream. It is clear from Figure 7 that the percentage of carbon recovered with the tails increased when a depressant was used. Starch, potassium permanganate and rubber cement did depress the carbon extremely well. Again these results remain inconclusive without examining the percentage of carbon in each flotation stream (see Figure 8). The percentage of carbon in each stream of the nonadditive runs were almost equal, i.e., the separation was poor. The rubber cement (Run 10) and potassium permanganate (Run 14) runs showed tails with carbon concentration of 80% and 93% respectively. These results are considered a great success.

If the depressant is to be recycled in the process, both the starch and sodium silicate runs are considered a success in separation. It should be mentioned here that because of the low solid percentage of it in the feed (2–5%) the additives or depressant to the sludge affected the calculation of the percentage of carbon in each stream. The numbers were extremely sensitive to the amount of additive in the sludge.

HYDROCYCLONE RUNS

The carbon separation results obtained using the hydrocyclone are summarized in Figures 9 and 10. The carbon split in

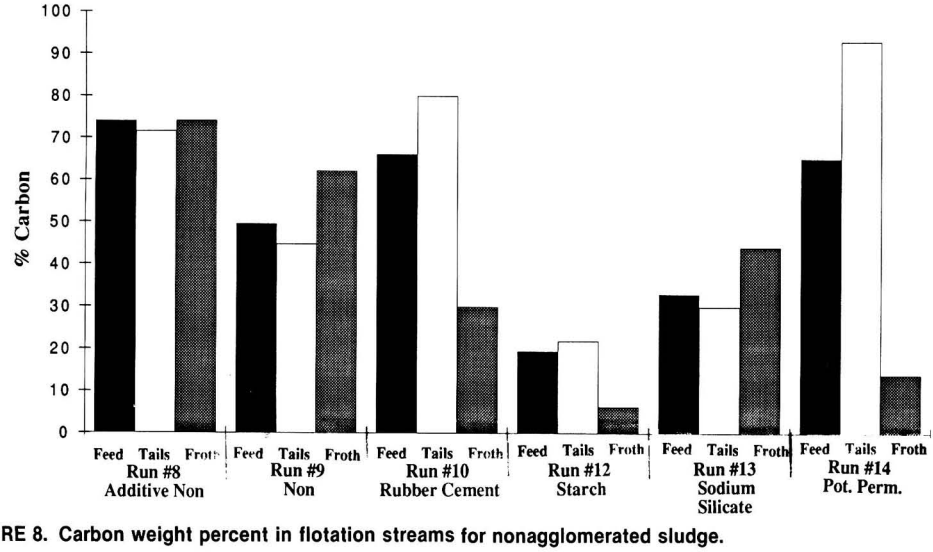

FIGURE 8. Carbon weight percent in flotation streams for nonagglomerated sludge.

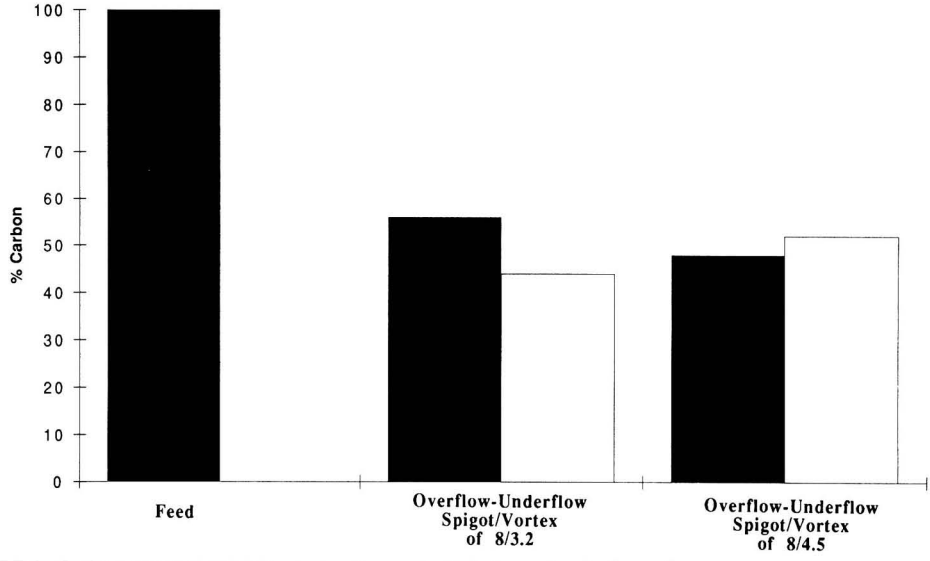

FIGURE 9. Carbon percent split for nonagglomerated sludge using hydrocyclone.

almost equal amounts between the overflow and the underflow regardless of the spigot/vortex combination. In addition, the percentage of carbon in the overflow stream was close to 50%. This means that both the impurities and the carbon were recovered in almost equal amounts in both the overflow and the underflow. In conclusion, the hydrocyclone failed to produce any separation regardless of the spigot/vortex combination. It should be mentioned here that the hydrocylone runs were difficult because of the existence of large plastic particles which caused plugging of the spigot.

CONCLUSIONS

The following are the conclusions resulting from this research:

- In general it was clear that the carbon in the nonagglomerated sludge was much easier to separate and to handle than that in the agglomerated sludge. The biomass was hard to break in the latter case. Even the existence of the polymer in the agglomerated sludge might have altered the performance of the flotation cell.
- The hydrocyclone failed to obtain any sludge separation. The flotation equipment was a more powerful tool in the separation process.
- Sodium silicate and starch appear to be excellent collectors and depressants for carbon.
- The concentration of the solids in the nonagglomerated sludge (1.5–5%) was considered very low. Any additive to the sludge will affect the final performance of the separation. The additives should be recycled back to the feed to make the process more attractive economically.

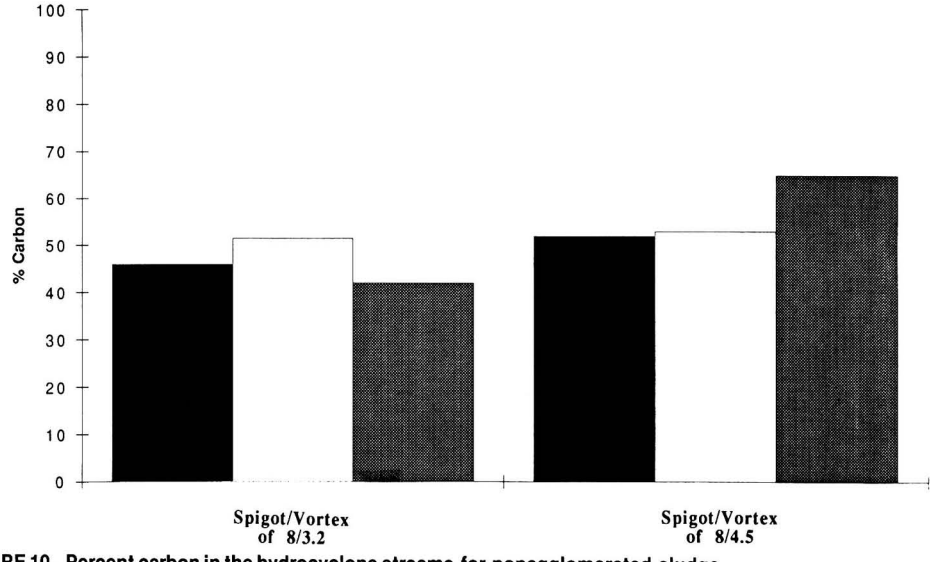

FIGURE 10. Percent carbon in the hydrocyclone streams for nonagglomerated sludge.

- The pH, hydrogen peroxide, and the attrition scrubber residence time increased the cell mass breakdown and consequently improved the carbon separation with flotation.
- If a good separation of carbon from the cell mass can be achieved, there is a good opportunity to decontaminate the discarded sludge and perhaps reactivate the carbon.

RECOMMENDATIONS

The following recommendations are made:

- Two-stage flotation is recommended to achieve a better carbon separation. In the first stage, plastic materials should be recovered using a cell mass/carbon collector such as sodium silicate. In the second stage, a carbon depressant, such as rubber cement or potassium permanganate, should be used to depress the carbon and float the cell mass.
- More work is needed in the biocell breakdown in order to obtain better carbon separation.
- The amount of the solids in the nonagglomerated sludge needs to be increased through decanting the water or filtration, thus eliminating the sensitivity of the results to the percentage of additive or depressant.

ACKNOWLEDGMENT

The authors appreciate the tireless efforts of Lynn Ann Smullen, who assisted with the experimentation and conducted most of the analytical work, and of Barbara Whitten, who also provided assistance in entering the data into spreadsheets and drawing most of the figures, as well as putting the text into its final form. Tom Wrobleski provided the sludge samples and described the operation of the plant wastewater system.

LITERATURE CITED

1. Gaudin, A. M., *Flotation*, McGraw-Hill Publishing Company, New York (1931).
2. *Chemical Engineering Progress Symposium Series*, No. 15, Collected Research Papers, AIChE, 1954.
3. Fuerstenau, M. C., *Flotation—A. M. Gaudin Memorial*, Vol. 1, American Institute of Mining, Metallurgical, and Petroleum Engineers, Inc., New York (1976).
4. Fuerstenau, M. C., *Flotation—A. M. Gaudin Memorial*, Vol. 2, American Institute of Mining, Metallurgical, and Petroleum Engineers, Inc., New York (1976).
5. Benefield, L. D., and C. W. Randall, "Evaluation of Comprehensive Kinetic Model for the Activated Sludge Process," *J. of the Water Pollution Control Federation*, **49**, pp. 1636-41 (1977).
6. Benefield, L. D., and C. W. Randall, *Biological Process Design for Waste-Water Treatment*, Prentice-Hall Inc., New York (1980).
7. Benjes, H. M., *Handbook of Biological Wastewater Treatment*, Garland STPM Press, New York (1980).
8. Cech, J. S., J. Chudoba, and P. Grau, "Determination of Kinetic Constants of Activated Sludge Micro-organisms," *Water Science and Technology*, **17**, 213, pp. 259-72 (1984).
9. Cole, C. A., J. B. Stamberg, and D. F. Bishop, "Hydrogen Peroxide Cures Filamentous Growth in Activated Sludge," *J. Water Pollution Control Federation*, **45**, pp. 829-36 (1973).
10. Demel, I., and C. H. Mobius, "Improving the Settling of Activated Sludge by Chemical Additives," *Water Science and Technology*, **20**(1), pp. 283-286 (1988).
11. Downing, A. L., and A. B. Wheatland, "Fundamental Consideration in Biological Treatment," *Transactions of the Institution of Chemical Engineers*, **40**, pp. 91-103 (1962).
12. Hopwood, S. R., and A. L. Downing, "Factors Affecting the Role of Production and Properties of Activated Sludge in Plants Treating Domestic Sewage," *Journal and Proceedings for the Institute of Sludge Purification*, **64**, pp. 435-452 (1965).
13. Parker, D. S., D. Jenkins, and W. J. Kaufman, "Physical Conditioning of the Activated Sludge Flow," *J. of the Water Pollution Control Federation*, **43**, pp. 1817-1824 (1971).
14. Randall, C. W., C. D. Benefield, and D. Buth, "The Effects of Temperature on the Biochemical Reaction Rates of the Activated Sludge Process," *Water Science and Technology*, **14**, pp. 413-430 (1982).
15. Cattar, S. A., S. Ramia, and J. C. N. Westwood, "Calcium Hydroxide (Lime) and the Elimination of Human Pathogenic Viruses from Sewage Studies with Experimentally-Contaminated (Poliovirus Type I, Sabin) and Pilot Plant Samples," *Canadian Journal of Public Health*, **67**, pp. 221-226 (1976).
16. Smith, P. G., and D. Coackley, "A Method for Determining Specific Surface Area of Activated Sludges by Dye Adsorption," *Water Research*, **17**, pp. 595-598 (1983).
17. Tomlinson, E. J., and B. Chambers, "Methods for Preventing of Bulking in Activated Sludge," *J. of Water Pollution Control*, **78**, pp. 524-538 (1979).
18. Zimmerman, R. E., "Froth Flotation," *Coal Preparation*, 3rd ed., Leonard, J. W., and Mitchell, D. R., eds., AIME, New York (1968).
19. Brady, G. A., and A. W. Gauger, "Properties of Coal Surfaces," *Industrial and Engineering Chemistry*, **32** (1940).
20. Horsley, R. M., and H. G. Smith, "Principles of Coal Flotation," *Fuel*, **30**, pp. 54-63 (1951).
21. Miller, F. G., "Reduction in Sulfur in Minus 28 Mesh Bituminous Coal," *Trans ASME*, **229**, pp. 7-14 (1964).
22. Neczaj-Hruzewicz, Jr., J. Szczypa, and H. Czarkowski, "Influence of Flotation Reagents on Formation of Gangue Slime Coatings on Coal," *Trans. Institution of Mining and Metallurgy*, **83**, pp. 261-3 (1974).

Field Testing Solar Photocatalytic Detoxification on TCE-Contaminated Groundwater

Mark S. Mehos and Craig S. Turchi

National Renewable Energy Laboratory, 1617 Cole Blvd., Golden, CO 80401

The Solar Detoxification Field Experiment was designed to investigate the photocatalytic decomposition of organic contaminants in groundwater at a Superfund site at Lawrence Livermore National Laboratory. The process uses ultraviolet (UV) energy available in sunlight in conjunction with a photocatalyst, titanium dioxide, to decompose organic chemicals into nontoxic compounds. The destruction mechanism, as in many other advanced oxidation processes, involves hydroxyl radicals. The field experiment was developed by three federal laboratories: the National Renewable Energy Laboratory, Sandia National Laboratory, and Lawrence Livermore National Laboratory. The United States Department of Energy funded the experiment. Groundwater at the test site was contaminated with trichloroethylene (TCE). A factorial test series examined four separate process variables: pH, catalyst loading, flow velocity, and solar intensity. Lowering the pH from pH 7 to pH 5 had the largest single effect, presumably by minimizing interference by bicarbonate. The catalyst was found to operate more efficiently at low, e.g. ambient sunlight, UV light levels. Information from these field tests suggest that treatment costs for the solar process would be similar to those for more conventional technologies.

INTRODUCTION

The ultraviolet (UV) light-induced photocatalytic oxidation of organic molecules is a recognized phenomenon [*1*]. The process uses UV light to activate a semiconductor catalyst and generate hydroxyl radicals, OH·, as depicted in Figure 1. The oxidation chemistry and potency of the photocatalytic process are similar to those of other chemical oxidation methods that generate hydroxyl radicals, e.g., UV/hydrogen peroxide and UV/ozone. Given sufficient exposure to hydroxyl radicals, most organic pollutants will oxidize into nontoxic materials, such as carbon dioxide and water. In the case of the commonly found chlorinated solvents, dilute hydrochloric acid is also formed.

The feasibility of using sunlight in conjunction with a photocatalyst to destroy organic water pollutants was demonstrated by researchers in the mid-1980s [*2, 3, 4*]. In the solar process, sunlight illuminates the contaminated water contained within a transparent receiver. The catalyst is either suspended as a slurry in the water or supported on some fixed matrix within the reactor. Although the chemistry can be driven by either sunlight or UV lamps, the solar process requires substantially less electric power. Thus, solar water detoxification contains benefits compared to other treatment technologies, notably low power consumption and on-site contaminant destruction.

The first solar detoxification field experiment was designed to investigate the photocatalytic decomposition of organic contaminants in groundwater at a Superfund site at Lawrence Livermore National Laboratory. The field experiment was developed by three federal laboratories: the National Renewable Energy Laboratory (NREL), Sandia National Laboratory Al-

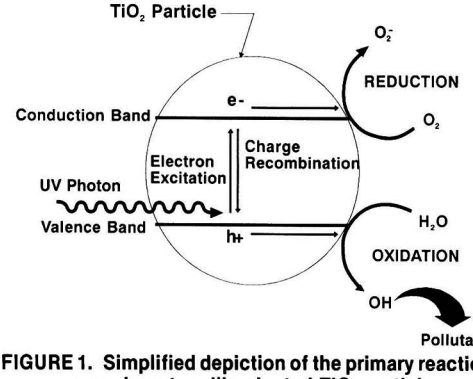

FIGURE 1. Simplified depiction of the primary reactions occurring at an illuminated TiO_2 particle.

Table 1 Inlet Groundwater Conditions from Monitoring Wells at Livermore Site

Constituent	Range
Trichloroethylene (TCE)	80–500 μg/L
Other Volatile Organic Compounds	< 10 μg/L
Bicarbonate	200–500 mg/L
pH	6.5–8.0

buquerque (SNLA), and Lawrence Livermore National Laboratory (LLNL). The objectives of the experiment include the advancement of the technology to on-site waste-treatment tests, the compilation of test data to verify laboratory research and guide future demonstrations, the development of safe operational procedures, and acquisition of data for process cost estimation.

SITE HISTORY

LLNL is located outside Livermore, CA, about 30 miles (50 km) east of the San Francisco Bay area. Groundwater contamination at LLNL dates from World War II when the facility was a Naval Air Station and training and maintenance facility. Large quantities of trichloroethylene (TCE) and other chemicals which were used to clean engine parts during this period now contaminate the groundwater in several locations. As part of the feasibility studies under the Comprehensive Environmental Response, Compensation, and Liability Act (CERCLA), LLNL is currently studying the operation of two electric UV/hydrogen peroxide treatment facilities to pump and treat the contaminated groundwater plumes resulting from this period. Other types of advanced oxidation systems, including the solar photocatalytic process, are being evaluated and planned for testing. The results of the pilot studies will lead to an approved plan for the clean up of the site.

The solar detoxification field experiment was positioned to draw off water from an existing well pipeline, treat it in the solar-driven system and return it to the pipeline so that it could be processed by a permitted treatment facility before being discharged. Four monitoring wells connected to the pipeline can be run individually or in parallel. This allowed some flexibility in choosing the water inlet conditions for the solar process (see Table 1).

EXPERIMENTAL APPARATUS

The system at Livermore had three major components: a concentrating solar collector, a receiver/reactor, and a mobile equipment skid. A sketch of the field experiment is shown in Figure 2 and a simplified operational schematic is provided as Figure 3. In addition, tanks were provided for settling the titanium dioxide (TiO_2) catalyst and for intermediate storage of the treated water. The collectors for this experiment consisted of two drive strings of commercially available concentrating parabolic solar troughs. The parabolic troughs were resurfaced for this experiment with a reflective film designed to enhance the UV reflectivity. The solar-UV weighted reflectivity of the film is nominally 85%. Each drive string is 120 ft long by 7 ft wide (36.6 m by 2.1 m) resulting in an aperture area of 840 ft^2 (78 m^2) per string. The troughs are aligned on an east-west axis and automatically tracked the sun during an experiment.

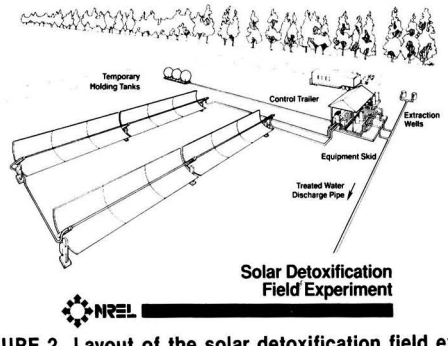

FIGURE 2. Layout of the solar detoxification field experiment at Lawrence Livermore National Laboratories (LLNL).

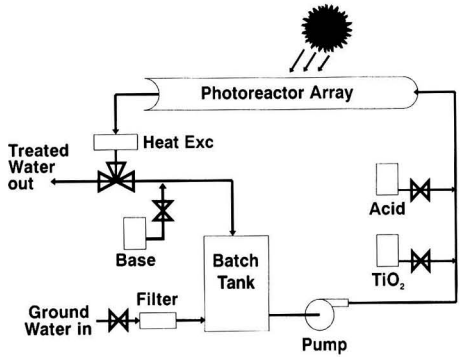

FIGURE 3. Flow schematic of the solar detoxification field experiment.

The receiver/reactor for these experiments consisted of a 2 inch (51 mm) diameter borosilicate glass pipe. The reactors ran along the length of the collectors at the focal line of the parabolic troughs. An effective sunlight concentration ratio of approximately 20 was calculated for this arrangement, based on the width of collector and the half-circumference of the glass pipe and including reflective and transmissive losses.

The third component of the system was the ancillary equipment necessary to support the experiment. This equipment consisted of the main process pump, a 150 gallon (570 L) tank, tanks and pumps required for pH adjustment and slurry addition, a heat exchanger for maintaining constant temperature, and a control panel. Information such as reactor inlet and outlet pH, inlet and outlet temperature, and rate of flow were logged at 30-second intervals and stored on a computer. In addition, solar radiometers recorded UV and full-spectrum sunlight. These instruments monitored direct-normal as well as global-horizontal insolation.

SYSTEM KINETICS AND MODELING

The field experiment was operated in both single-pass and recirculating-batch modes. In the more common recirculating operation, the fluid was continuously recirculated between the solar collector and a tank in which no reaction occurs (Figure 3). In the general case this system can be modeled as a plug flow reactor and a perfectly mixed tank connected in a loop. In these experiments, first order kinetics adequately described the kinetics within the photoreactor.

In the large field system, the amount of conversion per pass through the reactor can be appreciable. As the relatively clean water exiting the reactor is mixed with the "dirty" water in the batch tank the resulting water sent to the reactor has a lower concentration. Because rate usually decreases as concentration decreases, the overall rate in the system suffers. Thus, unless properly accounted for, the presence of the tank

will alter the perceived performance of the photoreactor. The fundamental equation describing the recirculating batch scheme is a partial differential equation in position and time. Although this expression can be rigorously solved, a simple, less computationally intensive, solution is possible. A procedure for properly evaluating kinetics from a recirculating batch system is discussed in reference [5].

To determine the true kinetic performance of an experimental reactor, one can correct for effects of a mixing tank. Yet in a full-scale system, where the goal is to obtain the best possible performance, mixing water from the reactor outlet in a large batch tank will decrease the overall processing rate. Thus, if a full scale system operates in a recirculating mode it is desirable to minimize the size of or eliminate the batch tank.

EXPERIMENTAL TEST PLAN AND RESULTS

The test plan for the field experiment was broken down into the following series of experiments:

—Single-pass experiments with groundwater
—Recirculating batch experiments with TCE-spiked deionized water
—Recirculating batch experiments with groundwater
—Recirculating batch follow-on experiments with groundwater

All experiments used a fresh sample of titanium dioxide. The TiO_2 was purchased from Degussa Corporation and used as supplied. According to the manufacturer's specifications, the P25 brand TiO_2 is a anatase/rutile mix that is approximately 75% anatase. The fundamental particle size is given as 30 nm. Experience shows that these particle agglomerate to larger sizes when in water. The powdered catalyst was added to the experiment as a concentrated slurry. During single-pass operation, destruction of TCE took place in one pass through the photoreactor. Samples were taken at the inlet and outlet to the solar collectors. (There were no intermediate sample ports in the solar array.) To maximize the level of destruction, the full set of collectors was based. In batch operation the contaminated water was recirculated continuously between the photoreactors and the batch tank on the skid. Samples were withdrawn from the tank at regular intervals. All batch experiments used only one drive string so that a detectable level of contaminant could be maintained over the 30 minute test period.

System performance was determined by measuring TCE concentration as a function of on-sun time. Water samples from the system were stored in 40 mL glass sample vials with Teflon-lined septa. The vials were stored upside down in a closed ice chest and transported to an on-site lab immediately following completion of the experiment. Samples were analyzed as soon as possible, usually within 24 hours. The samples were analyzed using a Hewlett-Packard 5880 gas chromatograph fitted with an electron capture detector. The chromatograph was connected to a Dynatech PTA-30 W/S autosampler and an OI Analytical 4460A purge and trap. The limit of detection of TCE for this arrangement is 0.5 μg/L.

Single-pass Experiments with Groundwater

The objective of the single-pass experiments was to verify that destruction of the contaminant to less than 5 μg/L (the U.S. Environmental Protection Agency's standard for drinking water) was possible in a single pass through the photoreactor. Prior laboratory tests showed that the high level of bicarbonate would slow the destruction process but that this effect could be offset by a reduction in pH. Therefore, destruction performance tests were performed with and without addition of dilute hydrochloric acid to the contaminated groundwater. The TiO_2 slurry metering pump was calibrated with water and adjusted to yield a catalyst loading of approximately 1.0 g/L TiO_2 (0.1 wt%) in the contaminated water entering the photoreactor.

Table 2 Single-Pass Experiments With and Without Acid Addition. Residence Time in Photoreactor was 10 Minutes.

Inlet [TCE] (μg/L)	pH	Outlet [TCE] (μg/L)
107	7.2±0.1	10
106	5.6±0.5	<0.5

Table 2 shows the results of the single-pass experiments. Two conditions were run: no pretreatment and adjustment of pH to approximately 5.6 by addition of dilute HCl. The flow rate through the reactor was maintained at approximately 4 gal/min (15 L/min) throughout the test, corresponding to a residence time of 10 minutes. The measured catalyst loading was 0.8 to 0.9 g/L of TiO_2.

Recirculating Batch Experiments with TCE-Spiked Deionized Water

The objective of these experiments was to establish a baseline TCE reaction rate in deionized water for comparison with other outdoor experiments and later groundwater experiments. These experiments were run near solar-noon using TCE spiked deionized water with initial concentrations representative of the groundwater (approx. 200 μg/L).

Prior to the baseline experiments, a series of leak tests and headspace-liquid equilibrium experiments were performed to ensure that loss of the contaminant was due solely to destruction by the solar detoxification process. An interesting discovery of these tests was that all glass piping and the translucent PVDF pipes leading to and from the photoreactors had to be covered even when the solar collectors were in the stowed position. If left uncovered, the TCE destruction due to ambient UV-light caused significant loss of the TCE before the solar troughs were focused on-sun. Subsequent leak tests verified that loss of TCE was due solely to photocatalytic oxidation.

Recirculating Batch Slurry Groundwater Experiments

The objective of the slurry groundwater experiments was to quantify TCE destruction rates in the groundwater and investigate the effects of several variables on the destruction process. A two-level factorial design was used for these experiments, which allowed us to determine the main effect of each variable (factor) on the system performance as well as any interaction effects that may have occurred. The experimental plan is shown in Tables 3 and 4.

Because it was not possible to rigidly control light intensity, all tests were run to investigate the variation in the first three factors around solar noon. An additional test was run in the mornings, thus providing several pairs of runs differing only

Table 3 Variables in Batch Slurry Tests with Livermore Groundwater

Variable	High Value (+)	Low Value (−)
Velocity in Reactor (Re)	63,000	21,000
pH	7.2 (as received)	5.0
Catalyst Loading (g/L)	1.0	0.3
UV Intensity	Solar noon	Off noon

Table 4 Test Matrix for Slurry Batch Groundwater Experiments

Replicate 1	Replicate 2	velocity	pH	catalyst loading	UV Intensity
S-01	S-09	−	−	−	+
S-02	S-10	+	−	−	+
S-03	S-11	−	+	−	+
S-04	S-12	+	+	−	+
S-05	S-13	−	−	+	+
S-06	S-14	+	−	+	+
S-07	S-15	−	+	+	+
S-08	S-16	+	+	+	+
S-17	S-25	−	−	−	−
S-18	S-26	+	−	−	−
S-19	S-27	−	+	−	−
S-20	S-28	+	+	−	−
S-21	S-29	−	−	+	−
S-22	S-30	+	−	+	−
S-23	S-31	−	+	+	−
S-24	S-32	+	+	+	−

in UV intensity. Two replicates of each test were run to determine the experimental error. This resulted in a total of 32 experiments.

A representative plot of three different runs is shown in

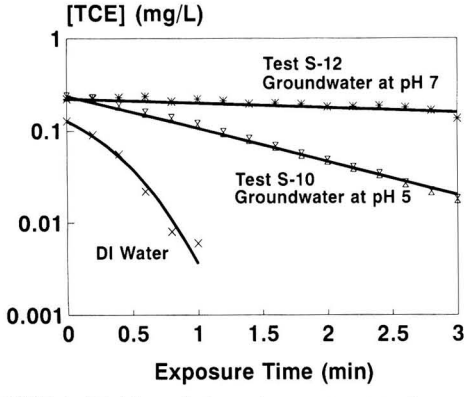

FIGURE 4. Trichloroethylene destruction data from recirculating batch tests.

Figure 4. The TCE concentration data are plotted versus exposure time. Lines represent model fits to the data. Exposure time represents the fraction of the total run time a given portion of water spends in the photoreactor ($t_{exposure} = tV_R/V_B$). Figure

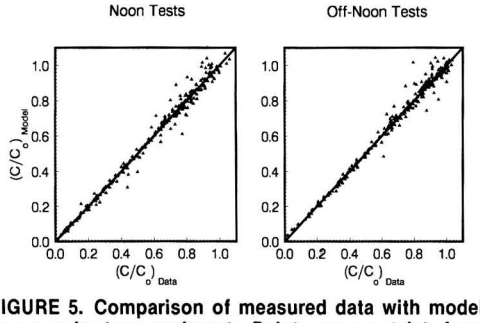

FIGURE 5. Comparison of measured data with model for groundwater experiments. Points represent data from tests S-01 through S-32, (see Tables 3 and 4).

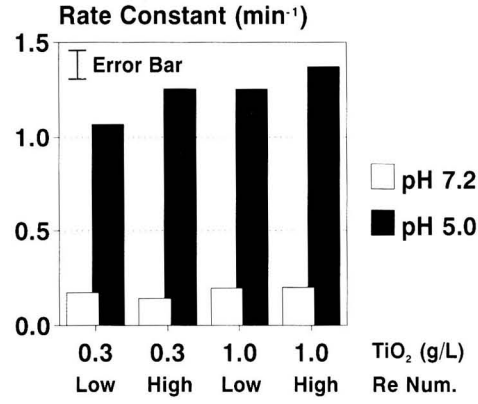

FIGURE 6. Calculated first-order rate constants from noon groundwater experiments outlined in Tables 3 and 4. Each bar represents the average of duplicate tests.

4 clearly shows the enhanced performance at pH 5 as opposed to pH 7. However, the rate of TCE destruction in deionized water is still much faster than in the groundwater. The lower rates in groundwater are likely due to interference from other, nonhazardous species present in the water. Performance estimates were based on the groundwater rates.

A comparison between the experimental data for the noon and off-noon tests and the model is shown in Figure 5. The results of this comparison indicate that the model provides a good representation of the system behavior.

Figure 6 shows the first-order rate constants for the noon experiments where each bar shown is the average of two replicate runs. An estimate of the error for each experiment was obtained by analyzing the variation in the duplicate experiments for all the different test conditions. As seen in the figure, lowering the pH of the groundwater significantly improved the performance of the destruction process. This improvement was likely due to the elimination of hydroxyl-scavenging bicarbonate ions which are converted to CO_2 at the lower pH. Catalyst loading and velocity effects were negligible.

Figure 7 shows the first order rate constants for the series of off-noon experiments. As seen in the figure, the estimated error for this series is approximately twice that of the noon experiments. However, the trends indicated in the figure reproduce those found in the noon experiments described above.

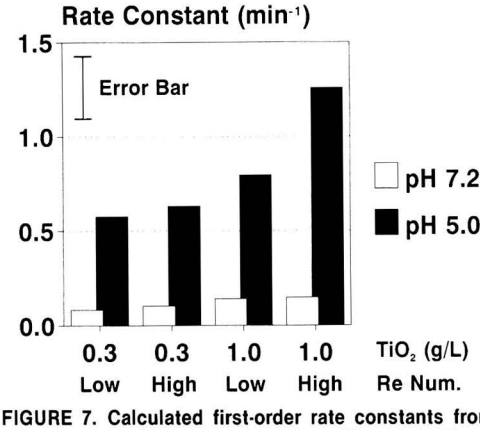

FIGURE 7. Calculated first-order rate constants from off-noon groundwater experiments outlined in Tables 3 and 4. Each bar represents the average of duplicate tests.

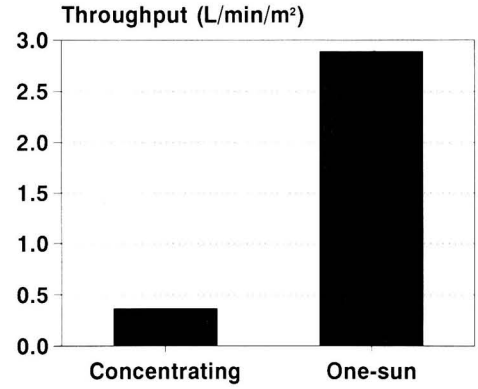

FIGURE 8. Comparison of system throughput for the best-case concentrating test and a one-sun test. Groundwater was adjusted to pH 5. Treatment reduces 200 μg/L TCE to 5 μg/L.

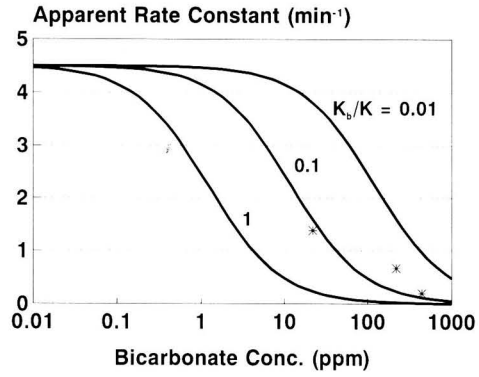

FIGURE 9. Effect of bicarbonate concentration on TCE destruction rate. Curves are calculated from a model that assumes bicarbonate behaves as a competitive reactant (see text).

Recirculating Batch Follow-on Experiments—One-sun Experiment

Laboratory and literature data suggested that the photocatalytic process may be more efficient at lower UV-light intensities. To test this possibility in the groundwater at LLNL an experiment was performed to compare the destruction of TCE under "one-sun" illumination with rates observed using concentrated light from the parabolic troughs. In the one-sun case, the troughs were positioned horizontally (pointed straight up). In this position the troughs do not concentrate any sunlight onto the photoreactor. As with the concentrated UV experiments, both direct-normal and diffuse UV radiation illuminated the side of the photoreactor tube facing the sun. Results of the analysis, shown in Figure 8, indicate the allowable flow rate per square meter of aperture area to maintain destruction of TCE from an initial concentration of 200 μg/L to a final concentration of 5 μg/L. The rates were normalized based on the aperture area for the concentrator (trough width × length) and the one-sun configuration (tube diameter × length).

When adjusted for aperture area as discussed above, the one-sun system uses sunlight eight times more efficiently than the concentrating system (Figure 8). This large increase in system efficiency is likely due to three effects: (1) elimination of concentrator optical and reflective losses, (2) ability of the one-sun system to capture diffuse UV light, and (3) improved catalyst efficiency at lower UV light intensity [*1*, *6*, *7*].

Recirculating Batch Follow-on Experiments—Effect of Bicarbonate

As shown previously, adjustment of the pH had a large impact on system performance. The improved performance at lower pH is believed to result from the reduction in the concentration of bicarbonate ion, a known scavenger of hydroxyl radicals. By reducing pH, the bicarbonate equilibrium is shifted toward dissolved carbon dioxide (carbonic acid). Changing from pH 7.2 to pH 5.0 reduces bicarbonate levels by 95%.

Using an expression such as equation (1), bicarbonate can be modeled as a simple competitor for hydroxyl radicals.

$$r = \frac{kC_{TCE}}{1 + KC_{TCE} + K_b C_{HCO_3}} \qquad (1)$$

The key parameter is a measure of the relative affinity of TCE and bicarbonate to attack by the hydroxyl radical, referred to as K_b/K. In Figure 9 the model curves for various K_b/K ratios are shown compared to the experimentally measured apparent rate constant for TCE destruction. The measured rate data points correspond to tests run with different levels of bicarbonate present in the groundwater. This included a test at the original pH of 7.2 (which had 440 mg/L bicarbonate), groundwater adjusted to pH 5.0 (22 mg/L bicarbonate), and groundwater diluted one-to-one with deionized water (220 mg/L bicarbonate). Literature values for hydroxyl reaction-rate constants suggest a K_b/K ratio of 0.002. This value is lower than the apparent best fit value on Figure 9; however, the literature rates are for homogeneous solutions and bicarbonate is likely to adsorb to TiO_2 thus bringing it into close contact with hydroxyl radicals. The model suggests that near complete elimination of the bicarbonate, e.g., by lowering pH to 4 or less, could result in a rate increase of roughly 300% from that observed at pH 5.0. Yet, this assumes that bicarbonate is the only inhibiting species; there is no guarantee that the rates seen with deionized water can be obtained with groundwater since other ions (sulfates, phosphates, nitrates, metals, etc.) may be slowing the TCE reaction rate.

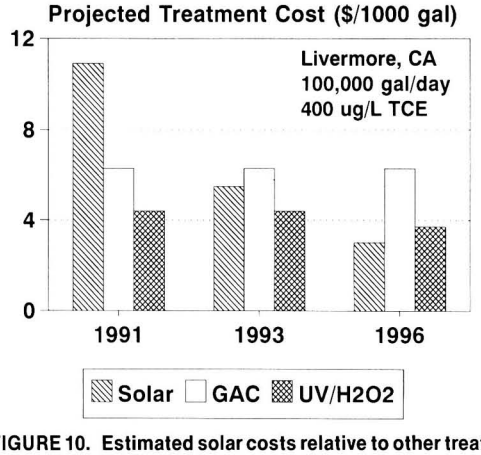

FIGURE 10. Estimated solar costs relative to other treatment options. The 1991 values are for a concentrating solar system similar to that used at the field tests, 1993 values show the current one-sun system estimates, and 1996 values are projections based on the use of advanced catalysts in one-sun collectors [*8*]. (1000 gal = 3.785 m³)

SYSTEM COST ESTIMATES

In 1990, LLNL performed a feasibility study for the remediation of a variety of sites at the laboratory. As part of this study, LLNL estimated the cost of a granular activated carbon (GAC) unit and an electric lamp, hydrogen peroxide oxidation unit for the site used during the solar detoxification field experiment. These cost projections provide a bench mark for comparison with the estimated cost of a solar facility. The kinetic data from the field experiments and cost data for new solar detoxification photoreactor designs were used to project the cost of a full-scale (100,000 gal/day) solar detoxification system at the Livermore site [8]. The results (Figure 10) predicted that the solar technology has a treatment cost similar to that for currently accepted treatment methods. The solar system also has the added advantage of on-site pollutant destruction (compared to GAC) and low power consumption (compared to UV/H_2O_2). Yet as a new technology, solar detoxification must demonstrate reliability and clear cost advantages before it will gain acceptance in the remediation market. To this end, process development and testing are continuing and further reductions in the solar treatment cost, via catalyst, reactor design, and operational improvements, are expected by the mid-1990's.

CONCLUSIONS AND RECOMMENDATIONS FOR FUTURE WORK

Engineers from three national laboratories successfully demonstrated, for the first time in the field, that solar energy can be used to destroy toxic organic compounds in groundwater. Data resulting from a carefully planned series of experiments performed at Livermore, CA showed that:

- Solar detoxification can reduce trichloroethylene in groundwater to levels below those required to meet drinking water standards.
- Lowering pH to offset high alkalinity substantially improved performance, demonstrating that simple pretreatment can deal with common nonhazardous water components such as bicarbonate.
- Catalyst loading and velocity through the photoreactor had a negligible effect on performance over the range these parameters were tested.
- A one-sun configuration performed roughly eight times more efficiently than the concentrator configuration when results were normalized by sunlight collection area.

In addition to these results, the field experiment at Livermore gave engineers valuable information on the costs of designing and fabricating solar detoxification systems. This information led to simplified system design and operating schemes. Current solar treatment costs are estimated to be similar to those for more conventional treatment methods used for the remediation of TCE in groundwater.

NREL is planning future field experiments and demonstrations of the solar process for groundwater and industrial waste water applications using photoreactors developed by industry specifically for solar detoxification. Future work will include an investigation of the lifetime and method of deployment (slurries or fixed) of photocatalysts. Ongoing laboratory research is investigating methods of increasing catalyst performance and developing more robust kinetic and engineering models for design and scale-up. The overall objective of this Department of Energy funded research is the commercialization of the solar detoxification technology by private industry. To that end, NREL is positioned to work with interested industry partners.

ACKNOWLEDGEMENTS

Funding for this research was provided by the Department of Energy through Environmental Restoration and Waste Management's Office of Technology Development and Conservation and Renewable Energy's Office of Industrial Technology. The authors greatly appreciate the assistance of Jim Pacheco of Sandia National Laboratories in the design, execution, and analysis of these tests. Also appreciated was the support and expertise of staff at Lawrence Livermore National Laboratories: A. J. Boegel, Marina Jovanovich, Tim Merrill, Rich Stanley, and Kena Stanley. Finally, the project would not have been possible without the guidance of Alan Laxson and Hal Link of NREL.

NOTATION

C_i = Concentration of species i, μg/L
k = First order rate constant, min^{-1}
K_b/K = Ratio of hydroxyl radical rate constants for bicarbonate and TCE
r = Rate of reactant destruction, μg/(L min)
Re = Reynolds number, $vD\rho/\mu$
t = Time, min
V_B = Total batch volume, m^3
V_R = Volume of photoreactor, m^3
V_T = Volume of the batch tank, m^3

LITERATURE CITED

1. Ollis, D. F., E. Pelizzetti, and N. Serpone, "Photocatalyzed Destruction of Water Contaminants," *Environ. Sci. Technol.*, **25**, p. 1523 (1991).
2. Ahmed, S., and D. F. Ollis, "Solar Photoassisted Catalytic Decomposition of the Chlorinated Hydrocarbons Trichloroethylene and Trichloromethane," *Solar Energy*, **32**, p. 597 (1984).
3. Matthews, R., "Photo-oxidation of Organic Material in Aqueous Suspensions of Titanium Dioxide," *Water Res.*, **20**, p. 569 (1986).
4. Barbeni, M., M. Morello, E. Pramauro, E. Pelizzetti, M. Vincenti, E. Borgarello, and N. Serpone, "Sunlight Photodegradation of 2,4,5-Trichlorophenoxy-acetic acid and 2,4,5-Trichlorophenol on TiO_2," *Chemosphere*, **16**, p. 1165 (1987).
5. Wolfrum, E., and C. S. Turchi, "Comments on Reactor Dynamics in the Evaluation of Photocatalytic Oxidation Kinetics," *J. Catal.*, **136**, p. 626 (1992).
6. Okamoto, K., Y. Yamamoto, H. Tanaka, and A. Itaya, "Kinetics of Heterogeneous Photocatalytic Decomposition of Phenol over TiO_2 Powder," *Bull. Chem. Soc. Jpn.*, **58**, p. 2023 (1985).
7. D'Oliveira, J.-C., G. Al-Sayyed, and P. Pichat, "Photodegradation of 2- and 3-Chlorophenol in TiO_2 Aqueous Suspensions," *Environ. Sci. Technol.*, **24**, p. 990 (1990).
8. Turchi, C. S., M. S. Mehos, and H. F. Link, "Design and Cost of Solar Photocatalytic Systems for Groundwater Remediation," NREL/TP-432-4865, May, 1992.

Computer Simulation of a Flue Gas Desulfurization Moving-Bed Reactor

Rachel J. Young and James T. Yeh

Pittsburgh Energy Technology Center, U.S. Department of Energy, P.O. Box 10940, Pittsburgh, PA 15236

This paper describes the methodology of computer simulation of a moving-bed reactor system utilizing a gravity-fed solid reactant and a cross-flow of reacting gas. The objective of this work was to predict the efficiency of a moving-bed reactor for generic solid-gas reactions with known reaction rate parameters. Since in a continuous cross-flow-moving-bed reactor the solid reactant at the inlet of the reactor is fresh (or freshly regenerated) and the solid reactant can be almost totally utilized, the break-through of the reactant gas is much less at the reactor top (solid inlet) than at the bottom. The simulation provides predictions of the reactant gas break-through concentration profile as well as the bulk reactant gas consumption within the moving-bed reactor. The reactor performance is modeled by both one-dimensional and two-dimensional series of imaginary micro-reactors. The computer code is listed and a sample calculation is presented for a flue gas desulfurization process utilizing copper oxide impregnated on alumina as a sorbent.

INTRODUCTION

A number of dry, regenerable metal oxide processes are under various stages of development for SO_2 and NO_x removal from coal combustion flue gas [*1*]. The removal of NO_x in the flue gas is usually accomplished by ammonia gas injection into the reactor and sorbent catalyzing the de-NO_x reaction. The absorption reactors can generally be classified into three types: the fluidized-bed reactor [*2*], the moving-bed reactor [*3*], and the fixed-bed reactor [*4*]. The simulation of a fluidized-bed reactor for SO_2 removal was described by Yeh et al. [*5*]. This paper focuses on the simulation of flue gas desulfurization by a moving-bed of supported metal oxide sorbents.

Chemical reactions occur when gaseous reactants contact solid reactants in a moving-bed reactor. Sulfur dioxide in flue gas is removed by the interaction of flue gas with the sorbent. A conceptual description of a moving-bed reactor is illustrated in Figure 1. The sorbent enters the top of the reactor and flows downward by gravity, creating a moving bed, and the flue gas enters the reactor in a cross-flow pattern. In the continuous life-cycle test system design at the Pittsburgh Energy Technology Center (PETC), as in the conceptual scheme, the spent

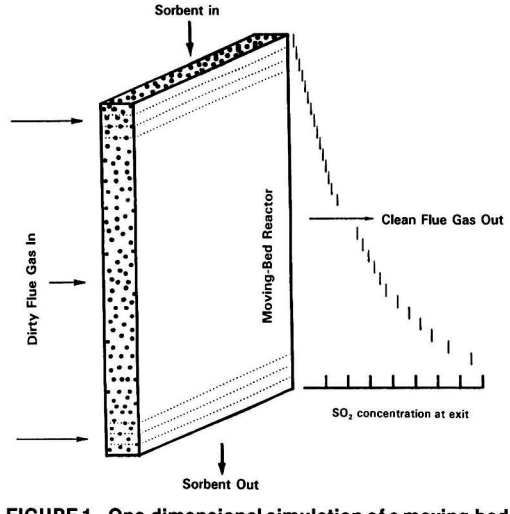

FIGURE 1. One-dimensional simulation of a moving-bed reactor.

Correspondence concerning this paper should be addressed to James T. Yeh.

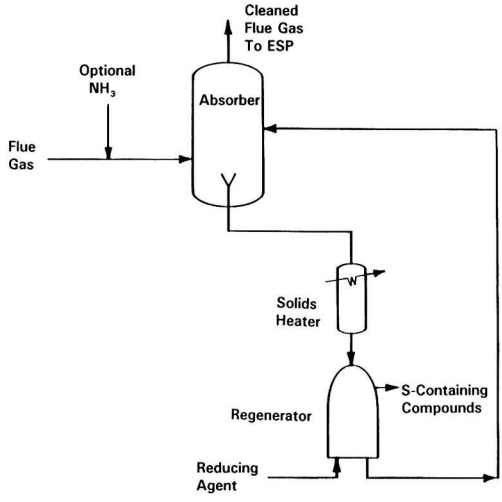

FIGURE 2. General schematic of dry, regenerable scrubbing process.

sorbent is regenerated in another vessel with a reducing gas and then recirculated to the absorber (reactor) for reuse (see Figure 2).

CHEMISTRY AND KINETICS

The chemistry of the sulfation of metal oxides can be represented by the following general equations.

$$aM + 1/2bO_2 \rightarrow M_aO_b \quad (1)$$

$$cM_aO_b + dSO_2 + eO_2 \rightarrow M_f(SO_4)_g \quad (2)$$

In the above equations, M_aO_b represents the metal oxide, and $M_f(SO_4)_g$ represents the metal sulfate.

The rate equation describing the sulfation of a supported metal oxide sorbent is given in equation 3. The rate equation has been derived from studies using a microbalance reactor [6]. The differential reactor used simulated flue gas and copper oxide sorbent supported on gamma-alumina pellets.

$$\frac{dx}{dt} = k(1-x)p \quad (3)$$

where,

x = fractional conversion of CuO on alumina
k = reaction rate constant, 1/h
p = fractional partial pressure of SO_2 (mole fraction of SO_2 in gas)
t = time, h

FLUIDIZED-BED REACTOR MODEL

A fluidized-bed reactor model was derived by Yeh *et al.* [5] using an Ideal-Flow Model approach. The model assumed plug flow behavior for the flue gas and completely mixed sorbent in the reactor.

The fraction of unreacted CuO is represented by

$$(1-x) = C/C_0 \quad (4)$$

C_0 = initial mass of CuO per unit mass of Al_2O_3
C = mass of unreacted CuO per unit mass of Al_2O_3

The weight of Al_2O_3 is determined by calculating the fraction of the CuO available (unreacted) and the amount of $CuSO_4$ formed in the sorbent. It is assumed that aluminum sulfate, if formed, would not participate in any subsequent chemical reactions (such as regeneration and absorption) beyond the first cycle of operation.

Following substitution of equation 4 into equation 3, the rate equation 3 is rewritten as below

$$\frac{-dC}{dt} = kpC \quad (5)$$

A model describing a perfectly-mixed sorbent reactor is developed by applying a material balance around a differential element of the reactor (see Figure 3). For a differential height (dZ) of the reactor, the decrease of SO_2 concentration within the finite element can be described by $-d(pV/G)$. G is the molar volume of gas at the reaction temperature. One mole of CuO reacts with one mole of SO_2. Therefore, in the elemental volume,

$$-d(pV/G) = \frac{kpCDA}{M}\,dZ \quad (6)$$

D = bulk density of the sorbent, lb/ft^3
A = reactor cross sectional area, ft^2
M = molecular weight of CuO, lb/lb-mol.

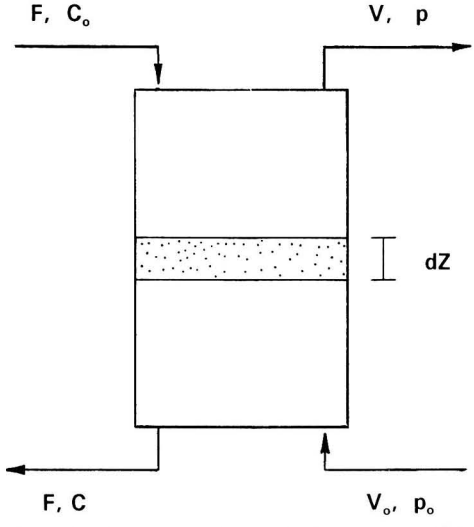

V: outlet flue gas volumetric flow rate (ft^3)
G: molar volume of gas (ft^3/lb-mol) at reaction temperature
D: density of moving bed, lb/ft^3
A: cross sectional area of moving bed, ft
Z: depth of moving bed, ft
M: molecular weight of metal
F: sorbent feed rate, lb alumina/h
p: outlet SO_2 concentration (mole fraction)
p_o: inlet SO_2 concentration
v_o: inlet flue gas volumetric flow rate, ft^3/h

FIGURE 3. Differential element of a perfectly-mixed sorbent model.

Substitution of equation 6 into equation 5 and solving after rearrangement, a reactor model is obtained:

$$p = \frac{(1-Q)p_0}{\exp\left[\frac{kDAGZC_0}{Mv_0}(1-Q)\right] - Q} \tag{7}$$

where,

$$Q = \frac{p_0 v_0 M}{GFC_0} = \frac{\text{moles } SO_2 \text{ feed/h}}{\text{moles CuO feed/h}} \tag{8}$$

F = sorbent feed rate, lb Al_2O_3/h

This model equation predicts outlet SO_2 concentration with conditions characterizing a perfectly-mixed sorbent reactor. Various operating conditions can now be simulated and tested using this equation. The primary assumption for this model's validity is that each sorbent particle is uniform and has the same properties. The sorbent particles exit with the same level of sulfation. Thus the overall level of SO_2 removal by the fluidized-bed reactor can be sufficiently described by this equation.

DESCRIPTION OF A MOVING-BED COMPUTER MODEL

However, in the case of a moving-bed reactor, the sorbent exists in a packed state and moves by gravity at a low velocity. The result of one particle's contact with the flue gas will not necessarily be the same as another's at a different location in the bed. Each particle's composition is dependent upon its particular position in the bed. Particles reacting at the flue gas entering point will remove a large portion of the SO_2, and as the flow continues across the reactor, the particles at the flue gas exiting point will have less sulfur loading (in the form of metal sulfate). Also, as the sorbent flows down through the reactor, similar differences occur. A particle located near the flue gas inlet face of the reactor is more utilized and has more sulfur than one located near the flue gas exit face (see Figure 1). A similar distinction can also be made between a particle near the flue gas inlet face at the bottom, which is more utilized and has more sulfur, than a particle near the flue gas inlet face at the top. This is because sorbent at the bottom of the reactor has experienced longer gas/solid contact time than sorbent at the top. In order to develop the model equation, a perfectly-mixed sorbent reactor system described previously can be adopted, in part, to simulate the moving-bed.

The moving-bed reactor is divided by imaginary horizontal and vertical divisions (see Figure 4). The horizontal divisions are called "stages" and the vertical divisions are called "cuts". The micro-reactors are bordered by stages and cuts. Each micro-reactor is treated like a perfectly-mixed reactor. The degree of sulfation of the sorbent is dependent on the position in height and depth of the micro-reactor. The particles remain packed in each micro-reactor, but the flue gas passes through and contacts the sorbent in a reduced area and thickness. As the grid size decreases, the difference between the entering and exiting sorbent particle compositions becomes smaller and each micro-reactor approaches that of a perfectly-mixed sorbent reactor.

A computer model has been formulated to test various microreactor/moving-bed designs (See Appendix A for the computer program code). The computer program requires input for process variables describing the reactor and predicts the resulting SO_2 concentration, removal efficiency, and degree of sulfation of the sorbent (expressed in weight percent of sulfur). Among the input variables are temperature, number of stages and cuts the reactor is to be divided into (micro-reactors), bed

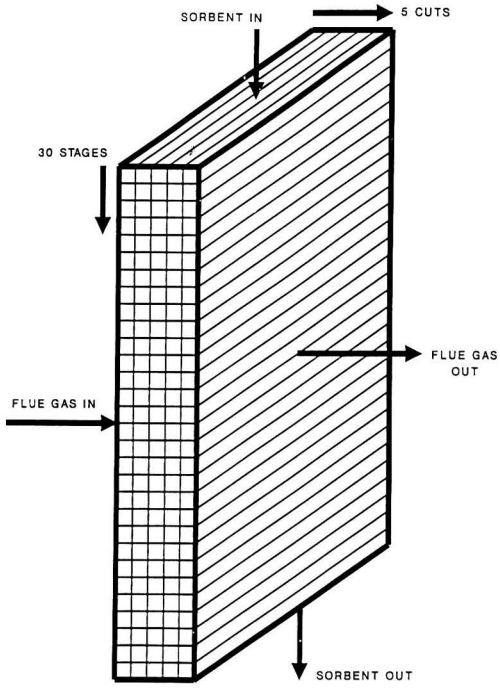

FIGURE 4. Two-dimensional simulation.

depth, bed cross sectional area, kinetic parameter, inlet flue gas properties (flow rate, SO_2 concentration), and sorbent properties (flow rate, bulk density, weight percent copper, weight percent sulfur). Next, the rate constant, volumetric flow rate, and molar volume constants are calculated.

The program then divides the reactor into the specified stages and cuts to prepare for stage by stage calculations. The sorbent flow rate into each micro-reactor is reduced according to the number of cuts. Likewise, the flue gas flow rate into each microreactor is reduced according to the number of stages. The sorbent exiting each stage has an increased weight percent of residual sulfur, so its value needs to be changed to be entered into the subsequent stage. The degree of sulfation of the sorbent is calculated from the values of the input process variables. The sorbent exiting each stage has an increased sulfur content. This new sulfur content is used as the initial sulfur content for the micro-reactor at the stage below, and so forth.

As the flue gas exits each cut of every stage, the value of SO_2 concentration is stored in the computer. The SO_2 concentration profile at the exit of one cut is used as the input SO_2 concentration profile for the next cut. This procedure continues until the SO_2 concentration is calculated at the exit of the last cut of every stage.

The simulation has adopted the following assumptions:

(1) The moving-bed reactor is isothermal.
(2) The sorbent in each micro-reactor is uniformly sulfated.
(3) The flue gas SO_2 flows through the moving-bed reactor in a plug flow manner.
(4) There is no back-mixing of the sorbent particles as they flow from one micro-reactor to the one below.

SIMULATION

A preliminary test of the computer model was made by using the model to simulate the performance of a moving-bed of copper oxide conducted by Stelman [3]. The test conditions

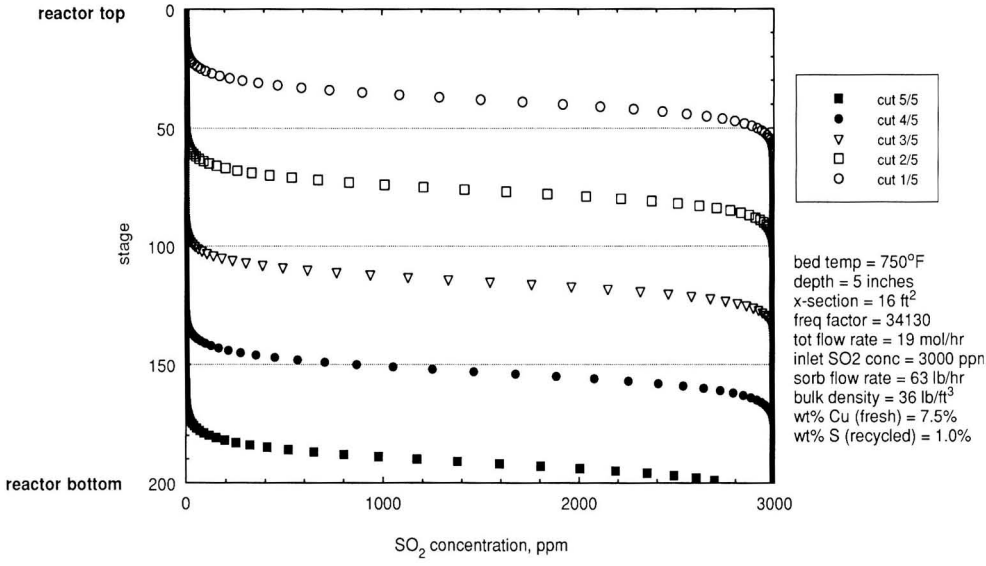

FIGURE 5. SO_2 concentration profile at outlet of cuts.

from the Rockwell study were entered into the model to predict the moving bed's desulfurization performance. The simulation (using 200 stages and 1 cut) predicts an 86% SO_2 removal at their test conditions as compared with 90% SO_2 removal from actual test results reported by Rockwell. Thus the model conservatively underestimated the performance of the moving-bed copper oxide reactor. The reactor parameters of the Rockwell test are given as follows: flue gas flow rate, 1 scfm; inlet SO_2 concentration, 3000 ppm; reactor temperature: 750°F; copper loading, 7.6%; sulfur on inlet sorbent, 0% (indicates fresh sorbent); sorbent feed rate, 0.007 lb/min; bed height 11.75″; bed width, 1.75″; and sorbent thickness, 1.75″.

Simulation studies can now be performed with various operating conditions. One case includes a reactor with a cross sectional area of 16 ft^2 (this is the cross-sectional area of the moving bed now under construction at the Pittsburgh Energy Technology Center) and depth of 5 in., divided into 5 cuts and 200 stages. The flue gas flow rate is 0.095 lb-mol/h for each stage with an inlet SO_2 concentration of 3000 ppm. The sorbent, with bulk density 36 lb/ft^3, has a flow rate of 63 lb/hr., 7.5 weight percent of copper, and an initial 1.0 weight percent of residual sulfur (simulating process conditions of the life-cycle test system). The reaction temperature is 750°F. The results for each cut are shown in Figure 5 and the total overall

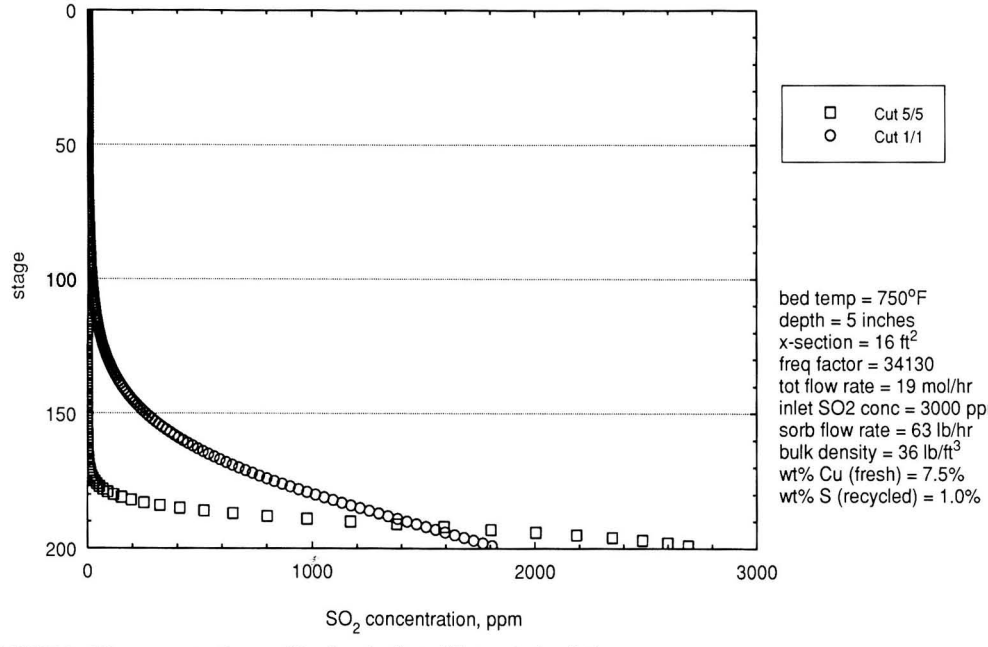

FIGURE 6. SO_2 concentration profiles for single and five cut simulations.

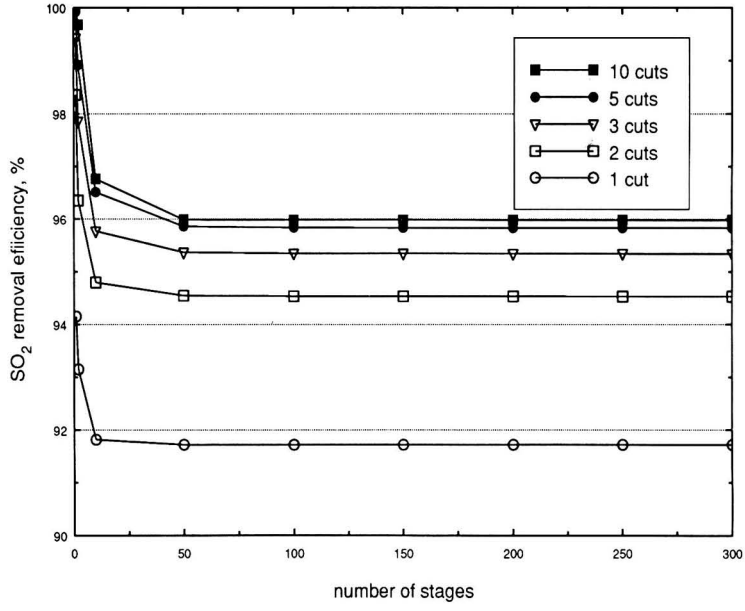

FIGURE 7. Sensitivity analysis on number of stages.

SO_2 removal is calculated as 95.8%. This is compared with a single cut simulation with SO_2 removal calculated at 91.7% (see Figure 6). Cut 5/5 from Figure 5 is also plotted in Figure 6 for the purpose of comparison.

Computing sensitivity analysis was made between 1 stage and 300 stages and between 1 cut and 10 cuts using the process inputs discussed above. Figure 7 illustrates the effects on calculated SO_2 removal by the choice of the number of stages. It indicates that at about 50 stages or greater the difference in calculated SO_2 removal results are negligible. Furthermore, the effects of number of cuts on calculated SO_2 removal is shown in Figure 8. It indicates that at 5 cuts or greater the effects on computation is diminishing. Therefore, excessive numbers of stages and cuts are not necessary to obtain a reasonable estimate of the reactor performance.

PARAMETRIC STUDY

Parametric studies were conducted in order to predict the trends in certain operating conditions. More specifically, emphasis was made concerning how changes in temperature and SO_2 concentration affected the sorbent flow rate with a 90

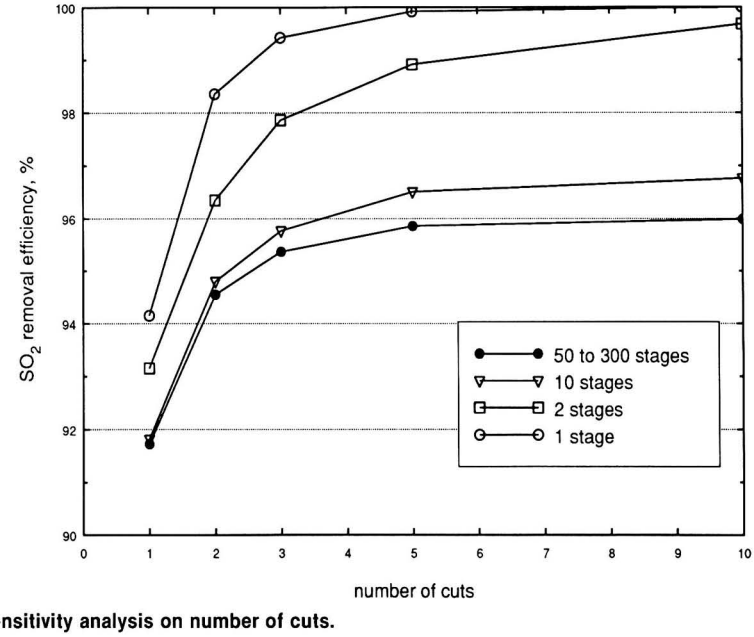

FIGURE 8. Sensitivity analysis on number of cuts.

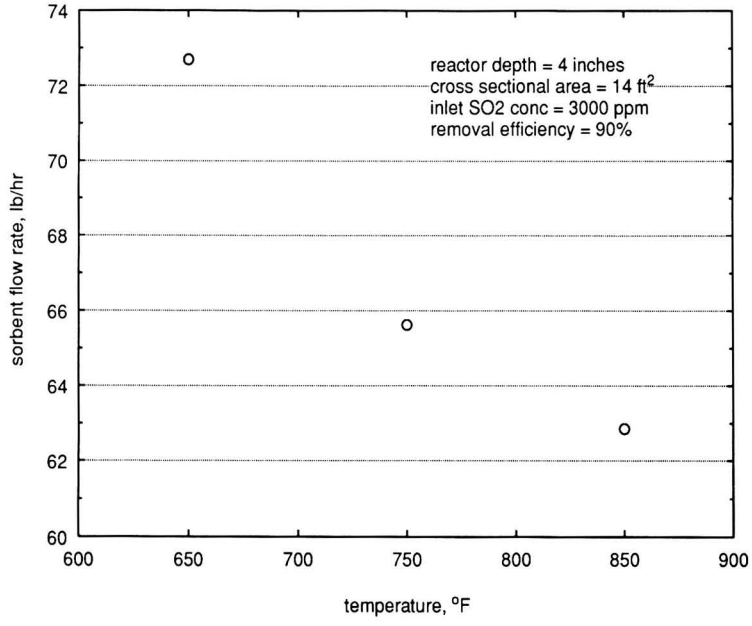

FIGURE 9. Effect of temperature on sorbent flow rate.

percent removal efficiency. Graphs depicting the trends are shown in Figure 9 and Figure 10. There are many other parameters that can be studied for their process sensitivity effects by using this computer model.

RECOMMENDATION

The present computer code could be improved by taking into account physical properties of the reactor that are not currently considered. The heat of reaction between sulfur dioxide and copper oxide under flue gas conditions is expected to create a temperature gradient across the moving bed and also from top to bottom of the moving bed. The current approach uses an average temperature of the moving bed in the calculations. In an actual test, a temperature profile of the moving bed should be measured. If the temperature gradient is large, then each of the micro-reactors should have a temperature which is different from its neighboring micro-reactors. Other properties such as sorbent density changes during the reaction,

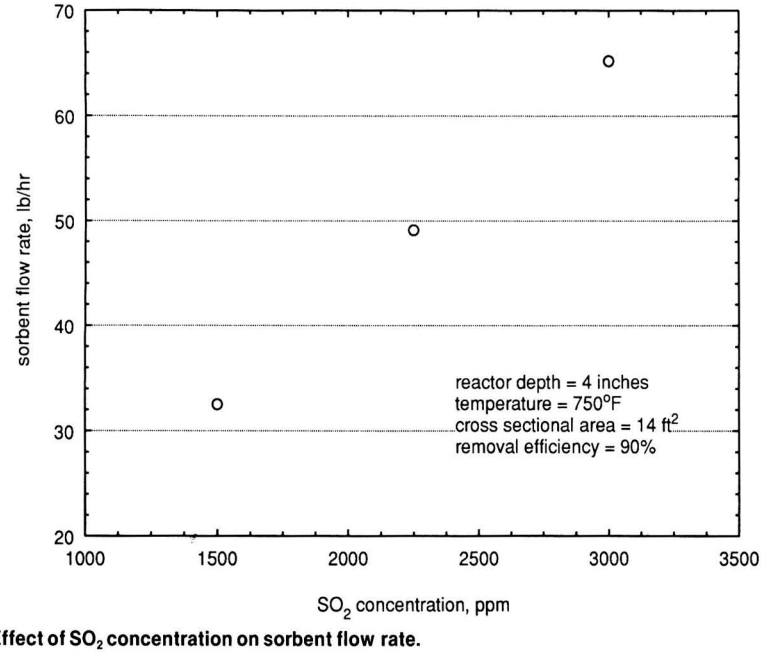

FIGURE 10. Effect of SO_2 concentration on sorbent flow rate.

and variation in the alumina property may also affect the simulation results to some extent.

ACKNOWLEDGEMENT

A version of the computer code in the C programming language has been recently made available by Dennis Chao of Princeton University. Mr. Chao is an Oak Ridge Associated Universities Professional Intern at PETC for the summer of 1992.

DISCLAIMER

References in this paper to any specific commercial product, process, or service is to facilitate understanding and does not necessarily imply its endorsement or favoring by the United States Department of Energy.

LITERATURE CITED

1. Hoffman, J. S., D. N. Smith, H. W. Pennline, and J. T. Yeh, "Removal of Pollutants from Flue Gas Via Dry, Regenerable Sorbent Processes," Presented at the AIChE Spring National Meeting, New Orleans, LA (Mar. 29–Apr. 2, 1992).
2. Yeh, J. T., R. J. Demski, and J. P. Strakey, and J. I. Jourbert, "Combined SO_2/NO_x Removal from Flue Gas," Detailed Discussion of a New Regenerative Fluidized-Bed Process Developed by the Pittsburgh Energy Technology Center, *Environmental Progress*, Vol. 4, No. 4, pp. 223–228 (1985).
3. Stelman, D., J. P. Ampaya, and J. C. Newcomb, "Simultaneous Removal of NO_x, SO_x, and Particulates from Flue Gas by a Moving Bed of Copper Oxide," US DOE Report DE-AC22-83PC60262, (Dec. 18, 1987).
4. Burk, J. M., "Shell NO_x/SO_2 Flue Gas Treatment Process: Independent Evaluation," US EPA Report No. EPA-600/7-82-064 (1982).
5. Yeh, J. T., C. J. Durmmond, and J. I. Joubert, "Process Simulation of the Fluidized-Bed Copper Oxide Process Sulfation Reaction," *Environmental Progress*, Vol. 6, No. 2, pp. 44–50 (1987).
6. Yeh, J. T., J. P. Strakey, and J. I. Joubert, "SO_2 Absorption and Regeneration Kinetics Employing Supported Copper Oxide," Presented at the AIChE Summer National Meeting, Cleveland, OH (August 1982).
7. Carnahan, B., J. O. Wilkes, "Fortran 77 with MTS and the IBM PS/2," The University of Michigan, Ann Arbor, MI (1989).

UNIT CONVERSION FACTORS

1 inch = 2.54 cm
1 lb = 453.6 grams
°C = (F-32)/1.8
1 ft^3 = 0.02832 m^3
1 ft^2 = 0.0929 m^3
1 ppm SO_2 = 2.86 mg/Nm^3

APPENDIX A

```
C      ----------PROGRAM:  MBED-----------
C       SIMULATION OF A MOVING-BED CuO PROCESS
C      -------FOR FLUE GAS DESULFURIZATION-----
C     (Computer simulation with 2-D cuts)
C      ---------------------------------------
C     A moving bed reactor is simulated with a
C     large number of mixed sorbent reactor
C     ****************************************
      REAL IN_CONC,K,INIT,M,L
      INTEGER STAGE,E,CUTS,C
      DIMENSION PPM(10,300),REM_EFF(10,300)
      DIMENSION SULF(10,300),AVG_PPM(10)
      DIMENSION AVG_REM(10)
      TOT_PPM = 0
      OPEN (6,FILE='LPT1')
      OPEN (7,FILE='MBED1.DAT')
C      ----------List of Variables-----------
C     TEMP,T,Y,P0,D,Z,AREA,RATE,PERCENT,SULFUR,
C     A,FLOW,K,V0,G,STAGE,FRAC,CuAVAIL,UNAVAIL,
C     AMOUNT,AVAIL,TOTAL,C1,S,DENSITY,Q,Q1,Q2,
C     Q3,Q4,Q5,P,PPM,REM_EFF,IN_CONC,OUTCONC,
C     GAIN,INIT,CHANGE,TOT_PPM,AVG_PPM,AVG_REM,
C     E,M,R,SULF,C,CUTS,SORB,DEPTH,L
C      ------------Input Variables-------------
C     Bed Temperature (K)      [T]
            WRITE (*,105)
            WRITE (6,105)
            READ (*,*) TEMP
            WRITE (6,90) TEMP
            T= (TEMP-32.)/1.8 + 273.16
C     Number of stages      [E]
            WRITE (*,155)
            WRITE (6,155)
            READ (*,*) E
            WRITE (6,95) E
C     Number of vertical cuts  [C]
            WRITE (*,170)
            WRITE (6,170)
            READ (*,*) C
            WRITE (6,95) C
C     Reactor depth (ft)        [Z]
            WRITE (*,110)
            WRITE (6,110)
            READ (*,*) Z
            WRITE (6,100) Z
C     Cross-sect area of reactor (sq.ft) [AREA]
            WRITE (*,115)
            WRITE (6,115)
            READ (*,*) S
            WRITE (6,90) S
            AREA = S/E
C     Frequency factor      [A]
            WRITE (*,120)
            WRITE (6,120)
            READ (*,*) A
            WRITE (6,100) A
C     Flow rate of flue gas (mol/h) [RATE]
            WRITE (*,125)
            WRITE (6,125)
            READ (*,*) RATE
            WRITE (6,100) RATE

C     Inlet SO2 Concentration (ppm)  [P0]
            WRITE (*,130)
            WRITE (6,130)
            READ (*,*) Y
            WRITE (6,90) Y
            P0 = Y/1000000.
C     Sorbent flow rate (lb/hr)  [FLOW]
            WRITE (*,135)
            WRITE (6,135)
            READ (*,*) SORB
            WRITE (6,90) SORB
            FLOW = SORB/C
C     Bulk density of sorbent (lb/cu.ft) [D]
            WRITE (*,140)
            WRITE (6,140)
            READ (*,*) D
            WRITE (6,90) D
C     Wt% Cu in fresh sorbent  [PERCENT]
            WRITE (*,145)
            WRITE (6,145)
            READ (*,*) PERCENT
            WRITE (6,90) PERCENT
C     Wt% residual S in recycled sorbent  [L]
            WRITE (*,150)
            WRITE (6,150)
            READ (*,*) L
            WRITE (6,90) L

C      ------------Calculations-------------
C     Rate constant (Aexp(-E/RT) (1/h))   [K]
            K = A*EXP(-2417.6/T)
C     Volumetric flow rate (scfh)      [V0]
            V0 = 0.7288462*RATE*(460.+TEMP)
C     Molar volume (cu.ft/lb-mole)      [G]
            G = 0.7288462*(460.+TEMP)
         DO 50 CUTS = 1,C
            WRITE (*,180) CUTS
            WRITE (6,180) CUTS
```

```
            WRITE (*,200)
            WRITE (6,200)
            TOT_PPM = 0
         DO 10 STAGE = 1,E
            IF (CUTS .GT. 1) THEN
            P0 = PPM((CUTS-1),STAGE)/1000000
            END IF
            IF (STAGE .EQ. 1) THEN
                SULFUR = L
            END IF
C     Amount of Cu available      [CuAVAIL]
             UNAVAIL = 1.9819089*SULFUR
             CuAVAIL = PERCENT - UNAVAIL
C     Amount of CuSO4 formed      [AMOUNT]
             AMOUNT = 4.976294*(SULFUR/100)
C     Amount of CuO available     [AVAIL]
             AVAIL = 1.2518099*(CuAVAIL/100)
C     Total Cu      [TOTAL]
                TOTAL = AMOUNT + AVAIL
            FRAC = 1.-TOTAL
C     lb CuO available/lb Al2O3      [C1]
            C1 = AVAIL/FRAC

C     Density of Al2O3 inside reactor
C     (lb Al2O3/cu.ft) [DENSITY]
C     Only to be calc. with initial conditions
      IF (STAGE .EQ. 1 .AND. CUTS .EQ. 1) THEN
                DENSITY = D*FRAC
            END IF
C        ------Calculations------

         Q = K*DENSITY*G*AREA*Z*C1/(79.54*V0)
         Q1 = V0*P0*79.54/(G*FLOW*C1)
         Q2 = 1.-Q1
         Q3 = Q*Q2
         Q4 = EXP(Q3)
         Q5 = Q4-Q1
C        SO2 output concentration     [M]
            P = Q2*P0/Q5
            M = P*1000000.
            TOT_PPM = TOT_PPM + M
C      Removal efficiency      [R]
            R = (P0-P)/P0*100
C      Store values in separate cells
            PPM(CUTS,STAGE) = M
            REM_EFF(CUTS,STAGE) = R
            SULF(CUTS,STAGE) = SULFUR

            WRITE (*,210) STAGE,PPM(CUTS,STAGE),
     1      REM_EFF(CUTS,STAGE),SULF(CUTS,STAGE)
            WRITE (6,210) STAGE,PPM(CUTS,STAGE),
     2      REM_EFF(CUTS,STAGE),SULF(CUTS,STAGE)
            WRITE (7,210) STAGE,PPM(CUTS,STAGE),
     3      REM_EFF(CUTS,STAGE),SULF(CUTS,STAGE)

C     Sulfur removed by sorbent (lb/hr)     [GAIN]
            IN_CONC = P0*RATE
            OUTCONC = P*RATE
            GAIN = (IN_CONC - OUTCONC) * 32.06
C     Sorbent sulfur concentration change[CHANGE]
                INIT = SULFUR/100*FLOW
                CHANGE = INIT + GAIN
            SULFUR = CHANGE/FLOW*100

   10  CONTINUE

       AVG_PPM(CUTS) = TOT_PPM/(STAGE-1)
       AVG_REM(CUTS) = (Y-AVG_PPM(CUTS))/Y*100

       WRITE (*,250) AVG_PPM(CUTS)
       WRITE (6,250) AVG_PPM(CUTS)
       WRITE (*,260) AVG_REM(CUTS)
       WRITE (6,260) AVG_REM(CUTS)

   50  CONTINUE

       STOP

   90  FORMAT (10X,F9.4)
   95  FORMAT (10X,I6)
  100  FORMAT (10X,F12.5)
  105  FORMAT (' Input the bed temperature (F)  ')
  110  FORMAT (' Input the reactor depth (ft)  ')
  115  FORMAT (' Input the total cross-sectional
     1        area (sq.ft)  ')
  120  FORMAT (' Input the frequency factor  ')
  125  FORMAT (' Input the flue gas flow rate
     1       (mol/h)  ')
  130  FORMAT (' Input the inlet SO2 conc.
     1       (ppm)  ')
  135  FORMAT (' Input the sorbent flow rate
     1       (lb/hr)  ')
  140  FORMAT (' Input the bulk density
     1       (lb/cu.ft)  ')
  145  FORMAT (' Input the wt% Cu in fresh
     1        sorbent  ')
  150  FORMAT (' Input the inital wt% residual
     1        S in recycled sorbent  ')
  155  FORMAT (' Input the number of stages  ')

  160  FORMAT (' Sorbent flow rate = ',F3.0)
  170  FORMAT (' Input the number of
     1        vertical cuts (pieces) ')
  180  FORMAT ('0'/'0'/' Cut : ',I2)
  200  FORMAT ('0'/' Stage',5X,'SO2 out.conc.'/
     1       '+',28X,'Rem.Eff.',9X,'Wt% S')
  210  FORMAT (I5,5X,F11.4,7X,F9.4,7X,F9.4)
  250  FORMAT ('0'/'0'/' Average SO2 output
     1        concentration:  ',F11.4)
  260  FORMAT (' Average removal efficiency:
     1       ',F8.4)

       END
```

APPENDIX B

```
Input the bed temperature (F)
        750.0
Input the number of stages
            50
Input the number of vertical cuts (pieces)
             1
Input the reactor depth (ft)
              .41677
Input the total cross-sectional area (sq.ft)
         16.0000
Input the frequency factor
        34130.00000
Input the inlet SO2 conc. (ppm)
       3000.0000
Input the sorbent flow rate (lb/hr)
         63.0000
Input the bulk density (lb/cu.ft)
         36.0000
Input the wt% Cu in fresh sorbent
          7.5000
Input the initial wt% residual S in recycled sorbent
           1.0000

Cut  :  1  (Only partial computer outputs are listed below)
```

Stage no.	SO_2 out.conc. ppm	SO_2 Removal Efficiency	Wt% S in sorbent
1	.1245	99.9958	1.0000
5	.2746	99.9908	1.2320
10	.7488	99.9750	1.5221
15	2.0751	99.9308	1.8120
20	5.8404	99.8053	2.1018
25	16.6686	99.4444	2.3909
30	48.0090	98.3997	2.6784
35	137.6298	95.4123	2.9611
40	378.1580	87.3847	3.2303
45	917.9393	69.4020	3.4656
50	1737.1490	42.0950	3.6363

```
Average SO2 output concentration:      248.1933
Average removal efficiency:    91.7269
```

** Computer codes on diskette may be obtained by writing to:
Dr. James T. Yeh, U.S.DOE, P.O.Box 10940, Pittsburgh, PA 15236

Pilot Scale Study and Design of a Granular Activated Carbon Regeneration Process Using Supercritical Fluids

David L. Tomasko, K. James Hay

Department of Chemical Engineering, University of Illinois, Urbana, IL 61801

Gregory W. Leman

Cabot Corp., P.O. Box 186, Tuscola, IL 61950

and

Charles A. Eckert

School of Chemical Engineering, Georgia Institute of Technology, Atlanta, GA 30332

A technology which has great potential for environmental control and waste remediation is contaminant removal and separation with supercritical fluids (SCF's) or supercritical fluid extraction (SFE). Pressure tuning of solvent power allows SCF processes to adapt to a wide variety of small batch oriented separations typified by environmental cleanup operations.

The ability of supercritical CO_2 to extract model contaminant compounds from GAC and subsequently drop out most of the contaminant in a liquid phase has been investigated in a pilot scale apparatus. Typical desorption profiles indicate an 85% removal of the compound from the carbon which allows for reuse. The desorption results have been interpreted with a generalized desorption-mass transfer model.

The results of the pilot plant studies have been applied to the design of a fixed-site GAC regeneration unit consisting of a three-element desorber with two-stage flash separation. Optimization of the process centers around minimizing the cost of recycling the SCF through an efficient recompression scheme and cycle configuration in the desorber unit. An economic evaluation shows a processing cost of 10.6¢/lb (23¢/kg) GAC which compares favorably with thermal regeneration and incineration. This non-destructive process allows re-use of the GAC while maintaining a high adsorbate capacity, which reduces carbon replacement costs and significantly decreases the need for carbon disposal by landfill or incineration.

INTRODUCTION

Environmental control and waste remediation are of immediate technological and political interest. The problem of removing potentially toxic compounds from waste streams or spill sites is exacerbated by their low concentrations and even lower allowable limits. With the advent of legislative controls on emissions and liability for contamination, the demand for economical treatment processes is growing stronger.

Although removal of contaminants from waste streams is usually considered an economic liability, any such problem has several potential solutions, some of which can be profitable. For instance, DuPont is recycling the wastes from their acrylonitrile and adipic acid processes to recover dibasic ester, 2-methylpentamethylenediamine, and acetonitrile, which yielded an estimated $70 million in profits for 1990 [1]. This solution shows a creative yet serious response to a problem which has long been ignored by industry and the government. Other wastes may not be amenable to such a solution but the renewed commitment to clean-up is motivation for development of treatment technologies.

One technology which has great potential is contaminant removal and separation with supercritical fluids (SCF's) or supercritical fluid extraction (SFE). In this process, a gaseous component is compressed and heated to a pressure and temperature above its critical point, where it has a substantial density and high compressibility. The density of the SCF is intermediate between that of a gas and a liquid, allowing the dissolution of non-volatile solid compounds up to 1-2 mole percent. The high compressibility in the supercritical region gives substantial change in density with small changes in pressure or temperature, allowing the solvent power of the fluid

Correspondence concerning this paper should be addressed to C. A. Eckert.

to be "tuned" so that contaminant mixtures may be separated in a series of steps. In addition, cosolvents added to the solvent in small quantities (1-5 mol%) can enhance absolute and relative solubilities by as much as several orders of magnitude in select cases. However, the level of predictive mathematical modeling of these systems for design purposes is hindered by a lack of molecular level understanding. In this paper, we give a broad overview of SCF phase equilibria and processing characteristics. For deeper insight, several excellent books and reviews are available [2-8].

Detoxification of soils, sludges and adsorbents such as granular activated carbon (GAC) appear amenable to SCF extraction. Detoxification processes will primarily be batch operations with widely varying feedstocks, a situation that demands a flexible separation strategy. Supercritical fluid extraction and separation may prove economically viable in such circumstances as indicated by model compound solubility studies and lab scale and feasibility studies demonstrating its use for the regeneration of GAC.

Supercritical fluid regeneration of GAC was first investigated by De Filippi and coworkers at Arthur D. Little in the early 1980's using pesticides from industrial wastewaters and model compounds [9, 10]. Carbon regenerated with CO_2 maintained a stable working capacity after 31 cycles whereas thermal regeneration typically reduces capacity 5-10% per cycle. An economic analysis showed that the processing costs depend predominantly on the specific waste properties and the regeneration throughput and were competitive with thermal regeneration. All of their regeneration experiments, however, were carried out at 120°C or 225°C (reduced temperatures of 1.29 and 1.64 respectively), where CO_2 is only supercritical in the technical sense of being above its critical point. Most of the unique characteristics of these fluids such has high compressibility and high diffusivities appear in the region of reduced temperature between 1.01 and 1.1, and many workers have since demonstrated the ability to extract contaminants from GAC and soil at these conditions [11-16]. Solubility and spectroscopic results in recent years have given new insight into the solubility mechanisms in SCF's and more sophisticated equations of state for determining phase behavior have been developed. It is useful therefore to apply some of the new knowledge to refine the application of this technology.

We report here the results of a pilot scale study of the SCF regeneration of GAC. The data obtained are used with a computer aided design package to produce a scaled up design of a fixed-site unit with economic analysis.

SOLUBILITY IN SUPERCRITICAL FLUIDS

We and others have made solubility measurements over the past decade using a variety of supercritical fluids over a range of temperatures. In the most common method an SCF is passed through a packed bed of solute and samples are either taken directly from the high pressure stream in a volume-calibrated sampling valve, or the saturated solution is flashed to atmospheric pressure where the solute drops out for weighing, and the gas flow is monitored. This technique can measure solute mole fractions in the range 10^{-5}-10^{-1} with a precision of about 10%. Carbon dioxide is the most often-used solvent because it is non-flammable and non-toxic; other common fluids with critical temperatures near room temperature are ethane, ethylene, fluoroform, and sulfur hexafluoride. Examples of medium temperature fluids are ammonia, propane, and butane, while very high temperature fluids include alcohols, toluene and water. Typical solutes of environmental significance are monofunctional alkanes and aromatics, phenol derivatives, and various pesticides [17-20].

The solvent power for the non-polar room temperature fluids appears to increase in the order $SF_6 < CO_2 < C_2H_6 < C_2H_4$. The solvent power of fluoroform increases with solute dipole moment; it is a better solvent for polar solutes but not as good as carbon dioxide for nonpolar compounds. For solutes of low volatility, the absolute solubility will depend greatly on the choice of solvent since solubility always increases with temperature at constant density. This indicates that although carbon dioxide is a convenient solvent because it is non-flammable and non-toxic, butane ($T_c = 152$°C) may be a better choice for many environmental applications.

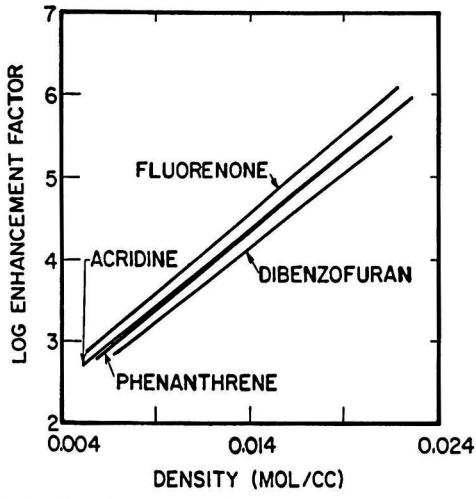

FIGURE 1. Enhancement factors for model compounds in supercritical CO_2 at 50°C.

The effect of solute properties on solubility is essentially two-fold: Solubility depends on the solute's volatility or vapor pressure and also on the strength of solute-solvent intermolecular forces. In order to compare the latter effects, a dimensionless enhancement factor is used which is defined as the ratio of a solute's partial pressure in the supercritical phase to its ideal gas partial pressure or vapor pressure (equation 1).

$$E = \frac{y_2 P}{P_2^{sat}} \tag{1}$$

By factoring out the solute's volatility, the enhancement factor allows comparison of solvent and secondary solute effects. Empirically, there is a linear relation between the log of the enhancement factor and solvent density. In fact, for the nonpolar and polar solutes shown in Figure 1 in supercritical CO_2, the enhancement factor plots almost coincide, indicating that differences in solubility are due primarily to vapor pressure differences. Non-linear behavior is noted for high solubilities (10^{-2}-10^{-1} mole fraction) as in the case of naphthalene in supercritical ethylene. The enhancement in pure fluids is relatively independent of solute structure but is sensitive to solvent polarity and density.

In pursuit of further solubility enhancements and solute selectivities, cosolvents (also known as entrainers) may be added to an SCF. Cosolvents are normally used at concentrations of 1-5 mole% with methanol and acetone being typical examples. The addition of cosolvent usually raises the mixture critical point several degrees and several bar above the pure solvent critical point with concentrations as small as 3-4%. This means that the operating conditions need to be altered accordingly to achieve similar supercritical properties and to maintain a single phase.

For nonpolar solutes containing no functional groups, the cosolvent-induced solubility enhancement is quite similar for all cosolvents and depends only on the concentration of cosolvent. This type of enhancement apparently results from

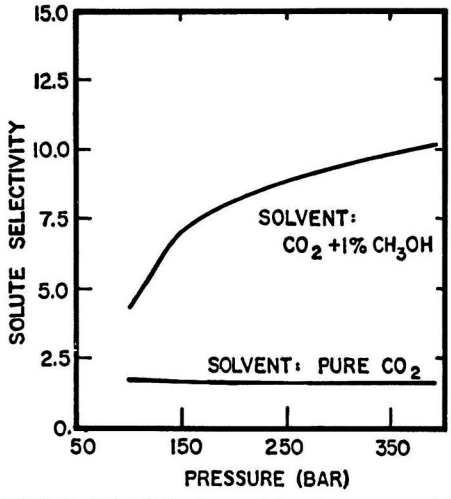

FIGURE 2. Selectivity for acridine from an acridine/anthracene mixture.

alteration of the solvent properties rather than any specific interaction. In the case of a polar or heterocyclic solutes, the nature of the cosolvent does become important in the magnitude of the enhancement factor, for example in hydrogen bonding or dipole-dipole interactions with the solute. It is these types of specific interactions that allow one to tailor a solvent/cosolvent mixture to enhance the solubility of a particular solute.

The preferential enhancement of one solute from a mixture of solutes then leads to novel separation processes. This enhancement of a single solute (or selectivity) is shown in Figure 2 for a mixture of acridine and anthracene, where the addition of methanol as a cosolvent in supercritical CO_2 yields a substantial increase in the selectivity of acridine. Again, this enhancement is due presumably to a specific hydrogen bonding interaction between the hydroxylic proton in methanol and the unpaired electrons on the amine nitrogen in acridine, whereas anthracene is not capable of participating in such an interaction.

The most widely used method for calculating high pressure gas phase thermodynamic properties is the cubic equation of state (e.g., Soave-Redlich-Kwong, Peng-Robinson). These equations have their basis in the classic van der Waals equation and their strength lies in their simplicity. They are cubic in volume (or density) and may be solved readily. They describe pure component PVT properties reasonably well and are readily extended to mixtures. Various attempts have been made to modify the molecular interactions in these models to describe more accurately the phase equilibria in the asymmetric solid-SCF system. The most difficult challenges an equation of state faces are the large differences in size and energy of the components and high compressibility of the solution which manifests itself in regions of augmented solvent density about a solute molecule. Reviews by Brennecke and Eckert [*6*] and Johnston and coworkers [*7*] provide excellent evaluation of the various approaches to modelling these solutions.

An approach for including cosolvent effects which appears promising is to treat the cosolvent-solute interaction by the law of mass action with an equilibrium constant and couple this chemical equilibrium with an equation of state that handles the physical interactions. These so called chemical-physical models are very versatile but suffer from too many adjustable parameters. It may be possible to reduce the number of such parameters, however, by measuring equilibrium constants spectroscopically [*21*]. It is likely that the most profitable applications of SCF technology will need to make use of cosolvent

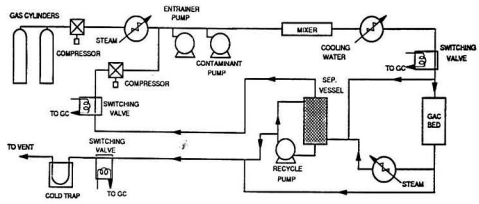

FIGURE 3. Schematic of pilot plant for GAC regeneration process.

effects to "tailor" a solvent for a particular solute and this type of model will likely be useful in the development of these applications.

PILOT PLANT EXPERIMENTS

The pilot plant is a two-part apparatus designed to carry out SCF regeneration of GAC and near-critical gas/liquid separations on a scale such that the data may be used directly in design calculations for a detoxification unit with reasonable scale-up factors (Figure 3). The two units are a GAC regeneration or desorption bed and a contaminant separation flash vessel, which may be operated separately or together. In addition to the pilot plant, another apparatus was constructed similar to that used by Tan & Liou [*14*] for preparing "contaminated" GAC by adsorbing the model compound onto the GAC from a nitrogen stream.

For GAC regeneration, liquid CO_2 was pumped to operating pressure and brought to temperature in a series of steam and cooling water heat exchangers. The system temperature and pressure were monitored with a thermistor probe (OMEGA OL-703) and pressure transducer (OMEGA PX302-3 KGV) respectively. Methanol was injected during the heat up stage by means of a high pressure syringe pump (ISCO μLC-500). The GAC bed consisted of an 18″ (45.7 cm) long, 3/8″ (0.95 cm) OD × 0.305″ (0.77 cm) ID piece of stainless steel tubing which was loaded with a preweighed sample of contaminated GAC. Glass wool plugs held the GAC in place during operation. An in-line high pressure UV monitor (Milton Roy Critical Extraction Monitor) was located downstream of the GAC bed to determine the concentration of contaminant in the SCF as a function of time. The output from the UV had to be back calibrated from the final contaminant concentration determined gravimetrically due to instrument deficiencies. Finally, the fluid mixture was flashed to atmospheric pressure through a micrometering valve where the contaminant dropped out of solution and was collected in a cold trap. The gas flow rate was monitored with a wet test meter.

The GAC (Calgon F-400) was washed once with distilled water to remove fines, dried under vacuum, then kept in a desiccator until ready for use. No screening for particle size was carried out. Carbon dioxide was bone dry grade (99.0%) from Linde. The 2-chlorophenol, methanol, toluene, and water were obtained from Aldrich and were used as received.

Regeneration experiments with CO_2 were carried out for 2-chlorophenol, 2-chlorophenol with methanol cosolvent, toluene, and toluene in the presence of water at 40°C and 10.4 MPa. Since the temperature and pressure effects on SCF phase and desorption behavior could be nominally predicted, these studies concentrated on flow rate effects and desorption profiles.

In order to model the rate of desorption it is also desirable to know the adsorption profile to help establish the equilibrium case. We previously carried out the adsorption of 2-chlorophenol from supercritical CO_2 at 17.3 MPa and 50°C. This adsorption profile resulted in a maximum loading of approximately 6 mmol/g GAC and was correlated with a Toth isotherm (equation 2),

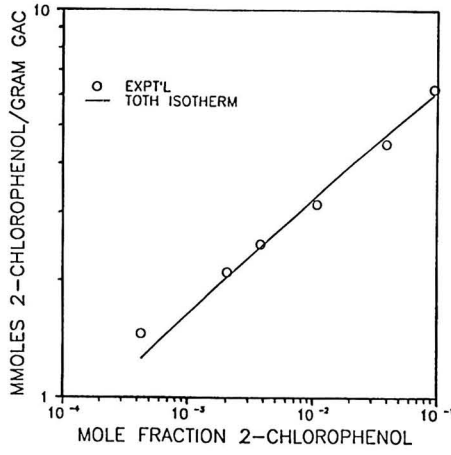

FIGURE 4. Adsorption of 2-chlorophenol from supercritical CO_2.

$$n = n_o \frac{c}{(b + c^m)^{1/m}} \quad (2)$$

where n is the amount adsorbed (mmol/g) and c is the concentration in the fluid phase (mmol/L). The regressed constants are: $n_o = 955$ mmol/g; $m = 0.0579$; and $b = 0.526$ (mmol/L)^m. The data and correlation are shown in Figure 4. To expedite sample preparation, further samples of GAC for the regeneration studies were prepared in a low pressure system using nitrogen as the carrier.

Using the nitrogen adsorption method, 2-chlorophenol showed a loading of 0.53 g/g GAC, while toluene adsorbed at 0.37 g/g GAC. These loadings were reproducible to within 2%.

The regeneration efficiency is defined as the percent of the initial concentration removed during regeneration. The desorption profile for toluene is shown in Figure 5 along with literature data for this system [*14*]. The data are plotted as a function of a dimensionless volume (volume of fluid at bed

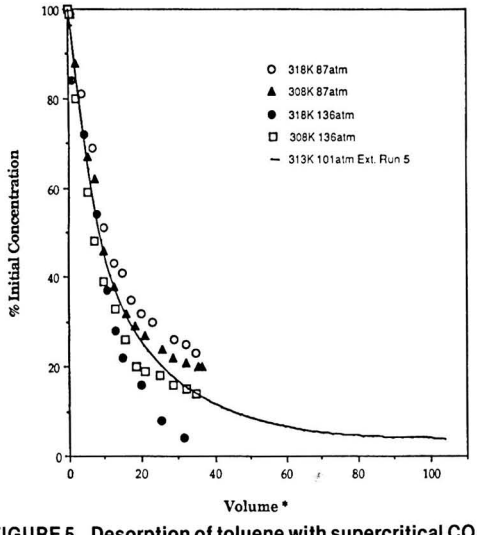

FIGURE 5. Desorption of toluene with supercritical CO_2, symbols are data of Tan & Liou. (V^* = dimensionless volume defined in text)

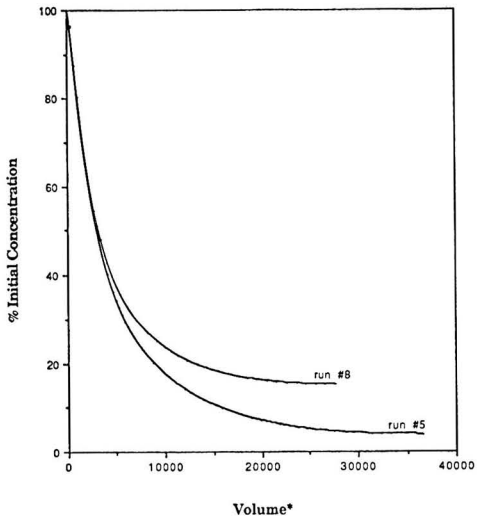

FIGURE 6. Desorption of toluene in the presence (#8) and absence (#5) of water. (V^* = dimensionless volume defined in text)

conditions/volume of GAC) in order to compare between our data and the literature data. The agreement is quite good despite differences in temperature, flow rate, and GAC. Figure 6 shows the effect of water on the desorption of toluene. The regeneration efficiency was 96% without water and 85% with water, but the initial rates of desorption (indicated by the slope of the desorption profile) are similar for both cases. Water apparently has a shielding effect for low concentrations of toluene. Efficiencies of 85% and 89% were observed for 2-chlorophenol in two separate trials.

In early studies the flow rate of CO_2 was varied to discern any mass transfer effects in terms of superficial velocity of solvent. No effect of superficial velocity was noted in our desorption profiles. The addition of methanol as a cosolvent to increase the regeneration efficiency actually does not help but appears to adsorb onto the carbon from the SCF phase. The GAC gained weight during a desorption run using methanol as a cosolvent.

The regeneration efficiency is determined by two competing effects, solvation and adsorption. The solvation is dictated by thermodynamic equilibrium and can be estimated using equation of state models for solid-SCF phase equilibria. The adsorption is determined by the characteristics of the GAC and the contaminant. Often the contaminant must compete for adsorption sites with other components of the solution (predominantly water), however, most chlorinated or polar aromatic compounds are easily adsorbed out of low concentration solutions. It appears that one layer of these strong adsorbates irreversibly adsorbs to the carbon causing a significant reduction in capacity after one adsorption/desorption cycle (30 + %). Acetic acid is one example of a weak adsorbate which can be fully desorbed [*9*]. Through repetitive cycles, other investigators have demonstrated sufficiently that SCF regenerated carbon retains consistently higher adsorption capacity than steam regenerated carbon [*9, 13*]. Such things as surface area per unit volume, heat treatment, and particle size, affect the adsorption/desorption properties but little can be done to predict these effects, and we did not have the facilities necessary to characterize fully the GAC. Further, it appears that contaminant type (which will be variable in practice), more strongly influences the economics than carbon properties. Therefore, adsorption/desorption experiments must be carried out for compounds of interest and the results fit to a model, as was shown above, which can then be extended in pressure and

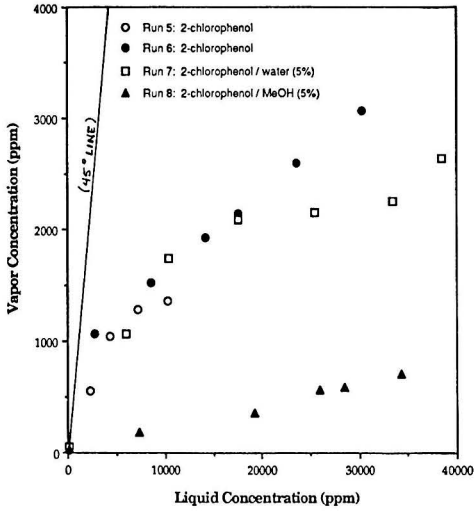

FIGURE 7. Vapor-liquid equilibria in the 2-chlorophenol/CO_2 system. (ppm = weight fraction times 10^6)

temperature space for that compound only.

For near-critical vapor-liquid separation, CO_2 was pumped through the heat exchangers and flashed through a micrometering valve into a separation vessel at a lower, but still elevated pressure. The gas phase from the separation vessel was recompressed and recycled to provide a recirculating flow while the liquid phase was pumped back to the top of the vessel to wash the gas stream. Once the desired conditions stabilized, the contaminant was injected into the stream and allowed to distribute between the two phases in the separation vessel. The vapor phase was then sampled and analyzed by gas chromatography. When water or methanol was used, it was added before the contaminant, and analysis was carried out before the contaminant was introduced.

The systems studies for separation include 2-chlorophenol/CO_2, 2-chlorophenol/water/CO_2, and 2-chlorophenol/methanol/CO_2. The concentrations of water and methanol were both 5 mole%. The results from these experiments are shown in Figure 7 as vapor concentration vs. liquid concentration. For a successful separation to occur, the contaminant must preferentially distribute into one of the two phases leaving the other phase relatively pure. This distribution will show up as a deviation of the data from the 45 degree line, which in the figure rises steeply away from the data due to the scales of the axes. The data indicate that most of the contaminant is in the liquid phase and that it would be possible to recycle the vapor phase as a solvent and concentrate the contaminants in a liquid phase.

Several recent publications discuss models for supercritical regeneration of GAC; Tan and Liou [*13*] present a model for the desorption of ethyl acetate which assumes no axial dispersion and which approximates the desorption kinetics as being linearly related to the adsorbed concentration. The resulting equation for desorption bed outlet concentration, $C(L, t)$ is:

$$C(L,t)=\frac{1-\alpha}{\alpha}C_{a_0}\left[\exp\left(-k\left(t-\frac{\alpha L}{u}\right)\right)-\exp(-kt)\right] \quad (3)$$

where k is defined as the kinetic desorption constant given by:

$$\frac{\partial C_a}{\partial t}=-kC_a \quad (4)$$

Recasens *et al.* [*22*] improved upon this model by incorporating the solid-SCF equilibrium and external mass transfer coefficient explicitly, assuming a parabolic concentration profile inside the particles. Analytical solutions were developed for two cases: 1) where equilibrium desorption occurs and is controlled by the external and intraparticle mass transfer rates and 2) where a first-order irreversible desorption step is controlling. The first of these was found to describe effectively the supercritical desorption of ethyl acetate. The solutions for exit concentration and desorbed fraction from carbon with an initial concentration C_{A0} are:

$$\frac{C(L,t)}{C_{a_0}/K}=\frac{b'}{b+b'}\exp[-(b+b')\theta][\exp(b+b')-1]+\exp[-(b+b')(\theta-1)]\sum_{m=0}^{\infty}(-1)^{m+1}\left(\frac{b}{b'}\right)^m\times\frac{A_m(b')A_m[b'(1-\theta)]}{(m!)^2} \quad (5)$$

where

$$\theta=\frac{tu}{L\alpha}$$

$$b=\frac{3k_pL\alpha}{r_0(\beta+\rho K)u}$$

$$b'=\frac{3(1-\alpha)k_pL}{r_0u} \quad (5a)$$

and A_m is related to the incomplete gamma function. The equilibrium constant K rigorously denotes the equilibrium between adsorbed concentration and concentration in the pore fluid:

$$C_a=KC_{pore} \quad (6)$$

The desorbed fraction is given by equation 7:

$$F=\frac{b}{b+b'}\left[1-\frac{\exp[-\theta(b+b')][\exp(b+b')-1]}{b+b'}\right]+\frac{1}{b+b'}\sum_{m=0}^{\infty}\frac{A_m(b')A_m[b(\theta-1)]}{(m!)^2}-\frac{b}{(b+b')b'}\exp[-(b+b')(\theta-1)]\times\sum_{m=0}^{\infty}(-1)^{m+1}\left(\frac{b}{b'}\right)^m\frac{A_m(b')A_m[b(1-\theta)]}{(m!)^2} \quad (7)$$

We found the first four terms in the summation sufficient to approximate the series.

In this work the data for SCF regeneration of GAC adsorbed with 2-chlorophenol have been modeled with these equilibrium desorption/mass transfer equations. Optimal fits for the equilibrium constant K and the overall mass transfer coefficient, k_p, were obtained by visual inspection using MathCAD software. The observed desorbed fraction may be reasonably predicted for a range of K, k_p combinations, but in order to simultaneously model the exit concentration, the values are constrained to a single pair. Figures 8 and 9 display a series of data in comparison with predicted values. The fitted values for equilibrium and mass transfer coefficients are 2.5×10^{-2} m^3/kg and 5.7×10^{-7} m/s respectively. These were used in the design study to determine cycle times and regeneration effectiveness for various fluid flow rates and bed lengths. Representative results for a fluid velocity of 0.05 m/s and 10 m bed length are shown in Figures 10 and 11.

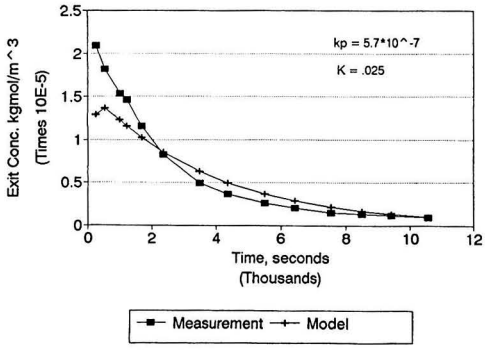

FIGURE 8. Model correlation of exit concentration data for 2-chlorophenol.

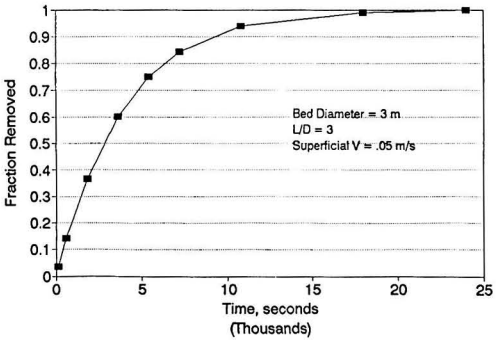

FIGURE 11. Calculated desorbed fraction profile for scaled-up desorber.

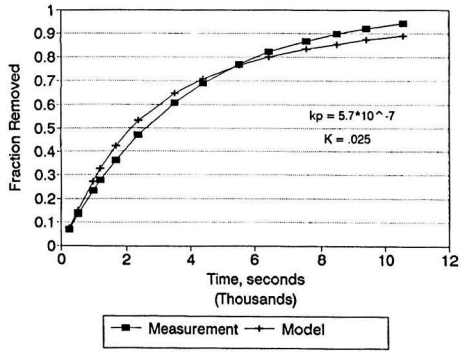

FIGURE 9. Model correlation of desorbed fraction of 2-chlorophenol.

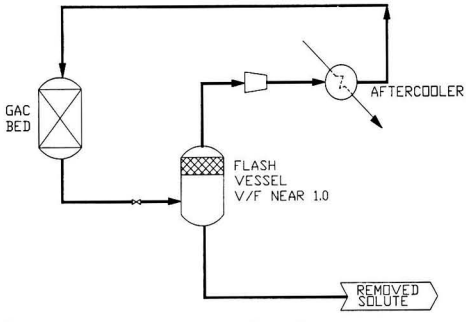

FIGURE 12. SCF recycling option 1.

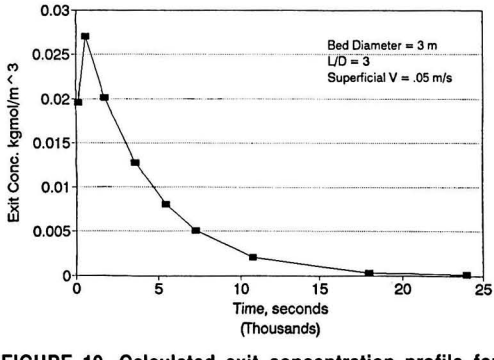

FIGURE 10. Calculated exit concentration profile for scaled-up desorber.

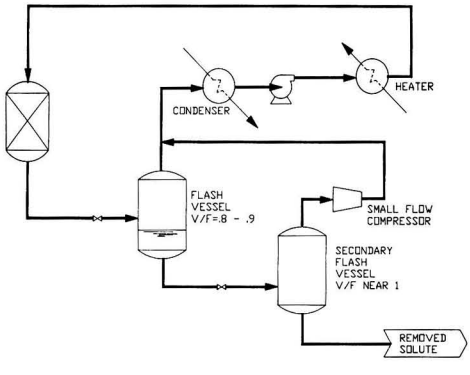

FIGURE 13. SCF recycling option 2.

APPLICATION TO DESIGN OF TREATMENT FACILITIES

Previous studies have shown that direct recycling of vapors (via recompression to supercritical pressure) is problematic in that demisting of the entrained solute is difficult and costly due to high compression of large vapor flows. An alternative which is often more economical and superior in operation is to condense the flashed vapors, pump the liquid phase to the desired pressure, and then heat to operating temperature. These processes, denoted as Options 1 and 2 respectively, are shown in Figures 12 and 13. Each of these options has been simulated with ChemCAD version 2.41 process simulation software.

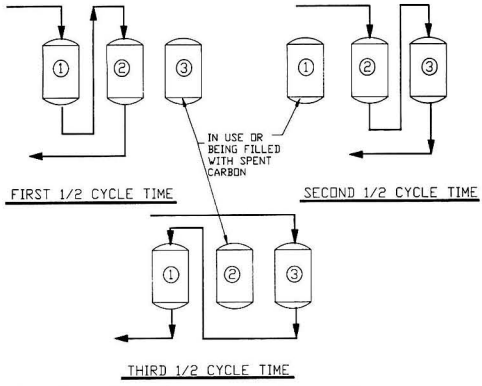

FIGURE 14. Desorber regeneration cycle sequence.

The regeneration data for 2-chlorophenol indicate the mass transfer kinetics are limiting. Thus the exit concentrations are not approaching the SCF solubility limits at any time, most particularly during the last half of the desorption cycle time. Consequently, it is advantageous to use a progressive sequence in which the SCF from a bed in the last half of its cycle is used to accomplish the first half of the cycle of another bed. With three beds as a unit, the cycle sequence is shown in Figure 14. The final flowsheet adopts this approach, minimizing cost of recycling the fluid and keeping the exit concentration fairly stable as a function of time. It is an assumption of this configuration that the individual regeneration vessels are being emptied of regenerated carbon and refilled during the off-line time. One half of a complete regeneration cycle should be adequate for the solids handling steps.

The model developed from analysis of the experimental data was used to examine the effects of bed height and fluid velocity over practical ranges. The optimal superficial velocity was determined by increasing the flow until further increments no longer result in decreased cycle time. This limit exists because the mass transfer rate is the desorption rate limiting step. A superficial velocity of 4.0 ft/min (2.0 cm/s) was found to be optimal and was adopted for the final flowsheet and economic analysis.

The cost calculations and analyses were performed on a computer spreadsheet. Cost/capacity relationships for major equipment inserted in the spreadsheet have been derived from cost data presented in Peters and Timmerhaus [*23*] and Guthrie [*24*]. For ease of use in the spreadsheet, all graphical data have been fit to equations which are described in the Appendix. The

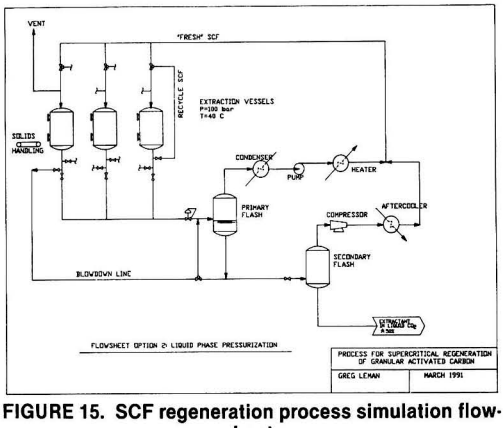

FIGURE 15. SCF regeneration process simulation flowsheet.

Table 1 Summary of Investment Costs ($10^3$$, 1991)

Direct Capital Costs:	
Extraction Vessels	345.7
Primary Flash Vessel	19.8
Reboiler for Primary Flash	42.1
Secondary Flash Vessel	3.8
Condenser	84.2
Refrigerated Condensate Loop	93.1
High Pressure Liquid Pump	43.4
Heater for High Pressure Liquid	49.2
Secondary Flash Recycle Compressor	93.1
After Cooler	72.6
Blowdown Recycle Compressor	49.2
After Cooler	1.8
Process Control/Instrumentation	250.0
Unlisted Equipment (35% of Total Dir.)	483.5
TOTAL DIRECT CAPITAL	1631.5
Indirect Costs (0.38 × Direct Costs)	620.0
Fees and Contingency (0.25 × Dir + Ind)	562.9
Working Capital (15% of Total Capital)	496.6
TOTAL CAPITAL INVESTMENT	3310.9

chemical engineering cost index for chemical process industries was used to convert purchased costs to a 1991 basis. The data from Guthrie includes ratios for total installed costs to purchased costs for each type of equipment, and these are used to develop the direct capital investment. Ratios for indirect capital are taken from Peters and Timmerhaus.

Supercritical fluid recycle efficiency determines operating feasibility and overall economy. As discussed above, the condensation of vapors from the first flash with a liquid pump for recompression and a gas compressor from the secondary flash vapors is much more economical than recompressing a vapor stream from a single flash. This scheme is more energy efficient primarily because the operating temperature is not far removed from ambient. This recycle scheme has been incorporated into a process simulation flowsheet (Figure 15) along with the 3-unit desorber described above.

The design presented is a fixed-site unit with a regeneration capacity of 24 tons (21.8 metric tons) of GAC per day. The capital cost does not include equipment for steam generation and so assumes that the plant is part of a larger industrial unit from which steam is supplied at $1.50/1000 lb ($3.30/metric ton) and cooling water at $1.00/10,000 gal (2.6¢/$m^3$). A summary of the direct capital investment costs is given in Table 1. Indirect costs are estimated as 38% of direct costs, then fees and contingencies are 25% of direct plus indirect costs. The total capital investment for the unit is 3.3 million dollars. Table 2 is a summary of operating costs for the regeneration unit on the basis of one operator per shift (24 hr operation), 0.5% loss rate for the SCF, and 4¢/lb (9¢/kg) replacement costs for CO_2, yielding a regeneration cost of 10.6¢/lb (23¢/kg).

Table 3 lists our costs along with those reported by De Filippi and co-workers [*9*, *10*] for phenol, dinitrobutylphenol, atrazine, and thermal regeneration. Comparisons of treatment costs with thermal regeneration are favorable. In addition to maintaining a stable capacity, SCF regeneration is consistently less expensive than thermal treatment. The final alternatives are incineration or disposal by landfill. Incineration of soils containing hazardous wastes is at least 20¢/lb (44¢/kg) for a similar scale unit [*25*]. This process compares favorably both economically and ecologically with the alternatives.

SUMMARY AND CONCLUSIONS

A primary key to designing any separation process is understanding the phase behavior in any particular mixture of

Table 2 Summary of Operating Costs ($10^3$$/YR, 1991)

DIRECT PRODUCTION COSTS:	
Make-up CO_2	271.4
Operating Labor	200.0
Direct Supervision	40.0
Utilities: Electricity	162.4
Steam	142.1
Cooling Water	2.5
Maintenance (7% of T.C.I.)	231.8
Operating Supplies (15% of Maint.)	34.8
Laboratory Charges (15% of Op. Labor)	30.0
FIXED CHARGES:	
Depreciation	163.1
Taxes & Insurance (3% of Fixed Cap.)	67.5
Plant Overhead (60% of Op. Lab. + Sup. + Maint.)	283.1
Administrative Costs (15% of Op. Lab. + Sup. + Maint.)	70.8
TOTAL TREATMENT COST	1699.4
UNIT TREATMENT COST	10.6¢/lb (23¢/kg)

components. This is especially so when proposing an unconventional process such as supercritical fluid extraction, where one cannot predict solution properties with any certainty. A substantial database of solubilities in supercritical fluids now exists and mathematical models can correlate the data. We are therefore at the stage of applying the knowledge of SCF thermodynamics to environmental and other separation applications. In this work, a pilot plant for the regeneration of GAC using supercritical carbon dioxide was constructed and operated demonstrating the feasibility of this application.

The ability of supercritical CO_2 to remove model contaminant compounds from GAC and subsequently drop out most of the contaminant in a liquid phase has been investigated. Model compounds 2-chlorophenol, and toluene were chosen to represent common features of hazardous waste chemicals and difficult desorptions providing a conservative basis for design. Contaminants were adsorbed onto GAC through either direct contact or by entrainment in a gas stream and desorbed with CO_2 at 40°C and 10.4 MPa. Typical desorption profiles indicate an 85% removal of the compound from the carbon. The presence of water on the GAC was shown to inhibit slightly the efficiency of the desorption. The desorption results have been interpreted with a generalized desorption-mass transfer model.

The results of the pilot plant studies have been applied to the design of a 24 ton/day (21.8 metric ton/day) fixed-site GAC regeneration unit consisting of a three element desorber with two stage flash separation. Optimization of the process centers around minimizing the cost of recycling the SCF through an efficient recompression scheme and cycle configuration in the desorber unit. An economic evaluation shows a processing cost of 10.6¢/lb (23¢/kg) GAC. The estimated capital and operating costs are valid within approximately 30%. If a small, mobile unit were to be built, the operating costs would be somewhat higher due to an economy of scaling which favors larger units and, the infeasibility of including a refrigeration system, forcing the use of the high cost flowsheet option which requires only cooling water.

The cost of this process compares favorably with thermal regeneration, the most often chosen alternative, but has the distinct advantage of maintaining a stable adsorbate capacity. This many-cycle regenerative use cuts carbon replacement costs and avoids landfill of spent material.

Table 3 Comparison of Operating Costs for Regeneration of GAC

Contaminant	Capacity/ Throughput (Ton/day)	Reported Unit Cost (¢/lb)	Adjusted Unit Cost[a] (¢/lb)
2-Chlorophenol	24	10.6	10.6
Atrazine	2.5	14[b]	29
Dinitrobutylphenol	1	29[b]	46.2
Phenol	5	8.5[c]	16.1
Thermal Regeneration		29-36[b]	46-57
Incineration (From data on Soils)		18-48[d]	20-53

[a]Adjusted to 1991 dollars assuming 6% inflation
[b]1983 dollars
[c]1980 dollars
[d]1989 dollars
(1¢/lb = 2.2 ¢/kg)

ACKNOWLEDGMENT

This project has been financed with federal funds as part of the program of the Advanced Environmental Control Technology Research Center—University of Illinois, at Urbana-Champaign, which is supported under cooperative agreement CR 812582 with the Environmental Protection Agency. The contents do not necessarily reflect the views and policies of the Environmental Protection Agency nor does the mention of trade names or commercial products constitute endorsement or recommendation for use.

NOTATION

Symbols

A = heat transfer area
$A_m(w)$ = incomplete gamma function
b, b' = dimensionless groups defined in equation 5a
C = concentration in SCF phase
C^{70} = cost in 1970 dollars
C^{79} = cost in 1979 dollars
D = diameter
DC^{91} = direct capital costs in 1991 dollars
E = enhancement factor
F = fraction desorbed
F_p = cost factor for pressure
K = adsorption equilibrium constant
k = desorption rate constant
k_p = overall mass transfer coefficient
L = length of carbon bed
P = pressure
Q = refrigeration system capacity
q = compressor intake flow rate
r_0 = GAC particle radius
t = time
u = superficial velocity of fluid at T&P of bed
w = dummy variable in incomplete gamma function

Superscripts

sat = saturation (VLE or SVE boundary)

Subscripts

a = adsorbed phase
cmp = compressor
hx = heat exchanger
int = internal support
o = initial
$pore$ = fluid in pore
rf = refrigeration system
vsl = pressure vessel

Greek symbols

α = void fraction of GAC bed
β = porosity of GAC particles
θ = dimensionless time defined in equation 5a
ρ = density of GAC particles

LITERATURE CITED

1. Reisch, M., *Chem. Eng. News*, **68**(43), 13 (1990).
2. Paulaitis, M. E., Krukonis, V. J., Kurnik, R. T., and R. C. Reid, "Supercritical Fluid Extraction," *Rev. Chem. Eng.*, **1**(2), 179 (1982).
3. Penninger, J. M. L., M. Radosz, M. A. McHugh, and V. J. Krukonis, eds., *Process Technology Proceedings Vol. 3, Supercritical Fluid Technology*, Elsevier Science Publishers, Amsterdam, The Netherlands (1985).
4. McHugh, M. A., and V. J. Krukonis, *Supercritical Fluid Extraction, Principles and Practice*, Butterworth Publishers, Boston, MA (1986).
5. Johnston, K. P., and J. M. L. Penninger, eds., *Supercritical Fluid Science and Technology, ACS Symp. Ser.*, **406** (1989).
6. Brennecke, J. F., and C. A. Eckert, "Phase Equilibria for Supercritical Fluid Process Design," *AIChE J.*, **35**(9), 1409 (1989).
7. Johnston, K. P., D. G. Peck, and S. Kim, "Modeling Supercritical Mixtures: How Predictive Is It?," *Ind. Eng. Chem. Res.*, **28**, 1115 (1989).
8. Bruno, T. J., and J. F. Ely, eds., "Supercritical Fluid Technology: Reviews in Modern Theory & Application," CRC Press, Boca Raton, FL (1991).
9. DeFilippi, R. P.,'V. J. Krukonis, R. J. Robey, and M. Modell, "Supercritical Fluid Regeneration of Activated Carbon for Adsorption of Pesticides," EPA Report EPA-600/2-80-054, United States Environmental Protection Agency, Washington, DC (1980).
10. DeFilippi, R. P., and R. J. Robey, "Supercritical Fluid Regeneration of Adsorbents," EPA Report EPA-600/2-83-038, United States Environmental Protection Agency, Washington, DC (1983).
11. Brady, B. O., C-P. C. Kao, K. M. Dooley, F. C. Knopf, and R. P. Gambrell, "Supercritical Extraction of Toxic Organics from Soils," *I&EC Res.*, **26**, 261 (1987).
12. Dooley, K. M., C-P. Kao, R. P. Gambrell, and F. C. Knopf, "The Use of Entrainers in the Supercritical Extraction of Soils Contaminated with Hazardous Organics," *I&EC Res.*, **26**, 2058 (1987).
13. Tan, C-S., and D-C. Lious, "Desorption of Ethyl Acetate from Activated Carbon by Supercritical Carbon Dioxide," *I&EC Res.*, **27**, 988 (1988).
14. Tan, C-S., and D-C. Liou, "Regeneration of Activated Carbon Loaded with Toluene by Supercritical Carbon Dioxide," *Sep. Sci. Tech.*, **24**(1 & 2), 111 (1989).
15. Tan, C-S., and D-C. Liou, "Supercritical Regeneration of Activated Carbon Loaded with Benzene and Toluene," *I&EC Res.*, **28**, 1222 (1989).
16. Hess, R. K., C. Erkey, and A. Akgerman, "Supercritical Extraction of Phenol from Soil," *J. Supercritical Fluids*, **4**, 47 (1991).
17. Van Leer, R. A., and M. E. Paulaitis, "Solubilities of Phenol and Chlorinated Phenols in Supercritical Carbon Dioxide," *J. Chem. Eng. Data*, **25**(3), 257 (1980).
18. Krukonis, V. J., and R. T. Kurnik, "Solubility of Solid Aromatic Isomers in Carbon Dioxide," *J. Chem. Eng. Data*, **30**(3), 247 (1985).
19. Schmitt, W. J., and R. C. Reid, "The Solubility of Paraffinic Hydrocarbons and Their Derivatives in Supercritical Carbon Dioxide," *Chem. Eng. Comm.*, **64**, 155 (1988).
20. Smith, R. D., H. R. Udseth, B. W. Wright, and C. R. Yonker, 'Solubilities in Supercritical Fluids: The Application of Chromatographic Measurement Methods," *Sep. Schi. Tech.*, **22**, 1065 (1987).
21. Eckert, C. A., M. M. McNiel, B. A. Scott, and L. A. Halas, "NMR Measurements of Chemical Theory Equilibrium Constants for Hydrogen-Bonded Solutions," *AIChE J.*, **32**(5), 820 (1986).
22. Recasens, F., B. J. McCoy, and J. M. Smith, "Desorption Processes: Supercritical Regeneration of Activated Carbon," *AIChE J.*, **35**(6), 951 (1989).
23. Peters, M. S., and K. D. Timmerhaus, *Plant Design and Economics for Chemical Engineers*, 3rd Ed., McGraw-Hill Book Co., New York, NY (1980).
24. Guthrie, K. M., *Process Plant Estimating Evaluation and Control*, Craftsman Book Company of America, Solona Beach, CA (1974).
25. Environmental Protection Agency, "Mobile/Transportable Incineration Treatment," *Engineering Bulletin*, EPA/540/2-9/014, Office of Research and Development, Cincinnati, OH (1990).

APPENDIX

The cost estimates for all equipment were adapted to use in a spreadsheet by fitting various graphical data to analytical expressions.

A. PRESSURE VESSELS (EXTRACTION UNITS & FLASH SEPARATORS)

Base cost in 1970 dollars for a vessel of diameter D (ft):

$$C_{vsl}^{70} = 294\ D^{1.825} \tag{A1}$$

Cost factors for pressure (F_p, P in psig) and internal support (C_{int}) are given by:

$$F_p = 0.057\ P^{0.625}$$
$$C_{int}^{70} = 35.2\ D^{1.37} \tag{A2}$$

(1 ft = 30.48 cm; 1 psi = 6.89 kPa)

For pressure vessels, the ratio of direct capital to purchased cost is 3.0, thus, the total direct capital (DC_{vsl}) in 1991 dollars is:

$$DC_{vsl}^{91} = \frac{450}{126} F_p[C_{vsl}^{70} + C_{int}^{70}] * 3.0 \tag{A3}$$

No allowances were made for stainless steel or better alloys. If specific applications require alloy construction, capital costs will increase accordingly.

B. HEAT EXCHANGERS

Base Cost in 1979 dollars for an exchanger with surface area A (ft^2):

$$C_{HX}^{79} = 547\ A^{0.543} \tag{A4}$$

The cost factor for pressure in excess of 1000 psig is given by:

$$F_p = 0.575 + 4.14 \times 10^{-4} P \tag{A5}$$

(1 ft^2 = 0.093 m^2; 1 psi = 6.89 kPa)

The ratio of direct capital to purchased cost is 2.30 for heat exchangers giving a total direct capital of:

$$DC_{HX}^{91} = \frac{450}{230} F_p C_{HX}^{79} * 2.30 \tag{A6}$$

C. INDUSTRIAL GAS COMPRESSORS

Costs for compressors, up to 3-stage with intercooling, are given by:

$$C_{cmp}^{79} = 2.59\ q_{fm}^{0.517} \tag{A7}$$

where q_{fm} is the intake flow in actual cubic feet per minute. The direct capital ratio is 1.57 and total direct capital is then:

$$DC_{cmp}^{91} = \frac{450}{230}\ C_{cmp}^{79} * 1.57 \tag{A8}$$

(1 $ft^3/min = 0.0005\ m^3/s$)

D. INDUSTRIAL REFRIGERATION

The flowsheet includes condensation of CO_2 at 51°F (11°C), thus requiring an ammonia refrigeration loop. The cost for this system and its operation costs are calculated as follows: The unit cost, in 1979 dollars, for a Q_{RF} ton (1 ton = 12,000 BTU/hr) unit operating at 20°F (−7°C), is:

$$C_{RF}^{79} = 3.098\ Q_{RF}^{0.742} \tag{A9}$$

Operating costs are approximately $1.20/ton-day and the direct capital ratio is 3.46, therefore, the total direct capital is:

$$DC_{RF}^{91} = \frac{450}{230}\ C_{RF}^{79} * 3.46 \tag{A10}$$

1 BTU/hr = 0.293 W

Hazardous Waste Source-Reduction Study With Treated Groundwater Recycling

Li-Yang Chang and Benjamin J. McCoy
Department of Chemical Engineering, University of California, Davis, CA 95616

A feasibility study is presented for modifying electroplating processes for source reduction. Ion exchange and reverse osmosis units are suggested to allow reclaiming and recycling of metal solutions. A particular example of water conservation in an electroplating shop is presented for the treatment and utilization of groundwater contaminated by hydrocarbon chemicals, including volatile organic compounds (VOCs) and gasoline products. Granular carbon adsorption, UV oxidation, and demineralization steps and alkalinity control measures for the groundwater are discussed. Engineering and economic analyses provide a basis for comparing alternative designs. An integrated scheme, including groundwater remediation and source reduction, is feasible for the plating shop. The removal of VOCs and demineralization of the polluted groundwater are important steps. With the integrated plan, 90% removal or recovery of heavy metals can be achieved, and water usage and wastewater can be reduced by 90%. Thus, it is feasible to prevent water pollution at the source and to recycle treated groundwater and wastewater for the manufacturing process.

INTRODUCTION—INCENTIVES FOR REDUCING WASTES

As pollution prevention requirements become mandatory, hazardous waste generators are being subjected to stringent regulations and strong economic pressures to reduce wastes. Several source reduction or waste minimization enactments are (1) the 1984 Hazardous and Solid Wastes Amendments (HSWA), specifically mandated by the U.S. Congress into the Resource Conservation and Recovery Act (RCRA), (2) the Clean Water Act (e.g., the national pollutant discharge elimination system or NPDES), (3) the Clean Air Act (e.g., the National Emission Standards for Hazardous Air Pollutants or NESHAPS program), (4) regulations from state governments, such as the California's Hazardous Waste Source Reduction and Management Review Act of 1989 (also known as SB 14 regulations), (5) the effluent discharge limits set by local wastewater treatment plants. Economic pressures, such an increasing permit application fees, insurance costs, and treatment, disposal, and storage fees, as well as water shortages and conservation, are driving individuals, industries, and farms to reduce water usage. Long-term liabilities, including potential criminal liability, as well as public relations are also motivating pollution prevention and risk reduction.

In California, effluent discharge limits for industries have become increasingly strict, and industries and businesses are being forced to treat wastewaters to remove dissolved metals and organic chemicals, and to reuse the treated water. For example, at the southern San Francisco Bay area (South Bay) in California, the Bay receives treated sewage wastewater from Silicon Valley business and industry as well as from homes. Several wastewater treatment plants in the South Bay area are able to remove as much as 75% of the toxic chemicals and heavy metals that enter through sewer lines. However, any chemicals remaining in the water after treatment are released into the Bay. Because the South Bay is constricted at the Dumbarton narrows, it is poorly flushed by currents and tidal action. This results in pollutants, primarily metals (e.g., silver, copper, nickel, lead) accumulating in the water, sediments, plants, and wildlife. High concentrations of these toxic metals have already been found in several species of clams and mussels.

In the South Bay area during the 1980s, several POTWs were able to reduce metal discharge to the Bay by 60% as a result of the industrial waste control program. For example, the discharge limit of metals of several water pollution control plants have been set at the following values: copper 2.7 mg/L, lead 0.4 mg/L, cyanide 1.0 mg/L, zinc 2.6 mg/L, nickel

2.6 mg/L, and several cities require that the concentrations of nickel and silver in the discharged wastewater should not exceed 1.0 and 0.2 mg/l, respectively. In the 1990s, new waste minimization programs will be developed to reduce harmful discharges from laboratories, photoprocessing facilities, hospitals, vehicle service facilities, etc.

In 1991 the California's SB 14 regulations mandated by the Hazardous Waste Source Reduction and Management Review Act of 1989 provided for new requirements from businesses generating hazardous waste in excess of specified annual amounts. The businesses were required to prepare a source reduction evaluation and review plan (Plan) and a hazardous waste management performance report (Report) by September 1, 1991, and every four years thereafter. The Plan must fully explain the decision process used to determine which source reduction measures to implement and must also include an implementation timetable. The Plan must consider the multimedia effect of a selected source reduction measure, and may not merely shift the hazardous waste from one medium (air, water, or land) to another. The Report must identify the factors that affect the management of hazardous waste of the generator. The Plan and Report must be available to state or local government agencies and to the public for reviewing.

Before wastes are land-disposed, both federal and state governments require minimization of free liquid, suppression of flash point, reduction of hazard potential, removal of volatile organics, and stabilization or removal of soluble metals from hazardous wastes. This land disposal restriction, or land ban, is mandated by RCRA.

Because of the above regulations, restrictions, and limits, alternative nonsludge-generating methods of hazardous waste management will see increasing utilization. Onsite waste reduction technologies are perceived as achievable and profitable methods to treat hazardous wastes. Techniques such as evaporation (EV), reverse osmosis (RO), ion exchange (IX), electrolytic cell (EC), electrodialysis (ED), ultrafiltration, liquid-liquid and supercritical fluid extraction, activated carbon adsorption, and distillation have already been applied, e.g., in the electroplating, aerospace, semiconductor, and electronics industries [*1–5*]. Detailed discussions of liquid/solid separation techniques can be found elsewhere [*3–7*]. A conclusion of recent studies [*8, 9*] is that the conventional sludge treatment method for managing hazardous waste in water is no longer economic and is not able to meet the stringent effluent discharge limits imposed on many wastewater treatment plants.

RAW MATERIALS AND MAJOR WASTE STREAMS IN THE ELECTRONICS INDUSTRY

Solvents and metals are the common hazardous chemicals used in the electronics, aerospace, and photoprocessing industries. Halogenated and oxygenated solvents, such as 1,1,1-trichloroethane (1,1,1-TCA), methylene chloride, perchloroethylene, Freon 113, isopropyl alcohol, and n-butyl acetate, are widely used for parts cleaning, degreasing, preparation, and for the developing and stripping of photoresist materials. Other solvents, such as acetone, methyl ethyl ketone (MEK), methanol, xylene, hydrofluoric acid, HNO_3, HCl, H_2SO_4, and alkaline solutions (ammonia, sodium hydroxide), are also used. The metals usually employed for plating are silver, gold, copper, nickel, zinc, tin, lead, and their alloys. Molybdenum, silicon, and cyanides are also used in the electronics industries.

Plating processes are central to the electronics and aerospace industries. Many steps are required to process the plated part, such as surface preparation and cleaning, catalyst application, electroless plating, image transfer for PC boards [*10*], electroplating, soldering, etching, striking, and rinsing [*1–3, 11, 12*].

The major sources of the inorganic and organic chemicals in wastestreams are the spent plating baths and rinses used in the plating process. Other sources of metallic contaminants are spent etchant, etch rinses, and sludges. Typical hazardous waste streams generated by plating-related processes are waste rinsing water, waste sludge, spent process baths, waste acids and bases, and metal salts. The major waste streams from 57 electronics firms show that more than 60% of the total hazardous waste consists of liquids with dissolved metals [*13*]. Only 4% of the total waste was recovered and recycled.

Chang and McCoy [*8, 9*] reported two feasibility studies of source reduction for small and large printed-circuit (PC) board manufacturing processes. The processes are generally divided into four categories: board and surface preparation, electroless plating, electroplating, and etching [*14, 15*]. As many as 20 to 40 operating steps may be involved in the whole manufacturing process. We will briefly review one case to set the stage for the particular example analyzed in the present work.

For a small PC board firm, nine dip-rinse and three spray-rinse operations are used; most are single-stage rinse units. A hazardous waste management plan was proposed, including waste treatment audit, manufacturing process evaluation, waste source identification, waste stream segregation, source reduction for electroplating and electroless coppering lines, manufacturing process modification with closed-loop rinse and recycling process, and water usage minimization. Originally the waste rinse water is treated at one industrial waste treatment plant with the conventional sludge treatment method, and the treated water is discharged to a local water pollution control plant.

In the source reduction scheme, two two-stage counter-current separation/rinsing systems were recommended to treat the waste rinsewater from the electroless copper line and the electroplating copper line. Three single-stage rinse units in the original copper plating process are replaced with three two-stage separation/rinsing systems. The separation/rinsing system for treating the spent rinsewater is composed of a strong acid cation resin and a weak base anion resin exchange column. The recovered metal salt in the regenerate solution (the IX resin was regenerated with sodium hydroxide [*5*]) and the rinsewater are reused in the process.

Based on the study of Gold et al. [*16*], an ion exchange system will be implemented to treat the spent electroless copper solution. The saturated resin can be regenerated with sodium-form EDTA (ethylenediamine tetracetic acid). The recovered EDTA-copper solution can be reused in the electroless process after passing through a filtration unit. The deionized water effluent from this separation unit will be recycled back to the rinse unit. The lightly polluted rinsewater from two single-stage rinse units of the etching and electroless copper processes can be reused for the next suggested two-stage rinse units. The used rinsewater from six two-stage rinse units (among them, three are in the electroless line and another three are in the etching line) can be mixed and treated with the existing wastewater precipitation, neutralization, and flocculation processes. The treated water will then be discharged to the sewer.

INTEGRATION OF SOURCE REDUCTION AND GROUNDWATER REMEDIATION FOR AN ELECTROPLATING SHOP—FEASIBILITY STUDY

The objective of this source reduction and water conservation study for a microwave parts manufacturer is to apply the integrated source reduction technologies that have been implemented for PC board manufacturers and to examine the feasibility of remediating groundwater for reuse. Since more than 60% (by weight) of waste from the plating line results in aqueous, acidic, and alkaline solutions with metals, and more than 25,000 gal/day or 95,000 L/day of water is used, water reuse and the reduction of these solutions are major concerns.

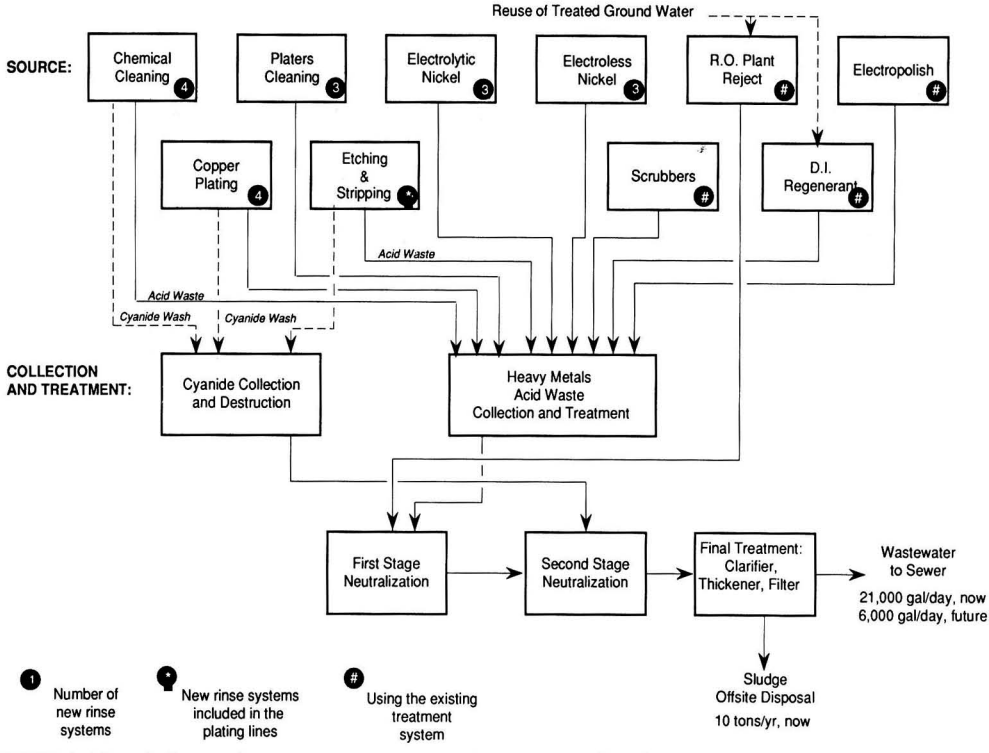

FIGURE 1. The plating and waste stream treatment processes of a microwave parts manufacturer.

Background

Several years ago in this microwave manufacturing facility, a polluted site was identified. Organic chemicals, such as trichloroethylene and dichloroethylene, were detected in both soil and groundwater samples. A groundwater remediation investigation and remediation feasibility study were conducted. Since the facility needs a huge amount of water each day, the manufacturer planned to reuse part of the treated groundwater for the plate shop. The rest of the treated groundwater could be used for irrigation or cooling purposes. Thus, the site remediation, water conservation, and source reduction projects can be integrated together. This will decrease the permitting efforts for discharge of the treated groundwater and used rinsewater (e.g., NPDES permit for storm sewer discharge). It will also reduce water usage in the plating process.

General Plating Process

Figure 1 shows a general waste-source and treatment process flow diagram of the plate shop. It includes chemical cleaning, plating-rack cleaning, nickel and copper plating, electroless nickel, polishing, striking, cyanide treatment, neutralization, reverse osmosis and ion exchange treatment, scrubbing, and miscellaneous processes. The plate shop of this manufacturer contains a cleaning line, electroless nickel line, nickel and copper plating lines, striking and stripping lines, and special application line. There are ten multi-stage deionized water rinsing units and thirty-four single-stage tap water rinsing units in the shop. Besides metals, other hazardous liquids, such as nitric acid, sulfuric acid, hydrochloric acid, sodium hydroxide, EDTA, and 1,1,1-TCA, are used in the shop.

FOUR HAZARDOUS WASTE MANAGEMENT APPROACHES

In the following section, we will examine four different hazardous waste management plans for this electroplating shop: the conventional end-of-pipe treatment, two zero-discharge schemes, and an integrated source reduction scheme.

Current Waste Treatment System (The End-of-Pipe Treatment Scheme)

A centralized wastewater treatment system including a cyanide destruction station, a two-stage neutralization station, a clarifier, thickener, and filtration station, and a final pH trim station are used in the plate shop. The system treats about 1.00×10^5 L/day of waste, and the effluent is discharged to a publicly-owned water-pollution control plant. Each year, 10 tons of sludge and 1.90×10^4 liters of oily waste are produced from this waste treatment plant.

The metal-bearing and metal-free solutions are first segregated and then collected in different floor sumps. Ferrous sulfate, sodium hydroxide, calcium chloride, and polyelectrolyte are used to treat the metal-bearing solutions. The treated solution is then combined with the metal-free streams and transported to the final pH trim station. The generated sludge is sent to the dewatering unit to reduce water content, and then placed into drums for offsite disposal. The effluent from this system is discharged to a public-owned water-pollution control plant. The capital and annual operation expenses, and maintenance costs of this system will be in the range of $80,000 and $150,000, respectively.

Mixed-Stream Zero-Metal Discharge Scheme 1

To reduce hazardous waste, a mixed-stream zero-metal discharge plan [6] was considered. The manufacturer can treat mixed waste rinsewater, alkaline solutions, and acidic solutions by filtration, carbon adsorption, and chelating ion exchange. The saturated resins are regenerated to produce a mixture of sulfuric acid and copper sulfate, which is mixed with spent etchant and spent plating solutions and treated in an electrolytic cell to recover copper or nickel. However, the treated rinsewater is discharged to a publicly-owned treatment facility. Since the total rinse flow rate is large, 1.0×10^5 L/day, the capital cost of this system is about $150,000 and the annual operating cost is about $100,000.

Semi-Segregated Stream Zero-Discharge Scheme 2

Another zero-discharge approach, a semi-segregated waste treatment scheme, was also considered [13]. Mixed dilute metal-containing rinsewater from the electroless line is treated by ion exchange while spent solutions, etchants, and spills are treated by an electrolytic cell. The developer and stripper solutions are first treated by a solid separation unit and then by an evaporation system. The resulting sludge is shipped for offsite disposal. The waste stream from the electroplating line is treated with a RO unit, and the treated water can be recycled. The water usage is about 5.0×10^4 L/day. The capital and annual operating costs are $250,000 and $100,000, respectively.

Waste Minimization via a Multi-Stage Separation/Recycling Rinse System

In Figure 2 is shown a suggested modification of the electroless-copper process for reducing water usage and wastewater generation rate. This approach has also been recommended in the EPA Guides to Pollution Prevention [17]. The two- or three-stage rinse system with or without the separation unit, which has been discussed in the above two case studies [8, 9], is also considered as a source reduction alternative to the present arrangement of the plating and rinse systems.

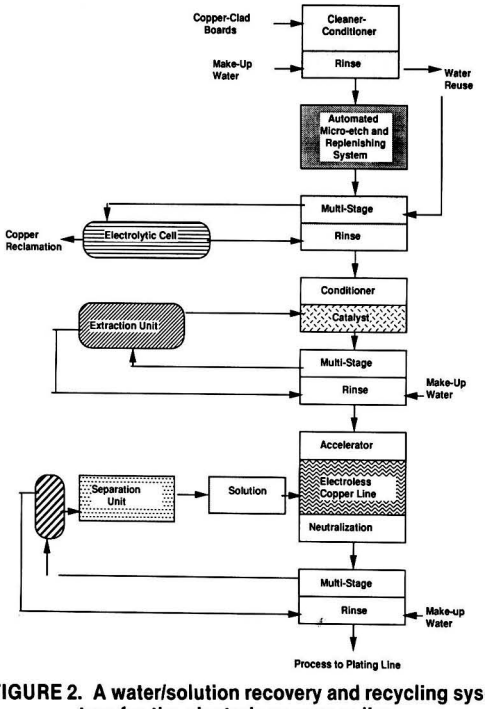

FIGURE 2. A water/solution recovery and recycling system for the electroless copper line.

Process Modifications for the Cleaning Lines

For the plating-rack cleaning line, the original six single-stage rinse systems (with ~340 L/hr flow rate per system) can be reorganized as three two-stage open-loop (no separation unit) rinse systems (with ~40 L/hr flow rate per system). For the chemical cleaning line, originally there are three acid-cleaning units, one alkaline-cleaning unit (which contains cyanide), and seven single-stage rinse units. These seven rinse units can be recognized as four two-stage open-loop rinse systems. For these two cleaning lines, it is found that the changes can greatly reduce daily water usage by 90%. The used rinsewater from these two lines can be treated either with the existing waste stream treatment plant (and then discharged to the sewer) or with a new separation/recycling unit (and then reused). The latter approach will recycle and reuse the treated water, thus further reducing the water usage by 90% (i.e., with 10% of make-up water).

Selection of Minimization Measures for the Electroless Nickel Line

For this line, there are six pre-treatment steps (including one acid dip and five single-stage water rinse tanks) and four post-treatment steps (including three single-stage rinse and one two-stage rinse). For the pre-treatment system, there are two minimization measures: (a) the first three single-stage rinse units can be reorganized as a three-stage countercurrent flow rinse unit and (b) the last two rinse units can be modified as a two-stage closed-loop rinse/separation system. For (b), the used rinsewater can be treated by the existing deionization system and then reused in the rinse unit.

For the electroless nickel bath and the post-treatment processes, a three-stage closed-loop rinse/separation system can be installed to treat the spent bath solution and wastewater from rinse tanks. The separation unit can be either (i) an ion exchange/electrodialysis system or (ii) a reverse osmosis system. As an alternative (i), a strong acid cation exchange unit may be used to treat the waste streams. Since the installation and capital costs of an ion exchange and electrodialysis system are high (approximately $65,000) and the operation procedures are relatively more complicated than for the RO system, the alternative (ii) is recommended. The equipment and installation cost of the alternative (ii) is about $50,000. A newly developed reverse osmosis (RO) system [18, 19] composed of a specific membrane designed for plating solution is also considered. The advantage of these new membranes is that they can withstand high pressure and wide pH range (1 to 13). This RO system can concentrate the dilute effluent to near bath strength (typically a concentration of 40% to 70%) without an evaporation unit. The concentrate can then be reused in the plating bath. The lifetime of the membrane is longer than 6 months [20]. A combination of IX and RO may also be selected for the final process design. However, the capital cost for the combination of IX and RO may be doubled.

Process Modifications for the Electroplating Lines

For both copper and nickel electroplating lines, five sets of two-stage rinse units with two ion exchange and reverse osmosis units (less than 30 gal/hr or 110 L/hr treatment capacity) are suggested to replace the original ten individual single-stage

Table 1 Estimated Waste Levels Of Different Waste Management Schemes

Operation	Conventional Treatment Scheme	Two Zero-Metal Discharge Schemes	Source Reduction Scheme
Water Usage (L/day)	$\sim 1.0 \times 10^5$	$10^5 \sim 5.0 \times 10^4$	$\sim 2.0 \times 10^4$
Sludge Generation (Tons/year)	10	6~8	~4
Capital Investment ($1,000s)	~80	~200	~130
Annual Operation and Maintenance Cost ($1,000s/year)	~150	~100	~50
Chemical Savings ($1,000s/year)	0	0	10~50

rinse systems. The used rinsewater from these two lines will be treated through the two separation units. Metals can be recovered and reclaimed and the treated rinsewater can be reused. The water usage and wastewater generation can be 95% lower than before. Since the cyanide destruction system will still be used to treat waste streams containing cyanides, the wastewater from this process will remain the same. Currently, about 1.7×10^4 L/day of waste flow into this destruction system.

Drag-out Control

The above estimation of water usage reduction is fully dependent on drag-out control practices. The effect of drag-out control can be observed from the mass balance calculations in our previous study [*8*]. Drag-out control can be conducted by the following methods: (a) minimizing bath concentration by maintaining chemistry at the lower end of the operating range; (b) increasing the bath temperature; and (c) withdrawing parts at slower rates, using drag-out tanks to recover process chemicals for reuse, etc.

Non-Cyanide Cleaning or Etching

In alternative (a), non-cyanide strong acid or strong caustic etchant may replace the alkaline ferricyanide solution as a cleaning or etching solution. A nitric/sulfuric acid mixture may be applicable. However, since the acid mixture may raise solution temperature because immersing the parts into acid generates heat, the etching or cleaning process is more difficult to control. Thus, the implementation potential of this alternative is low. For alternative (b), alkaline water-base surface cleaning agents may be used to clean the part surfaces. For example, an agent with 70% to 90% of water, approximately 10% to 30% of NaOH, and 0.1% of combination of EDTA, nitrite, borates, and triethanolamine can be very effective to clean equipment or metal parts. After cleaning, the part or equipment is dried in a heating oven to remove water residue. This alternative is highly recommended.

Non-Cyanide Plating

As a source reduction alternative, replacement of cyanide plating solution with cyanide-free solutions is attractive, since it reduces the health and safety hazard of handling cyanide solution and eliminates the cyanide waste destruction efforts and cost. Non-cyanide cadmium and zinc plating processes have been applied for several cases [*21*]. However, the drawbacks of this source reduction measure are: (i) reduced ductility, (ii) requirement of tighter chemical control, (iii) higher equipment cost (due to corrosion protection), (iv) upgrading of cleaning/degreasing techniques, (v) poorer product quality. Thus, in this study the implementation potential of this source reduction measure is low.

Wastewater and Sludge Reductions

With the suggested multi-stage rinse and separation systems, the rinsing rate of every rinse unit can be as low as 10 gal/hr, or 38 L/hr [*8*]. Since these new rinsing/separation systems are closed-loop systems (except the systems of cleaning lines), the water usage and wastewater generation can be 90% lower than the original open-loop rinse systems in the plate shop. With these new systems and the existing cyanide destruction system, we estimate that only 2.0×10^4 L/day wastewater (i.e., ~25% of the original volume) will be generated from this facility.

Since only about 2.0×10^4 L/day of wastewater will be transported to the two-stage neutralization and flocculation systems, the sludge quantity will also be greatly reduced. From our calculation [*8*], we find that if the drag-out rate from the plating bath is 1000 g/hr, the recovered solution flow rate from a separator will be about 700 g/hr. Since the recovered solution can be reused in the plating processes, the metal content in wastewater can be reduced by 40% to 80%. This will reduce metal content in sludge and thus reduce its toxicity. Based on the process modification, it is estimated that less than four tons/year (compared to the original 10 tons/year) of sludge would be generated from the existing wastewater treatment plant. We also find that the metal weight fraction in the recovered solution ranges from 0.37 to 0.59 if the metal weight fraction in the drag-out from the plating bath is 0.29. Therefore, about 150 to 300 g/hr of metal will be recovered, i.e., 20 to 30 kg/month. This will further save chemical purchasing costs.

Cost Analyses of the Modified Process

In our modified rinsing processes, four separation units will be installed at a total cost of $130,000. The total operating and maintenance fee is expected to be within $50,000/year for the first three years. This modified process can save water treatment chemical, sludge treatment, and process material costs of about $50,000 per year.

The economic analyses of the four different hazardous waste management schemes are summarized in Table 1, which shows that the source reduction scheme is superior to the others.

Since treated groundwater can be used in the plate shop, the manufacturer can both conserve water and reduce water pollution risk in the future. In the following sections, we will briefly discuss the feasibility analysis of groundwater treatment and water softening and demineralization processes.

Summary of Groundwater Remedial Investigation and Feasibility Studies

The evaluation of the contaminated site showed concentrations of volatile chlorinated hydrocarbons such as 1,1,1-trichloroethane (TCA), 1,1-dichloroethene (DCE), tetrachloroethylene (PCE), and trichloroethylene (TCE) in the groundwater near the plate shop. Gasoline products, including benzene, toluene, xylene, and ethylene (BTXE), were also found in both the soil and groundwater. The observed concentrations

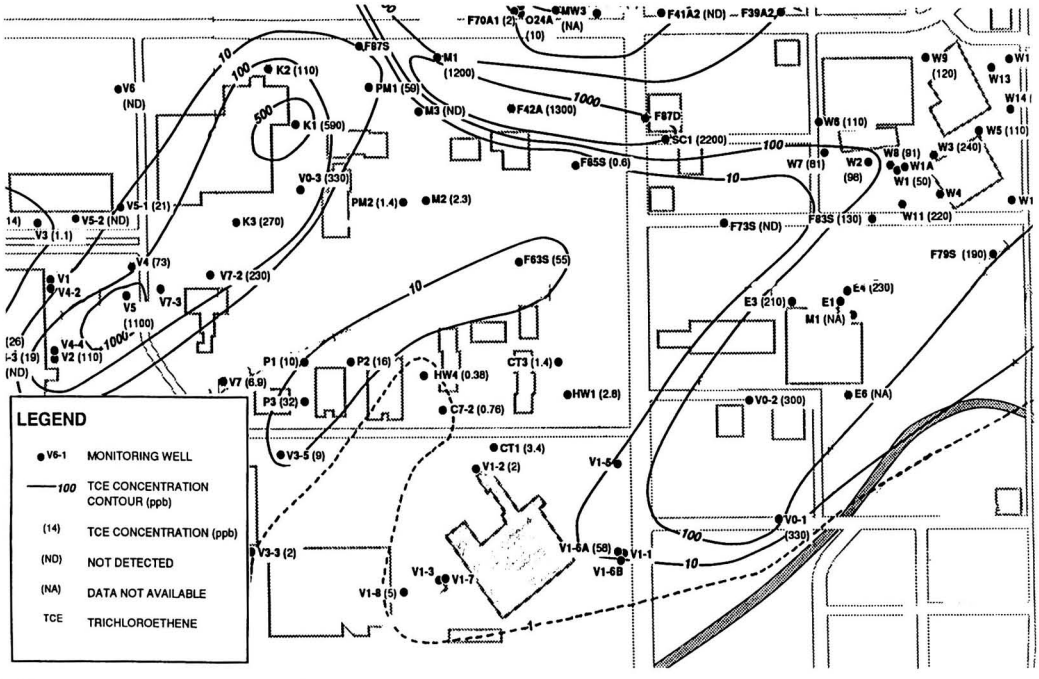

FIGURE 3. TCE concentration (ppb) contour in the shallow groundwater bearing zone.

of TCE (3100 ppb) and DCE (83 ppb) are above the maximum concentration limits set by California EPA. Figure 3 shows the TCE concentration contour in the shallow groundwater zone near the plate shop.

To decrease the rate of spread of chemicals in the shallow groundwater (25–40 ft below surface) and to reduce the source of organic chemicals migrating in the soil in the plating shop area, an interim remediation feasibility study was performed. To meet the remediation objectives, in-situ cleanup of groundwater was recommended. Four treatment technologies were evaluated: hydrodynamic control (extraction), air stripping, carbon adsorption, and UV oxidation. The screening of the proposed technologies was based on the following four criteria: implementability, effectiveness, regulatory compliance, and economic analysis. The definition of each criterion is given below.

Implementability is the evaluation of the appropriateness of a technology and how it can be put into effect. The limitation of space may preclude technologies that require large-scale construction activities. Effectiveness consists of evaluating how well a technology will meet stated objectives, e.g., to prevent volatile organic chemicals and gasoline products from migrating through the subsurface, and to remove them from the groundwater. Several factors are considered in evaluating regulatory compliance: the health and safety of remediation workers, the safety and health of properties and public in offsite areas, and how well a technology option meets the anticipated cleanup goal. The appropriate treatment and monitoring must be utilized to ensure the organic chemicals are contained, immobilized, removed or destroyed to minimize impacts to humans or environment. Economic analysis is based on engineering evaluations, including cost estimates of preliminary process design, installation, operation and maintenance, and the potential use as a final remedial measure.

To evaluate regulatory compliance, the treated groundwater disposal should also be considered. Three options, disposal at a local wastewater treatment plant, disposal at surface water, or reinjection to groundwater, have been considered. The latter two options were rejected since in the South Bay area approval by local government agencies would be difficult. Thus, the first option was selected. However, to reduce the wastewater discharge cost and water usage cost to the shop, recycling of the treated groundwater to the plating process is also recommended.

Based on the evaluation, carbon adsorption with granular activated carbon (GAC) and UV oxidation were selected as two final candidate technologies. Although the capital cost of UV oxidation was higher than for GAC, the latter has a higher operation and maintenance cost (due to regeneration) than the former. Thus these two technologies were selected for final evaluation, including benchscale treatability studies.

The groundwater cleanup system will start with a single groundwater extraction pump and well installed near the building at the well VI-3 (see Figure 3). A new well is also recommended to permit greater infusion from the shallow aquifer. The extracted groundwater will be routed through a treatment until that includes a particulate filter, a UV oxidation unit, or a GAC system, or both prior to discharge to the demineralization system. Table 2 shows a screening matrix for evaluating the groundwater treatment technologies.

Table 2 Screening Matrix for Groundwater Treatment Technologies

Technology	Implementability	Effectiveness	Compliance	Cost
Bioremediation	Limited Cases	Unknown	Fair	Medium
Air Stripping	Vapor Abatement Needed	Good	Fair	High
GAC	Good	Good	Good	High
UV Oxidation	Good	Good	Good	High

WATER SUPPLY FROM THE REMEDIATION PROCESS

In this plate shop the modified process requires no more than 3.0×10^4 L/day of water, which can easily be supplied by the groundwater treatment process with capacity 2.0×10^5 L/day. Before reuse of the treated groundwater in the process, the water chemistry must be considered.

The water sample taken from wells onsite in early 1991 provided the following results: pH 7.0, temperature 20°C, bicarbonate alkalinity (as $CaCO_3$) 400 mg/L, calcium 120 mg/L, chloride 130 mg/L, magnesium 71 mg/L, sodium 91 mg/L, sulfate 200 mg/L, hardness 590 mg/L, total dissolved solids (TDS) 890 mg/L, trichloroethylene (TCE) 3.1 mg/L, 1,1-dichloroethylene (DCE) 0.083 mg/L, and the concentrations of heavy metals are relatively low or below the detection limits.

Groundwater Treatment

The organic chemicals found in groundwater will be removed by granular activated carbon (GAC) adsorption or UV oxidation. These two technologies are widely used in groundwater treatment process for removal of volatile organic chemicals [*22*]. A disadvantage of the GAC technique is high regeneration cost; however, the preliminary bench pilot tests showed that the GAC technique can remove at least 99% of TCE and DCE with relatively lower operating and maintenance costs.

Since the alkalinity, calcium, magnesium, hardness, and TDS concentrations are high in groundwater samples, the water effluent from the GAC or UV system cannot be directly used in the plating process or cooling system. Further treatments, such as lime-soda ash or zeolite softening, ion exchange, reverse osmosis, deareation, neutralization, or reduction [*23*], of the treated water are thus necessary.

Water Chemistry

The alkalinity of most natural water supplies is caused by dissolved bicarbonate salt. However, when CO_2 dissolves in water, it reacts with water to produce the hydrogen and bicarbonate ion. The reaction of bicarbonates with $CaCO_3$ or $MgCO_3$ further increases the alkalinity (and pH value also) of water. When water contacts soil and rock containing $CaCO_3$ and $MgCO_3$, the chemical reactions produce extra hardness [*23*]. The following equations show the reactions in water.

$$CO_2 + H_2O \leftrightarrow H_2CO_3 \leftrightarrow H^+ + HCO_3^-$$

$$CO_2 + H_2O + CaCO_3 \leftrightarrow Ca^{2+} + 2HCO_3^-$$

$$H^+ + CaCO_3 \leftrightarrow Ca^{2+} + HCO_3^-$$

Two thermodynamic factors, pressure and temperature, dominate the solubility of CO_2 in water. Because the pressure underground is higher than at the surface, usually groundwater contains more dissolved CO_2 than surface water. Sometimes the groundwater is cooler than surface water, thus the solubility of CO_2 in groundwater is also higher. In one previous case that we have examined we found that the analyses of water samples from an extraction well showed the following results: bicarbonate alkalinity = 730 mg/L (as $CaCO_3$), pH = 6.9, and calcium = 130 mg/L. After passing a water sample through an air stripper, the alkalinity and calcium contents were dropped to 580 and 80 mg/L, respectively, and at the same time, pH was increased to 8.0. Substantial $CaCO_3$ precipitation was observed during the test run. If extra acid is injected in water, $CaCO_3$ can be dissolved or stabilized.

Demineralization

Since only 3.0×10^4 L/day (21 L/min) of the extracted groundwater will be used as make-up water in the plate shop, a small size zeolite resin softener and dealkalization system can be used to treat the effluent from the GAC or UV unit. The treated water is then pumped to the existing RO or IX system to further purify the water used in the plate shop.

Anions, such as alkaline carbonate and bicarbonate, and sulfate, chloride, etc., will pass through the softener unchanged. Therefore, a dealkalization unit after the softener is needed to remove anions. The existing ion exchanger of the plate shop can be upgraded to an anion exchange unit, such as a strong-base chloride-anion exchanger.

Free CO_2 in the water is also removed by adding a small amount of caustic to the salt-brine regenerate. The TDS content of the water can be lowered by both ion exchange or softener and reverse osmosis systems. After passing through GAC, zeolite softener, ion exchange, and/or reverse osmosis processes, the purified groundwater can be reused in the plating process. The existing sludge collection system (see Figure 1) can collect the sludge, such as $CaCl_2$, that will be generated from the resin regeneration process. Based on the hardness content of 590 mg/L, it is estimated that the demineralization process with 90% efficiency may generate as much as 5.7 tons/year of non-hazardous sludge.

The reactions of the zeolite resin softener (symbolized as Z), which exchanges calcium and magnesium ions (symbolized as M^{2+}) for sodium ion, are given as

$$M^{2+} + Na_2Z \leftrightarrow MZ + 2Na^+$$

The following equations show the dealkalization reaction, where R represents the resin:

$$HCO_3^- + RCl \leftrightarrow RHCO_3 + Cl^-$$

$$SO_4^{2-} + 2RCl \leftrightarrow R_2SO_4 + 2Cl^-$$

The capital cost of this demineralization system, including piping, installation, and softener unit, will not exceed $30,000. Because both RO and IX are existing units in the shop, there will be no extra operating and maintenance costs for these two units. The cost of zeolite softener regeneration and non-hazardous sludge disposal is estimated at $5,000 per year.

CONCLUSIONS

Based on case-study calculations [*8*, *9*], EPA documents [*17*], California State reports [*13*, *18*, *20*, *21*], and example studies of source reduction schemes for the electronics industries, we summarize the following conclusions.

Hazardous waste management plans should include source reduction, water usage minimization, waste stream segregation, process modifications, and management commitment. The source reduction study should incorporate and evaluate alternative processing methods for generating less waste. We found that an integrated groundwater remediation and source reduction plan is feasible for a plating shop with contaminated groundwater. Both VOC removal and demineralization of the polluted groundwater are important. With the integrated scheme, 90% removal or recovery of heavy metals can be achieved, and water usage and wastewater can be reduced by 90%. It is feasible to prevent water pollution at the source and recycle the treated groundwater and wastewater to the plating process. The total cost of the proposed plan is competitive with the conventional-sludge scheme and other zero-metal discharge schemes.

LITERATURE CITED

1. Kemp, D. W., "The Application of Ion-Exchange and Modified Rinsing Procedures to Minimize Treatment Costs," the Fourth Conference on Advanced Pollution Control for the Metal Finishing Industry, pp. 59-63, Florida, 1982.
2. Kokjohn, C. W., *Advances in Aqueous Dry Film Development and Control*, in *Seminar: Chemical Metal Deposition for PCB; Conference: Economics and Cost Saving*, pp. 2-7-1 to -12, Edited by M. G. Fassini, European Institute of Printed Circuits, 1983.
3. Cushnie, Jr., G. C., *Electroplating Wastewater Pollution Control Technology*, pp. 152-219, Noyes Publications, N.J., 1985.
4. Palmer, S. A. K., M. A. Breton, T. J. Nunno, D. M. Sullivan, and N. F. Surprenant, *Metal/Cyanide Containing Wastes Treatment Technologies*, pp. 66-335, Noyes Data Corporation, N.J., 1988.
5. "Control and Treatment Technology for the Metal Finishing Industry: Ion Exchange," Summary Report, EPA 625/8-81-007, June 1981.
6. Higgins, T., *Hazardous Waste Minimization Handbook*, pp. 75-116, Lewis Publishers, Inc., MI, 1989.
7. Schweitzer, P. A. (Editor), *Handbook of Separation Techniques of Chemical Engineers*, pp. 2.89-2.103, McGraw-Hill Book Co., N.Y., 1979.
8. Chang, L. Y., and B. J. McCoy, "Waste Minimization For Printed Circuit Board Manufacture," pp. 293-318, Hazardous Waste & Hazardous Materials, Vol. 7, No. 3, 1990.
9. Chang, L. Y., and B. J. McCoy, "Alternative Waste Minimization Analyses for The Printed Circuit Board Industry: Examples for Small and Large Manufacturers," *Environmental Progress*, pp. 110-121, May, 1991.
10. Wallig, L. R., "Image Transfer," Chapter 11 in *Printed Circuit Handbook*, (3rd Edition), edited by C. F. Coombs, Jr., McGraw-Hill Co., New York, 1988.
11. Moleux, P. G., "Pollution Control and Recovery Systems," Chap. 15 in *Printed Circuits Handbook*, (3rd edition), edited by C. F. Coombs, Jr., McGraw-Hill Co., N.Y., 1988.
12. Duffek, E. F., "Plating," Chap. 12 in *Printed Circuits Handbook*, (3rd edition), edited by C. F. Coombs, Jr., McGraw-Hill Co., N.Y., 1988.
13. Judd, R. L., B. Fleet, C. E. Small, G. A. Davis, B. Piasecki, and M. J. Muller, Final Report to Department of Health Services, State of California, "Waste Reduction Strategies for the Printed Circuit Board Industry," 1987.
14. Chang, L. Y., and B. J. McCoy, "An Integrated Waste Minimization Scheme for the Electronics Industry," Paper presented at the AIChE Meeting, Houston, April, 1991.
15. Nunno, T., S. Palmer, M. Arienti and M. Breton, *Toxic Waste Minimization in the Printed Circuit Board Industry*, Noyes Data Corporation, New Jersey, 1988.
16. Gold, H., G. Czupryna, R. D. Levy, C. Calmon, and R. L. Gross, "Purifying Plating Baths by Chelate Ion Exchange," pp. 619-42, in *Metals Speciation, Separation, and Recovery*, edited by J. W. Patterson and R. Passino, Lewis Publishers, 1987.
17. US EPA, *Guides to Pollution Prevention—The Fabricated Metal Products Industry*, EPA/625/7-90-006, July, 1990; US EPA, *Guides to Pollution Prevention—The Printed Circuit Board Manufacturing Industry*, EPA/625/7-90-007, June, 1990.
18. Rich, R. R., and T. Von Kuster, Jr., "Recovery of Rinse Water and Plating Bath from Process Rinses Using Advanced Reverse Osmosis," PP.91-8, *Metal Waste Management Alternatives*, 1989 Symposium Proceedings, California State Department of Health Services.
19. Malmberg, J., "Advanced Reverse Osmosis for Hazardous Waste Recovery," pp. 801-6, *Proceedings of the 6th Annual Hazardous Waste Materials Management Conference West*, Long Beach, California, 1990.
20. Cartwright, P. S., "Membrane Separation Processes for Treatment of Hazardous Waste," pp. 171-185, *Metal Waste Management Alternatives*, 1989 Symposium Proceedings, California Department of Health Services.
21. Foecke, T., "Source Reduction Opportunities in the Plating Industry," pp. 45-55, *Metal Waste Management Alternatives*, 1989 Symposium Proceedings, California Department of Health Services.
22. Stenzel, M. H., and W. J. Merz, "Use of Carbon Adsorption Processes In Ground Water Treatment," Vol. 8, pp. 257, *Environmental Progress*, 1989.
23. "*Betz Handbook of Industrial Water Conditioning*," 6th Edition, Betz, 1962.

Hydrophobic Zeolite Adsorbent: A Proven Advancement in Solvent Separation Technology

Stephen W. Blocki

Dürr Industries, 40600 Plymouth Rd., Plymouth, MI 48170

With the passage of the Clean Air Act Amendment (CAAA) of 1990, solvent emission regulations continue to become ever more stringent. An ongoing and increasingly strong incentive exists to develop and apply to the solvent emission control industry more efficient and cost effective control technologies.

This paper presents a new technology used for solvent separation and concentration, hydrophobic zeolite adsorbent. Because of its unique physical properties, solvent control systems using hydrophobic zeolite may exhibit separation capacity equal to or better than systems using activated carbon without requiring much of the support equipment. Though activated carbon remains the adsorbent of choice for many applications, hydrophobic zeolite represents an efficient alternative for many niche applications. Extensive tests have proven its capabilities and the results are presented here.

Also presented is the modular solvent concentrator (MSC) designed to handle up to 50,000 scfm (79,000 Nm^3/h)—up to 50% more air flow as current concentrators—in the same area. The MSC is flexible enough to handle any currently available adsorbent. Several case studies are presented to illustrate use of hydrophobic zeolite as well as the MSC.

TECHNOLOGY ADVANCEMENT IN SOLVENT SEPARATION

Activated Carbon for Solvent Separation

A simple, cost-effective, and very effective process for controlling dilute solvent emissions is solvent concentration/oxidation. The process first concentrates the dilute solvents into an airstream 6–18 times smaller than the original exhaust before final destruction in a small thermal oxidizer.

The intermediate stage in many solvent emission control systems is solvent separation from the process air, most commonly using activated carbon. Though widely applied, activated carbon presents several problems.

- Flammable material
- High-boiling solvents (bp >300° or >150°C) cannot be desorbed
- Promotes polymerization or oxidization of some solvents to toxic or insoluble compounds
- Can efficiently handle only minor concentration fluctuations
- Hygroscopic, requiring relative humidity control

Carbon is flammable, potentially promoting a fire when heated above 250°F (120°C). Even at ambient conditions, readily oxidizing solvents such as ketones can initiate a fire when adsorbed onto carbon. An effective fire protection system can be cost prohibitive and operationally cumbersome. Carbon's flammability limits the practical solvent desorption temperature to about 250°F (120°C) at which solvents boiling over 300°F (150°F) cannot be efficiently removed.

Impurities naturally occurring in carbon can act as catalysts and promote polymerization or oxidization of some solvents such as Styrene, MEK, Cyclohexanone, etc., resulting in by-products which cannot be desorbed or which might be haz-

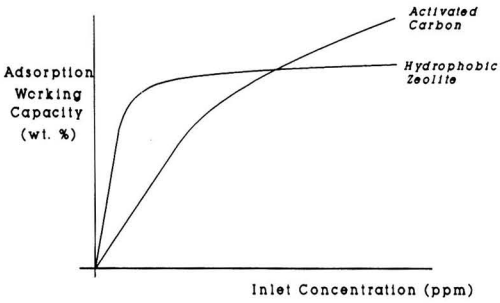

FIGURE 1. Hydrophobic zeolite vs. activated carbon. Capacity vs. relative humidity.

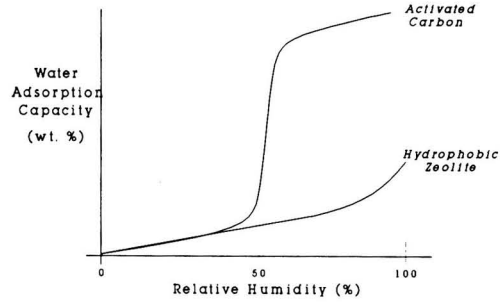

FIGURE 2. Hydrophobic zeolite vs. activated carbon. Adsorption capacity.

ardous. Carbon's inability to handle wide solvent fluctuations means a granular activated carbon (GAC) bed must be installed upstream to dampen concentration variations. Because carbon's adsorption capacity drops greatly at relative humidity of 50–60%, relative humidity control upstream is often required, especially when a wet spraybooth is being abated.

The Next Generation in Solvent Separation—Hydrophobic Zeolite

Hydrophobic zeolite, a new synthetically-produced adsorbent with expanded physical characteristics, offers a distinct advancement in solvent separation technology. It can be integrated easily into a solvent recovery or oxidation system to achieve one of the safest, most cost effective systems possible.

Zeolites, porous alumina silicates, occur naturally as different minerals but also can be synthesized. All zeolites are inorganic and therefore are non-flammable, capable of withstanding very high temperatures. Zeolites sometimes are called molecular sieves because of their crystalline framework with channels (pores) and interconnecting voids. The resulting homogenous pore size prevents molecules larger than a certain size from passing within the lattice. By varying the chemistry in the basic structure, different pore sizes, hence different selectivity, can be achieved. Unfortunately, the selectivity results in limitations in where it can be applied. Hydrophobic zeolite often exhibits lower separation efficiency for some relatively common solvents such as xylene and solvesso 100. Because it has a wide variety of pore sizes, these individual inefficiencies do not exist with activated carbon. Depending on the end user's solvent mix, either hydrophobic zeolite or activated carbon may be the ideal adsorbent media. The two technologies are complementary rather than competing solutions.

Zeolites have been used as catalysts for petroleum cracking since the early 1960's and as water softening agents in detergents. Most zeolites are hydrophilic (attracting water) and therefore not well suited for separating VOC's in a humid atmosphere.

Recent advancements have made it possible to manufacture a hydrophobic zeolite with adsorption characteristics suitable for solvent separation. Hydrophobic zeolite's properties can be summarized as follows.

- Non-flammable material
- Can withstand temperatures up to 1800°F (1000°C)
- Can handle a wide variety of solvents
- Efficient adsorption at a wide range of concentrations
- Does not promote solvent polymerization or reaction
- Hydrophobic, repels moisture

Hydrophobic zeolite is non-flammable and therefore will not contribute to a fire in a solvent laden atmosphere. Even under ambient conditions, readily oxidizing solvents such as ketones will not initiate a fire when adsorbed.

Hydrophobic zeolite can withstand temperatures as high as 1800°F or 1000°C (1100°F or 600°C when impregnated on a honeycomb structure); therefore it can be desorbed at a higher temperature than activated carbon effectively removing solvents boiling in excess of 350°F (175°C) and maximizing its working capacity. GAC beds often are not needed. As shown in Figure 1, hydrophobic zeolite has a much greater adsorption capacity at low solvent concentrations.

Because it is hydrophobic, the zeolite has a low affinity for water. Figure 2 compares the adsorption working capacities of hydrophobic zeolite to activated carbon with respect to relative humidity, clearly showing the advantages of hydrophobic zeolite at high relative humidities. Up to 85% relative humidity can be handled with little adverse effect on adsorption.

The system simplifications resulting from using hydrophobic zeolite for solvent separation can be summarized as follows.

- Inert gas or sophisticated wet/dry fire protection not needed
- Sacrificial adsorbent bed not needed
- Flattening bed generally not needed
- Relative humidity control not needed

The result is a less expensive, simpler system achieving equal or greater efficiencies. Hydrophobic zeolite is available as pellets or on a honeycomb structure.

Modular Solvent Concentrator

Continuous concentrators are manufactured as rotating discs for air flows between approximately 6,000-30,000 SCFM (9,500-47,500 Nm^3/h), while the Molecular Solvent Concentrator (MSC) utilizing a cylindrical construction with honeycomb blocks provides a more volume efficient design for higher air flows.

The MSC (see Figure 3) is a compact, efficient device for removing solvents from dilute air streams. It separates solvents from the process air, concentrating them into a smaller air stream to allow more economical final treatment—either by thermal oxidation or recovery.

The adsorbing elements consist of a honeycomb structure containing the hydrophobic zeolite, activated carbon or other commercially available adsorbing materials (see Figure 4). Should the solvent mix requiring separation be changed, the adsorbent exhibiting the maximum efficiency may very well change. Interchangeable elements mean the same MSC can be

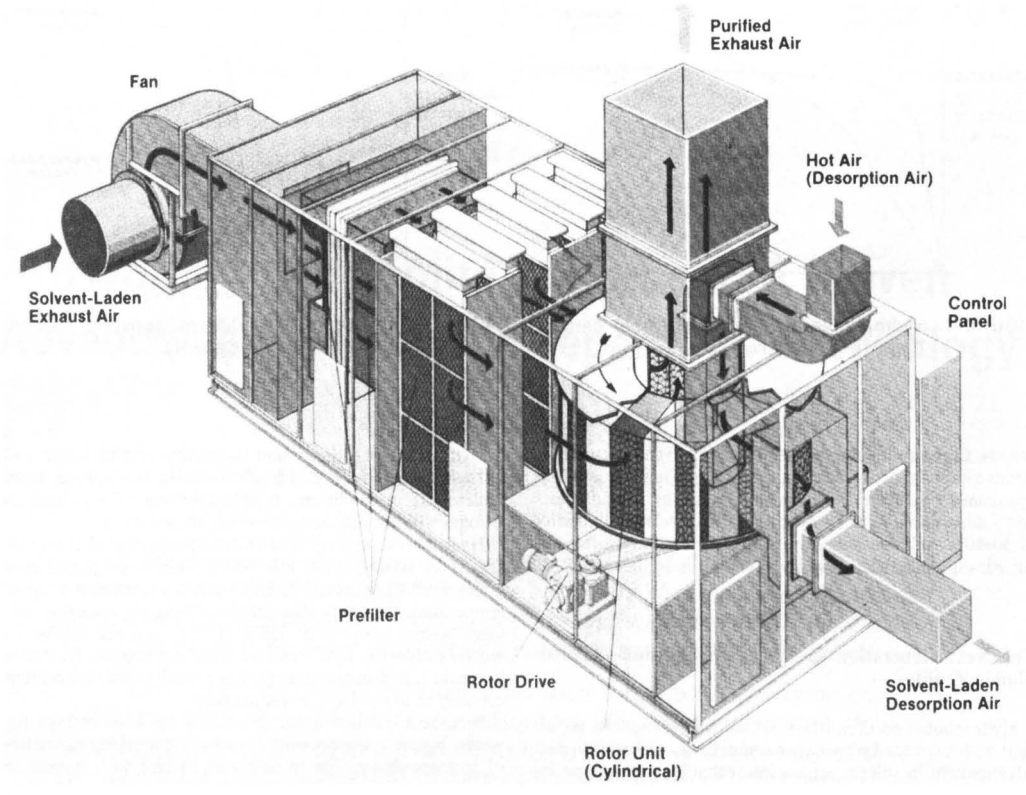

FIGURE 3. Molecular solvent concentrator.

used with different adsorbent media for continued maximum performance.

The element are attached to a frame (see Figure 5) which rotates through three distinct zones: an adsorption zone, where solvents are separated from the process air; a desorption zone, where the solvents are stripped from the adsorbing elements by a hot gas stream; and, a cooling zone, where the elements are cooled for maximum efficiency before reentering the adsorption zone.

During operation the process air blown into the enclosure passes through the honeycomb elements and flows radially into the center of the cylinder. Adsorbing material impregnated to the surface of the elements adsorbs the solvents, leaving purified process air to exit through the inner cylinder (as indicated by the arrows in Figure 3).

As the cylinder rotates it moves into the desorption zone, where a smaller heated gas flow (air or nitrogen, for example) strips off the solvents, reactivating the adsorbing material. The desorption air also flows radially, but opposite the process air flow direction. The desorption air containing concentrated solvents exits the system for recovery or thermal oxidation. The cylinder then rotates through a cooling zone where a cool

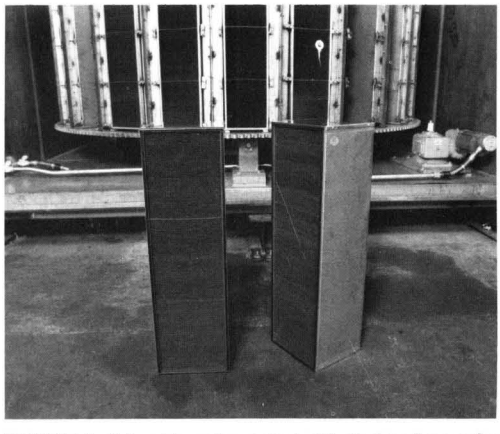

FIGURE 4. Adsorbing elements (activated carbon or hydrophobic zeolite).

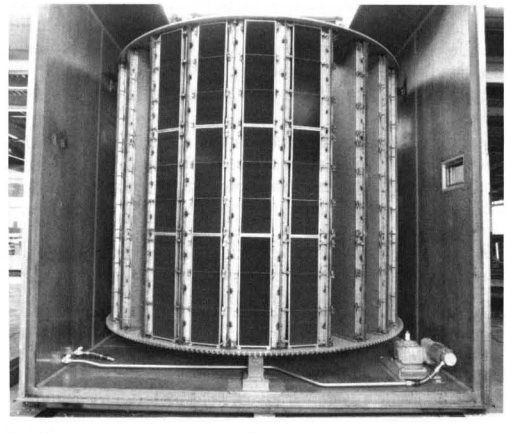

FIGURE 5. Rotating cylinder housing adsorbing elements.

Test Conditions

Inlet Gas Temperature (°C)	32°C
Inlet Gas RH (%)	60
Face Velocity (m/s)	1.8
Reactivation	160°C
Concentration Ratio	10

Solvent Composition One

				Concentration (ppm)		
Solvent	MW	vol. %	BP °C	In	Out	Efficiency
Solvesso 100	---	20	160	14	1.72	87.7
Ethanol	46.1	21.9	78	15.3	3.37	78
MAK	114.2	16.1	150	11.3	N.D.	100
MEK	72.1	8.3	80	5.9	0.05	99.1
MIBK	100.2	7.6	118	5.3	N.D.	100
n-Butyl Acetate	116.2	9.9	126	6.9	N.D.	100
Xylene	106	9.7	138	6.7	1.15	82.8
Octyl Acetate	172	6.5	200	4.6	N.D.	100
	wt'd avg.		127	70	6.29	91

Solvent Composition Two

				Concentration (ppm)		
Solvent	MW	vol. %	BP °C	In	Out	Efficiency
Butyl Cellosolve Acetate	160	5.0	192	4.3	0	100
Xylene	106	80.0	138	68.0	3.3	95.2
I.P.A.	60	8.0	66	6.8	0.8	88.0
Ethyl Acetate	88	3.0	77	2.6	0	100
Butyl Cellosolve	118	4.0	168	3.4	0	100
	wt'd avg.		134	85.0	4.1	95.2

FIGURE 6. Adsorption efficiency test results.

air stream flows through the honeycomb structure. This lowers the adsorber temperature near optimal operating temperature for maximum efficiency before reentering the adsorbing zone.

The MSC design offers the following features:

- Continuous regeneration, providing higher on-line time compared to fix bed systems.
- Honeycomb adsorbers result in low pressure drop for lower power consumption.
- New, space efficient arrangement of multiple elements provides large adsorber area capable of handling up to 30-50% more air volume than other configurations.
- Interchangeable modular blocks—each element is an interchangeable unit for easy maintenance. Adsorbents can be changed if solvents emitted are changed to ensure the most efficient separation possible.
- Modular construction results in minimal field installation work, maximum quality control.
- Shop preassembled and tested for simplified shipping and installation, and reduced field start-up time.

The MSC is optimal for handling low to medium solvent concentrations in the air flow range of 6,000-50,000 SCFM/unit (9,500-79,000 Nm^3/h) and will provide removal efficiencies up to 99%.

Test Results

A simulated MSC loaded with hydrophobic zeolite adsorber media has been tested thoroughly under simulated production conditions at the Dürr Industries Research and Development Center in Plymouth, Michigan from August to October of 1992. The tests were run to determine the influence on performance when using different solvents, solvent concentrations, process air flow, concentration factor, desorption temperature, and rotational speed.

These tests together with environmental compliance testing and performance check-ups of installed VOC control systems using the same type of hydrophobic zeolite media as the MSC, verify removal efficiency in excess of 95%, and frequently show performance in the 96-98% range.

Figure 6 summarizes two tests conducted to determine the adsorption efficiency of hydrophobic zeolite. Removal efficiency is largely independent of solvent concentration within a wide range. The hydrophobic zeolite also shows good performance for a variety of different solvents, non-polar as well as polar and high boiling as well as those with a fairly low-boiling point.

The selectivity of hydrophobic zeolite's homogenous pore sizes can be seen when tested with solvent composition one. Unlikely activated carbon, hydrophobic zeolite shows inefficient performance for selected solvents like solvesso 100 and xylene whose diameters fall in between hydrophobic zeolite's pore sizes. The removal efficiency of solvesso 100 and xylene, 87.7% and 82.8% respectively, are significantly lower than the other solvents. With solvent mix two, however, the removal efficiency of xylene is much higher, over 95%. The tests demonstrate that hydrophobic zeolite can be successfully applied to many, though certainly not every emission stream.

Hydrophobic zeolite and activated carbon are complementary adsorbents whose selection should be determined on a case by case basis. As of December 1992, over 80 MSCs have been in operation handling over 3,000,000 SCFM of solvent laden air.

Table 1

Case One	Regenerative Thermal Oxidation	Carbon Rotor Concentration/ Thermal Oxidation	Hydrophobic Zeolite Concentration/ Thermal Oxidation	Basis
Investment Cost (Base = 100)	100	102.8	91.7	68,000 cfm
Fuel Gas	$145,300	$45,800	$45,800	$4.00/MMBTU
Electricity	$105,200	$25,800	$25,800	$0.05/KWH
Dry Filters	$19,300*	$19,300	$19,300	1.0 gr/kSCF inlet
Total Utility Cost	$269,800	$90,900	$90,900	

*Dry filters are not mandatory for the regenerative thermal oxidation option. Without filters, a bake-out feature is typically purchased. When operated, fuel gas expense will be higher than stated above.

Table 2

Case Two	Direct Regenerative Thermal Oxidation	Hydrophobic Zeolite Concentration/ Thermal Oxidation	Basis
Complete Cost	$8,200,000	$7,800,000	327,000 cfm
Fuel	$574,600	$79,200	$4.00/MMBTU
Electricity	$496,100	$134,900	$0.06/KWH
Dry Filters	$0*	$60,200	1.5 gr/kSCF inlet
Total Annual Cost	$1,070,700	$274,300	

*Dry filters are not mandatory for the regenerative thermal oxidation option. Without filters a bake-out feature is typically purchased. When operated, fuel gas expense will be higher than stated above.

Case Studies

Two case studies presented below illustrate the advantages of using solvent concentration and hydrophobic zeolite to control solvent emissions present in dilute exhaust streams.

In case one, an exhaust stream of 68,000 cfm (115,000 m^3/h) containing about 30 ppmv required >90% abatement. The stream contained 5–7% methanol and almost 30% ketones. Three possible systems were evaluated: direct regenerative thermal oxidation, carbon concentration/thermal oxidation, and hydrophobic zeolite concentration/thermal oxidation. Each system was capable of meeting the performance criteria.

Because the solvents are in very low concentrations, direct regenerative thermal oxidation would result in excessive purchased fuel cost, as well as high electrical cost. The installation cost of carbon concentration/thermal oxidation is competitive and its operating costs are much lower. Carbon concentration, however, presents two problems; carbon's adsorption capacity for methanol is very low, and the readily-oxidizing ketones represent a greater-than-normal fire hazard.

Hydrophobic zeolite concentration/thermal oxidation has the lowest installed cost and its utility costs are equal to those of the carbon system. Its adsorbent replacement cost is much higher than with activate carbon. Because GAC beds are generally not needed, the cost of GAC replacement is eliminated. Because hydrophobic zeolite adsorbs methanol to a much greater extent than carbon and because it is not flammable, the problems cited earlier are not applicable with this option. Table 1 summarizes the costs associated with each option.

In case two, an exhaust stream of 327,000 cfm (560,000 m^3/h) containing about 90 ppmv required >95% abatement. Because of the fire hazard presented by the stream containing 30–40% ketones, the customer immediately eliminated carbon adsorption as an option.

Two possible systems then were evaluated; direct regenerative thermal oxidation and hydrophobic zeolite concentration/thermal oxidation. Each system was capable of meeting the performance criteria.

A key driving force for direct regenerative thermal oxidation was its perceived simplicity. A basic review of the hydrophobic zeolite concentration/thermal oxidation system reinforces that it is a very simple system whose key components generally are expected to give a very high uptime. The concentrator rotates at 1–3 revolutions per *hour*. Because of the very low pressure drop of the main air flow (~5–7″ w.c. or ~1.2–1.7 kPa), the main blower is relatively low horsepower. Conversely, the high pressure drop of the regenerative thermal oxidizer (~30″ w.c. or ~7.5 kPa) results in a blower with 4–6 times greater horsepower. Beyond the main blower, the balance of the system handles only 5–14% of the air volume, making all its other components very small. Final oxidation also handles 5–14% of the main air volume, making it more compact.

Table 2 summarizes the costs of each option. The hydrophobic zeolite/thermal oxidation is lower in installed cost. More importantly, the utility costs are almost *$800,000* per year less!

CONCLUSION

Hydrophobic zeolite adsorbent is a new technology representing a distinct advancement in solvent separation and concentration technology. Because of its unique physical properties, solvent control systems using hydrophobic zeolite, when applied to many solvent mixes, exhibit separation capacity equal to or better than systems using activated carbon without requiring much of the support equipment. Because of its homogenous pores, hydrophobic zeolite exhibits limited performance for some common solvents. Hydrophobic zeolite represents a technology complementary to rather than competing with activated carbon.

Tests conducted on the hydrophobic zeolite both in the laboratory and in actual installations confirm its performance. A summary of actual test results have been presented. A modular solvent concentrator (MSC), an efficient enclosure designed to handle hydrophobic zeolite or any other commercially available adsorbent, also was presented. Two case studies were outlined to demonstrate the advantages of using a MSC with hydrophobic zeolite.

LITERATURE CITED

1. Blocki, S. W., "New Solvent Control Strategies—The Systems House Approach," Hydrophobic Zeolite Adsorbent; presented at Finishing '91 sponsored by the Society of Manufacturing Engineers, Cincinnati, OH, September, 1991.
2. Crompton, D., and A. Gupta, "Removal of Air Toxics: A Comparison of the Adsorption Characteristics of Activated Carbon and Zeolites," for presentation at the 86th Annual Conference of the Air and Waste Management Association, Denver, CO, June, 1993.
3. Crompton, D., "Carbon Adsorption for VOC Emission Control," *Industrial Finishing*, March, 1990.

Detoxification of Chlorinated Organic Compounds Using Hydrodechlorination on Sulfided $NiO\text{-}MoO_3/\gamma\text{-}Al_2O_3$ Catalyst. Kinetic Analysis and Effect of Temperature

Fabio Murena, Vittorio Famiglietti, Francesco Gioia

Dipartimento di Ingegneria Chimica, Università di Napoli Federico II, Piazzale Tecchio, 80125, Napoli, Italy

The kinetics of the catalytic hydrodechlorination (HDCl) process in the liquid phase of 1,2,3-trichlorobenzene was studied. A commercial Ni-Mo type catalyst, previously sulfided, was used. Experiments were run in the temperature range 280–350°C in a stirred tank reactor under a hydrogen pressure of approximately 100 bar. The reaction network was identified and the kinetic constants have been evaluated using Arrhenius' law and a hypothesis of first order kinetics. The data obtained have been compared with those from an earlier experiment carried out using the same catalyst in unsulfided form. We observed that the sulfidation treatment notably increased the activity of the catalyst. The results have also been reported in terms of the degree of detoxification. The possibility of reaching detoxification efficiency levels, even in mild operating conditions, comparable with those required by legislation for incineration of chlorinated organic compounds, have been demonstrated.

INTRODUCTION

Chlorinated organic compounds, other than those which by nature are inert, are classified by both Italian and international legislation among those compounds which if present in industrial waste render it hazardous and toxic. Following this legislation, more severe and more restrictive directives were issued to regulate the disposal of these categories of industrial waste.

In the past the most striking cases of pollution by chemical substances have been caused by the accidental release of chlorinated organic compounds, such as the case of ICMESA at Seveso [1] where 2,4,5-trichlorophenyl was produced, or the contamination caused by polychlorinated biphenyls (PCBs) [1].

Many chlorinated organic compounds play an important role in the chemical industry both as intermediates as well as final products. Various industries use these chemicals as degreasing solvents (trichloroethylene and trichloroethane), dry cleaning (perchloroethylene and 1,1,2-trichloro-1,1,2-trifluoroethane), electrical isolating fluids (trichlorobenzenes), disinfectants, and herbicides. For those compounds such as the PCBs which can no longer be sold on the market, the problem remains of how to dispose of them [2].

At the present time, the disposal of chlorinated compounds takes place mainly in hazardous waste landfills or in incinerators where they are treated thermally according to precise regulations issued with the aim of guaranteeing the safety of the environment and public health.

In the case of incineration the problem is resolved with the thermal degradation of the chlorinated molecules by means of combustion at a high temperature. It is known, however, that the combustion of chlorinated compounds can give rise to polychlorinated dibenzodioxins (PCDDs) or polychlorinated dibenzofurans (PCDFs) [3, 4]. Even the use of waste fuel in cement kilns is not without hazard, as shown by Mix and Murphy [5].

It is thus to be hoped that treatment processes alternative or complementary to those described will be used. Logically, treatment processes which yield an economic gain or at least reduce costs in terms of a savings of energy or chemical products are to be preferred.

To this end, a particularly interesting means of detoxifying chlorinated organic compounds in the liquid phase is catalytic HDCl [6, 7].

By this process, in fact, the chlorinated organic compound, following the removal of the chlorine as hydrochloric acid (HCl) and its substitution with a hydrogen atom, is transformed into the corresponding hydrocarbon which results in less or zero toxicity. For this reason, the whole HDCl process is termed a detoxification process. The removal of chlorine, as hydrochloric acid, is a technically resolvable problem. The final product is, thus, a mixture of hydrocarbons that can be used in many different ways.

The HDCl process belongs to the category of the catalytic hydrogenolysis processes which are well known to the chemical industry, in particular, in the petrochemical industry. The halogenated compounds' content in crude oil is not significant, however, and specific data on HDCl are not available from this technological sector.

Kinetics data on the catalytic hydrogenolysis of chlorinated compounds is fragmentary and are much less numerous than

for other classes of toxic compounds containing nitrogen, sulfur, and oxygen [7, 8]. The data available in the literature are reviewed below. A review of thermal hydrogenolysis kinetics of chlorinated organic compounds is reported by Converti *et al.* [9].

Concerning catalytic hydrogenolysis, there are data on the chlorobenzene HDCl with sulfided $CoO\text{-}MoO_3/\gamma\text{-}Al_2O_3$ and $NiO\text{-}MoO_3/\gamma\text{-}Al_2O_3$ catalysts at only one operating condition ($T=340°C$ and $p_{H2}=70$ bar) [10], and with Pd/Al_2O_3 and Rh/Al_2O_3 catalysts at $T=80°C$ (gas phase reaction) [11, 12]. More complete data can be found in Hagh and Allen [13] who report the HDCl rates of 1,2-dichlorobenzene and of chlorobenzene for $T=275\text{-}375°C$.

For the most complex chlorinated compounds information is still lacking. For hexachlorobenzene with Ni-Mo sulfided catalyst, the HDCl rates are reported [14] but only at one temperature of $T=325°C$. For PCDDs, the removal levels obtainable with Pt catalysts are reported in operating conditions similar to those found after incineration, but without any information on the reaction mechanisms [15]. Kinetic data on the catalytic activity of copper on the decomposition of ottaCDD and of ottaCDF have been calculated by Gioia [7] from the experimental results of Hagenmaier *et al.* [16] at $T=285°C$ and in the absence of gaseous hydrogen.

On the other hand, experiences of detoxification of mixtures of waste containing chlorinated organic compounds have been developed on pilot-plant scale with commercial catalysts and have produced encouraging results [17].

In the present study, the effect of the temperature on the catalytic HDCl of 1,2,3-trichlorobenzene using a commercial catalyst $NiO\text{-}MoO_3/\gamma\text{-}Al_2O_3$ previously sulfided has been investigated. We preferred to operate with a less toxic compound such as 1,2,3-trichlorobenzene rather than with PCDDs or PCDFs for obvious safety reasons. The data obtained can be used, however, for evaluating the HDCl kinetics of more complex and toxic compounds.

EXPERIMENTAL

The HDCl runs were carried out in a steel reactor (SS316) 300 ml capacity with magnetic stirring at 1200 rpm. Pure hexadecane was used as the reacting medium. It was loaded in the reactor and heated to the reaction temperature. When this temperature was reached, a mixture of 1,2,3-trichlorobenzene, sulfided catalyst, hexadecane and carbon disulfide (CS_2) was placed in the reactor and the hydrogen pressure was adjusted to the set value. The reacting mixture was injected instantaneously by a pressurized loader connected to the reactor head. In this way, the catalytic reaction took place at a constant temperature from $t=0$ reducing the thermal transients. In all runs, 0.4 g of CS_2 were loaded to maintain the catalyst in the sulfided form.

Operating conditions selected for experimental runs are reported in Table 1. As can be seen, the runs were carried out at temperatures between 280 and 350°C and under a constant total hydrogen pressure of 100 bar. The total pressure corresponds to the partial pressure of hydrogen because the vapor pressure of the solvent (hexadecane) is negligible ($p^v=3.24$ bar @ $T=350°C$). The way the experiments were performed ensured that the liquid phase was always saturated with hydrogen.

Table 1 Operating Conditions. CS_2 loaded = 0.4 g for all runs

T [°C]	p_{H2} [bar]	W_{TCB} [g]	W_E [g]	W_C [g]	W_C/W_L	W_{TCB}/W_C
280	100	5.02	171.3	1.11	$6.28\cdot10^{-3}$	4.52
300	100	5.03	163.6	1.04	$6.15\cdot10^{-3}$	4.84
320	100	5.03	163.6	0.90	$5.32\cdot10^{-3}$	5.58
350	100	5.03	163.6	1.20	$7.10\cdot10^{-3}$	4.19

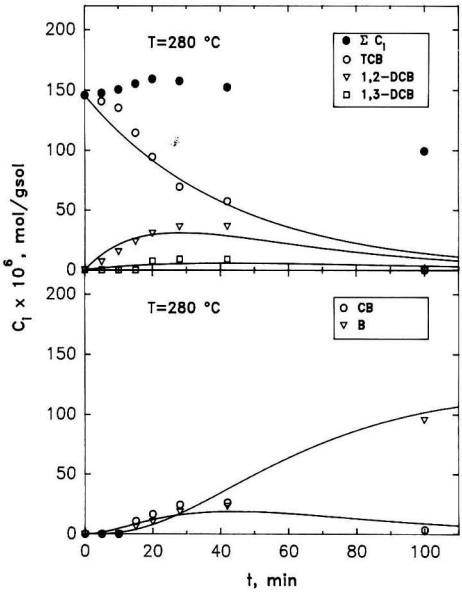

FIGURE 1. Experimental concentrations of reactant and reaction products vs. time at $T=280°C$. Filled circles represent the sum of the concentrations of identified products (ΣC_i). Curves represent the kinetic model.

The catalyst was American Cyanamid HDS-9A. Its composition is $NiO=3.1\%$, $MoO_3=18.3\%$, $WO_3=0.04\%$ and $Na_2O=0.05\%$ (weight percent). The specific surface is 149 m^2/g and the porosity is 0.51 cm^3/g. Before the sulfidation the catalyst was grounded and sieved and the fraction between 74–105 micron (mesh 200-140) was used. The operating conditions adopted for the sulfidation treatment correspond to those that can be considered as standard conditions ($T=400°C$; $t=4$ hr; $[H_2S]=10\%$ in H_2). These operating conditions determine high levels of sulfidation [18] making the catalyst more active in relation to the reactions of hydrogenolysis than to the hydrogenation reactions [19].

The HDCl process has been controlled by regular sampling of the liquid phase carried out, at fixed reaction times, using a sampling line in the bottom of the reactor. A sintered steel filter, at the beginning of the sample line, prevented loss of catalyst.

Liquid samples have been analyzed with a gas chromatograph PE-8500 equipped with a column 50 m HP-1 (Cross-linked Methyl Silicone Gum) $L=50$ m, $D=0.2$ mm thickness of the film = 0.5 micron and with a flame ionization detector. Further details on the experimental and analytical apparatus are reported elsewhere [20]. The following compounds have been identified by gas chromatographic analysis: 1,2,3-trichlorobenzene (TCB), 1,2-dichlorobenzene (1,2-DCB), 1,3-dichlorobenzene (1,3-DCB), chlorobenzene (CB) and benzene (B). The corresponding concentrations have been evaluated by the internal standard technique.

RESULTS

Compound concentrations as a function of reaction time for the runs carried out at $T=280°C$ and $T=350°C$ are reported in Figures 1 and 2. The interpolation curves of the experimental data represent the pattern predicted by the kinetic model which is discussed below.

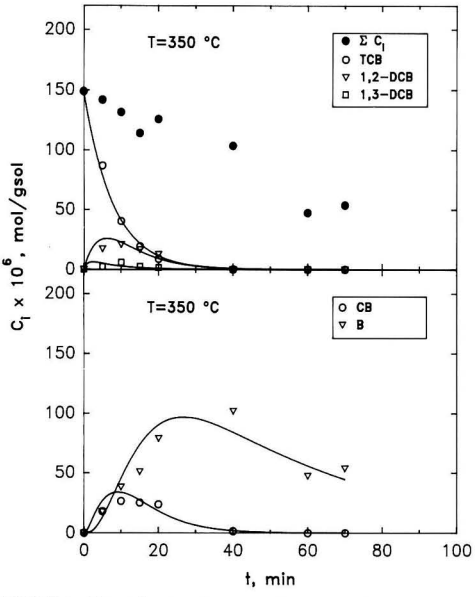

FIGURE 2. Experimental concentrations of reactant and reaction products vs. time at $T = 350°C$. Filled circles represent the sum of the concentrations of identified products (ΣC_i). Curves represent the kinetic model.

Examination of Figures 1 and 2, and of the analogous experimental results at intermediate temperatures [*20*], allows us to hypothesize that, in the operating conditions adopted, the HDCl process of 1,2,3-trichlorobenzene takes place in successive steps each one of which removes a chlorine atom from the aromatic ring. In fact, the only reaction products with derivative (dC_i/dt) different from zero for $t = 0$ are the compounds with two chlorine atoms (1,2-DCB and 1,3-DCB). The formation of chlorobenzene takes place successively followed by that of benzene.

The significant presence of other reaction products does not show up on the chromatographic output. In particular, hydrogenation products of the aromatic ring such as: cyclohexane, cyclohexene and cyclohexadiene were not detected. This finding agrees with the results of other authors obtained in similar experimental conditions [*10, 14*]. Numerous "light" compounds, however, present in low concentrations have been detected in samples removed after long reaction times.

The detected "light" compounds may be considered as hydrocracking reaction products of benzene. The fact that the benzene hydrogenation products were not detected may be explained considering that they crack more rapidly than they are formed. As a consequence, the pattern of the concentration of benzene vs. time shows a maximum and then decreases, and the total balance (ΣC_i) of the moles of the identified compounds decreases with time (Figures 1, 2).

The reaction network reported in Figure 3 has been identified on the basis of the above evidence after only a few attempts. The reactant H_2 and the product HCl are not reported in Figure 3 for clarity. The reported network differs from that identified for the same process with the same catalyst in unsulfided form [*21*] because of the presence of the reaction of benzene consumption and of the absence of inverse reactions.

The kinetic analysis has been developed by hypothesizing that all the reactions in the network of Figure 3 were first order in the concentration of organic compounds. This hypothesis is confirmed by other authors [*13*] when low concentrations of reactants are used as in this case ($C_i < 0.1$ M for TCB and $C_i \ll 0.1$ M for all the other compounds).

The reaction rate for the generic reaction $i \rightarrow j$ is thus:

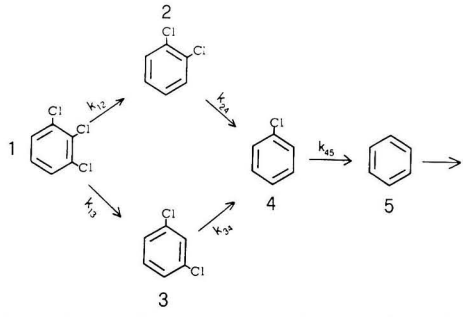

FIGURE 3. Reaction network for the hydrodechlorination of 1,2,3-trichlorobenzene using sulfided Ni-Mo catalyst.

$$r'_{ij} = k''_{ij} C_i f(p_{H2}) \quad (1)$$

where the dependence on the hydrogen pressure is not specified. Since all the runs have been carried out at the same hydrogen pressure ($p_{H2} = 100$ bar) the term $f(p_{H2})$ can be included in the kinetic constant:

$$k'_{ij} = k''_{ij} f(p_{H2}) \quad (2)$$

so equation (1) reduces to:

$$r'_{ij} = k'_{ij} C_i \quad (3)$$

where k'_{ij} is a pseudo first order kinetic constant.

The kinetic constants k'_{ij}, corresponding to the reactions in network of Figure 3, have been evaluated using a regression procedure, reported in the literature [*22*], and verified as reliable and rapid [*23*].

Kinetic constants have been expressed in terms of catalyst weight by the expression:

$$k_{ij} = k'_{ij} (W_L/W_C) \quad (4)$$

from which also the reaction rate can be expressed in terms of the unit weight of catalyst:

$$r_{ij} = k_{ij} C_i$$

The kinetic constants k_{ij} are reported in Table 2. The theoretical curves, obtained by the integration of the system of differential equations representing the network of Figure 3, are reported in Figures 1 and 2. The correlation with the experimental data is satisfactory. The same correlation quality has also been observed for the runs carried out at intermediate temperatures [*20*].

Table 2 Kinetic constants and Arrhenius' law parameters corresponding to reactions of the network in Figure 3 and to reaction (8)

	280°C	300°C	320°C	350°C	k^*_{ij} [gsol/gcat·min]	ΔE_{ij} [kJ/mol·min]
k_{12}	3.26	7.08	8.00	10.38	$5.69 \cdot 10^4$	44.06
k_{13}	0.41	1.88	4.40	7.35	$5.74 \cdot 10^{10}$	116.40
k_{24}	8.12	8.94	14.93	27.97	$7.20 \cdot 10^5$	52.96
k_{34}	4.36	9.27	36.00	131.42	$1.49 \cdot 10^{14}$	143.83
k_{45}	13.29	6.80	15.00	31.20	$1.01 \cdot 10^5$	43.07
k_{56}	0.30	0.31	0.52	3.16	$3.02 \cdot 10^8$	97.27
k_o	4.24	4.51	7.90	17.50	$1.89 \cdot 10^6$	60.61

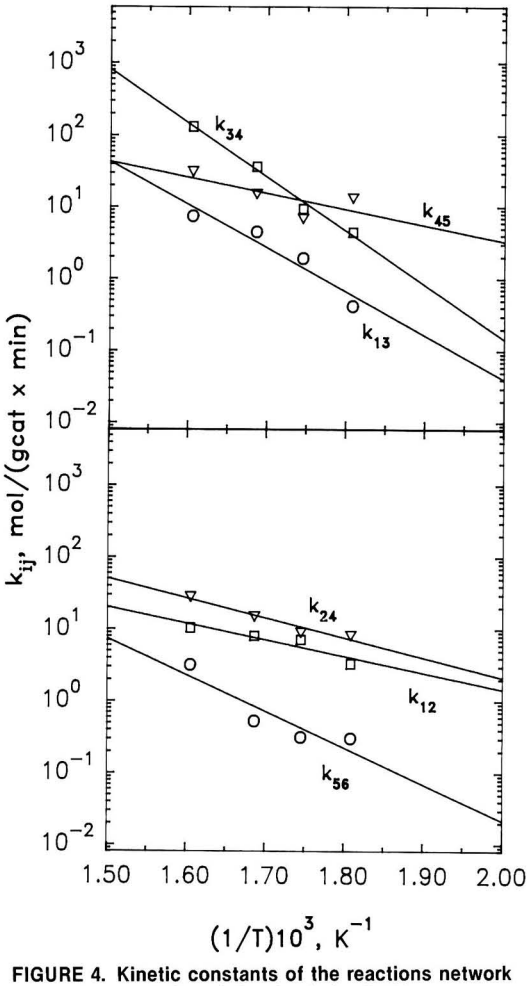

FIGURE 4. Kinetic constants of the reactions network in Fig. 3. Correlation by Arrhenius' law.

Arrhenius's law has been used to model the dependence of the kinetic constants on the temperature:

$$k_{ij} = k_{ij}^{\circ} \exp(-\Delta E_{ij}/RT)$$

The diagrams $\log k_{ij}$ vs. $1/T$ are shown in Figure 4. The values of the prexponential factor and of the activation energy, for the different reactions of the network identified, are reported in Table 2.

DISCUSSION

It is interesting to elucidate the effect of sulfidation of the catalyst on the HDCl reactions. It is well known that the sulfidation process improves or modifies the activity of the catalysts of the transition metals used in hydrocracking. Experience with sulfided Ni-Mo catalysts is reported by various authors: hydrogenation and hydrogenolysis of benzene and substituted benzenes [*10*, *24*]; hydrogenation of benzothiophene and its derivatives [*25*]; of thiophene [*26*]; and of quinoline [*27*]. The results generally show a noticeable improvement of catalytic activity after the sulfidation treatment. The most salient aspects of the role played by sulfur in HDS catalysts have been dealt with by Topsoe and Clausen [*28*].

As far as substituted benzenes are concerned it is interesting to observe that the sulfidation process improves the hydrogenolysis activity more than the hydrogenation activity for slightly electron-donating substituents (e.g., Cl) [*10*].

By comparing the results of this work with those reported by Gioia et al. [*21*], we observe the following features peculiar of the sulfided form of the catalyst.

The HDCl rate increases notably, following the sulfidation process. The kinetic constants ratio (k_{ij} sulfided/k_{ij} not sulfided [*21*]), for the reaction network in Figure 3, are at $T = 350°C$: 1.38 for the reaction 1→2; 2.72 for the reaction 1→3; 7.13 for the reaction 2→4; 47.4 for the reaction 3→4 and 36.7 for the reaction 4→5. It is clear from these results that the fewer the number of chlorine atoms bonded to the benzene ring and the greater the distance between them, the greater the increase of the hydrogenolysis activity.

The sulfidation treatment of the catalyst thus determines an increase in the reaction rate of all the HDCl reactions, particularly of chlorobenzene, which is no longer the slower step, and of 1,3-dichlorobenzene [*21*].

Furthermore, when sulfided catalyst is used, the inverse (chlorination) reactions do not occur. Conversely, when unsulfided catalyst was used, the statistical analysis of data indicated that the inverse reactions 5→4, 4→3 and 4→2 also took place [*21*].

As a minor feature, the sulfided catalyst, as can be seen from the experimental pattern of benzene's concentration curves (Figures 1 and 2), shows a certain activity in the hydrocracking of benzene. On the contrary, hydrocracking activity does not take place when the unsulfided form of the Ni-Mo catalyst is used [*21*]. Hydrocracking reactions of benzene have been globally reported in the network of Figure 3 introducing the reaction 5→6 (benzene→"light" reaction products).

The observation of C_i vs. t curves, with both the unsulfided [*21*] and the sulfided catalyst (Figures 1, 2), does not seem to indicate the presence of reactions involving the simultaneous removal of two or three chlorine atoms from the benzene ring. The C_i vs. t curves at $T = 280°C$, reported in Figure 1, show that $dCi/dt = 0$ both for benzene and for chlorobenzene, at time $t = 0$. Therefore, reactions TCB→CB and TCB→B do not take place or are not relevant. In any case, the reactions with a simultaneous removal of two or three chlorine atoms have been added to the reaction network of Figure 3 as a test. The results obtained were generally inconsistent. Results statistically consistent were obtained only for the reaction 1,2-DCB→B at the two intermediate temperatures ($T = 300$ and $T = 320°C$), while still inconsistent results were obtained for the runs at the extreme temperatures ($T = 280$ and $T = 350°C$). Therefore, we may conclude that reactions involving the simultaneous removal of two or three chlorine atoms are not relevant in our experiments.

Finally, it must be noted that thermal hydrogenolysis plays an insignificant role in the range of temperatures investigated. At $T = 350°C$ the ratio between catalytic HDCl with sulfided catalyst ($W_C/W_L = 7.11 \cdot 10^{-3}$) and thermal HDCl (with the contribution of the catalytic effect of the inner walls of the reactor) is between $0.3 \cdot 10^2$ and $5.5 \cdot 10^2$ (k'_{ij} sulfided/k'_{ij} thermal) [*20*], for all the different reactions of the network in Figure 3. Thermal reactions are reported [*9*] to take place at higher temperatures 600–900°C.

Calculation of the Degree of Detoxification

If we take the 1,2,3-trichlorobenzene and its chlorinated reaction products (1,2-DCB, 1,3-DCB, CB) to be toxic compounds we can define the detoxification degree as [*6*]:

$$\varphi_d = 1 - (C_{TCB} + C_{1,2DCB} + C_{1,3DCB} + C_{CB})/C_{TCB}^{\circ} \qquad (7)$$

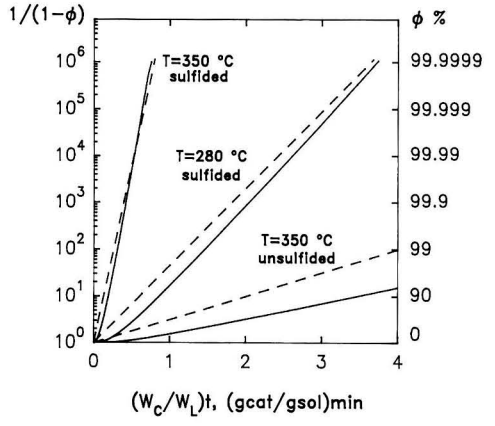

FIGURE 5. Pattern of detoxification degree φ_d (solid line) and of hydrodechlorination degree φ_h (dashed line). Curves for unsulfided catalyst are from Gioia et al. [21].

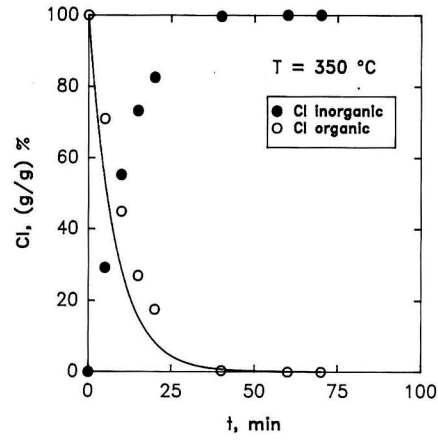

FIGURE 6. Pattern of global hydrodechlorination reactions of 1,2,3-trichlorobenzene (organic chlorine→inorganic chlorine). The curve represents equation (11) with k_o of Table 2 at $T=350°C$.

After defining the reaction network and evaluating the kinetic constants, we can calculate the detoxification degree of 1,2,3-trichlorobenzene as a function of the operating conditions.

In Figure 5, the pattern of φ_d is plotted vs. the operating parameter $(W_C/W_L)t$ at $T=280°C$ and $T=350°C$, using the kinetic model developed in this study (kinetic constants of Table 2 applied to the reaction network of Figure 3). The adopted representation immediately shows the operating conditions, reaction time and catalyst concentration, required to reach fixed levels of detoxification.

In Figure 5 the pattern of φ_d corresponding to the use of the same catalyst in unsulfided form [*21*, *29*] is also shown for comparison. It can be seen that the use of the sulfided catalyst, in the same experimental conditions, drastically reduces the detoxification time. Moreover, it allows values of φ_d%, corresponding to low values of the parameter $(W_C/W_L)t$, comparable with those required by legislation on thermal destruction plants: $\varphi_d\% \geq 99.99$ for each specific toxic compound (Resource Conservation and Recovery Act), and $\varphi_d\% \geq 99.9999$ for PCBs (Toxic Substances Control Act) [*1*, pp. 208-209]. Figure 5 shows that $\varphi_d\% > 99.9999$ at $T=350°C$ with $(W_C/W_L)t \approx 1$, or at $T=280°C$ with $(W_C/W_L)t \approx 4$. To reach the same levels of φ_d with the unsulfided catalyst, values of $(W_C/W_L)t$ about 20 times greater would be required than those reported previously.

Overall Kinetics

It is useful to depict the reaction network in Figure 3 in the following overall reaction:

$$\text{organic chlorine} \rightarrow \text{inorganic chlorine} \qquad (8)$$

where organic chlorine is defined as that bonded to the benzene ring and inorganic chlorine as that present as HCl which, for the stoichiometry of the reactions, equals twice the moles of the H_2 consumed.

In the reaction system studied the concentration of organic chlorine atoms ($C_{C\text{-}Cl}$) present in the reaction mixture at time t is:

$$C_{C\text{-}Cl} = 3C_{TCB} + 2(C_{1,2\text{-}DCB} + C_{1,3\text{-}DCB}) + C_{CB} \qquad (9)$$

If we also hypothesize a first order kinetics for reaction (8) we have:

$$dC_{C\text{-}Cl}/dt = -k_o(W_C/W_L)C_{C\text{-}Cl} \qquad (10)$$

and

$$C_{C\text{-}Cl} = C^{\circ}_{C\text{-}Cl}\exp[-k_o(W_C/W_L)t] \qquad (11)$$

where $C^{\circ}_{C\text{-}Cl}$ is the initial concentration of organic chlorine in the reactor which, in the specific reaction system, is equal to three times the initial concentration of 1,2,3-trichlorobenzene. Correlating the experimental data with equation 11 we obtain, at $T=350°C$, the curve shown in Figure 6. Considering the simplifications adopted, the first order hypothesis is quite satisfactory. The correlation of experimental data with equation 11 provides the values of k_o reported in Table 2. The dependence of the kinetic constant k_o on the temperature, according to Arrhenius' law, is expressed by the following equation:

$$k_o = 1.89 \cdot 10^6 \exp[-60.61 \cdot 10^3/RT] \qquad (12)$$

We can define the HDCl degree φ_h, by analogy with the detoxification degree φ_d (equation 7), as the ratio between the concentration of the atoms of inorganic chlorine produced (equal to the atoms of organic chlorine hydrogenated) and the concentration of the atoms of organic chlorine initially present:

$$\varphi_h = (C^{\circ}_{C\text{-}Cl} - C_{C\text{-}Cl})/C^{\circ}_{C\text{-}Cl} \qquad (13)$$

Using equation (11) we obtain:

$$\varphi_h = 1 - \exp[-k_o(W_C/W_L)t] \qquad (14)$$

The patterns of φ_d and φ_h vs. $(W_C/W_L)t$ are reported in Figure 5 at $T=280°C$ and $T=350°C$. Since, as shown in Figure 5, $\varphi_h \approx \varphi_d$, equations (14) with equation (12), for practical applications, can be used to easily obtain a valuable prediction of the detoxification degree φ_d in the operating conditions of interest.

Conceptually, φ_h must be always $\geq \varphi_d$. In fact, φ_h and φ_d are defined so that:

$$\varphi_h - \varphi_d = (C_{1,2DCB} + C_{1,3DCB} + 2C_{CB})/3C^{\circ}_{TCB} \qquad (15)$$

The fact that in Figure 5 the curves of φ_d and φ_h ($T=350°C$

with sulfided catalyst) cross over each other is thus conceptually erroneous and is due to the approximation of the first order kinetics adopted to model the global reaction [8].

For polychlorinated compounds the HDCl degree, in the first stage of the chemical process, increases more rapidly than the detoxification degree because the reaction intermediates, which contain organic chlorine, are also toxic. Where an unsulfided catalyst is used the patterns of φ_d and φ_h (see Figure 5) are further apart, since the HDCl kinetics of intermediate reaction products (1,2-DCB; 1,3-DCB and CB) are slower.

CONCLUSIONS

The sulfided form of a commercial NiO-MoO_3/γ-Al_2O_3 catalyst has shown a marked improvement of activity, over the unsulfided catalyst, on the HDCl process of 1,2,3-trichlorobenzene, in particular on the HDCl rates of 1,3-dichlorobenzene and of chlorobenzene. As a result, the detoxification times are significantly reduced. Levels of detoxification of 1,2,3-trichlorobenzene, comparable with those required for incineration, can be reached by the HDCl process even in mild operating conditions.

The HDCl process follows a parallel-series reaction network in which the chlorine atoms are progressively removed from the benzene ring. A simplified representation of the process, reducing the reaction network to a single first order reaction, is possible for design purposes. This makes it easier to predict the detoxification degree as a function of temperature, reaction time, and catalyst concentration.

These results can also be used to estimate the HDCl kinetics of more toxic compounds (PCDDs, PCDFs, PCBs) for which direct experiments are dangerous. Bearing this in mind, the HDCl kinetics of intermediates (chlorobenzene, 1,2-dichlorobenzene, 1,3-dichlorobenzene) and of 1,2,3-trichlorobenzene itself, can be used in the presence of the following: a single chlorine atom, two chlorine atoms in ortho position, two chlorine atoms in meta position and three chlorine atoms in positions 1,2,3. The experiments do not, however, provide an evaluation of the hydrogenolysis kinetics of chlorine atoms in para position, even if a value similar to meta or ortho can be hypothesized.

NOTATION

$C_{C\text{-}Cl}$ = organic chlorine concentration; mol/gsol
C_i = concentration of compound i; mol/gsol
ΔE_{ij} = activation energy of the reaction $i \rightarrow j$ (i and j as reported in the reaction network of Figure 3); kJ/mol
k'_{ij} = pseudo first order kinetic constant (i and j as above); min^{-1}
k_{ij} = kinetic constant (i and j as above); gsol/(gcat·min)
k^o_{ij} = prexponential factor (i and j as above); gsol/(gcat·min)
k_o = kinetic constant of the global reaction of hydrodechlorination; gsol/(gcat·min)
p^v = vapor pressure of Hexadecane; bar
p_{H2} = partial pressure of Hydrogen; bar
R = gas constant; $R = 8.314$ J/(mol·K)
r_{ij} = reaction rate (i and j as above); mol/(gcat·min)
r'_{ij} = reaction rate (i and j a above); mol/(gsol·min)
T = temperature; K
W_C = weight of catalyst loaded; g
W_E = weight of hexadecane loaded; g
W_L = weight of solution loaded; g
W_{TCB} = weight of 1,2,3-trichlorobenzene loaded; g

Greek letters

φ_d = detoxification degree; see equation (7)
φ_h = HDCl degree; see equation (13)

ACKNOWLEDGMENT

This work was financed by research grants from "Ministero dell'Università e della Ricerca Scientifica e Tecnologica" and from "Consiglio Nazionale delle Ricerche."

The assistance of Mr. Giuseppe Cutillo for the experimental parts of this work is gratefully acknowledged.

LITERATURE CITED

1. C. A. Wentz, "Hazardous Waste Management," McGraw-Hill, New York, NY (1989).
2. Maroni, M., A. Colombi, P. Carrer, F. Barbieri, V. Foa', G. Dal Frate, and C. Bossi, "Stima Delle Giacenze di PCB Presenti in Italia e Loro Soluzioni di Smaltimento," *Acqua Aria*, **8**, pp. 761-767 (1991).
3. Buser, H. R., and H. P. Bosshardt, "Formation of Polychlorinated Dibenzofurans (PCDFs) from the Pyrolysis of PCBs," *Chemosphere*, **7**, pp. 109-119 (1978).
4. Buser, H. R., "Formation of Polychlorinated Dibenzofurans (PCDFs) from the Pyrolysis of Chlorobenzenes," *Chemosphere*, **8**, pp. 415-424 (1979).
5. Mix, T. W., and B. L. Murphy, "Risks Associated with Waste-Fuel Use in Cement Kilns," *Environ. Progr.*, **3**, pp. 64-70 (1984).
6. Gioia, F., "La Tecnica dell'Idrogenazione Nella Gestione dei Rifiuti Tossici," *Rifiuti Solidi*, **4**, pp. 197-201 (1990).
7. Gioia, F., "Detoxification of Organic Waste Liquids by Catalytic Hydrogenation," *J. Hazardous Mater.*, **26**, pp. 243-260 (1991).
8. Gioia, F., "Idrogenazione di Rifiuti Organici Tossici," *Chimica Industria*, **72**, pp. 915-921 (1990).
9. Converti, A., M. Zilli, D. M. De Faveri, and G. Ferraiolo, "Hydrogenolysis of Organochlorinated Pollutants: Kinetics and Thermodynamics," *J. Hazardous Mater.*, **27**, pp. 127-135 (1991).
10. Moreau, C., J. Joffre, C. Saenz, and P. Geneste, "Hydroprocessing of Substituted Benzenes Over a Sulfided CoO-MoO_3/γ-Al_2O_3 Catalyst," *J. Catal.*, **122**, pp. 448-451 (1990).
11. Coq, B., G. Ferrat, and F. Figueras, "Conversion of Chlorobenzene over Palladium and Rhodium Catalysts of Widely Varying Dispersion," *J. Catal.*, **101**, pp. 434-445 (1986).
12. Bodnariuk, P., B. Coq, G. Ferrat, and F. Figueras, "Carbon-Chlorine Hydrogenolysis Over PdRh and PdSn Bimetallic Catalysts," *J. Catal.*, **116**, pp. 459-466 (1989).
13. Hagh, B. F., and D. T. Allen, "Catalytic Hydroprocessing of Chlorobenzene and 1,2-Dichlorobenzene," *AIChE J.*, **36**, pp. 773-778 (1990).
14. Hagh, B. F., and D. T. Allen, "Catalytic Hydroprocessing of Chlorinated Benzenes," *Chem. Eng. Sci.*, **45**, pp. 2695-2701 (1990).
15. Hiroaka, M., N. Takeda, S. Okajima, T. Kasakura, and Y. Imoto, "Catalytic Destruction of PCDDs in Flue Gas," *Chemosphere*, **19**, pp. 361-366 (1989).
16. Hagenmaier, H., H. Brunner, R. Haag, and M. Kraft, "Copper-Catalyzed Dechlorination/Hydrogenation of Polychlorinated Dibenzo-*p*-Dioxins, Polychlorinated Dibenzofurans and Other Chlorinated Aromatic Compounds," *Environ. Sci. Technol.*, **21**, pp. 1085-1088 (1987).
17. Kalnes, T. N., and R. B. James, "Hydrogenation and

Recycle of Organic Waste Streams," *Environ. Progr.*, **7**, pp. 185–191 (1988).
18. Massoth, F. E., "Studies of Molybdena-Alumina Catalysts. IV. Rates and Stoichiometry of Sulfidation," *J. Catal.*, **36**, pp. 164–184 (1975).
19. Voorhoeve, R. J. H., and J. C. M. Stuiver, "Kinetics of Hydrogenation on Supported and Bulk Nickel-Tungsten Sulfide Catalysts," *J. Catal.*, **23**, pp. 228–235 (1971).
20. Cutillo, G. P., "Idrodeclorazione di 1,2,3-Triclorobenzene su Catalizzatore NiO-MoO_3/γ-Al_2O_3. Effetto della Sulfurazione del Catalizzatore," Tesi di Laurea in Ingegneria Chimica, Napoli (1991).
21. Gioia, F., V. Famiglietti, and F. Murena, "Catalytic Hydrogenation of 1,2,3-Trichlorobenzene," *J. Hazardous Mater.*, **33**, pp. 63–73 (1993).
22. Himmelblau, P. M., C. R. Jones, and K. B. Bishoff, "Determination of Rate Constants for Complex Kinetic Models," *Ind. Eng. Chem. Fundam.*, **6**, pp. 539–543 (1967).
23. Hosten, L. H., "A Comparative Study of Short Cut Procedure for Parameter Estimation in Differential Equation," *12th Symp. Comput. Appl. Chem. Eng.*, **1**, pp. 169–183 (1979).
24. Aubert, C., R. Durand, P. Geneste, and C. Moreau, "Factors Affecting the Hydrogenation of Substituted Benzenes and Phenols Over a Sulfided NiO-MoO_3/γ-Al_2O_3 Catalyst," *J. Catal.*, **112**, pp. 12–20 (1988).
25. Aubert, C., R. Durand, P. Geneste, and C. Moreau, "Hydroprocessing of Dibenzothiophene, Phenothiazine, Phenoxathiin, Thianthrene and Thioxanthene on a Sulfided NiO-MoO_3/γ-Al_2O_3 Catalyst," *J. Catal.*, **97**, pp. 169–175 (1986).
26. De Beer, V. H. J., T. H. M. van sint Fiet, G. H. A. M. van der Steen, A. C. Zwaga, and G. C. A. Schuit, "The CoO-MoO_3/γ-Al_2O_3 Catalyst. V. Sulfide Catalysts Promoted by Cobalt, Nickel, and Zinc," *J. Catal.*, **35**, pp. 297–306 (1974).
27. Gioia, F., and V. Lee, "Effect of Hydrogen Pressure on Catalytic Hydrodenitrogenation of Quinoline," *Ind. Eng. Chem. Process Des. Dev.*, **25**, pp. 918–925 (1986).
28. Topsoe, H., and B. S. Clausen, "Active Sites and Support Effects in Hydrodesulfurization Catalysts," *Appl. Catal.*, **25**, pp. 273–293 (1986).
29. Famiglietti, V., "Idrodeclorazione Catalitica di 1,2,3-Triclorobenzene," Tesi di Laurea in Ingegneria Chimica, Napoli (1991).

Effects of Particle Size Distribution on Limestone Dissolution in Wet FGD Process Applications

Naohiko Ukawa, Toru Takashina and Naoharu Shinoda

Hiroshima Research & Development Center, Mitsubishi Heavy Industries, Ltd., 4-6-22, Kanonshin-machi, Nishi-ku, Hiroshima 733 Japan

and

Taku Shimizu

Engineering and Construction Center, Mitsubishi Heavy Industries, Ltd., 15-1, Tomihisa-cho, Shinjuku-ku, Tokyo 162 Japan

The kinetics of limestone dissolution in the wet type flue gas desulfurization (FGD) processes has been studied. The rates of dissolution and particle size reduction were measured in both batch and continuous reaction systems for limestone of different size distribution. A predictive model was developed based on mass transfer mechanism. It was in good agreement with experimental data. Moreover, the rate of dissolution for 25 limestones of different composition and size distribution were measured in apparatus with a sulfur dioxide absorber which simulated FGD processes. The model was also in good agreement with these results.

INTRODUCTION

The mainstay of flue gas desulfurization (FGD) processes for thermal power plants with the object of environmental protection has been the wet type limestone scrubbing process. In this process, limestone dissolves into absorbent slurry and neutralizes sulfur dioxide, so the dissolution rate of limestone is one of the most essential kinetics in FGD processes; therefore, accurately evaluating the dissolution of limestone is important for not only designing of a FGD process but also operation of the plant [8].

Many studies on limestone dissolution have been carried out so far. Morse and Plummer *et al.* discussed the basic kinetics of dissolution [7, 9]. Generally, the limestone dissolution is considerably affected by the pH value of liquid and the particle size of limestone. The correlation between the pH value and limestone dissolution rate was studied by Chan *et al.* and Ellis [2, 5], and research regarding the particle size was studied by Tress *et al.* [11]. Compton *et al.* carried out experiments on the morphology of the limestone dissolution [3, 4]. Furthermore, the model being able to predict limestone reactivity as well as FGD performance was developed by Gage *et al.* [6]. Few previous studies, however, have discussed the variation of the particle size distribution during dissolution, although the particle size is one of the most significant factors in dissolution.

In this study, the variation of the particle size distributions of limestone through the dissolution reaction were measured both in the batch and continuous type test apparatus. The obtained data were compared with the results which were expected by the mathematical model. Furthermore, the dissolution rates of limestone having various particle size distributions and compositions were measured, using wetted-wall column equipment which simulated the absorber of wet FGD process.

MODEL DESCRIPTION

In the vicinity of pH 5, the dissolution of limestone in solution is supposed to be the reaction between the limestone and hydrogen ions and is expressed as follows:

$$CaCO_3 + 2H^+ \rightarrow Ca^{2+} + CO_2 + H_2O \qquad (1)$$

Correspondence concerning this paper should be addressed to Naohiko Ukawa.

On the dissolution equation 1, Toprac *et al.* proposed dissolution rate equations by combining the rate in a stagnant fluid and an agitated fluid as mentioned below [*10*]. When the limestone particles are assumed to be spherical, the dissolution rate can be expressed by equation 2, and the mass transfer coefficient in the stagnant fluid is given by:

$$\frac{dV_p}{dt} = -\frac{\pi d_p^2 k_L}{\rho_m} \Delta C \tag{2}$$

$$Sh = \frac{k_L \cdot d_p}{D} = 2 \tag{3}$$

From equation 2 and 3:

$$\frac{dV_p}{dt} = -\frac{\pi \Delta C}{\rho_m} 2Dd_p \tag{4}$$

The correlation equation of the mass transfer coefficient in the agitated fluid was studied by Calderbank *et al.* [*1*] who presented as:

$$k_L \cdot Sc^{2/3} = 0.13 \left(\frac{\epsilon \cdot \nu_c}{\rho_c^2}\right)^{1/4} \tag{5}$$

$$Sc = \frac{\nu_c}{D} \tag{6}$$

From equation (2), (5) and (6), the dissolution rate in the agitated fluid is given by:

$$\frac{dV_p}{dt} = -\frac{\pi \Delta C}{\rho_m} \cdot 0.13 \left(\frac{\epsilon \cdot \nu_c}{\rho_c^2}\right)^{1/4} \left(\frac{\nu_c}{D}\right)^{-2/3} d_p^2 \tag{7}$$

When equation (4) and (7) are combined, the dissolution rate is obtained as follows:

$$\frac{dV_p}{dt} = -\frac{\pi \Delta C}{\rho_m} \left[2Dd_p + 0.13 \left(\frac{\epsilon \cdot \nu_c}{\rho_c^2}\right)^{1/4} \left(\frac{\nu_c}{D}\right)^{-2/3} d_p^2 \right] \tag{8}$$

Equation 8 can be rewritten as:

$$\frac{dV_p}{dt} = -kcV_p^{1/3} - kcBV_p^{2/3}$$

$$\left(\text{Where} \quad kc = \frac{3.63 D \Delta C \pi^{2/3}}{\rho_m} \right.$$

$$\left. B = \frac{0.08065}{D} \left(\frac{\epsilon \cdot \nu_c}{\rho_c^2}\right)^{1/4} \left(\frac{\nu_c}{D}\right)^{-2/3} \right) \tag{9}$$

Equation 9 can be solved analytically. When the fraction of unreacted limestone is used instead of volume of particle as:

$$t = \frac{3}{kcB^2} \left(\ln\left(\frac{1 + BV_j^{1/3} f_j^{1/3}}{1 + BV_j^{1/3}}\right) + BV_j^{1/3}(1 - f_j^{1/3}) \right) \tag{10}$$

This equation shows a fraction of dissolution of limestone having a same particle size in the batch reaction system. Usually, the limestone used in the FGD process has broad particle size distribution. Therefore, equation 10 should be solved per each particle size, and the fraction of dissolution of limestone with a particle size distribution the batch reaction system is expressed by:

$$F_B = \sum_{j=1}^{n} (\phi_j f_j) = 1 - \eta_B \tag{11}$$

Meanwhile, the reaction of limestone in most of the FGD process happens to a continuous reaction system, so the consideration on the residence time distribution of CSTR for the limestone particles should be required. Eventually, the fraction of dissolution in the continuous reaction system is given by:

$$F_C = \sum_{j=1}^{n} \left[\phi_j \frac{1}{\tau} \int_0^{\infty} f_j \cdot \exp\left(-\frac{t}{\tau}\right) dt \right] = 1 - \eta_c \tag{12}$$

As is clear from its definition, *kc* in equation 10 is proportional to a difference in the concentration which is the driving force when the diffusion coefficient and molar density of limestone are constant. At the pH value prevailing in the absorber of FGD process, this difference in concentration can be considered to be hydrogen ion concentration. If the activity coefficient of the hydrogen ion is presumed to be constant, *kc* is further defined by:

$$kc = ka \cdot 10^{-\mathrm{pH}} \tag{13}$$

EXPERIMENT

Apparatus

Figure 1 shows batch type test apparatus. Two reactors which had different volume were prepared. One reactor, a volume of 2l, was used to obtain the data regarding the fraction of dissolution vs. the particle size distribution. The other reactor, a volume of 0.2l, was used to obtain the data regarding the time vs. the fraction of dissolution. The liquid in the reactor was kept at a constant temperature through the jacket. During all the tests, the constant pH was kept by means of adding acid with pH controller. The particle size distribution of unreacted limestone was measured by standard sieves for over 20 μm and photo extinction apparatus for under 20 μm. The test conditions were as follows: Reactor volume—2l (0.2l); limestone concentration—45g/900 ml (0.5g/100ml); acid solution—6N-HCl (1N-HCl); liquid pH—5.0; and temperature—50°C. The values in the parenthesis show the test conditions for the time vs. the fraction of dissolution. The continuous type test apparatus is shown in Figure 2. The reactor had a volume of 8l and was kept at a constant temperature in the same way as the batch type test apparatus. In this apparatus, an acid was quantitatively added (this corresponds to the absorbed amount of sulfur dioxide in the FGD process) and limestone was fed continuously to keep constant pH value. This apparatus can simulate feeding of limestone and discharging of gypsum in the absorber tank in FGD process. In

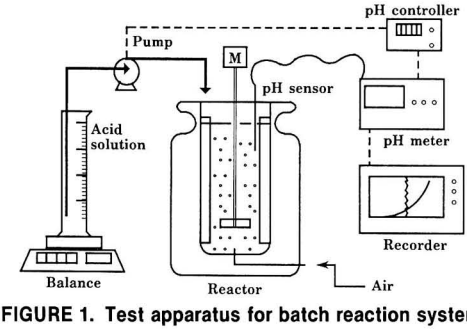

FIGURE 1. Test apparatus for batch reaction system.

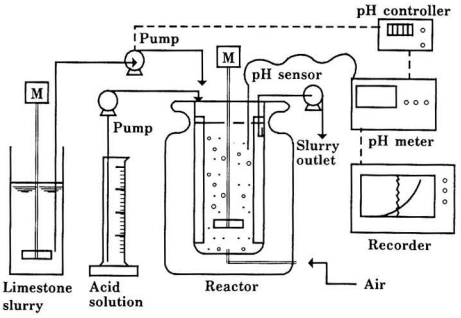

FIGURE 2. Test apparatus for continuous reaction system.

order to simulate the FGD process more accurately, it might be better to use sulfuric acid to be added, but hydrochloric acid was used in this tests to prevent formation of gypsum, because if gypsum particle was formed, it would be difficult to measure the particle size distribution of unreacted limestone. Using the continuous type test apparatus, data regarding the fraction of dissolution and particle size distribution of unreacted limestone were obtained. The particle size distribution was measured by the same way as the batch type test. The test condition were as follows; Hydrochloric acid load—100mmol/l. h; liquid pH—4.8 to 5.5; and temperature—50°C.

The wetted-wall column apparatus is shown in Figure 3. The wetted-wall column can simulate the practical absorber in an actual FGD process. Table 1 summarizes the specifications of the test apparatus and the operating conditions. Synthetic flue gas fed at the top of the wetted-wall column came in contact with a co-current flow of liquid film falling down the column wall. Air was sparged into the tank to oxidize dissolved sulfite completely. The dissolution rate of limestone was calculated from the amount of absorbed sulfur dioxide; however, the particle size distribution of unreacted limestone could not be measured in this test due to coexistence of gypsum particles.

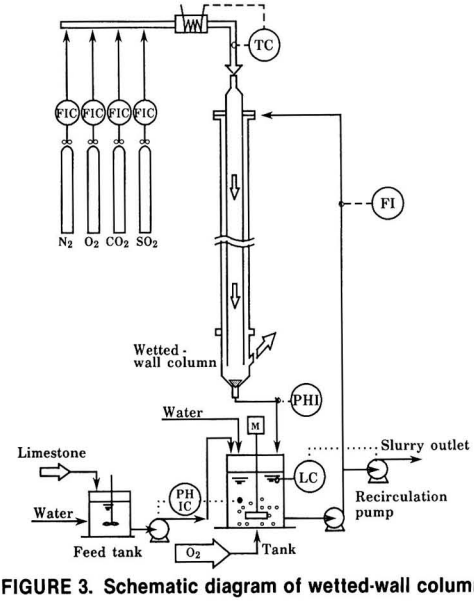

FIGURE 3. Schematic diagram of wetted-wall column.

Table 1 Specifications and Operating Conditions for Wetted-Wall Column

Synthetic flue gas	
Flow rate	: 2.15 [m^3N/h]
Composition	: 6 [%] O_2, 12 [%] CO_2, 82 [%] N_2, 3000 [ppm] SO_2
Temperature	: 100 [°C]
Absorber	
Wetted-wall column	: 15 [mm] ID, 6000 [mm] Height L/G = 22 [l/m^3N] Pressure = 1 [atm] Exit gas temperature = 50 [°C]
Tank	: 2.0 [l]
Slurry composition	
Limestone	= 0.01-0.02 [mol/l]

Material

A limestone produced in Japan was used for testing with the batch and continuous type test. This limestone had the following composition: Purity of calcium carbonate—98.0 wt. %; MgO—0.4%; and acid insoluble—0.28%. Three limestone samples having different particle size distribution were prepared as follows:

(1) Limestone, 95 wt. % of which passed through a 45 μm sieve and a mean diameter of which was 9.3 μm.

(2) Limestone, 95 wt. % of which passed through a 75 μm sieve and a mean diameter of which was 10.5 μm.

(3) Limestone, the particle size of which was adjusted from 20 μm to 45 μm by standard sieves.

For wetted-wall column test, 25 samples of limestone collected from various places of the world were prepared.

Results and Discussion

Figure 4 shows the relationship between the time and the fraction of dissolution in the batch test. In this figure, the limestone which reaches a higher fraction of dissolution in shorter reaction time has a higher reactivity. In the test, limestones with different particle sizes of the sample were used. The relation of the particle size distributions of the limestone was 45 μm 95% passing <75 μm 95% passing <20-45 μm. The measured values show higher reactivity in this order. The solid curves in the figure show the calculated values by equation 10 and 11, and they are in good agreement with the obtained data. The following values were used at the dissolution rate

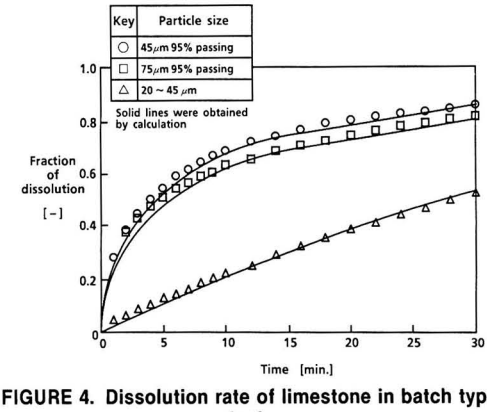

FIGURE 4. Dissolution rate of limestone in batch type test.

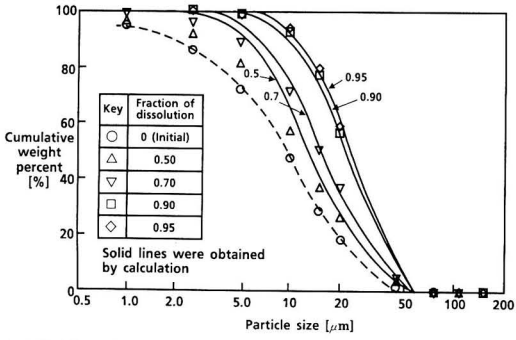

FIGURE 5. Particle size distribution of unreacted limestone in batch type test (particle size distribution of initial limestone; 45μm 95% passing).

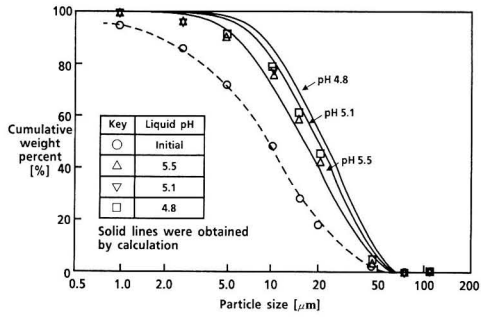

FIGURE 6. Particle size distribution of unreacted limestone in continuous type test (particle size distribution of initial limestone; 45μm 95% passing).

constant and enhancement factor which were dissolution parameters.

$$ka = 3.4 \cdot 10^{-9},\ B = 200000$$

The value of B is relatively higher than those (26000 to 88000 [l/m]) obtained by Toprac. The reason might be attributed to the difference of agitating conditions. The fact that the limestone of the same composition and from the same place but having different particle sizes can be expressed by the same dissolution parameters show that equations (10) and (11) allow accurate calculations of the effect of particle size. The particle size distribution of unreacted limestone in the batch type test was measured at several fractions of dissolution. Figure 5 shows the particle size distribution of the unreacted limestone. It indicates that as the dissolution progresses, the particle size of unreacted limestone shifts to the larger values. This can be simply explained by the fact that as: smaller particles have larger specific areas dissolve at a greater rate, and they disappear sooner than coarser one. The solid curves in Figure 5 give the values calculated by the dissolution rate equations like those in Figure 4. The measured values are in good agreement with the calculated values.

The fractions of dissolution measured and calculated at various pH values in the continuous reaction system are shown in Table 2. Figure 6 and 7 show the particle size distributions of unreacted limestone samples of 45 μm 95 wt. % passing and 75 μm 95 wt. % passing. The particle size distributions of unreacted limestones obtained in the continuous type test also shift to the larger values when the fraction of dissolution become greater, like in the batch type test, but the degree of shifting is smaller than in the batch system. For instance, for the sample of 45 μm 95 wt. % passing, the fraction of dissolution at which mean diameter of unreacted limestone becomes 18 μm is 95% in the continuous type test but 70% in the batch type test. It is considered that as fresh limestone of smaller particle size is constantly fed into the continuous reaction system, smaller particles are more likely to exist in it than in the batch reaction system. The calculated values in Table 2 and the solid curves in Figures 6 and 7 are values obtained by using equation (12). For the dissolution parameters, the same values as for the batch type test were used. In the continuous type test, the measured and calculated values are in good agreement, and they confirm that the dissolution rate equations in this study also holds good for the continuous type test and can be expressed by the same dissolution parameters. In addition, the results with the continuous type test show that the measured and calculated values at various pH values correspond well each other, and that equation 13 holds good in the pH range in this test.

The tests and analyses described above have shown that the dissolution rate equation in this study is applicable to the particular limestone produced in Japan. However, limestone used in a FGD process is usually produced from a mine near the plant, due to economical reasons, of which the characteristics may vary from quarry to quarry. Moreover, hydrochloric acid was used in the test as an acid to dissolve the limestone, but in an actual FGD plant, limestone reacts with an acid formed by absorption of sulfur dioxide. Therefore, 25 limestones were collected from various places of the world and were examined for their dissolution rates using the wetted-wall column apparatus which can simulate the absorption of sulfur dioxide. Figure 8 shows the relation between the dissolution rate constants and pH values of these limestones. In this test, the dissolution rate constants in the wetted-wall column and in the tank can be separately obtained through measuring the amount of absorbed sulfur dioxide in the wetted-wall column and pH values at both the bottom of the wetted-wall column and the tank. Therefore, the data shown in Figure 8 includes the rate constants obtained in both the wetted-wall column

Table 2 Fractions of Dissolution Obtained by Experiment and Calculation

Particle size of initial limestone	Liquid pH	Fractions of Dissolution (−) Observed	Calculated
45μm 95% passing	5.5	0.895	0.877
	5.1	0.950	0.947
	4.8	0.963	0.973
75μm 95% passing	5.5	0.852	0.853
	5.1	0.912	0.915
	4.8	0.934	0.955

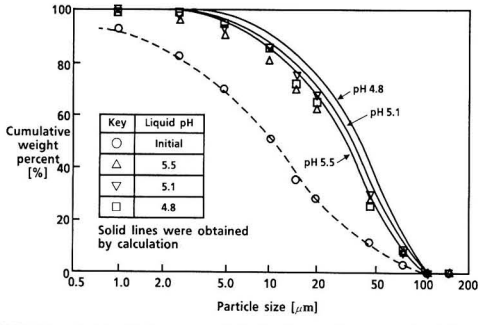

FIGURE 7. Particle size distribution of unreacted limestone in continuous type test (particle size distribution of initial limestone; 75μm 95% passing).

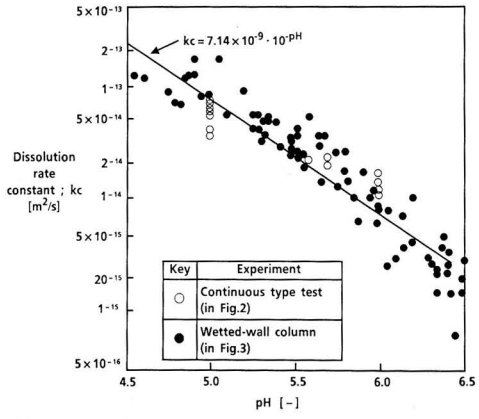

FIGURE 8. Relation between dissolution rate constant and pH value.

and the tank, which are related to pH values at the bottom of the wetted-wall column and at the tank respectively. The dissolution rate constants of many limestones gather along the primary straight line of 10^{-pH}. The results indicate that the dissolution rate equation in this study is applicable to limestone of various particle sizes, composition and place of production. These data were processed by the method of non-linear least squares and $ka = 7.14 \cdot 10^{-9}$ was obtained. This ka value is larger than the ka value obtained in either batch or continuous type test because chloride ions accumulated in the liquid and might reduce the ka value in wetted-wall column test.

CONCLUSIONS

In this study, the dissolution kinetics of limestone in the FGD process were examined, and the following results were obtained: (1) The dissolution rate equation introduced by the mass transfer rate in an agitated fluid gives results in good agreement with the measured values of dissolution rate and the reduction rate of the particle size distribution of unreacted limestone in both batch and continuous type tests. (2) The above dissolution rate equation gives values also in good agreement with the dissolution rate of 25 limestone samples from different places in the world having various particle sizes and compositions in the wetted-wall column test apparatus simulating the absorber tower and tank in the actual FGD process. (3) According to this evaluation, it is possible to calculate the reactivity of high calcium limestone with specified level of the particle size distribution and design the FGD process more accurately.

NOTATION

B = enhancement factor [m^{-1}]
ΔC = concentration gradient [kgmol/m^3]
D = diffusion coefficient [m^2/s]
d_p = particle size of limestone [m]
F = overall fraction of unreacted limestone [−]
f = fraction of unreacted limestone [−]
ka = dissolution rate constant (corrected by pH value) [m^2/s]
kc = dissolution rate constant [m^2/s]
k_L = mass transfer coefficient [m/s]
Sc = Schmidt number (ν_c/D) [−]
Sh = Sherwood number ($k_L \cdot d_p/D$) [−]
t = time [s]
V = initial volume of limestone particle [m^3]
V_p = volume of limestone particle [m^3]
ϵ = agitation power per unit weight of fluid [W/kg]
η = overall fraction of dissolved limestone [−]
ν_c = kinematic viscosity of fluid [m^2/s]
ρ_c = density of fluid [kg/m^3]
ρ_m = molar density of limestone [kgmol/m^3]
τ = average residential time [s]
ϕ_j = fraction of limestone with initial diameter d_{pj} [m]

Subscripts

B = batch reaction system
C = continuous reaction system
j = jth particle group

LITERATURE CITED

1. Calderbank, P. H., and M. B. Moo-Young, *Chem. Eng. Sci.*, **16**, p. 39 (1961).
2. Chan, P. K., and G. T. Rochelle, *ACS Symp. Ser.*, **188**, p. 75 (1982).
3. Compton, R. G., P. J. Daly and W. A. House, *J. Colloid Interface Sci.*, **113**, p. 12 (1986).
4. Compton, R. G., and P. J. Daly, *J. Colloid Interface Sci.*, **115**, p. 493 (1987).
5. Ellis, A. R., *Inst. Chem. Eng. Symp. Ser.*, **106**, p. 251 (1989).
6. Gage, C. L., and G. T. Rochelle, 1990 SO_2 Control Symposium, New Orleans, LA, May 8-10 (1990).
7. Morse, J. W., *Amer. J. Sci.*, **274**, p. 97 (1974).
8. Muramatsu, K., T. Shimizu, N. Shinoda, and A. Tatani, *Chem. Economy Eng. Review*, **16**, p. 15 (1984).
9. Plummer, L. N., T. M. L. Wigley, and D. L. Parkhurst, *Am. J. Sci.*, **278**, p. 179 (1978).
10. Toprac, A. J., and G. T. Rochelle, *Environ. Prog.*, **1**, p. 52 (1982).
11. Tress, M. V., R. H. Loeppert, and J. H. Matis, *Soil. Sci. Soc. Am. J.*, **49**, p. 302 (1985).

PROCESS CONTROL THEORY AND THE CPI...

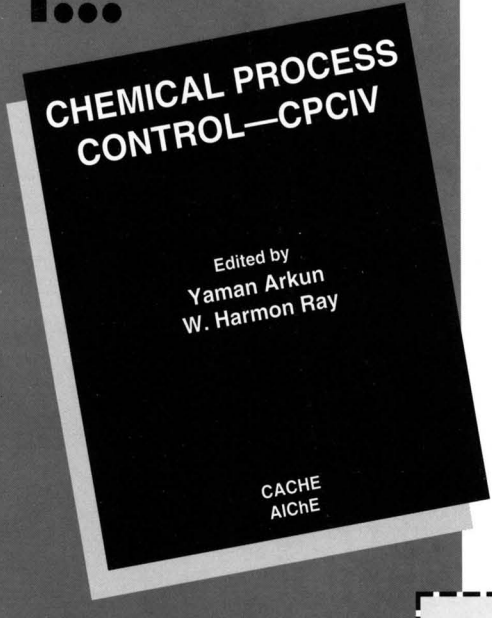

IS THERE A BRIGHTER FUTURE SHINING THROUGH ALL THAT JARGON?

Despite its advances, process control theory has been slow to realize its full potential in the chemical processing industry.Control experts have "theorized" themselves out of the industrial loop. Control remains mostly an afterthought to process design.Yet safety and economics clearly demand more high-performance, non-linear control techniques in the CPI. Those are among the important issues addressed in the new volume of Chemical Process Control—CPCIV. This 700-page compendium contains 37 of the most significant papers from the Fourth International Conference on Chemical Process Control. It covers virtually every topic in the field that chemical engineers should know about. From inventory control in Japanese plants to modeling in neurobiology, these papers sum up five years of the very latest control applications from industry, academia, and government. This fully indexed volume covers:

- Industrial overviews from Japan, Europe, and North America
- On-line sensors and data analysis
- Dynamic process simulation, modeling, and identification
- Model-based process modeling and control
- Recent approaches to the control of nonlinear processes
- Learning systems, adaptive, and AI control
- Control technology in the year 2000

CHEMICAL PROCESS CONTROL—CPCIV, 1991, edited by Yaman Arkun,Georgia Institute of Technology, and W. Harmon Ray, University of Wisconsin. BE SURE TO ORDER YOUR COPY OF THIS IMPORTANT NEW REFERENCE! Mail this form to: AIChE Publications Dept. 345 E. 47th St., New York, NY 10017. or call (212) 705-7657, Fax (212) 752-3294.

Please send me a copy of CHEMICAL PROCESS CONTROL—CPC IV ISBN 0-8169-0549-5

___ Enclosed is my check or money order for $95.00. AIChE members take 20% off list price. International Price $133.00

Please bill my ____Visa ____Mastercard # _____

Expiration date _____ Signature_____

SHIP TO:

Name _____

Organization _____

Address _____

City_____State_____Zip _____

Country _____

Pollution Prevention:

Homework and Design Problems for Engineering Curricula

"One of the greatest needs in industry, as we approach waste elimination, is to change the mindsets of people who have been trained to maximize yield or minimize immediate process costs. This manual goes a long way toward teaching tomorrow's engineers that the real 'process' does not end with just the intended product."

Earl R. Beaver
Monsanto Company

"Through the use of this manual, we hope to instill increased recognition and acceptance of the professional and ethical responsibilities which engineers must have as they develop the next generation of environmentally-compatible, cost-effective process technologies."

Lawrence L. Ross
AIChE's Center for Waste Reduction Technologies

The American Institute of Chemical Engineers' Center for Waste Reduction Technologies is offering a workbook introducing a new resource of pollution prevention technologies and methodologies. This workbook is of value to the novice as well as expert environmental engineers working in the pollution prevention field. Ordered by 600+ faculty members, it is ideal for those seeking:

- Review of pollution prevention techniques
- Introduction to pollution prevention
- Environmental research
- Pollution prevention tutorials
- Use as an educational supplement
- Integration of environmental issues into existing company training courses

Filled with quantitative engineering problems and solutions, this 155 page workbook provides background material, case studies, references, and coverage of six significant pollution prevention concepts.

A driving force behind the creation of this workbook was the American Institute of Pollution Prevention with their members, comprising experts drawn from a wide range of professional and trade organizations, contributing key case studies. The workbook was developed by faculty and professionals active in pollution prevention research, teaching, and practice. Each problem has been reviewed for accuracy, completeness and applicability by engineers in industry, and critiqued by members of CWRT.

Order your Workbook Now!

Call (212)705-7657, Fax (212)752-3294, Or send your order to:

Center for Waste Reduction Technologies
The American Institute of Chemical Engineers

Publication Sales Department, 345 E. 47th Street, New York, NY 10017
All orders must be prepaid (US $35.00). International prices slightly higher.